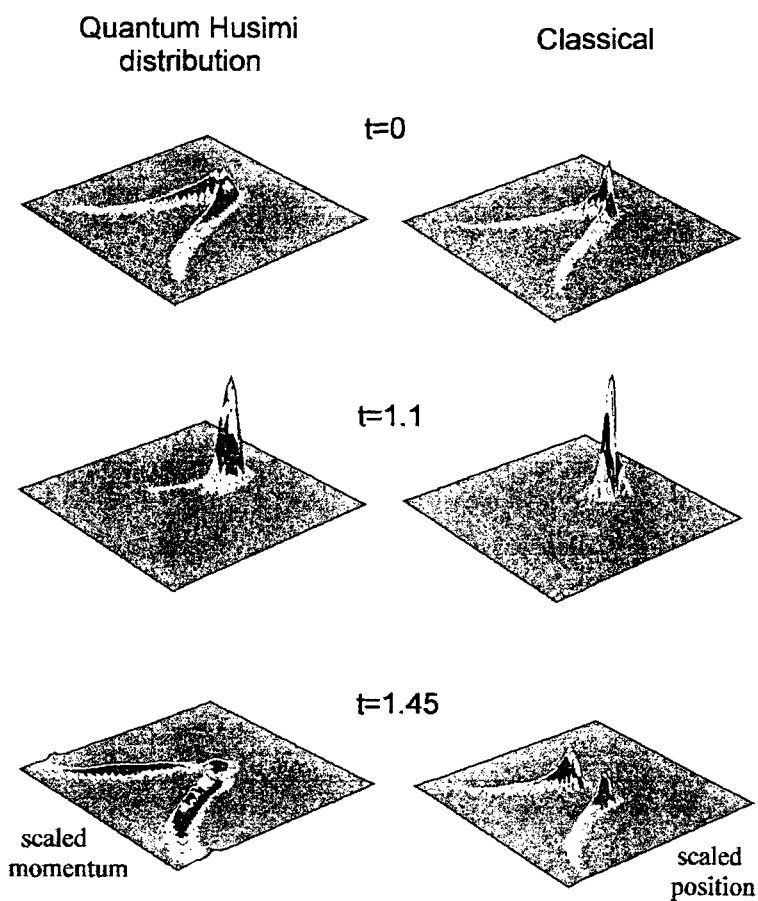


2002 Atomic, Molecular and Optical Sciences Research Meeting



Sponsored by:
U.S. Department of Energy
Office of Basic Energy Sciences
Chemical Sciences, Geosciences & Biosciences Division

Front Cover:

Quantum (left) and classical (right) calculations of the probability density for finding the Rydberg electron with a given position and momentum for two different times after a strongly polarized Rydberg atom was subjected to a half-cycle pulse at $t=0$ (in units of the average Kepler period). The agreement between quantum and classical dynamics indicates that the overall behavior of the Rydberg wavepacket can be explained classically. These results also illustrate the creation of non-stationary wavepackets that become transiently localized in phase space at certain times, i.e., $t=1.1$.

Graphic courtesy of Carlos Reinhold, Oak Ridge National Laboratory. For more information see: "Transient Phase Space Localization," C.L. Stokely, F.B. Dunning, C.O. Reinhold and A.K. Pattanayak, Phys Rev A Vol. 65 (2002) 021405(R).

Foreword

This volume summarizes the scientific content of the 2002 Research Meeting of the Atomic, Molecular and Optical Sciences (AMOS) Program sponsored by the U. S. Department of Energy (DOE), Office of Basic Energy Sciences (BES). This meeting is held annually for the DOE laboratory and university principal investigators within the BES AMOS Program in order to facilitate scientific interchange among the PIs and to promote a sense of program identity. For the past four years, the meeting has included significant participation from scientists outside of the BES AMOS Program and has had a specific topical focus. The 2002 meeting continues this format with a topical focus on "Quantum Information Science," an area of intense current scientific interest and one that has received substantial funding from the national security and defense agencies.

The BES AMOS Program continued on a path of modest growth in FY2002. In large measure this growth has been due to successful competition in recent BES research initiatives, including Complex and Collective Phenomena in FY1999, Novel X-Ray Light Sources in FY2000, and Nanoscale Science, Engineering and Technology in FY2001 and FY2002. This growth has helped to spur the evolution of the program from one of purely atomic physics to a more diverse portfolio that includes the interactions of intense laser fields with atoms and molecules, coherent control of quantum processes, development and application of novel x-ray light sources, ultracold collisional interactions, quantum condensates and electron-driven processes. At the same time, the traditional role of the program continues through support of AMO science at the DOE synchrotron facilities and via ongoing projects involving highly charged atomic ions.

In February 2002 BES hosted its first Committee of Visitors (COV), formally organized under the auspices of the Basic Energy Sciences Advisory Committee (BESAC). The COV was charged with reviewing the management and peer review practices of the research programs in the Chemical Sciences at BES. The AMOS and Chemical Physics programs were reviewed as a unit and found to be "very strong, active, well managed" and with "science viewed as first rate." Clearly, the quality of science in the AMOS program is entirely attributable to the PIs in the program – keep up the good work! The quality of program "management" is also largely attributable to the excellent peer reviews obtained from the AMOS community. I want to thank all of you who have given of your valuable time in this service, either in mail reviews of grant applications or on-site reviews of multi-PI programs. Thorough and thoughtful reviews take time and effort, but they are absolutely vital to the continued scientific health and growth of the BES AMOS Program.

I gratefully acknowledge the contributions of this year's speakers, particularly those not supported by the BES AMOS program, for their investment of time and for their willingness to share their ideas with the meeting participants. Thanks also to the staff of the Oak Ridge Institute of Science and Education, in particular Julie Malicoat, and the Airlie Conference Center for assisting with logistical aspects of the meeting.

Eric Rohlffing, Program Manager
Atomic, Molecular and Optical Sciences
Chemical Sciences, Geosciences and Biosciences Division
Office of Basic Energy Sciences
August 2002

Agenda

U. S. Department of Energy
Office of Basic Energy Sciences

2002 Meeting of the Atomic, Molecular and Optical Sciences Program
Quantum Information Science

Sunday, Oct. 6

3:00-6:00 pm ***** Registration *****
6:00 pm ***** Reception (No Host) *****
7:00 pm ***** Dinner *****

Monday, Oct. 7

7:00 am ***** Breakfast *****
8:00 am *Introductory Remarks*
Eric Rohlfing, BES/DOE
Session I Chair: **Eric Rohlfing**
8:10 am *U.S. and International Programs in Quantum Information*
Henry Everitt, U.S. Army Research Office
9:00 am *Quantum Computing with Quantum Optics*
Peter Zoller, University of Innsbruck
9:50 am ***** Break *****
10:20 am *So You've Built a Quantum Computer, Now What Are You Going to do With It?*
Seth Lloyd, Massachusetts Institute of Technology
11:10 am *Scaling the Ion Trap Quantum Computer*
Christopher Monroe, University of Michigan
12:00 pm ***** Lunch *****
5:00 pm ***** Reception (No Host) *****
6:00 pm ***** Dinner *****

Session II Chair: **Phil Bucksbaum**

7:20 pm *Quantum Key Distribution Through the Atmosphere in Daylight and at Night*
Richard Hughes, Los Alamos National Laboratory
8:10 pm *Atom + Cavity Systems for Quantum Information Processing*
Michael Chapman, Georgia Tech
9:00 pm *Few-Body Reaction Imaging*
Jim Feagin, Cal State Fullerton

Tuesday, Oct. 8

- 7:00 am **** Breakfast ****
- Session III** Chair: **Henry Kapteyn**
- 8:00 am *Investigation and Control of Strong-Field Processes in Atoms, Molecules and Clusters*
Robert Jones, University of Virginia
- 8:30 am *Multiphoton Quantum Dynamics and Optimal Generation of Coherent X-Ray Harmonic Emission*
Shih-I Chu, University of Kansas
- 9:00 am *High-Intensity Laser Interactions with Atomic Clusters*
Todd Ditmire, University of Texas
- 9:30 am *High Harmonic Cutoff Extension Due to Ionization Suppression*
Zenghu Chang, Kansas State University
- 10:00 am **** Break ****
- 10:30 am *Experiments in Molecular Optics*
Robert Gordon, University of Illinois, Chicago
- 11:00 am *X-ray Scattering by Atoms and Molecules Dressed with Femto-second Laser Fields*
Ali Belkacem, Lawrence Berkeley National Laboratory
- 11:00 am *Quantum Trajectory Monte Carlo Method Describing the Production and Destruction of Coherence*
Carlos Reinhold, Oak Ridge National Laboratory
- 12:00 pm **** Lunch ****
- Session IV** Chair: **Mike Prior**
- 4:00 pm *Development and Utilization of Bright Tabletop Sources of Coherent Soft X-Ray Radiation*
Jorge Rocca, Colorado State University
- 4:30 pm *Ultrafast Coherent Soft X-Rays: A Novel Tool for Spectroscopy of Collective Behavior in Complex Materials*
Keith Nelson, Massachusetts Institute of Technology
- 5:00 pm *A Quantum Mechanically Complete Experiment on Photo-Double Ionization of Helium*
Bertold Krässig, Argonne National Laboratory
- 5:30 pm *Site-Specific Target Orientation Dependence of Charge Fractions Observed for F^{q+} Ions Backscattered from a (100) Surface of RbI*
Herb Krause, Oak Ridge National Laboratory
- 6:00 pm **** Reception (No Host) ****
- 7:00 pm **** Dinner ****

Wednesday, Oct. 9

7:00 am **** Breakfast ****

Session V Chair: **Jim Feagin**

8:00 am *Theory of Fragmentation and Rearrangement Processes in Ion-Atom Collisions*
Joe Macek, University of Tennessee

8:30 am *Molecular Structure and Collisional Dissociation and Ionization*
Kurt Becker, Stevens Institute of Technology

9:00 am *Polyatomic Excitation Effects in Electron-Molecule Collisions: A First-Principles Study of Electron-CO₂ Scattering*

Tom Resicigno, Lawrence Berkeley National Laboratory

9:30 am *Triply Excited States in Three-Electron Ions*

Pat Richard, Kansas State University

10:00 am **** Break ****

10:30 am *Dissociation and Coulomb Explosion of Model Molecular Hydrogen Ions by Intense Short Laser Pulses*

Uwe Thumm, Kansas State University

11:00 am *Quantum/Classical Atomic Interactions*

Francis Robicieux, Auburn University

11:30 am *Double K-Photoionization of Heavy Atoms*

Elliott Kanter, Argonne National Laboratory

12:00 pm *Closing Remarks*

Eric Rohlfig, BES/DOE

12:10 pm **** Lunch ****

Table of Contents

Invited Presentations (Ordered by Agenda)

<i>U.S. and International Programs in Quantum Information</i> Henry O. Everitt	1
<i>Quantum Computing with Quantum Optics</i> Peter Zoller	2
<i>So You've Built a Quantum Computer, Now What are You Going to do With It?</i> Seth Lloyd	3
<i>Scaling the Ion Trap Quantum Computer</i> Christopher Monroe	4
<i>Quantum Key Distribution Through the Atmosphere in Daylight and at Night</i> Richard J. Hughes	5
<i>Atom + Cavity Systems for Quantum Information Processing</i> Michael Chapman	6
<i>Few-Body Reaction Imaging</i> James M. Feagin	7
<i>Quantum Control of Time-Dependent Electron Correlation</i> Robert R. Jones	11
<i>Multiphoton Quantum Dynamics and Optimal Generation of Coherent X-Ray Harmonic Emission</i> Shih-I Chu	13
<i>High Intensity Laser Interactions with Atomic Clusters</i> Todd Ditmire	17
<i>High Harmonic Cutoff Extension Due to Ionization Suppression</i> Z.Chang	21
<i>Experiments in Molecular Optics</i> Robert J. Gordon, Langchi Zhu, W. Andreas Schroeder	22
<i>X-ray Scattering by Atoms and Molecules Dressed with Femto-Second Laser Fields</i> Ali Belkacem	26
<i>Quantum Trajectory Monte Carlo Method Describing the Production and Destruction of Coherences</i> C.O. Reinhold	28
<i>Development and Utilization of Bright Tabletop Sources of Coherent Soft X-ray Radiation</i> Jorge J. Rocca, Henry C. Kapteyn, Carmen S. Menoni	29

<i>Ultrafast Coherent Soft X-rays: A Novel Tool for Spectroscopy of Collective Behavior in Complex Materials</i> Keith A. Nelson, Henry C. Kapteyn, Margaret M. Murnane	33
<i>A Quantum-Mechanically Complete Experiment on Photo-Double Ionization of Helium</i> B. Krässig	37
<i>Site-Specific Target Orientation Dependence of Charge Fractions Observed for F⁹⁺ Ions Backscattered from a (100) Surface of RbI</i> H.F. Krause, F.W. Meyer, C.R. Vane	38
<i>Theory of Fragmentation and Rearrangement Processes in Ion-atom Collisions</i> J.H. Macek	40
<i>Molecular Structure and Collisional Dissociation and Ionization</i> Kurt H. Becker	43
<i>Polyatomic Excitation Effect in Electron-Molecule Collisions: a First-Principles Study of Electron-CO₂ Scattering</i> Thomas N. Rescigno	47
<i>Triply Excited States in Three-Electron Ions</i> Patrick Richard	48
<i>Dissociation and Coulomb Explosion of Model Molecular Hydrogen Ions by Intense Short Laser Pulses</i> Uwe Thumm, Bernold Feuerstein	49
<i>Quantum/Classical Atomic Interactions</i> F. Robicheaux	50
<i>Double K-Photoionization of Heavy Atoms</i> E.P. Kanter, R.W. Dunford, D.S. Gemmell, B. Krässig, S.H. Southworth, L.Young	53
 Research Summaries (Multi-PI Programs, Alphabetical by Institution)	
<i>X-Ray and Inner-Shell Interactions</i> R.W. Dunford, E.P. Kanter, B. Krässig, S.H. Southworth, L. Young	54
<i>Ultracold Atoms: Applications</i> R.W. Dunford, S. H. Southworth, L. Young	58
<i>Generation and Characterization of Attosecond Pulses</i> L.F. DiMauro, K.C. Kulander, I.A. Walmsley, R.W. Boyd	61

<i>Structure and Dynamics of Atoms, Ions, Molecules, and Surfaces: Atomic Physics with High Velocity, Highly Charged Ion Beams</i> Patrick Richard	65
<i>Structure and Dynamics of Atoms, Ions, Molecules, and Surfaces: Atomic Physics with Ion Beams, Lasers and Synchrotron Radiation</i> C.L. Cocke	69
<i>Structure and Dynamics of Atoms, Ions, Molecules, and Surfaces: Molecular Dynamics with Ion and Laser Beams</i> Itzik Ben-Itzhak	73
<i>Molecular Dissociation imaging of Collision-Induced Dissociation and Dissociative Capture in Slow $H_2^+ + Ar$ (He) Collisions</i> D. Hathiramani, I. Ben-Itzhak, J.W. Maseberg, A.M. Saylor, M.A. Smith, K.D. Carnes	73
<i>Ultrafast X-ray Source and Detector</i> Z. Chang	77
<i>Ion and Photon Interactions with Laser Cooled Targets</i> B.D. DePaola	81
<i>Structure and Dynamics of Atoms, Ions, Molecules and Surfaces: Atomic Physics with Ion- and Electron-Beams</i> S. Hagmann	85
<i>Theoretical Studies of Interactions of Atoms, Molecules and Surfaces</i> C.D. Lin ..	89
<i>Theoretical Studies of Interactions of Atoms, Molecules, and Surfaces: Dynamics of Few-Body Systems</i> B.D. Esry	93
<i>Interactions of Ions and Photons with Atoms, Surfaces, and Molecule</i> Uwe Thumm	97
<i>Inner-Shell Photo-Ionization of Atoms and Small Molecules</i> A. Belkacem, M. Prior	101
<i>Research with Cold Molecules and Cold Atoms</i> Harvey Gould	105
<i>Electron-Atom and Electron-Molecule Collision Processes</i> C.W. McCurdy, T.N. Rescigno	109
<i>Femtosecond X-ray Beamline for Studies of Structural Dynamics</i> Robert W. Schoenlein	113

<i>Atomic and Molecular Physics Research at Oak Ridge National Laboratory</i> <i>M.E. Bannister, C.C. Havener, H.F. Krause, J.H. Macek, F.W. Meyer, C. Reinhold,</i> <i>D.R. Schultz, C.R. Vane</i>	117
---	-----

Research Summaries (Single-PI Grants, Alphabetical by PI)

<i>Properties of Transition Metal Atoms and Ions</i> <i>D.R. Beck</i>	125
<i>Probing Dynamics and Structure in Atoms, Molecules and Negative Ions Using the Advanced Light Source</i> <i>Nora Berrah</i>	129
<i>Coherent Control of X-rays</i> <i>P.H. Bucksbaum</i>	133
<i>Low Energy Ion-Surface and Ion-Molecule Collisions</i> <i>R.L. Champion</i>	137
<i>Theoretical Investigations of Atomic Collision Physics</i> <i>A. Dalgarno</i>	141
<i>Femtosecond Photon Echo Techniques for Manipulation of Quantum States and Computation</i> <i>Marcos Dantus</i>	144
<i>Chemistry with Ultracold Molecules</i> <i>Bretislav Friedrich, Dudley R. Herschbach</i>	148
<i>Theoretical Studies of Atomic Transitions</i> <i>Charlotte Froese Fischer</i>	150
<i>Studies of Autoionizing States Relevant to Dielectronic Recombination</i> <i>T.F. Gallagher</i>	154
<i>Experiments in Ultracold Collisions</i> <i>Phillip L. Gould</i>	157
<i>Physics of Correlated Systems</i> <i>Chris H. Greene</i>	160
<i>Quantum Theory of Collective Effects in the Atom Laser</i> <i>Murray J. Holland</i>	163
<i>Toward Cooper Pairing of Fermionic Atoms</i> <i>Deborah Jin</i>	167

<i>Non-Perturbative Laser Atom Interactions for Nonlinear Optics</i> Henry C. Kapteyn, Margaret M. Murnane	170
<i>Spectroscopy of Nanoparticles Produced by Laser Ablation of Microparticles</i> John W. Keto	172
<i>Physics of Low-Dimensional Bose-Einstein Condensates</i> Eugene B. Kolomeisky	177
<i>Ion/Excited-Atom Collision Studies with a Rydberg Target and a CO₂ Laser</i> Stephen R. Lundeen	180
<i>Correlation in Dynamic Multi-Electron Systems</i> Jim McGuire	183
<i>Electron-Driven Processes in Polyatomic Molecules</i> Vincent McKoy	187
<i>Atomic Collisional Processes Investigated Through the Generalized Oscillator Strength</i> Alfred Z. Msezane	191
<i>Study of Near-Field Optical Interactions Between a Molecule and a Laser Illuminated Metal Tip</i> Lukas Novotny	195
<i>Energetic Photon and Electron Interactions with Positive Ions</i> Ronald A. Phaneuf	199
<i>Mode-Specific Polyatomic Photoionization far from Threshold: Molecular Physics at 3rd Generation Light Sources</i> Erwin Poliakoff	203
<i>Isotopically Enriched Thin Films and Nanostructure by Ultrafast Pulsed Laser Deposition</i> Peter P. Pronko	207
<i>Cold Rydberg Atom Gases and Plasmas in Strong Magnetic Fields</i> G. Raithel	211
<i>Measurement of Electron Impact Excitation Cross Sections of Highly Ionized Atoms</i> A.J. Smith	215
<i>Dynamics of Few-Body Atomic Processes</i> Anthony F. Starace	219
<i>Femtosecond and Attosecond Laser-Pulse Energy Transformation and Concentration in Nanostructured Systems</i> Mark I. Stockman	223
<i>Correlated Charge-Changing Ion-Atom Collisions</i> J.A. Tanis	227

Invited Presentations
(ordered by agenda)

U.S. and International Programs in Quantum Information

Henry O. Everitt
Associate Director
Physics Division
U.S. Army Research Office

Current U.S. and international activities in quantum information science will be surveyed, including quantum cryptography, quantum communication, and quantum computing. State of the art research will be assessed relative to critical performance milestones. Progress in various physical implementations for quantum computing and quantum communications will be compared.

Quantum Computing with Quantum Optics

Peter Zoller
Institute for Theoretical Physics
University of Innsbruck
Austria

We discuss theoretical aspects of implementation of quantum computers with quantum optics. Quantum optics proposals typically assume that qubits are stored in longlived atomic states of single atoms. We discuss the underlying techniques of trapping and cooling of atoms. As a digression, we emphasize the role of the recently observed superfluid-Mott insulator transition of atoms as a loading technique for a large number of qubits in optical lattices, and the engineering of Hubbard type models with controllable parameters in atomic physics. Furthermore, we discuss in detail the realization of single and two-qubit gates with ions, atoms and in Cavity QED, and comment on the scalability of quantum optical proposals. Furthermore, we present new results on quantum computing with cold atoms in 1D optical lattices, where qubits are encoded in small Schrödinger cat states, and a collectively enhanced entanglement due to cold collisions between atoms implements the two-qubit gates. We conclude with a brief discussion of the role of atomic ensembles in quantum information processing, and draw a connection between quantum dot proposals as "artificial atoms".

So You've Built a Quantum Computer, Now What are You Going to do With It?

Seth Lloyd
MIT Mechanical Engineering

A large number of techniques for building quantum computers have been proposed, and several relatively simple quantum information processors have been constructed. This talk reviews techniques for constructing quantum computers and quantum communication systems, compares the advantages and drawbacks of each, and examines their prospects. The talk will propose a number of things to do with simple quantum computers, including investigating quantum algorithms and quantum entanglement, using quantum information processors as environmental sensors, and analog quantum computation.

Scaling the Ion Trap Quantum Computer

Christopher Monroe
University of Michigan

Trapped atomic ions are among the most attractive physical candidates for scalable quantum computing. Quantum bits derived from internal electronic states offer isolation that is unmatched in other systems, and the Coulomb-mediated interaction between qubits can be accurately controlled with appropriate external laser sources. Scaling this system towards large numbers of quantum bits appears straightforward, but presents several key challenges – both technical and economic. Many proposed schemes for the scale-up will be outlined, including the use of “quantum CCD” ion trap arrays with multiple ion species, strong laser fields for application of extreme dipole forces, and high finesse optical cavities. Some of these schemes will be discussed in the context of current efforts at Michigan involving trapped cadmium isotopes.

Quantum key distribution through the atmosphere in daylight and at night

Richard J. Hughes
Physics Division,
Los Alamos National Laboratory,
Los Alamos, NM 87545

Quantum key distribution (QKD) is an emerging technology that uses single-photon transmissions to generate the shared, secret random number sequences (cryptographic keys) that are used to encrypt and decrypt secret communications. The unconditional security of QKD is based on the interplay between fundamental principles of quantum physics and information-theoretic techniques. An adversary can neither successfully tap the transmissions, nor evade detection (eavesdropping raises the key error rate above a threshold value). QKD could enable “on demand” re-keying of secure communications systems. Particularly attractive uses of QKD are in free-space optical communications, both ground-based and for satellite communications.

We have developed a QKD test bed to investigate key transfer over multi-kilometer ground-based, line-of-sight links, and to serve as a model for a satellite-to-ground key distribution system [1]. Our system, which uses non-orthogonal single-photon polarization states to implement the BB84 QKD protocol without active polarization switching, is capable of continuous, unattended operation throughout the day and night. It incorporates reconciliation and privacy amplification to produce error-free, secret key bits protected against technologically feasible eavesdropping. Other novel features of our system include: the use of distinct wavelengths to perform key transfer and synchronization; quantum mechanical random number generation at the receiver; and cryptographic testing of the key material produced. We will describe the operation of our QKD system in daylight to generate cryptographic quality key material at practical rates over a 10-km distance and the implications of these results for using QKD for secure satellite communications.

1. R. J. Hughes, et al., *New Journal of Physics* 4, 43 (2002).

Atom + cavity systems for quantum information processing

Michael Chapman

*School of Physics, Georgia Tech
Atlanta, GA 30332*

We are developing neutral atom cavity QED systems capable of storing and coherently manipulating quantum information coded in long-lived ground states of trapped atoms. This requires successful integration of two leading quantum information technologies — atom-based quantum memories and cavity QED-based entanglement generation and manipulation. Our configuration employs movable laser traps for individual atoms that will permit us to store a chain of individually addressable atoms and to manipulate these atoms in arbitrary combinations using the quantum field of the optical cavity.

We have recently guided and transported atoms into our high-finesse optical cavities using a translating one-dimension optical lattice, and we have observed the signals from single atoms as they are transported through the cavity. In the strong coupling regime of our atom + cavity system, just a single atom interacts strongly enough with the quantum field of the cavity to create a measurable change in the transmission of a weak cavity probe.

I will also discuss two related experimental efforts in cold atom manipulation, all-optical Bose-Einstein condensation and neutral atom magnetic guiding. This past year, we successfully created an atomic Bose-Einstein condensate using all-optical methods, realizing a long-term objective in the field. Remarkably, our method is simpler and faster than traditional BEC experiments and offers unique capabilities for atoms and molecules not amenable to traditional methods. The use of BEC's for entanglement generation and other quantum information purposes is currently an area of active investigation.

Also, we have recently demonstrated the first storage ring for neutral atoms. The ring employs a two-wire magnetic guiding structure and a novel mechanism to transfer atoms to the ring from a magneto-optic trap. This experiment represents a significant step towards utilizing ultracold, guided atoms in ring-based atom interferometry experiments, and such magnetic guiding techniques can be used to coherently transport atomic qubits.

Few-Body Reaction Imaging

Department of Energy 2002

James M Feagin

Department of Physics

California State University-Fullerton

Fullerton CA 92834

jfeagin@fullerton.edu

Over the past decade we have witnessed the evolution of a new generation of experiments demonstrating isolation and control of individual atoms and molecules. Correlations and entanglements among groups of particles can now be orchestrated, and their internal and motional states encoded, transformed, read, and even teleported. While many of the gedanken experiments familiar in quantum traditions have become reality, strong evidence has been established that one can store and process information in quantum systems with efficiencies exponentially superior to classical computation and communication. Besides the profound impact on the foundations of quantum mechanics, these experimental and accompanying theoretical advances conspire to establish a newcomer technology *quantum information processing*.¹

Much of the progress with quantum information has relied heavily on quantum optics and manipulating photons. There is thus fundamental interest in demonstrating analogous control with massive charged particles, for example correlated electrons and ions for which the DOE Office of Basic Energy Sciences has a long and distinguished history. With *few-body reaction imaging* we are working to develop tools for quantum control from the highly-evolved AMO industry of collision and few-body phenomena. Our research remains nevertheless part of a general effort in the AMO community to advance the basic understanding of collective few-body excitations. We are thus investigating the physics of nanoscale science, engineering, and technology (NSET) based on a long-time experience in AMO collision physics. We find there exists opportunity to contribute to at least two goals of the NSET initiative of the DOE: (i) Attain a fundamental understanding of nanoscale phenomena, and (ii) develop experimental characterization tools and theory to understand, predict, and control nanoscale phenomena.

We consider few-body reaction and fragmentation detection from the more general perspective of reaction imaging. We accordingly distinguish two parallel efforts with (i) new emphasis on *detection with interferometers* while (ii) pursuing ongoing work on *collective Coulomb excitations*.

Detection with Interferometers

Advances in coincidence detection technology for collisions involving charged particle or photon impact have evolved into a new field of few-body fragmentation spectroscopy.² Full kinematic information can now be extracted systematically on all collision fragments of few-body states from measurements of the momentum vectors of each fragment. With supersonically cooled targets, momentum detection to 0.1 au is now routinely achieved. With confined and cooled targets in magneto-optical traps, this precision is likely to improve in the near future by an order of magnitude. For example, N. Andersen and coworkers in Copenhagen used this technique recently to resolve diffraction patterns in differential charge-transfer cross sections.³ Parallel

¹Two excellent resources have recently appeared: *Quantum Computation and Quantum Information*, M. A. Nielsen and I. L. Chuang, Cambridge University Press (2000); and *The Physics of Quantum Information*, D. Bouwmeester, A. Ekert and A. Zeilinger (Eds.), Springer-Verlag (2001).

²R. Dörner et al., Phys. Rep. **330**, 95 (2000).

³M. van der Poel et al., Phys. Rev. Lett. **87**, 123201-1 (2001).

to this remarkable progress have been the developments in the field of atom optics concerned with manipulating with micro-structures and light fields the motion of atoms and molecules and Bose-Einstein condensates to observe their interference and diffraction just like waves of light. For example, A. Zeilinger and coworkers in Vienna demonstrated recently the diffraction of fullerene molecules by standing light waves.⁴

In pioneering work on quantum correlation, Wootters and Zurek⁵ analyzed how two-slit interference with photons changes when the recoil of a distant collimator slit is monitored. Motivated by the experimental interests of L. Cocke (Kansas State) and R. Dörner (Frankfurt), we have extended the description of Wootters and Zurek to particle impact ionization involving projectile interferometry and target-fragment recoil detection. Our intention is to combine few-body fragmentation spectroscopy with tools from atom optics to extract additional amplitude and phase information from the reaction dynamics. This effort is thus much in the spirit of recent work by Forrey and coworkers to determine electron scattering amplitude information with electron interferometry.⁶

Our projectile wavefunction is just one component of an entangled ‘projectile + target’ state required by momentum conservation and generated when a projectile m_1 is scattered with momentum components $\mathbf{k}_1 \rightarrow \mathbf{k}_{f\pm} = \mathbf{k}_f \pm \mathbf{k}_0$ towards the entrance of a two-slit interferometer, as in the Wootters and Zurek analysis of photon diffraction.⁷ Here, $\mathbf{k}_0 = \pi\mathbf{s}/\lambda L$ with slit separation s , target-to-slit distance L , and projectile deBroglie wavelength λ . The fuzziness of the recoil momentum $\mathbf{K} = \mathbf{k}_2 + \mathbf{k}_3$ of the target-atom center of mass (CM) derives from that of the scattered projectile, viz. $\mathbf{K}_{f\pm} = \mathbf{K}_c - \mathbf{k}_{f\pm}$, since the system CM momentum \mathbf{K}_c is conserved. Thus, for a given \mathbf{K}_c component the system is described just outside the entrance of the interferometer by

$$|\chi_{nP\&T}\rangle = P_n^{-1/2} [f_{n+}|\mathbf{k}_{f+}\rangle|\mathbf{K}_{f+}\rangle + f_{n-}|\mathbf{k}_{f-}\rangle|\mathbf{K}_{f-}\rangle], \quad (1)$$

where $f_{n\pm} \equiv f_n(\mathbf{k}_{f\pm})$ are the amplitudes for projectile scattering into the two slits with excitation of the target atom to the state n . Here, $P_n = |f_{n+}|^2 + |f_{n-}|^2$ is the probability that the scattered projectile enters the interferometer through one or the other slit.

To maintain the necessary momentum fuzziness, there has to be a measurement of the target CM position $\mathbf{r}_T = (m_2\mathbf{r}_2 + m_3\mathbf{r}_3)/(m_2 + m_3)$, the whereabouts of which is required for good fringe visibility. In the Wootters and Zurek analysis, this quantity is essentially fixed by the position \mathbf{r}_3 of the rigid support m_3 to which a spring and collimator slit m_2 are attached. In a scattering experiment with a massive recoil ion m_3 , $\mathbf{r}_T \simeq \mathbf{r}_3$ could be a nearly fixed point inside a sufficiently compact reaction volume, say a magneto-optical trap, or the anchor point of a target atom to a surface. The CM position measurement implies a corresponding reduction of the state vector Eq. (1), $|\chi_{nP\&T}\rangle \rightarrow |\chi_{nP}\rangle = \langle \mathbf{r}_T | \chi_{nP\&T} \rangle$, or equivalently of the system density operator, $\rho_{nP\&T} \rightarrow \rho_{nP} = |\chi_{nP}\rangle\langle \chi_{nP}|$, which retains the requisite cross terms for interference. The projectile interference pattern is then the probability of finding the superposition $|S_P\rangle = e^{ik_0\xi}|\mathbf{k}_{f+}\rangle + e^{-ik_0\xi}|\mathbf{k}_{f-}\rangle$, so that projectile detection inside the interferometer introduces the additional reduction $|\chi_{nP}\rangle \rightarrow \chi_n(\xi) = \langle S_P | \chi_{nP} \rangle$, where

$$\chi_n(\xi) = P_n^{-1/2} [f_{n+} e^{-ik_0\xi + i\mathbf{K}_{f+} \cdot \mathbf{r}_T} + f_{n-} e^{ik_0\xi + i\mathbf{K}_{f-} \cdot \mathbf{r}_T}], \quad (2)$$

and thus the interference pattern

$$I_n(\xi) = 1 + \frac{2|f_{n+}||f_{n-}|}{P_n} \cos(2k_0\xi + 2k_0x_T - \Delta_n) \quad (3)$$

⁴O. Nairz et al., Phys. Rev. Lett. **87**, 160401-1 (2001).

⁵W. K. Wootters and W. H. Zurek, Phys. Rev. D **19**, 473 (1979).

⁶R. C. Forrey, A. Dalgarno and J. Schmiedmayer, Phys. Rev. A **59**, R942 (1999), and references therein.

⁷J. M. Feagin and Si-ping Han, Phys. Rev. Lett. **86**, 5039 (2001).

with $x_T \equiv \hat{\mathbf{k}}_0 \cdot \mathbf{r}_T$, since $\mathbf{K}_{f-} - \mathbf{K}_{f+} = \mathbf{k}_{f+} - \mathbf{k}_{f-} = 2\mathbf{k}_0$.⁸ As a rule of thumb, the lateral width Δx_T of the reaction volume must be on the order of the slit separation s to ensure enough transverse coherence for good fringe visibility. In the Fraunhofer limit which defines $|S_P\rangle$, the fringe spacing $\Delta\xi$ is large compared to s , and so taking $\Delta x_T \ll \Delta\xi$, i.e. setting $x_T = 0$, is an ideal but appropriate limit.

The state n describes target internal excitation and an additional degree of freedom for sorting alternative subensembles of projectile-target entanglement. It was the essential element of our analysis, which follows closely that of Wootters and Zurek. Along these lines, we have thus also had in mind the introduction of a second interferometer to probe the target recoil and alternative entanglements equivalent to Eq. (1).⁹ In effect, one could then replace the recoil states $|\mathbf{K}_{f\pm}\rangle$ with for example the *marker* basis $|\tilde{\mathbf{K}}_{\pm}\rangle = |\mathbf{K}_{f+}\rangle \pm |\mathbf{K}_{f-}\rangle$ and reexpress Eq. (1) as

$$|\chi_{nP\&T}\rangle = |\chi_{nP}^+\rangle|\tilde{\mathbf{K}}_+\rangle + |\chi_{nP}^-\rangle|\tilde{\mathbf{K}}_-\rangle \quad (4)$$

with $|\chi_{nP}^{\pm}\rangle = P_n^{-1/2} [f_{n+}|\mathbf{k}_{f+}\rangle \pm f_{n-}|\mathbf{k}_{f-}\rangle]$. If one now considers a target-recoil measurement of say $|\tilde{\mathbf{K}}_+\rangle$ correlated to the projectile measurement $|S_P\rangle$, one obtains Eq. (2) with $\mathbf{r}_T = 0$ but now describing a *joint* projectile-target-recoil interference amplitude, i.e. $\langle S_P \tilde{\mathbf{K}}_+ | \chi_{nP\&T} \rangle = \chi_n(\xi)$ with $\mathbf{r}_T = 0$. Experiments of this sort could be used to examine a number of outstanding issues fundamental to quantum mechanics.

Along with teleportation of trapped-ion states, we are working to extend detection interferometry to include n -slit diffraction and other *quantum tomographic* techniques to image in addition the extremely fragile few-body Coulomb states generated near fragmentation thresholds¹⁰ and fundamental to the few-body Coulomb problem.

Single-Electron Circular Dichroism

Parallel to advances in double ionization with circularly polarized photons has been a renewed interest in recent years in photo *single* ionization and the resulting photoelectron angular distributions for departures from the dipole approximation. Following the theoretical work of Cooper,¹¹ Bechler and Pratt,¹² and others, Krässig and coworkers have reported measurements of nondipolar asymmetries in photoelectrons from Ar and Kr ionized with x rays in the 3–5 keV energy range from the National Synchrotron Light Source.¹³

Two-slit detection would provide new probes of these photoionization angular distributions. Even in photo *single* ionization of unoriented atoms, it appears possible¹⁴ to generate a circular dichroism analogous to the well established effect seen in photo *double* ionization.¹⁵ Thus, circular dichroism is observed in the angular distributions of photoionized electron pairs and has been used to extract phase information unavailable using linearly polarized photons. (We have also considered the generalization of this effect to molecular photo double ionization.¹⁶) In the case of photo single ionization, the idea is this: Introduce a two-slit detector and let the pair of momentum vectors \mathbf{k}_{\pm} of the ionized electron amplitude entering each slit take on the chiral role of the electron-pair momentum vectors \mathbf{k}_1 and \mathbf{k}_2 in photo double ionization. In

⁸J. M. Feagin and Si-ping Han, Phys. Rev. Lett. **89**, in press (2002).

⁹We especially enjoy the review of such alternative “as-if realities” in the context of two-way interferometry by B.-G. Englert in Z. Naturforsch. C **54a**, 11 (1999)

¹⁰J. M. Feagin, J. Phys. B: At. Mol. Phys. **28**, 1495 (1995).

¹¹J. W. Cooper, Phys. Rev. A **47**, 1841 (1993) and references therein.

¹²A. Bechler and R. H. Pratt, Phys. Rev. A **42**, 6400 (1990) and references therein.

¹³B. Krässig et al., Phys. Rev. Lett. **75**, 4736 (1995); M. Jung et al., Phys. Rev. A **54**, 2127 (1996).

¹⁴J. M. Feagin, Phys. Rev. Lett., **88**, 043001-1 (2002).

¹⁵V. Mergel et al., Phys. Rev. Lett. **80**, 5301 (1998) and references therein. (*Feagin is a coauthor on this paper.*)

¹⁶T. J. Reddish and J. M. Feagin, J. Phys. B: At. Mol. Opt. Phys. **32**, 2473 (1999).

effect, the handedness of the incident photons would be used to distinguish right and left slits. One thus obtains a one-electron circular dichroism of the form $\Delta \sim (\mathbf{k}_+ \times \mathbf{k}_-) \cdot \mathbf{k}_\gamma$ as well as nondipolar phase information unavailable with linearly polarized photons. A new generation of experiments to study nondipolar effects is underway in a number of laboratories.

A related dichroism and nondipolar probe is expected for excitation and fluorescence in which the fluorescence photon takes the role of the photoionized electron and would thus be analyzed by two-slit interferometry. Such an experiment is currently underway by T. Gay and coworkers at the University of Nebraska. Nondipolar effects which can be probed in this way are being calculated for various atomic and molecular systems.¹⁷

Collective Coulomb Excitations

The conventional detection of two electrons following photo-double ionization or electron-impact single ionization of simple atoms and molecules is already a highly-advanced technology, and one which has contributed enormously to our understanding of the correlated motion of electrons in the field of a positive ion. Thus, the study of the photo double ionization of the helium atom near threshold has played a significant role. Not only is the final state one involving three unbounded particles interacting via pure Coulomb forces, but the dipole symmetry change is simple and well defined. This system has thus served as a benchmark for both experimental¹⁸ and theoretical¹⁹ work.

The coincident measurement of two continuum electrons has been extended to the photo double ionization of molecular hydrogen in the isotopic form D_2 ,²⁰ and recently including coincident detection of the deuterons.²¹ We have thus developed a basic description of the photo double ionization cross section for diatomic molecules²² based closely on the cross section for helium. We derive a dependence of molecular excitation amplitudes on electron energy sharing and dynamical quantum numbers labeling internal modes of excitation of the escaping electron pair. We consider both linear and circular polarizations. The model is currently being analyzed along with detailed D_2 fragmentation data by T. Weber as part of his PhD thesis in Frankfurt.²³

Publications

Energy Sharing and Asymmetry Parameters for Photo Double Ionization of Helium 100 eV Above Threshold, A. Knapp et al, J. Phys. B: At. Mol. Opt. Phys., in press (2002).

Reply-Comment on Reaction Imaging with Interferometry, J. M. Feagin and Si-ping Han, Phys. Rev. Lett. **89**, in press (2002).

Circular Dichroism in Photo Single Ionization of Unoriented Atoms, J. M. Feagin, Phys. Rev. Lett., **88**, 043001-1 (2002).

Reaction Imaging with Interferometry, J. M. Feagin and Si-ping Han, Phys. Rev. Lett. **86**, 5039 (2001).

Molecular Symmetries of Electron-Pair Atomic States, M. Walter, J. S. Briggs and J. M. Feagin, J. Phys. B: At. Mol. Opt. Phys. **33**, 2907 (2000).

¹⁷B. Zimmermann and J. M. Feagin, Phys. Rev. A, in preparation (2002).

¹⁸R. Dörner et al, Phys. Rev. A **57**, 1074 (1998). (*Feagin is a coauthor on this paper.*)

¹⁹M. Walter, J. S. Briggs and J. M. Feagin, J. Phys. B: At. Mol. Opt. Phys. **33**, 2907 (2000).

²⁰T. J. Reddish et al., Phys. Rev. Lett. **79**, 2438 (1997); N. Scherer et al., J. Phys. B: At. Mol. Opt. Phys. **31**, L817 (1998); J. P. Wightman et al., J. Phys. B: At. Mol. Opt. Phys. **31**, 1753 (1998).

²¹R. Dörner et al., Phys. Rev. Lett. **81**, 5776 (1998). (*Feagin is a coauthor on this paper.*)

²²J. M. Feagin, J. Phys. B: At. Mol. Opt. Phys. **31**, L729 (1998).

²³T. Weber et al., Phys. Rev. A, in preparation (2002). (*Feagin is a coauthor on this paper.*)

Quantum Control of Time-Dependent Electron Correlation

Robert R. Jones, Physics Department, University of Virginia,
382 McCormick Road, P.O. Box 400714, Charlottesville, VA 22904-4714
rj3c@virginia.edu

Program Scope

We use intense and/or short laser pulses to (1) manipulate and view the time-dependent interaction between electrons in two-electron atoms; and (2) investigate and control strong-field ionization and fragmentation of multi-electron atoms, molecules, and clusters. In the first class of experiments, coherent pulse sequences are used to generate doubly-excited Rydberg wavepackets in atoms with two valence electrons. By controlling the excitation pulses, we can manipulate dielectronic dynamics and alter the branching ratio for electron ejection into different energy and angularly resolved continua. In the second line of experiments we are studying the role of electronic structure and electron correlation in strong field processes such as population trapping via AC Stark shifted resonances and the apparent suppression of ionization in diatomic molecules with triplet ground states. We are also examining the competition between laser induced ionization and fragmentation in larger molecules and small clusters. Our experiments compare and contrast process yields for different molecular species as a function of laser intensity, polarization, and wavelength. In addition, a liquid-crystal-based laser-pulse shaper is being used in conjunction with a genetic feedback algorithm to explore the enhancement and/or suppression of these phenomena through the manipulation of the time-dependent laser field.

Recent Results

I. Suppression of Strong-Field Ionization in Molecules

In the past year, we have continued our investigation of intense laser ionization of molecules. While atomic ionization is relatively well described by single-active-electron tunneling or multiphoton models, in general, molecular ionization and fragmentation yields cannot be accurately predicted at this time. For example, our measurements with D_2 , F_2 , S_2 , SO , NO , and CO targets are at odds with current theoretical predictions. We know of no simple physical picture for why ionization is suppressed in some molecular species, particularly those with triplet ground states, but not in others. However, due to their relative insensitivity to absolute laser intensity and focussing parameters, our systematic precision measurements of molecular/atomic ionization yield ratios should provide strict tests of new theoretical work in this area. Our recent results have been published in PRL [4] and PRA [1].

II. Control of Intense-Laser Fragmentation of Clusters*

When molecules and clusters are subjected to intense laser fields, both ionization and fragmentation of the molecule can occur. In some applications, however, it may be desirable to produce only the parent molecular ion or specific charged fragments. Not surprisingly, the ionizing laser's color, intensity, and/or temporal structure can often be adjusted to manipulate the relative yield into particular fragments. Unfortunately, due to the complexity of these systems, it is not generally possible to know *a priori* the specific laser characteristics that will maximize the desired yield for a particular target.

We are currently using a liquid-crystal based, laser pulse-shaper in combination with an adaptive feedback algorithm to investigate control of intense laser fragmentation of small clusters.[6-9] For example, we recently found that the branching ratio and absolute yield for production of particular charged fragments, S_n^+ , from S_8 clusters could be enhanced by >300% using either “phase-only” field shaping or combined amplitude- and phase-shaping. Our measurements indicate that two technical obstacles limit further selectivity in these, and other, strong-field laser control experiments. The first problem is the distribution of peak intensities experienced by ion fragments originating from different positions within the laser focal volume. We will reduce this effect in our continuing experiments by installing a small extraction aperture so that only those fragments produced in a small volume within the laser focus are detected. The second issue is the small number of control parameters (typically a maximum of 32, or so) that can be used in the search algorithm if convergence is to be achieved. While typical pulse-shapers have a significantly greater number of independently variable parameter “knobs” (256 pixels in a standard liquid crystal light modulator) we typically reduce the search space by constraining groups of knobs so that they do not vary independently. This approach severely restricts the types of laser pulses that can be produced. Importantly, in a cluster fragmentation experiment, key molecular rearrangement may require that the laser pulse have structure over times-scales of several picoseconds or more. Such pulses are not obtainable using the standard pixel clustering method. We have developed two different laser pulse-shape parameterization schemes that enable us to use the full resolution of the pulse-shaper, and generate pulses with significantly longer temporal structure while still searching over 32 (or fewer) independent knobs. We intend to compare and contrast the effectiveness of these two parameterization schemes relative to the previous pixel clustering approach.

III. Pondermotive-Gradient Field Ionization**

In an attempt to explore multi-electron effects in strong field processes, we recently began a systematic study of electron population trapping in highly-excited ionic states during intense-laser ionization of atoms and diatomic molecules. Specifically, we measured Rydberg ion population produced during multiphoton ionization of alkali atoms, rare-gas atoms, and diatomic molecules. We saw no evidence for population trapping in excited alkali or molecular ions. However, consistent with previous results,[10] we did observe Ar^+ , Kr^+ , Xe^+ , Kr^{2+} , and Xe^{2+} Rydberg ions. For the noble gases, a sequential excitation/ionization model severely over estimates (by as much as 5 orders of magnitude) the number of trapped, highly charged Rydberg ions that are produced. In the model, neutral Rydberg atoms are created via AC Stark-shifted resonances during the leading edge of the laser pulse followed by inner-electron ionization in the higher intensities available near the temporal peak of the pulse. The model implicitly assumes that the intense laser cannot ionize Rydberg electrons that are far from the atomic nucleus.

However, the assumption of Rydberg transparency breaks down if we consider the spatial variation of the pondermotive potential in the laser focus. The force associated with the *gradient* of the pondermotive potential can be considered acts as an effective half-cycle field pulse that can ionize Rydberg atoms. The same field is responsible for the scattering of free electrons in the Kapitza-Dirac effect [11]. Interestingly, when the gradient field-ionization mechanism is taken into account, nearly all of our measurements are in good agreement with the predictions of the modified sequential excitation/ionization model. The sole exception is Xe^{2+} , whose relative yield

Multiphoton Quantum Dynamics and Optimal Generation of Coherent X-Ray Harmonic Emission

Shih-I Chu

Department of Chemistry, University of Kansas
Lawrence, Kansas 66045
E-mail: sichu@ku.edu

Program Scope

In this research program, we address the fundamental physics of the interaction of atoms and molecules with intense ultrashort laser fields. The main objectives are to develop new theoretical formalisms and accurate computational methods for *ab initio* comprehensive investigations of multiphoton quantum dynamics and very high-order nonlinear optical phenomena of one- and multi-electron quantum systems in intense and superintense laser fields, taking into account detailed atomic and molecular structures. Particular attention will be paid to the exploration of novel physical mechanisms, time-frequency spectrum, and coherent control of multiple high-harmonic generation (HHG) processes for the development of tabletop x-ray laser light sources. Also to be investigated is the fundamental AMO theory on the interactions of ultrafast, intense x-ray pulses with atomic and molecular systems, including multiphoton and high-field effects.

Recent Progress

1. Optimization of Multiple High-Order Harmonic Generation by Genetic Algorithm and Wavelet Time-Frequency Analysis

The study of coherent control of atomic and molecular processes is a subject of much current interest in science and technology. In the area of the interaction of atoms with intense laser pulse, the optimization of high-order harmonic generation (HHG) is a topic of particular interest to the future technological development of x-ray laser, attosecond laser pulse generation, and many other applications. Recently the JILA high-field experimental group has shown that it is possible to perform “intra-atomic” phase matching, allowing the enhancement of the intensity of a specific harmonic [1]. Although qualitative picture of such an intra-atomic phase matching may be roughly explained by the quasi-classical electron trajectory picture [2], the quantum nature of this process such as the time-dependent quantum wave function, and the delicate quantum interference pattern, etc., is not yet known. To advance this important field, we have recently pursued the first fully *ab initio* quantum 3D study of the coherent control of HHG in intense laser fields by means of the *genetic algorithm* (GA) of the laser-pulse amplitude and phase [3]. Accurate time-dependent wave function and HHG power spectrum of atomic H are obtained by the recently developed *time-dependent generalized pseudospectral method* [4] and the *wavelet transform* is used to obtain the quantum dynamical phase associated with the dipole-emission time profile. It is shown that “intra-atomic” dynamical phase matching on the sub-optical cycle, atto-second, time scale can be achieved, leading to nearly perfect constructive interference between different returning quantum electronic wave packets and marked improvement in both emission intensity and purity of a given harmonic.

2. Development of Self-Interaction-Free Time-Dependent Density Functional Theories for Nonperturbative Treatment of Many-Electron Quantum Systems in Intense Laser Fields

To study strong-field processes of many-electron systems using the *ab initio* wave function approach, it is necessary to solve the time-dependent Schrödinger equation of $3N$ spatial dimensions in

space and time (N = the number of electrons), which is beyond the capability of current supercomputer technology. The *single-active-electron* (SAE) model with *frozen core* is commonly used and has been successful for some strong-field processes where only one valence electron plays the dominant role. However, within the SAE model, important physical phenomena such as excited state resonances, different dynamical response from different valence spin-orbitals, inner core excitation, and the dynamical electron correlations cannot be treated. Clearly, a more complete formalism beyond the SAE model is very desirable for further progress in the study of the atomic and molecular physics in strong fields. Recently we have initiated a series of new developments of *self-interaction-free* time-dependent density functional theory (TDDFT) for probing strong-field processes of many-electron atomic systems, taking into account electron correlations and detailed electronic structure [5-7]. Since last year, we have also begun to develop self-interaction-free TDDFT for the two-center diatomic molecular systems as well [8,9,10]. Given below is a brief summary of the progress in 2001-2002.

2a) *High-Order Harmonic Generation of Rare Gas Atoms in Intense Laser Pulsed Fields*

We perform a detailed *all-electron* study of multiphoton ionization (MPI) and high-order harmonic generation (HHG) processes of rare gas atoms (He, Ne, and Ar) in intense pulsed laser fields [7] by means of the *self-interaction-free* TDDFT recently developed in our group. The time-dependent exchange-correlation (xc) potential with proper short- and long- range potential is constructed by means of the *time-dependent optimized effective potential* (TD/OEP) method and the incorporation of an explicit *self-interaction-correction* (SIC) term. The TD/OEP-SIC equations are solved accurately and efficiently by the use of the *time-dependent generalized pseudospectral* technique [4]. In this study, all the valence electrons are treated explicitly and nonperturbatively and their partial contributions to the ionization and HHG are analyzed. The results reveal qualitatively different behavior from each subshell orbital. Moreover, we found that the HHG yields from Ne and Ar atoms are considerably larger than that of the He atom in strong fields. Two main factors are identified for accounting the observed phenomena: (a) the binding energy of the subshell valence electron, and (b) the orientation of the valence electron orbital (with respect to the electric field polarization) [7].

2b) *Multiphoton and High-Order Harmonic Generation of H_2 in Intense Laser Fields*

While the study of atomic processes in intense laser fields has been a very active field of strong field AMO physics research both experimentally and theoretically in the last decade, the study of strong-field molecular progress begins to receive much attention only quite recently. The high-field phenomena in molecular systems are a largely unexplored area of frontier research. *Ab initio* theoretical studies of many-*electron* molecular processes in strong fields are considerably much more challenging than the corresponding atomic processes due to the multi-center problems and the additional nuclear degrees of freedom. Thus most theoretical studies on strong-field molecular processes up to today were based on simple models and did not take into account the effect of detailed molecular structure.

We have recently initiated the development of general *self-interaction-free* TDDFT for nonperturbative and comprehensive treatment of multiphoton processes of *multi-electron molecular* systems in intense laser fields [8]. The resulting TDDFT equations are structurally similar to the time-dependent Hartree-Fock equations, but include the many-body (electron-correlated) effects through an orbital-independent single-particle *local* time-dependent exchange-correlation (xc) potential. The latter is constructed by means of the time-dependent OEP/SIC method. A numerical time-propagation technique is introduced for accurate and efficient solution of the TDDFT/OEP-SIC equations for two-center diatomic molecular systems. The procedure involves the use of a *generalized pseudospectral method* for *nonuniform* optimal grid discretization of the Hamiltonian in prolate spheroidal coordinates

[9] and a split-operator scheme in the *energy* representation for the time development of individual electron orbital wave functions. High-precision time-dependent wave functions can be obtained by this procedure with the use of only a modest number of grid points. The theory is applied to the first *all-electron* study of HHG processes of H_2 molecules in intense pulsed laser fields. Particular attention is paid to the exploration of the spectral and temporal structures of HHG by means of the wavelet time-frequency analysis. The results reveal striking details of the fine structures (sub-peaks) of the time profile of individual harmonic, providing new insights regarding the underlying HHG mechanisms in different energy regimes, including low-lying multiphoton dominant regime, near ionization-threshold regime, plateau regime, and near cut-off regime, for a molecular system for the first time [8].

2c) *Multiphoton Processes and Dynamical Response of Individual Valence Electrons of N_2 in Intense Laser Fields*

Recently we have presented a molecular TDDFT with proper long-range potential for the first *all-electron* nonperturbative detailed study of multiphoton ionization (MPI) and high-order harmonic generation (HHG) of N_2 in intense laser fields [10]. A time-dependent generalized pseudospectral method is extended for precision solution of the TDDFT equations for two-center diatomic systems. The results reveal unexpected and intriguing nonlinear optical response behaviors of the individual valence spin orbital to strong fields. In particular, it is found that the dominant contribution of total HHG power spectrum of N_2 is due to the constructive and destructive interferences of the induced dipoles of the two highest-occupied bonding ($3\sigma_g$) and antibonding ($2\sigma_u$) molecular orbitals in the presence of intense laser fields [10].

3. Quantum Fluid Dynamics Approach to Strong-Field Processes

We explore the feasibility of extending the quantum fluid dynamics (QFD) approach for nonperturbative investigation of many-electron quantum systems in strong fields. Through the amalgamation of the QFD and density functional theory (DFT), a single time-dependent hydrodynamic equation can be derived. This equation has the form of a generalized nonlinear Schrodinger equation (GNLSE) but include the many-body effects through a local time-dependent exchange-correlation potential. A time-dependent generalized pseudospectral method is developed to the solution of the GNLSE in spherical coordinates, allowing *nonuniform* and optimal spatial discretization and accurate solution of the hydrodynamic wave function and density in space and time. The procedure is applied to the study of MPI and HHG of He and Ne atoms in intense laser fields [11]. Excellent agreement with the TDDFT/OEP-SIC calculations [7] is obtained for He, and for Ne, good agreement is achieved. The QFD/DFT method offers a conceptually appealing and computational practical approach for nonperturbative treatment of complex many-electron systems well beyond the time-dependent Hartree-Fock level. More exploration of this formalism is in progress.

4. Generalized Floquet Formulation of TDDFT for Intense-field Multiphoton Processes of Atomic Systems

Recently we have initiated the development of the generalized Floquet formulation of TDDFT for general nonperturbative treatment of multiphoton processes of many-electron atomic systems [12,13]. The Floquet-TDDFT approach allows exact transformation of *periodically* (one-color) or *quasi-periodically* (multi-color) time-dependent Kohn-Sham equation into an equivalent *time-independent* generalized Floquet eigenvalue problem. We further develop an exterior-complex scaling (ECS) – generalized pseudospectral (GPS) method for accurate solution of the non-Hermitian Floquet-TDDFT Hamiltonian [14]. We applied the new procedure to the study of one- and two-photon detachments of Li^- negative ions. For the one-photon case, the photodetachment cross sections are in good agreement

with experimental data. In the two-photon case, both the partial detachment rates and electron angular distributions for the dominant and above-threshold channels are determined for a range of laser frequencies and intensities. Dramatic transformation of the angular distributions in the vicinity of the two-photon threshold are observed and analyzed in details [14].

Future Research Plans

In addition to continuing the ongoing researches discussed above, we plan to initiate the following several new project directions: (a) Extension of the genetic algorithm and wavelet time-frequency analysis to the optimization of HHG processes of more complex many-electron systems. (b) For the self-interaction-free TDDFT, so far the nuclear vibrational degrees of freedom have not yet fully incorporated. We will continue the main efforts in this direction in the future. (c) Development and extension of the Floquet formulation of TDDFT to the molecular systems. (d) Further exploration of the quantum-fluid dynamics/DFT approach for the investigation of multiphoton processes of complex many-electron quantum systems in strong fields.

References Cited (* Publications supported by this DOE program.)

- [1] R. Bartels, S. Backus, E. Zeek, L. Misoguti, G. Vdovin, I. P. Christov, M. M. Murnane, and H. C. Kapteyn, *Nature (London)* **406**, 164 (2000).
- [2] I. P. Christov, R. Bartels, H. C. Kapteyn, and M. M. Murnane, *Phys. Rev. Lett.* **86**, 5458 (2001).
- *[3] X. Chu and S. I. Chu, *Phys. Rev. A* **64**, 021403 (R) (2001).
- [4] X. M. Tong and S. I. Chu, *Chem. Phys.* **217**, 119 (1997).
- [5] X. M. Tong and S. I. Chu, *Phys. Rev. A* **57**, 452 (1998).
- [6] X. M. Tong and S. I. Chu, *Int. J. Quantum Chem.* **69**, 305 (1998).
- *[7] X. M. Tong and S. I. Chu, *Phys. Rev. A* **64**, 013417 (2001).
- *[8] X. Chu and S. I. Chu, *Phys. Rev. A* **63**, 023411 (2001).
- *[9] X. Chu and S. I. Chu, *Phys. Rev. A* **63**, 013414 (2001).
- *[10] X. Chu and S. I. Chu, *Phys. Rev. A* **64**, 063404 (2001).
- *[11] A. K. Roy and S. I. Chu, *Phys. Rev. A* **65**, 043402 (2002).
- [12] D. Telnov and S. I. Chu, *Chem. Phys. Lett.* **264**, 466 (1997).
- *[13] D. Telnov and S. I. Chu, *Phys. Rev. A* **63**, 012514 (2001).
- *[14] D. Telnov and S. I. Chu, *Phys. Rev. A* (submitted).

High Intensity Laser Interactions with Atomic Clusters

Progress report (Fall 2002)

Principal Investigator:

Todd Ditmire

Department of Physics

University of Texas at Austin, MS C1600, Austin, TX 78712

Phone: 512-471-3296

e-mail: tditmire@physics.utexas.edu

Program Scope:

The development of ultrashort pulse table top lasers with peak pulse powers in excess of 1 TW has permitted an access to studies of matter subject to unprecedented light intensities. Such interactions have accessed exotic regimes of multiphoton atomic and high energy-density plasma physics. Very recently, the nature of the interactions between these very high intensity laser pulses and atomic clusters of a few hundred to a few thousand atoms has come under study. Such studies have found some rather unexpected results, including the striking finding that these interactions appear to be more energetic than interactions with either single atoms or solid density plasmas. Recent experiments have shown that the explosion of such clusters upon intense irradiation can expel ions from the cluster with energies from a few keV to nearly 1 MeV. This phenomenon has been exploited to produce DD fusion neutrons in a gas of exploding deuterium clusters. Under this project, we have undertaken a general study of the intense femtosecond laser cluster interaction. Our goal is to understand the macroscopic and microscopic coupling between the laser and the clusters with the aim of optimizing high flux fusion neutron production from the exploding deuterium clusters or the x-ray yield in the hot plasmas that are produced in this interaction. In particular, we are studying the physics governing the cluster explosions. The interplay between a traditional Coulomb explosion description of the cluster disassembly and a plasma-like hydrodynamic explosion is not entirely understood, particularly for small to medium sized clusters (<1000 atoms) and clusters composed of low-Z atoms. We are focusing on experimental studies of the ion and electron energies resulting from such explosions through various experimental techniques. We are also examining how an intense laser pulse propagates through a dense medium containing these clusters.

Recent Progress

Much of the research undertaken previously under this project has been focused on the interaction of a intense 30 fs pulses with deuterium clusters. These initial experiments utilized the 5 TW Falcon laser at LLNL. This work is motivated by the recent observation of DD fusion in a gas of laser irradiated deuterium clusters. One of the principal goals of this project is to understand the explosion mechanisms of these clusters so that they can be manipulated to enhance the fusion yield. Work during the past year has concentrated on the explosion dynamics of deuterium clusters and deuterated methane clusters. Most of the experiments have been performed on the LLNL JanUSP laser which delivers pulses with pulse duration as short as 100 fs and energy up to 10J.

1) Interactions with deuterium clusters

We have examined fusion yield and ion energies from irradiation of D₂ clustering gas jets with laser energy up to 10 J. Ion time-of-flight measurements were conducted on D⁺ ions escaping the plasma in a

high density gas jet irradiated with peak intensity up to 10^{20} W/cm². This measurement indicated that ions with energy out to 100 keV are produced in the exploding clusters. One of the principal diagnostics in these experiments has been the measurement of the 2.45 MeV fusion neutron production. To gain information on the explosion mechanisms, we examined the fusion neutron yield as a function of laser energy at different pulse durations. These data are shown in figure 1. We find that the fusion yield increases rapidly as a function of energy, increasing roughly as the square of the energy for all pulse durations.

More striking, however, is the observation that the yield is strongly dependant on pulse duration. We have conducted particle dynamics simulations of the exploding deuterium clusters and we attribute this shift in yield to an effect arising from the rise time of the laser pulse. In a pure Coulomb explosion, the highest ion energy, and highest fusion yield, will occur if the cluster electrons are stripped while the atoms are at their equilibrium positions. If the pulse rises more slowly, the atoms in the cluster will be ionized over a finite time, during which the cluster can expand a small amount. Therefore, the final Coulomb explosion energy will be reduced from that expected from an explosion at the equilibrium position. This effect illustrates the importance of using femtosecond pulses.

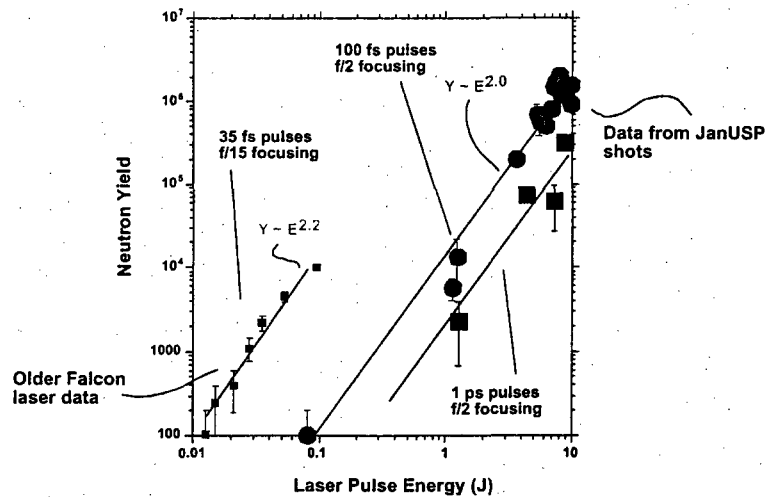


Figure 1: Measured fusion yield per laser shot vs energy for three different laser pulse durations

2) Interactions with deuterated methane clusters

In addition to the exploding D₂ cluster experiments, we conducted experiments on exploding CD₄. Heteronuclear clusters like deuterated methane are very interesting for a number of reasons and have not been studied in any detail under very intense laser irradiation. These mixed ion clusters may exhibit enhancements in ion energy through a dynamical effect in the Coulomb explosion. The Coulomb explosion of a single species cluster, like D₂ clusters will eject deuterons with an energy given directly by the potential energy of the ion as it is initially in the fully stripped cluster. In exploding mixed ion clusters like CD₄ the light deuterons will outrun the heavier ions, explode in an out shell with a higher average energy than would be expected from the naïve estimate of ion energy based on initial potential energy. This implies that the fusion yield could be substantially increased in plasmas formed from explosions of heteronuclear clusters over that of neat D₂ clusters of the same size because of this kinematic enhancement of ion energies in the mixed ion case.

We examined the explosion of CD_4 clusters irradiated at intensity up to 10^{20} W/cm^2 . These clusters were produced by the same jet used in the D_2 experiments. The measured average D^+ ion energies for these clusters are shown in figure 2 and are compared to average ion energies from D_2 cluster of comparable size ($\sim 5 \text{ nm}$ as determined by Rayleigh scattering measurements). These data suggest that an enhancement in ion energy does occur in the CD_4 clusters, though we intend to conduct additional measurements to confirm this.

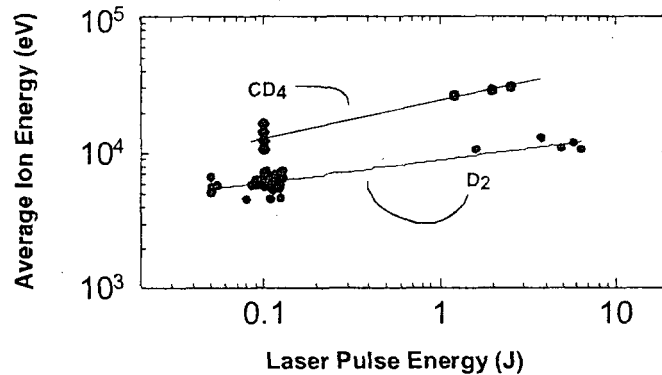


Figure 2: Measured average D^+ ion energy from exploding D_2 and CD_4 clusters

3) Two color pump probe experiments

We have constructed an experiment to examine the third harmonic generation of 800 nm pulses in a gas of xenon clusters as the clusters expand from the photoionization and heating of a an initial pump pulse (which has a wavelength of 400 nm). This pump-probe experiment is designed to yield information on the nonlinear oscillation dynamics of the electron cloud in an expanding cluster. This experiment follows on experiments conducted at LLNL on the linear absorption of a probe laser pulse in xenon clusters as a function of delay after an ionizing pump.

We conducted initial experiments using the Falcon laser at LLNL and during the past year reassembled this experiment at UT on the terawatt laser in the laboratory of Mike Downer. We have seen some variation of third harmonic signal as delay between the 800 nm and 400 nm pulses. Experiments on the scattering intensity as a function of time have also been started. These experiments are continuing.

Future Research Plans

Our future research plans are aimed at an understanding of the interactions between the laser and single clusters to understand in more detail the energy deposition mechanisms. In particular, the striking variation in fusion yield with pulse duration suggests that more detailed studies of Coulomb explosion energy be conducted as pulse duration and chirp is varied.

To do these experiments we use a time-of-flight spectrometer coupled to a molecular beam. We have fitted the chamber with a cryogenically cooled gas jet, identical to that used in the experiments described above. Laser pulses are focused with an aspheric lens into this beam of clusters and fast ejected particles are detected along an axis perpendicular to both the laser and the cluster beam. This spectrometer is designed to yield information on both ion and electron energy spectra. Ion spectra will be characterized both through direct, field free ion time of flight as well as through the use of charged retarding grids. This spectrometer will allow us to examine ions with energy up to 1MeV and will allow charge state

differentiation on ions with energy to charge state ratios up to 20 keV/Z. We will also analyze electron spectra, which will be measured by scanning the voltage on the retarding grids.

1) Our next set of experiments at UT will be to examine the ion energy distributions from hydrogen clusters. We plan to carefully study pulse rise time effects, as well as the consequences of pulse intensity and chirp. We will study both electrons and ions. Information derived here will then be used to optimize fusion yield in the high density deuterium gas jet experiments.

2) These experiments will be followed by greater attention to heteronuclear clusters. Note only will we examine the electron and ion energies from CD₄ clusters but we will examine other mixed species clusters, like HI.

3) We then intend to examine spectra from higher Z species (namely N₂, Ar, Kr and Xe) This will allow us to explore the nature of the cluster explosions as it evolves from a pure Coulomb explosion to a hydrodynamic explosion. Here, electron and ion spectra will be compared with particle dynamics simulations (conducted by Richard Fitzpatrick) as well as with hydrodynamic simulations (simulated with the Hyades hydro-code).

4) Additional experiments will follow up on the two color pump probe experiments. While we intend to continue the third harmonic experiments in Xe clusters, we will also begin to look at electron and ion spectra from these two pulse interactions. Once again, we will likely concentrate on deuterium clusters with an eye toward optimizing ion energies for fusion studies.

Papers published or to appear on work supported by this grant:

- 1) J. Zweiback, R.A. Smith, T.E. Cowan, G. Hays, K.B. Wharton, and T. Ditmire, "Nuclear Fusion Driven by Coulomb Explosions of Large Deuterium Clusters," *Phys. Rev. Lett.* **84**, 2634 (2000).
- 2) T. Ditmire, J. Zweiback, V. P. Yanovsky, T. E. Cowan, G. Hays, and K. B. Wharton, "Studies of Nuclear Fusion in Gases of Deuterium Clusters Heated by a Femtosecond Laser," *Phys. Plas.* **7**, 1993 (2000).
- 3) J. Zweiback, T.E. Cowan, J. Hartley, G. Hays, R. Howell R.A. Smith, C. Steinke, and T. Ditmire, "Characterization of Fusion Burn Time in Exploding Deuterium Cluster Plasmas," *Phys. Rev. Lett.* **85**, 3640 (2000).
- 4) T. D. Donnelly, M. Rust, I. Weiner, M. Allen, R. A. Smith, C. A. Steinke, S. Wilks, J. Zweiback, T. E. Cowan, and T. Ditmire, "Hard X-ray Production from Intense Laser Irradiation of Wavelength-Scale Particles" *J. Phys. B: At. Mol. Opt. Phys.* **34**, L313 (2001).
- 5) J. Zweiback, T. Ditmire, "Femtosecond Laser Energy Deposition in Strongly Absorbing Cluster Gases Diagnosed with Blast Wave Trajectory Analysis," *Phys. Plas.*, **8**, 4545 (2001).
- 6) J. Zweiback, T.E. Cowan, R. A. Smith, J. H. Hartley, R. Howell, G. Hays, K. B. Wharton, J. K. Crane, V. P. Yanovsky and T. Ditmire "Detailed Study of Nuclear Fusion From Femtosecond Laser-Driven Explosions of Deuterium Clusters" *Phys. Plas.* **9**, 3108 (2002).
- 7) K. W. Madison, P. K. Patel, M. Allen, D. Price, T. Ditmire, "An investigation of fusion yield from exploding deuterium cluster plasmas produced by 100 TW laser pulses" *J. Opt. Soc. Am. B* to be published.
- 8) K. W. Madison, R. Fitzpatrick, P. K. Patel, D. Price, T. Ditmire, "Laser driven Coulomb explosions of clusters at relativistic intensity" *Phys. Rev. Lett.* submitted.
- 9) K. Madison, P. Patel, D. Price, A. Edens, M. Allen, T. E. Cowan, J. Zweiback, and T. Ditmire "Nuclear fusion from explosions of deuterated methane clusters" *App. Phys. Lett.*, submitted.

High Harmonic Cutoff Extension Due to Ionization Suppression

Z. Chang

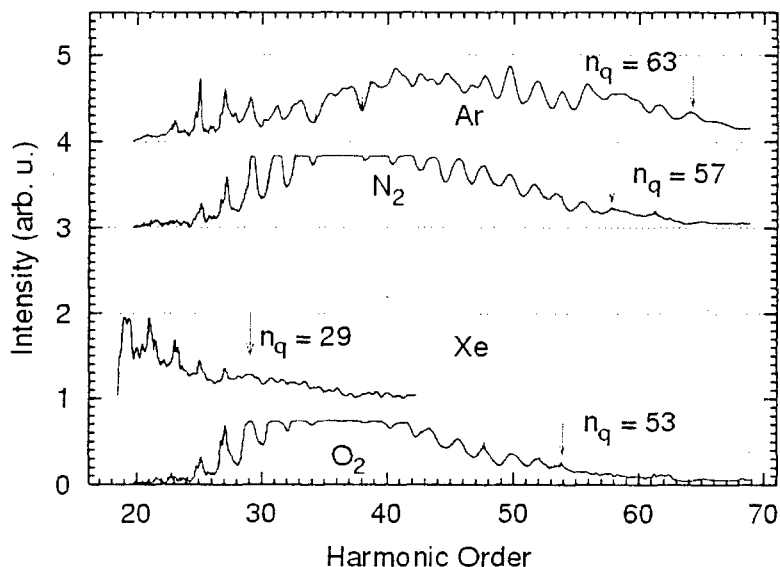
J. R. Macdonald Laboratory, Kansas State University [chang@phys.ksu.edu]

So far most of the studies on high harmonic generation (HHG) have been concentrated on rare gas atoms. On the other hand, few experiments have been done on molecules. In an earlier experiment, it was found that “the harmonic spectra from molecular gases are very similar to those obtained in the atomic gases, with a plateau and a cutoff whose location is strongly correlated to the value of the ionization potential”.

Recently it was found that the ionization of O_2 is suppressed by about one order of magnitude when comparing with Xe, which has nearly the same ionization potential as O_2 . As is known, HHG is closely related to ionization in the intense laser. The suppressed ionization of O_2 should lead to a significant extension of harmonic spectra. We studied the HHG cutoff behavior for molecules and their companion atoms to confirm this prediction.

The experiment was carried out with the newly established high intensity laser facility at the J. R. Macdonald laboratory. We compared Ar and N_2 , which have nearly the same ionization potentials, at 15.76 eV and 15.58 eV, respectively, and we found they have nearly identical harmonic cutoffs (The cutoff positions for Ar and N_2 are $q_c = 63$ and $q_c = 57$, respectively). On the other hand, while Xe and O_2 have nearly the same ionization potentials, at 12.13 eV and 12.06 eV, respectively, the harmonic cutoff for O_2 ($q_c=53$) is much higher than for Xe ($q_c=29$). The spectra are shown in the figure. We attributed this difference to the O_2 molecule being much harder to ionize than the Xe although they have the same ionization potential.

Fig.1 Comparisons of HHG spectra from atoms and their companion molecules. Ar and N_2 spectra were obtained under the same experimental conditions. So were Xe and O_2 .



Contradictory to previous results, our experiments show that the high harmonic cutoff of molecules can be significantly different from that of their companion atoms with almost identical ionization potentials. Our results indicate that the harmonic cutoff extension and the ionization suppression are strongly correlated. The cutoff extension caused by the ionization suppression provides another avenue for obtaining energetic x-ray photons.

EXPERIMENTS IN MOLECULAR OPTICS

Robert J. Gordon,^{a,b} Langchi Zhu,^a and W. Andreas Schroeder^c

^aDepartment of Chemistry (m/c 111), University of Illinois at Chicago,
845 West Taylor Street, Chicago, IL 60607-7061, ^bemail address: rjgordon@uic.edu

^cDepartment of Physics (m/c 273), University of Illinois at Chicago,
845 West Taylor Street, Chicago, IL 60607-7061

1. Program Scope

The objectives of this program are to develop optical methods of deflecting, focusing, and aligning beams of neutral molecules. Optical manipulation of molecules is a powerful tool for controlling chemical reactions, enhancing selected optical transitions, and creating nanostructures on surfaces. The central idea is to use the dipole force produced by a focused non-resonant laser beam to induce a dipole moment in a polarizable molecule. The potential energy of a molecule with dipole moment μ and polarizability α (with tensor components α_{\parallel} and α_{\perp}) is given by¹

$$U(r, \theta, t) = -\mu E(r, t) \cos \theta - \frac{1}{2} E^2(r, t) (\alpha_{\parallel} \cos^2 \theta + \alpha_{\perp} \sin^2 \theta),$$

where $E(r, t)$ is the electric field of the laser and θ is the angle between the principle axis of the molecule and the electric vector. Averaging the potential for a Gaussian field over a single optical cycle gives

$$U(r, \theta, t) = -\frac{1}{4} E_0^2 e^{-2r^2/\omega^2} (\Delta\alpha \cos^2 \theta + \alpha_{\perp}) f_{\text{env}}(t),$$

where $\Delta\alpha$ is the polarizability anisotropy, and $f_{\text{env}}(t)$ is the temporal envelope of the field. The derivative of U with respect to r gives a radial force that may be used to deflect and focus a beam of neutral particles, whereas the derivative with respect to θ gives a torque that may be used to align the molecules. These results are very general and are limited only by the requirement that the laser intensity lies below the ionization threshold of the molecule.

Several projects concurrent in our laboratory are the separation of molecules in different rotational states, production of aligned rotational wave packets with ultrashort laser pulses, deflection of molecules in high Rydberg states, the study of alignment effects in dissociative ionization, and a theoretical study of nanolithography using a focused molecular beam.

2. Recent Progress

During the past year, most of our effort has been devoted to deflecting molecules in states having different rotational projection quantum numbers, M_J . The underlying principle is that the effective polarizability of a molecule depends on its alignment in the field.² For example, a molecule with $|M_J| = J$ rotates in a plane perpendicular to the field vector, so that E interacts with α_{\perp} , whereas for $M_J = 0$ the molecule rotates in a plane

containing E , and only α_H interacts with the field. This effect may be put on a quantitative basis by solving for the eigenvalues of $\mathcal{H}_{\text{rot}} + U(r, \theta)$, shown in Figure 1 for the HI molecule. The dipole force, which is proportional to the slopes of the curves in this figure, is seen to vary with $|M_J|$.

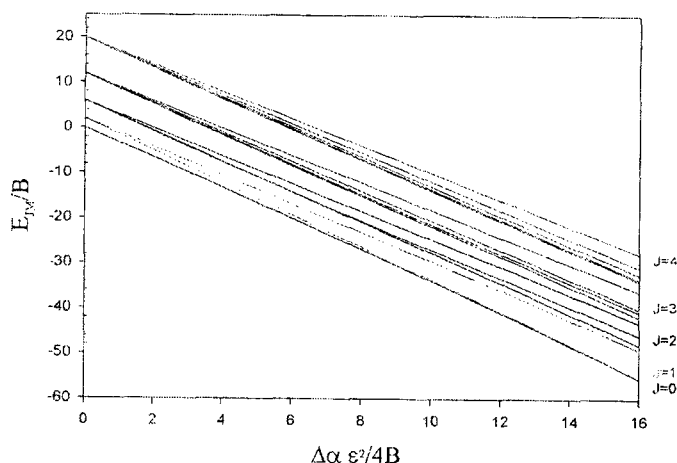


Figure 1. Eigenvalues of the rotational Hamiltonian in an electric field, scaled by the rotational constant, B . The various curves are for rotational quantum numbers $J = 0-4$ and $|M_J| = 0, \dots, J$.

The experiment is performed by focusing a Nd:YAG laser onto a molecular beam between the electrodes of a Wiley-McLaren time-of-flight mass spectrometer. Molecules in specific rotational states are detected by resonance-enhanced multiphoton ionization (REMPI), using a tunable dye laser. The parent ions are focused onto a microchannel plate at the end of the flight tube, and the ion image produced on a phosphor screen is captured by a CCD camera. The Nd:YAG laser creates the molecular lens that deflects molecules in different $|M_J|$ states, which should appear as a series of spots on the screen. The probe laser is scanned across the molecular lens, in order to locate the region of the lens that produces maximum deflection.

Preliminary results showing the deflection of CS_2 without state selection are displayed in Figure 2. The dipole force, which is calculated by taking the derivative of the Gaussian intensity profile along a Cartesian axis, produces the dispersion-like deflection curve shown in the figure.

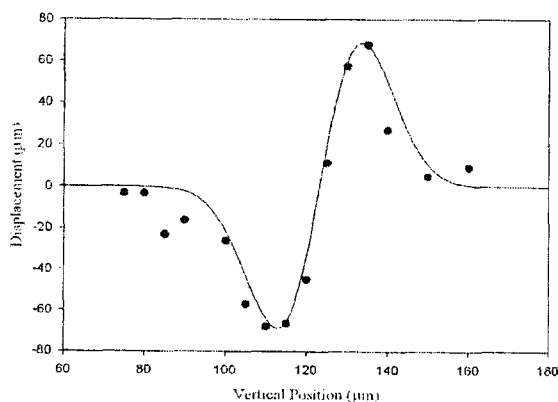


Figure 2. Deflection of CS_2 by a focused Nd:YAG (1064 nm) laser beam. Shown is the displacement of the CS_2^+ image as a function of the vertical position of the focused (358 nm) probe beam.

The magnitude of the deflection is proportional to $\Delta\alpha/m$, where m is the molecular mass. Acetylene is a molecule that has both a large $\Delta\alpha/m$ ratio and a rotationally resolved REMPI spectrum. Based on our preliminary results with CS_2 and HI, we estimate that the resolving power of our apparatus needs to be increased by a factor of ~ 6 in order to separate $J = 1, M_J = 0$ from $J = 1, |M_J| = 1$ of acetylene. To achieve this goal, we have designed a thick Einzel lens that should increase the flight-time (and hence the lateral displacement) of the ions by a factor of >20 .

A project that we completed this year is a study of alignment effects in multiphoton photodissociation. We previously observed unusual velocity-map images of the photofragments of iodobenzene and I_2 characterized by an "hourglass" shaped angular distribution and a continuous energy distribution peaked at zero kinetic energy. We interpreted these findings in terms of a dissociative ionization mechanism, in which a gateway state is initially populated, and competition between ionization and dissociation of a super-excited Rydberg state produces the characteristic recoil distribution. In the past year, we extended this study to ICl, using two colors to access the gateway and super-excited states independently. By varying the wavelengths, polarizations, and pulse times of the two lasers, we identified the gateway state and showed that the angular distribution is determined by the multiphoton dissociative step.

In a theoretical study, in collaboration with Tamar Seideman, we have shown that it is possible to focus a molecular beam onto a surface with a continuous laser beam. Previous work required that the laser beam be pulsed in order to achieve the requisite field strengths. Difficulties with this approach include the low duty cycle of the laser and the large background of molecules reaching the surface when the laser is off. We have shown that by using a grazing incidence configuration it is possible to reduce the required laser intensity by several orders of magnitude, thereby opening the possibility of using continuous beams of particles and photons.

3. Future Work

Once the deflection study is completed, we plan to resume two ongoing experiments that were postponed because they share key components (lasers and molecular beam) of the deflection apparatus. The first one is the alignment of molecules with picosecond laser pulses. The advantage of using short pulses is that the coherent wave packet of rotational states that is produced displays periodic revivals long after the pulse is over, allowing one to achieve field-free alignment.³ The amount of alignment that can be achieved is limited by the requirement that the aligning laser does not ionize the molecule. One possibility for increasing the alignment is to use a sequence of pulses spaced by the revival period of the wave packet. To a first approximation, the extent of alignment by N pulses of intensity P equals that of one pulse of intensity NP . The maximum alignment achievable by this strategy reaches a saturation limit. Averbukh⁴ has shown, however, that it is possible to exceed this limit by using a series of aperiodic pulses that "squeeze" the molecule. We plan to implement this method, using a spatial light modulator to create a pulse train from a stretched Ti:Sapphire laser pulse. We intend to use for this purpose a 2 mJ/pulse, 1 kHz, 50 fs laser, recently purchased with an

NSF/CRIF grant and scheduled for delivery in October, 2002. This experiment will be conducted using the existing molecular beam imaging apparatus.

A second ongoing experiment is the deflection of molecules in high Rydberg states. The idea behind this experiment is that the polarizability varies strongly with the principle quantum number, n , and that at large n it becomes negative. In this regime, the focused laser field acts as a molecular mirror. We have prepared molecules in high Rydberg states, using a different molecular beam apparatus. Our plan is to measure the ionization threshold of such molecules induced by the ponderomotive force of the deflection laser. We will then proceed to measure the sign and magnitude of the deflection produced by the laser field.

4. Publications in 2000-2002

A. Sugita, M. Mashino, M. Kawasaki, Y. Matsumi, R. J. Gordon, and R. Bersohn, "Control of Photofragment Velocity Anisotropy by Optical Alignment of CH_3I ," *J. Chem. Phys.* **112**, 2164 (2000).

S. Unny, Y. Du, L. Zhu, K. Truhins, R. J. Gordon, A. Sugita, M. Kawasaki, Y. Matsumi, R. Delmdahl D. H. Parker, and A. Berces, "Above-Threshold Effects in the Photodissociation and Photoionization of Iodobenzene," *J. Phys. Chem. A* **105**, 2270 (2001).

R. J. Gordon, L. Zhu, S. Unny, Y. Du, K. Truhins, A. Sugita, M. Mashino, M. Kawasaki, and Y. Matsumi, "Photofragment Imaging Studies of Aligned Molecules," *Imaging Chemical Dynamics*, A. G. Suits and R. E. Continetti, eds, (ACS, Washington, DC, 2000) pp 87-112.

S. Unny, Y. Du, L. Zhu, R. J. Gordon, A. Sugita, M. Kawasaki, Y. Matsumi, and T. Seideman, "Above-Threshold Dissociative Ionization in the Intermediate Intensity Regime," *Phys. Rev. Lett.* **86**, 2245 (2001).

H. Yamada, N. Taniguchi, M. Kawasaki, Y. Matsumi, and R. J. Gordon, "Dissociative Ionization of ICl Studied by Ion Imaging Spectroscopy," *J. Chem. Phys.* **117**, 1130 (2002).

¹ B. Friedrich and D. Herschbach, *J. Phys. Chem.* **99**, 15686 (1995).

² T. Seideman, *J. Chem. Phys.* **107**, 10420 (1997).

³ T. Seideman, *Phys. Rev. Lett.* **83**, 4971 (1999).

⁴ I. Sh. Averbukh, R. Arvieu, and M. Leibscher, *Phys. Rev. Lett.* **87**, 163601 (2002).

X-ray scattering by atoms and molecules dressed with femto-second laser fields.

Ali Belkacem

Chemical Sciences Division
Lawrence Berkeley National Laboratory

Multiphoton processes driven by combined synchrotron (x-ray) and laser (optical) radiation provide a basis for novel scientific directions. From a fundamental perspective, synchrotron x-rays can probe unique states of matter formed while a gaseous or solid target is exposed to intense electromagnetic (laser) radiation. An atom is a multielectron system that responds as a whole when perturbed by a strong laser field. The modifications to the atomic structure by the femto-second laser (acting on the outer electrons only) can indirectly extend to inner-shells through electron correlation. In particular the presence of the laser during relaxation of an atom with an inner-shell hole will modify the autoionization of the upper states as well as the post-collision interactions (e.g. between photo- and Auger electrons) changing the end products. In addition to its importance from the fundamental perspective, gaining knowledge on the relaxation of atoms and small molecules in high femto-second fields is an important stepping stone to understanding the process by which, more complex molecules that are x-ray excited come apart in such fields. This situation is likely to occur at experiments planned for fourth generation light sources.

Synchrotron x-rays address primarily core levels and probe the modifications these levels undergo when the atom is immersed in an intense femto-second field. One distinguishes two very important aspects in these studies. a) Synchrotron x-rays are used as a probe of the structure of the laser dressed atom or molecule and the time evolution of the laser-excited system. b) The interaction of x-rays with inner-shell electrons as well as the relaxation of the "x-ray-excited or ionized" atom both are modified by the presence of the high intensity laser field.

The focus, for this fiscal year, is on point b and our ongoing and planned experiments is to study the time evolution of post-collision interactions using the ALS x-ray pulse as a pump (creation of K-vacancy) and the intense laser pulse as a probe.

Using the synchronization techniques we learned from dense matter experiments we set up a gas phase experiment in beam line 5.3.1 to study the charge state distribution of argon when a K-shell electron is removed by a synchrotron radiation x-ray. We built and installed a very efficient time-of-flight and target system that can accommodate high gas densities. Measurements of the "laser-off" charge state distribution show very clear post-collision interaction effects on the charge state distribution of Ar ions when the x-ray

energy is tuned through the K-edge. Our “laser-off” results are in very good agreement with similar measurements found in the literature.

We measured argon charge state distribution with “laser-on”, where the laser is overlapped in time (100 ps) and space ($< 100 \mu\text{m}$) with the camshaft pulse of the ALS x-ray pulse-train. We found a unexpected time dependence, in the nanosecond time scale, of the electron yield. This electron yield is correlated with the production of high charge-state argon ions. One possible interpretation is that the relaxation of the Ar K-vacancy results in a number of excited metastable (tens of nanosecond time scale) low charge state ions, with several electrons in the excited state. The short laser pulse interacts very efficiently with this highly excited system accelerating its further ionization. These preliminary data are currently being analyzed and more experimental work is planned for this fiscal year.

These first successful experimental runs on beamline 5.3.1 using a combination of 100 psec laser and 30 psec x-ray pulses show that we are able to overcome several problems associated with the mismatch of the kilo-Hz laser and half giga-Hz ALS repetition rates. Since we needed a high gas densities to have a reasonable data rate we used differential pumping techniques to keep the microchannel plate detectors under high vacuum while the density of the Ar gas is varied from a fraction of a mTorr to a few Torr.

Quantum trajectory Monte Carlo method describing the production and destruction of coherences

C.O. Reinhold*

Oak Ridge National Laboratory

The internal electronic state of a fast atom (or ion) traversing solids is an example of an open quantum system in contact with a "large reservoir". The large number of degrees of freedom of the environment refers here to the electronic and nuclear degrees of freedom of the solid. Moreover, for highly charged ions the coupling to the vacuum fluctuations of the radiation field becomes comparable to the coupling to the particles in the solid. Therefore, the reservoir of the open quantum system should include both the radiation field and the degrees of freedom of the solid. We study this problem as a prototype of open quantum systems. One of our ultimate goals is to be able to simulate the decoherence of "open" excited states of atoms as exactly as possible.

We have studied the dynamics of hydrogenic one-electron ions traversing amorphous carbon foils, for which accurate experimental data have recently become available [1]. We have derived from first principles a general theoretical framework describing the evolution of the internal state of the ion. We employ an open quantum system approach [2-3] that incorporates the complex array of collisions with electrons and ionic cores. Interactions with the solid environment and the radiation field are treated on the same footing and the quantum master equation for the reduced density matrix of the electronic state of the ion is approximated by a Lindblad equation. The latter allows the solution of this multi-state problem in terms of Monte Carlo sampling of quantum trajectories whose dynamics is governed by a stochastic non-linear Schrodinger equation [3]. Our approach provides an extension to methods used in quantum optics and models previously employed in ion-solid interactions. Our focus is on the transient build-up and destruction of coherences by stochastic processes. One main development is that we go beyond the standard secular approximation and provide a Monte Carlo method that gives good account for the short time evolution of the coherences of the system. We apply our method to the study of coherence properties of the internal state of a fast Kr^{35+} ion traversing carbon foils. Simulations exhibit clear signatures of partially coherent transitions and are found to be in good agreement with experimental data.

* In collaboration with T. Minami and J. Burgdorfer

- [1] T. Minami, C.O. Reinhold, M. Seliger, J. Burgdorfer, C. Fourment, B. Gervais, E. Lamour, J-P. Rozet, and D. Vernhet, *Phys. Rev. A* 65, 032905 (2002).
- [2] C. Cohen-Tannoudji, J. Dupont-Roc, and G. Grynberg, *Atom-Photon Interactions*, (Wiley Interscience, 1992)
- [3] C.W. Gardiner and P. Zoller, *Quantum Noise* (Springer, 1999).

D.O.E. grant DE-FG 03-00ER15084

Development and utilization of bright tabletop sources of coherent soft x-ray radiation

Principal Investigators:

Jorge J. Rocca,

Electrical and Computer Engineering Department, Colorado State University, Fort Collins, CO 80523-1373

Telephone: (970)-491- 8514/8371, Fax: 970 (491) – 8671, e-mail: rocca@enr.colostate.edu

Henry C. Kapteyn

JILA/Physics Department, University of Colorado, Boulder, CO 80309-0440

Telephone (303) 492-8198, Fax:(303) 492-5235 , e-mail: kapteyn@jila.colorado.edu

Carmen S. Menoni

Electrical and Computer Engineering Department, Colorado State University, Fort Collins, CO 80523-1373

Telephone: (970)-491- 8659, Fax: 970 (491) – 8671, e-mail: carmen@enr.colostate.edu

Program Description

Compact capillary discharge lasers and high order harmonic up conversion of ultrashort pulse lasers can both produce very high brightness beams of coherent soft x-ray radiation [1,2]. These sources are very compact, yet can generate soft x-ray radiation with peak spectral brightness several orders of magnitude larger than synchrotrons. These characteristics, coupled with an excellent spatial coherence, make possible new applications. Recent demonstrations include time-resolved surface spectroscopy [3], material characterization [4], material ablation [5], characterization of soft x-ray optics [6] and plasma interferometry [7]. This project investigates aspects of the development of these compact XUV sources, including the characterization of some the important parameters that enable their use in unique applications, such as the degree of spatial coherence and the wavefront characteristics that affect their focusing capabilities. In relation to source development we are investigating the amplification of high order harmonic pulses in a discharge pumped soft x-ray amplifier. This work is motivated by the possibility of obtaining pulses that combine some of the advantages of these two types of sources in terms of pulse energy and duration, and also with the opportunity to investigate aspects of seeded amplification in the soft x-ray regime. Results to date include the demonstration of an ultra-compact discharge pumped 46.9 nm amplifier that can be operated either in the seeded or unseeded modes. In term of source characterization we have completed measurements that show that the output of these sources can reach essentially full spatial coherence [8,10]. We have also recently fully characterized the beam of a discharge-pumped tabletop soft x-ray laser in term of amplitude and phase utilizing a novel soft x-ray Shack-Hartmann soft x-ray wavefront sensor [11].

Demonstration of an ultra-compact desk-top 46.9 nm discharge-pumped amplifier for high order harmonic amplification and other applications.

A new ultra-compact capillary discharge Ne-like Ar amplifier capable to amplify high order harmonic pulses was designed and constructed. It is designed to allow the free propagation of high order harmonic pulses along the axis for seeded operation. The amplifier provides a gain of approximately e^{10} at 46.875 nm using a 10 cm long plasma column. An increase of the plasma column length to 20 cm produces saturation of the amplified spontaneous emission, generating an intense laser beam on its own. In this unseeded mode the laser produces pulses of up to 10 mJ of energy and ~ 1.2 ns duration. This soft x-ray laser amplifier has a dimension of about $40 \times 40 \times 15$ cm³ and can easily fit on top of a very small desk (Fig. 1a). It is to our knowledge the most compact source of coherent soft x-ray radiation presently available. Figure 2b shows the temporal evolution of the laser pulse measured with a vacuum photodiode. The laser beam was attenuated to avoid saturation of the photodiode. The intensity of the laser pulse is observed to completely dominate the spectrally integrated spontaneous emission of hundreds of lines emitted by the hot dense plasma column. Fig 1c shows a corresponding spectrum that illustrates the monochromaticity of the source. The observed linewidth is limited by the instrumentation, which can not resolved the estimated linewidth of $\Delta\lambda/\lambda \sim 5 \cdot 10^{-5}$. For all the tests reported herein the laser amplifier was operated at repetition rates of 0.5 to 1 Hz, but operation at higher repetition rates should be possible.

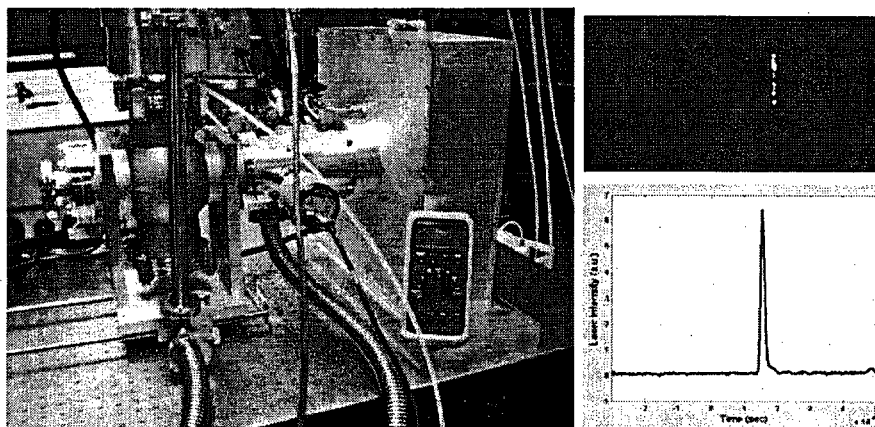


Fig 1. a) Photograph illustrating the size of saturated desk-top Ne-like Ar laser compared with a hand-held multimeter. b) Axial spectra of the capillary discharge plasma in which only the amplified laser line is observed. c) Temporal characteristics of the 46.9nm laser pulse

Applications experiments of this discharge-pumped amplifier, such as the amplification of high order harmonic pulses, requires a precise synchronization. To achieve necessary the low discharge jitter we have developed a high voltage spark gap that is triggered by a femtosecond laser pulse of a few hundred microjoules of energy. Such trigger pulse can be extracted from the same Ti:sapphire laser amplifier that is used to create the high order harmonic seed pulses. We have developed a spark-gap switch with a shot-to-shot time delay statistical of $\sigma = 0.1\text{ns}$ for voltages of 10 KV [12]. At the high power levels required to pump the capillary discharge amplifier the jitter is higher, however sub-nanosecond jitter of the laser amplifier has been demonstrated under optimized conditions.

Full characterization of the Electromagnetic Field Distribution in a Soft X-Ray Laser Beam

These compact tabletop coherent soft x-ray sources make possible a large number of applications in several disciplines, using techniques such as interferometry, holography, and microscopy. However, many of these applications require accurate characterization of the coherent wavefront. With this objective in mind, a wavefront sensor for the soft X-ray wavelength range was developed and used to fully characterize the electromagnetic field distribution in a soft x-ray laser beam [11]. The sensor is based on the Shack-Hartmann concept and is composed of a 20×20 array of diffraction Fresnel lenses etched on a reflective multilayer mirror. This design avoids optical aberrations and overcomes the limitations imposed by the strong absorption of all materials in this spectral range. Using this instrument, the wavefront of a neonlike Ar soft x-ray laser ($\lambda=46.9\text{ nm}$) [2] was fully characterized in a single shot with an estimated resolution of $\lambda/100$. Figure 2 shows the experimental set up used in the measurements. The wavefront characteristics were observed to be dependent on the discharge pressure and on the capillary length, as a result of beam refraction variations in the capillary plasma. The results show a dramatic improvement of the soft X-ray laser beam wavefront with increased capillary plasma column length, leading to an improvement of the focal spot. Figure 3 illustrates the results obtained operating the discharge-pumped at a pressure of 420 mTorr, near the optimum for maximum amplification. The measurements show that for a 34 cm capillary about 70 percent of the SXRL beam energy could be focused into an area about four times the size of the diffraction-limited spot, reaching intensities of $\sim 4 \times 10^{13}\text{ W/cm}^2$. The achievement of such high intensity in the soft X-ray wavelength range with a table-top device opens the possibility of new applications.

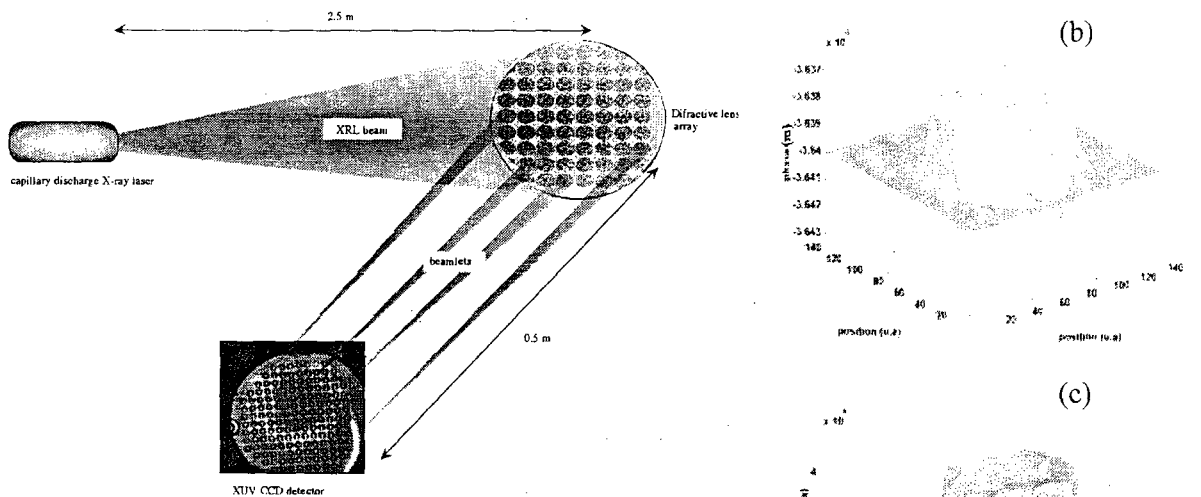


Fig.2: (a) Schematic representation of the experimental set used to measure the wavefront of a 46.9 nm capillary discharge soft x-ray laser showing the lens array and a measured image of focal spots. Measured wavefront shape (b), and corresponding intensity distribution (c) for an the laser beam produced operating the discharge at a an Argon pressure of 420 mTorr. The radius of curvature of the wavefront is 6.5 meters. The annular shape of the beam a is due to the refraction the laser beam in the plasma column. (Phys. Rev. Lett. **88**, 192001 (2002))

Progress towards the amplification of high order harmonic pulses in a discharge pumped soft x-ray amplifier

Seeding of a discharge-pumped amplifier with high harmonic (HH) pulses could produce soft x-ray pulses with energy several orders of magnitude larger than the HH seed pulse, and with pulse width more than two orders of magnitude shorter than those of the unseeded discharge-pumped amplifier. Moreover, such experiment provides a test-bed for the technical development and understanding necessary to seed soft x-ray amplifiers. The results obtained could impact the seeding of proposed x-ray free-electron laser amplifiers. To conduct this experiment we have development the compact discharge-pumped amplifier described above that has an open-end structure to allow the injection and extraction of the HH pulses, and have optimized the generation of HH pulses at 46.9 nm utilizing phase-matching and pulse-shaping techniques.

We are presently working to obtain temporal and spatial overlap of the HH pulses with the gain pulse in the discharge amplifier, in order to demonstrate seeded amplification. Figure 3 shows the harmonic amplification experimental set up. The high order harmonic pulse is generated using phase-matched frequency conversion in a gas cell. This setup uses a laser generating 20 mJ pulses at 10 Hz repetition rate. Optimum conversion of light into the 17th harmonic of 800 nm, corresponding to 47 nm, requires a large-area (i.e. long focal length) focus into a low-pressure xenon or krypton gas cell. This setup has been implemented, and harmonic generation into the 17th harmonic has been verified using a small spectrometer. Presently, estimates of flux at this photon energy are being done to verify recent results from other groups measuring microjoule pulse energy using similar configurations.[9] In parallel, we are setting-up a high-resolution spectrometer that will make it possible to spectrally resolve the high harmonic emission. This will allow us to optimize the HHG for the 46.9 nm wavelength of the discharge.

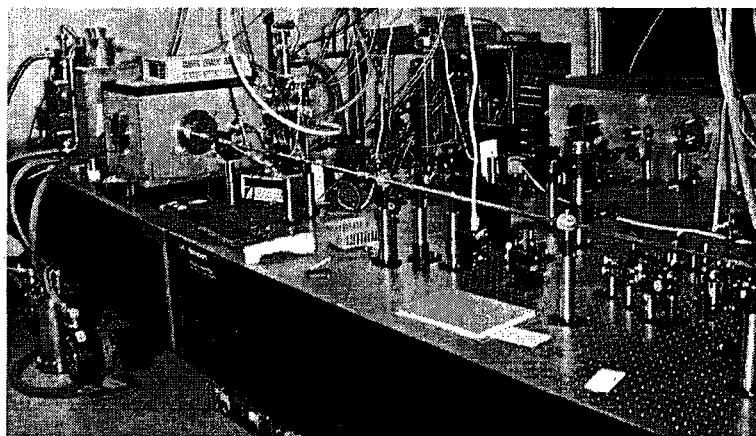


Fig. 3: Set up for the amplification of high order harmonic pulses.

References

1. C.D. Macchietto, B.R. Benware, J.J. Rocca, "Generation of millijoule-level soft-x-ray laser pulses at a 4-Hz repetition rate in a highly saturated tabletop capillary discharge amplifier", *Opt. Lett.* **24**, p. 1115-1118, (1999).
2. A. Rundquist, C. Durfee, S. Backus, C. Herne, Z. Chang, M. Murnane, H. Kapteyn, "Phase-Matched generation of Coherent Soft-X-Rays", *Science*, **280** (5368) p. 1412 – 1415 (1998).
3. M. Bauer, C. Lei, K. Read, R. Tobey, J. Gland, M. M. Murnane, and H. C. Kapteyn, "Direct observation of surface chemistry using ultrafast soft-x-ray pulses," *Phys. Rev. Lett.* vol. 8702, pp. 5501-U59, 2001.
4. I.A. Artioukov, B.R. Benware, J.J. Rocca, M. Forsythe, Yu. A. Uspenskii, and A.V. Vinogradov, "Determination of XUV Optical Constants by Reflectometry Using a High-Repetition Rate 46.9nm Laser", *IEEE J. Quan. Elec.* vol. 5, 1495-1501, (1999).
5. B.R. Benware, A. Ozols, J.J. Rocca, I.A. Artioukov, V.V. Kondratenko and A.V. Vinogradov, "Focusing of a soft x-ray laser beam and laser ablation", *Opt.Lett.* **24**, 1714, (1999).
6. B.R. Benware, M. Seminario, A.L. Lecher, J.J. Rocca, Yu A. Unspenskii, A.V. Vinogradov, V.V. Kondratenko, Yu P. Pershing, and B. Bach, "Generation and applications of a high average power polarized soft x-ray laser beam", *J.of the Optical Soc. of America*, **18**, 1041-1045 (2001).
7. J. Filevich, K. Kanizay, M.C. Marconi, J.L.A. Chilla and J.J. Rocca, "Dense plasma diagnostics with an amplitude division laser interferometer based on diffraction gratings", *Optics Lett.* **25**, 356, (2000).
8. R. A. Bartels, A. Paul, H. Green, H. C. Kapteyn, M. M. Murnane, S. Backus, I. P. Christov, Y. W. Liu, D. Attwood, and C. Jacobsen, "Generation of spatially coherent light at extreme ultraviolet wavelengths," *Science*, vol. 297, pp. 376-378, 2002.
9. K. Midorikawa, presented at the 8th International Conference on X-ray Lasers, Aspen, CO May 2002.

Publications

10. Y. Liu, M. Seminario, F. G. Tomasel, C. Chang, J. J. Rocca and D. T. Attwood, "Achievement of Essentially Full Spatial Coherence in a High Average Power Soft X-Ray Laser," *Phys. Rev. A*, 63 033802, (2001).
11. S. Le Pape, Ph. Zeitoun, M. Idir, P. Dhez, J.J. Rocca, and M. François, "Electromagnetic field distribution measurements in the soft x-ray range: full characterization of a soft x-ray laser beam", *Phys. Rev. Lett.* **88**, 183901 (2002).
12. B. Luther, L. Furfaro, A. Klix and J.J. Rocca, "Femtosecond laser triggering of a sub-100 picosecond jitter high voltage spark gap", *Appl. Phys. Lett.*, **79**, 3248-3250 (2001)

**Ultrafast Coherent Soft X-rays:
A Novel Tool for Spectroscopy of Collective Behavior in Complex Materials**

Keith A. Nelson
Department of Chemistry
Massachusetts Institute of Technology
Cambridge, MA 02139
Email: kanelson@mit.edu

Henry C. Kapteyn
JILA
University of Colorado and National Institutes of Technology
Boulder, CO 80309
E-mail: kapteyn@jila.colorado.edu

Margaret M. Murnane
JILA
University of Colorado and National Institutes of Technology
Boulder, CO 80309
E-mail: murnane@jila.colorado.edu

Program Scope

In this project, nonlinear time-resolved spectroscopy of condensed matter with coherent soft x-rays is being attempted. The primary experimental objective is to obtain direct access to both femtosecond time resolution and mesoscopic length scale resolution. The length scale is defined through transient grating, or time-resolved four-wave mixing, measurements in which the grating spacing is on the order of the soft x-ray wavelength. The primary scientific objective is to measure both the correlation length scale and the correlation time scale, and to determine whether there is any direct association between them, for collective responses including structural relaxation in polymers, supercooled liquids, and other complex materials. A broader objective is to enable nonlinear time-resolved x-ray spectroscopy of condensed matter generally, including investigation of electronic as well as structural evolution on short length and time scales.

Femtosecond pulses at soft x-ray wavelengths are produced through high harmonic generation. [1] It is now possible to reach nanojoule energies in such pulses, sufficient for nonlinear time-resolved spectroscopy of condensed matter. Given the high spatial coherence and focusability of the output, intensity levels comparable to those typically used in condensed-matter femtosecond spectroscopy with visible pulses can be reached. Thus there is strong reason to hope for successful extension of spectroscopic methods now widely used in visible and nearby wavelengths to the soft x-ray regime.

In current time-resolved measurements of condensed-matter collective dynamics, the relevant time scales may be measured but the relevant length scales are rarely determined and often are not well understood. For example, structural relaxation in simple molecular liquids occurs in femtosecond/picosecond time scales and is only weakly temperature-dependent. In supercooled liquids, the responses are often highly nonexponential, extending over a wide range

(several decades) of time scales even at a simple temperature and changing enormously (i.e. by many decades) as the temperature is cooled and the viscosity increases. [2] A great many materials including synthetic polymers and biopolymers, molecular and ionic liquids, and some aqueous solutions show this behavior. In the case of polymers, it is tempting to associate time scales with length scales, i.e. to imagine that the faster components of structural relaxation correspond to the motions of end groups, somewhat slower components to small side chain motions, still slower components to polymer backbone rearrangements, and the slowest components to relative motions of whole polymer molecules. However, supercooled polymer and small-molecule or ionic liquids show very similar temperature-dependent dynamics, and in the latter cases there is no obvious hierarchy of length scales based on structural elements like those of polymers. How are we to understand the observed hierarchy of time scales? Current time-resolved measurements cannot resolve this issue since essentially all the important correlation lengths are far smaller than any length scale that is defined experimentally. In this respect the situation is similar to ultrafast measurements of molecules, but in the case of molecules we have extensive independent information about bond lengths and molecular potentials to guide our understanding of the dynamical responses observed. In the case of collective dynamics, we usually do not have such guidance concerning correlation length scales. Thus we do not know whether small or large groups of constituents are involved in different components of structural relaxation, or whether there is any consistent or systematic connection between length and time scales.

In transient grating measurements, the grating fringe spacing defines the length scale over which correlated dynamics are measured. [3] In familiar cases, the fringe spacing is used to define an acoustic wavelength or the length scale over which thermal or mass diffusion is measured. In such cases the observed dynamics can be associated directly with the experimentally defined length scale. This is the basis for transient grating study of a wide range of phenomena including thermal, compositional, collective vibrational and electronic dynamics. However, structural relaxation dynamics are associated with density or molecular orientational correlation lengths or polymer persistence lengths that generally extend over nanometers, not microns. Direct measurement of the length and time scales is still possible through transient grating experiments, but the light wavelength must be sufficiently short that fringe spacings on the order of the correlation lengths can be produced. This requires soft x-ray wavelengths, i.e. wavelengths on the order of tens of nanometers or shorter.

In our experiments, two coherent soft x-ray pulses produced through high harmonic generation are crossed to excite the sample in a grating pattern with nanometer fringe spacing. The sample response is monitored through diffraction of probe x-ray pulses that are incident at the phase-matching angle for diffraction off the induced grating pattern. The excitation pulses may induce both permanent and transient samples responses, and both may be observed. Of primary interest in our measurements is heating of the sample at the transient grating maxima, which will lead to thermal expansion and acoustic wave generation. The time-dependent diffraction intensity is expected to show acoustic oscillations and thermal diffusion, in both cases associated with the grating spacing. From the acoustic responses, measured as functions of temperature and grating spacing (i.e. acoustic wavelength or wavevector), complex structural relaxation dynamics can be determined. The measurements should extend those made with visible wavelengths, yielding acoustic responses throughout much of the Brillouin zone. In particular, acoustic responses at wavelengths ranging from about 50 nm to 500 microns, corresponding to acoustic frequencies in roughly the 10 MHz – 100 GHz frequency range, will

be characterized. The results, along with complementary optical measurements of slower structural relaxation dynamics, will yield relaxation dynamics in the 10 ps – 1 ms range. This is sufficient for description of complex structural relaxation dynamics at most temperatures significantly above the liquid-glass transition temperature. Crucially, the correlation length scales can also be determined in the soft x-ray measurements. Association of these with relaxation time scales will be examined in detail.

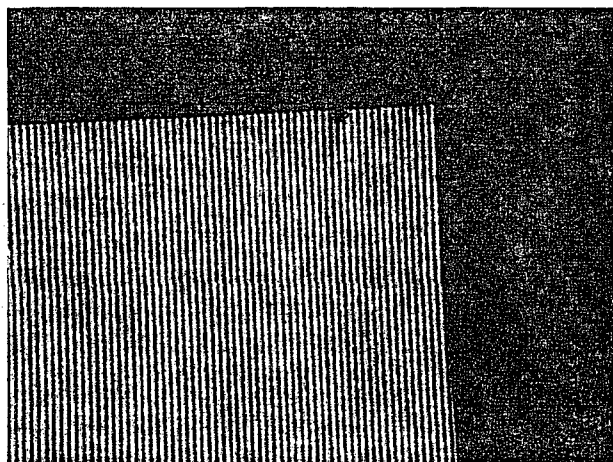
Measurements are under way using timed sequences of visible light pulses to excite acoustic waves in strongly absorbing metal films, which are then used as transducers to launch the acoustic waves into adjacent liquid samples. The acoustic waves may be observed optically after passing through the liquid. These measurements are only possible when the acoustic damping rate is sufficiently low to permit acoustic propagation through a macroscopic volume of liquid. The damping rate increases sharply (roughly quadratically) as a function of acoustic frequency, so these measurements are expected to provide access to a lower acoustic frequency range than that accessible to the coherent soft x-rays measurements. The combination of these measurements and transient grating measurements with visible and x-ray pulses will yield acoustic responses throughout most of the Brillouin zone without gaps in the frequency ranges covered.

Recent Progress

In the initial stages of the project, mask patterns for soft x-ray photolithography were fabricated by the group of Prof. H.I. Smith of the MIT Dept. of EECS. These are designed for diffraction-based generation of transient gratings with 50-nm fringe spacings. These are free-standing SiN gratings that are 4 mm x 4 mm in size, with a fringe spacing of only 100 nm. This means that there are 40,000 lines at that spacing, with spatial coherence maintained throughout the entire grating. An interferometer that permits mounting and precise alignment of two grating patterns has been also been constructed for diffraction of an incident soft x-ray pulse into two orders which are then recombined through diffraction to meet at the sample. These play the role of the transient grating excitation pulses. The final stages of grating mounting and alignment in the interferometer are currently under way. The probe pulse may be incident on the same interferometric setup to generate variably delayed probe and reference pulses, the latter used for heterodyne detection of diffracted signals.

In preliminary soft x-ray experiments, a single 100-nm grating fabricated as described above was placed directly above a PMMA sample and irradiated with high harmonic output at 30 nm wavelength (41 eV photon energy). This resulted in a "shadow" masking effect, producing a spatially varying pattern of illumination at the sample with the same 100-nm period. Irradiation resulted in photolithographic etching of permanent patterns in the PMMA sample, at a rate that was in excellent agreement with estimates of the necessary flux. This is an important result in several respects. First, it shows that pulsed irradiation of 100-nm grating patterns is possible in a simple manner. Second, it demonstrates a simple method for soft x-ray lithography that may have practical importance. Third, it indicates promise for our next set of experiments in which pulsed excitation will be used to generate a transient, high-frequency acoustic response that will be monitored with variably delayed soft x-ray pulses.

Figure 1: Exposure of PMMA when a grating placed above the PMMA was irradiated with high harmonic output at 30 nm wavelength (41 eV photon energy). This is an example of EUV lithography with high harmonic radiation



Other efforts are under way to generate the two excitation pulses through two separate fiber-optic high-harmonic generation systems. In this case the two outputs will be directed to meet at the sample, at which grating formation will take place. This arrangement offers higher total intensity, but may prove less robust since the interference pattern may be more susceptible to fluctuations. Initial experiments that confirm that the soft-x-ray beams can be focused to intensities sufficient to excite the sample have been carried out.

Measurements of lower-frequency acoustic responses using femtosecond optical pulses and pulse sequences have begun. Using single optical excitation pulses, broadband acoustic wavepackets with frequency components up to 20 GHz have been detected after passage through liquid samples. Using pulse sequences to concentrate the acoustic energy in narrowband waves of selected frequency, somewhat higher frequencies should prove detectable.

Future Plans

Transient grating measurements with soft x-ray wavelengths are currently being attempted. Demonstration and optimization of the experimental method are the first objectives. Key issues are successful generation of transient grating signals, determination of the responses of interest, and elucidation and understanding of any competing signals. Simple samples will be examined at first for the purpose of methodology development. Following this stage, systematic study of supercooled liquid structural relaxation dynamics will follow. In parallel with this effort, measurements with optical pulse sequences will permit characterization of acoustic responses at lower frequencies, completing our access to essentially all wave vectors at which acoustic waves propagate in the liquid state.

References

1. "Phase-Matched Generation of Coherent Soft-X-Rays," A. Rundquist, C. Durfee, Z. Chang, S. Backus, C. Herne, M. M. Murnane and H. C. Kapteyn, *Science* **280**, 1412 – 1415 (1998).
2. See e.g. *Supercooled liquids: Advances and novel applications*, ACS Symp. Ser. **676**, J. T. Fourkas D. Kivelson, U. Mohanty and K. A. Nelson, eds. (Amer. Chem. Soc., Washington, D.C. 1997).
3. "Testing of Mode-coupling Theory Through Impulsive Stimulated Thermal Scattering", by I.C. Halalay, Y. Yang, and K.A. Nelson, *Transport Theory and Stat. Phys.* **24**, 1053-1073 (1995).

A quantum-mechanically complete experiment on photo-double ionization of helium

B. Krässig

Argonne National Laboratory, Argonne, IL 60439

kraessig@anl.gov

The breakup of the helium atom during photo-double ionization is the classic case of a three-body Coulomb problem. The most detailed information on this process is obtained from measurements of the cross section that is differential in the electron emission angles and in the energy sharing between the electrons. It has been shown that the functional form of this differential cross section depends on just two complex correlation functions that are functions of the energy sharing and the mutual angle between the outgoing electrons. The fact that these functions enter coherently into all observables of this process has so far hampered their direct experimental determination. In this work a method will be presented with which the correlation functions and their relative complex phase can be obtained directly from experiment, without making any assumptions on the functional form of the correlation functions. The method has been applied to the event mode data set of a COLTRIMS experiment at 99 eV photon energy in which the momentum components of the ionization fragments were recorded with 4π angular acceptance.

Site-Specific Target Orientation Dependence of Charge Fractions Observed for F^{q+} Ions Backscattered from a (100) surface of RbI

H.F. Krause, F.W. Meyer and C.R. Vane

*Physics Division, Oak Ridge National Laboratory
P.O. Box 2008, Oak Ridge, TN 37831-6372*

Beam-surface investigations at the ORNL MIRF focus on the fundamental physics describing the interaction of slow, highly-charged ions with metal, semiconductor and insulator surfaces[1]. In the past, experimental and theoretical studies of insulator surfaces (e.g., ionic crystals) have concentrated primarily on grazing surface collisions where the projectile approaches the surface very slowly over a long interaction length. Surface studies involving a backscattering technique [2], where the approaching ion interacts essentially with one atom in the incident trajectory but leaves along a grazing trajectory, provides different information. Now we have applied this technique to study interactions of F^{q+} with RbI, where the exit ions analyzed are scattered at the fixed angle of 120 degrees from the incident beam direction.

When an incident F^{q+} ion is scattered 120 degrees in elastic binary collisions from a RbI surface, the product ion energy, E_r , depends on whether it scattered from a Rb or an I atom and the kinetic energies can be experimentally resolved (e.g., $E_r/E_0 = 0.507$ and 0.636 for Rb and I, respectively, where E_0 is the incident beam energy). If recoil ions pass through a long electrically biased time-of-flight region, then the final charge states and neutrals are separated in time, and the Rb and I binary peaks within each charge state can be resolved (site specificity). The experimental ratio of these binary peaks indicates the relative efficiency for the production of each final charge state. Interesting possibilities arise when an ionic crystal such as RbI is studied.

RbI has a diatomic cubic structure (rock salt) of alternating atoms ABAB on each side of the unit cell (e.g., a $\langle 100 \rangle$ direction, 0.366 nm atomic spacing). In a $\langle 110 \rangle$ direction, there are alternating parallel rows AAAA and BBBB (0.517 nm atomic spacing). When the crystal is rotated so that a $\langle 100 \rangle$ direction is aligned to the scattering plane, the projectile's interaction with an atomic string of alternating atoms is sampled, and whether it initially hit atom A or B can be experimentally measured. Similarly, interaction with a string of either AAAA or BBBB is sampled when a $\langle 110 \rangle$ direction is selected to lie in the scattering plane. Moreover, interaction with widely spaced A_B_A_B atomic strings (0.818 nm spacing) can be measured when a $\langle 210 \rangle$ direction lies in the scattering plane.

We have performed experiments at the ORNL MIRF using F^{q+} ions ($q=1, 2, 6, \text{ and } 7$) in the 2-10 keV regime at a variety of incident polar and azimuthal angles; product cation, anion and neutral species were observed. Results demonstrate that i) the final charge state distribution and ii) the ratio of binary hits associated with Rb and I change when the ion approach direction is changed from $\langle 100 \rangle$ to $\langle 110 \rangle$ (see Fig. 1). Differences between the $\langle 100 \rangle$ and $\langle 210 \rangle$ are also observed. Effects observed for both cation and anion products are particularly dramatic when the incident ion enters about 20 degrees from normal incidence and leaves along a grazing exit trajectory (10 degrees above the surface plane). With the possible exception of an extreme grazing exit trajectory, most of the observed effects are probably controlled by the binary collision species and its nearest neighbor in the exit direction. The relative production efficiency associated with these "quasi-binary" collisions with Rb and I atoms (i.e., a "hard" binary loss collision followed by a soft grazing collision of very small energy loss) vs the crystallographic direction is being analyzed and these results will be discussed. Trajectory simulations using the MARLOWE code [3] will be used to interpret the experimental results.

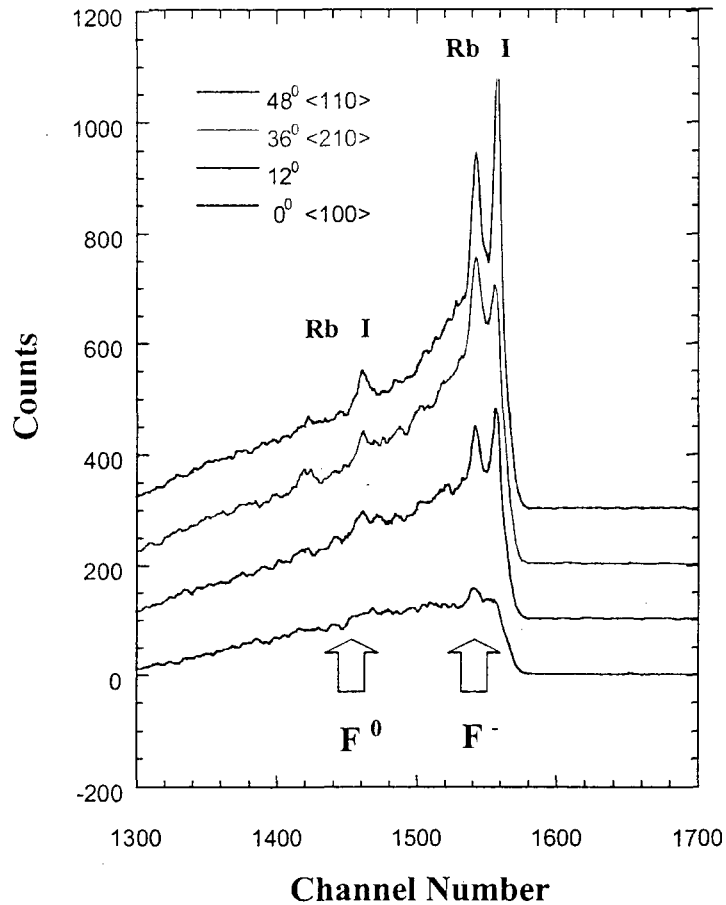


Fig. 1. Azimuthal dependence for 4.2 keV F^+ ions backscattered from a (100) surface of RbI. The incident beam direction is tilted 20° from the surface normal. Only the F and F^- products are shown; the F^+ product channel will be discussed. The prominent peaks to the right correspond to the Rb and I binary peaks for F^- , respectively. The binary intensity ratio, Rb/I, depends on the crystallographic direction.

- [1] F.W. Meyer et al., see other program abstracts of this conference.
- [2] V.A. Morozov and F.W. Meyer, Rev. Sci. Instr. **70**, 4515 (1999); Phys. Rev. Lett. **86**,736 (2001).
- [3] M.T. Robinson, Radiat. Eff. Defect. Solid. **130**, 3 (1994); Phys. Rev. **B40**, 10717 (1989).

Theory of fragmentation and rearrangement processes in ion-atom collisions

J. H. Macek

*Department of Physics and Astronomy,
University of Tennessee, Knoxville, Tennessee and
Oak Ridge National Laboratory, Oak Ridge, Tennessee
email:jmacek@utk.edu*

1 Program scope

The interactions of bare charged particles with one-electron atoms are prototypes for atomic collision processes generally. At the present time, computer simulation of processes involving only two-body channels, *e. g.* excitation and particle transfer, have reached a high level of reliability. Attention now focuses on ionization and fragmentation which involve three-body channels in the final state. In this case, simulations of total cross sections have reached a level of reliability comparable to that for two-body channels, however, energy and angular distributions of particles in the final state have only recently been simulated. Even here the distributions of slow electrons in 1-5 keV proton-hydrogen atom collisions is difficult to extract owing to the need for high accuracy over large volumes. One aspect of our work is to supplement *ab initio* calculations with analytic treatments at large distances where numerical methods are impractical. A second project seeks exact results of soluble models of physical systems that can be used to test numerical procedures[1,2,3]. A third aspect of our work is to further develop the hidden crossing theory so that reliable distributions can be obtained. Finally we plan to use the hidden crossing theory to examine weak processes that are difficult to simulate numerically owing to their small probability relative to more dominant processes.

2 Recent progress

Computer simulation of ionization in proton and antiproton collisions with hydrogen atoms by Schultz and co-workers have obtained electron distribu-

tions for 1-5-keV projectiles for a small selection of impact parameters. For protons, these distributions show a π -orbital shape centered near the top of the potential barrier between the two protons, in qualitative agreement with approximate hidden crossing calculations. Neither distribution is in qualitative agreement with COLTRIMS measurements of electron distributions in proton-helium atom collisions.

It is thought that the simulations diverge from measurements because the computations extract the distributions at finite, and relatively modest, values of the internuclear separations. We have tested this hypothesis by using our analytic top of barrier propagator to propagate the ionization amplitude computed by Schultz and co-workers to infinite distances. We find that the resulting distribution is narrowed in directions perpendicular to the projectile velocity and broadened in parallel directions, in qualitative agreement with observations.

With the addition of top of barrier propagation we conclude that complete computer simulations of all processes occurring in ion-atom collisions are in hand. Further testing of this hypothesis by computations over a wide range of ionic species, impact parameters, and projectile velocities are needed.

Two projects seeking exact results have been initiated. Preliminary results for antiproton collisions with hydrogen[4] and more extensive results for a zero range potential (ZRP) model of negative ions colliding with neutral atoms[1,2] have been obtained. Previous work has employed the ZRP model, but only for zero impact parameter. We have solved this model for non-zero impact parameters. The effect of "rotational coupling in the continuum", missing in the zero impact parameter case, are computed. These results have been used to assess the validity of the hidden crossing theory for ionization[4]. Finally, we have obtained an exact theorem for transitions between states of positively charged ions in the limit of vanishing momentum transfer[3].

3 Future plans

Projects are underway to include top-of-barrier propagation in other ab initio simulations of fragmentation. Virtually any theory that gives an electron distribution for finite internuclear separations can be propagated to infinite distances using the top of barrier propagator. We will use this method to-

gether with the hidden crossing theory to elucidate the origin of the π electron distributions in proton-hydrogen collisions. Preliminary results suggest that such distributions occur when the σ components are anomalously small owing to Stuekelberg minima. We will examine the distributions in regions where there are maxima rather than minima to see if σ -like distributions emerge. Close coordination with the computer simulations of David Schultz's group are envisioned.

The hidden crossing theory will also be further developed to examine the formation of bound proton-antiproton species in collisions of antiprotons with positronium. This requires extending the hidden crossing theory to allow for heavy particle bound states.

4 References to DOE sponsored research that appeared in 2000-2002

1. Harmonic oscillator Green's function J.H. Macek, S.Yu. Ovchinnikov, D.B. Khrebtukov, *Radiation Physics and Chemistry* **59**, 149 (2000).
2. Exact electron spectra in collisions of two zero-range potentials with non-zero impact parameters S.Yu. Ovchinnikov, D.B. Khrebtukov, and J.H. Macek, *Phys. Rev. A* **65**, 032722 (2002).
3. Lassetre's theorem for excitation of ions by charged particle impact, J. H. Macek and N. B. Avdonina *J. Phys. B.* **35** 1775, (2002).
4. Ionization of atoms by antiproton impact, J. H. Macek in *Electron Scattering From Atoms, Molecules, Nuclei and Bulk Matter*, Ed. by C. Whelan, (Kulwar Scientific 2002).

Molecular Structure and Collisional Dissociation and Ionization

Kurt H. Becker

Department of Physics and Engineering Physics,
Stevens Institute of Technology, Hoboken, NJ 07030
phone: (201) 216-5671; fax: (201) 216-5638; kbecker@stevens-tech.edu

Program Scope:

This program is aimed at investigating the molecular structure and the collisional dissociation and ionization of selected molecules and free radicals. The focus areas are (1) ionization studies of selected molecules and free radicals and (2) the study of electron-impact induced neutral molecular dissociation processes. Targets of choice for ionization studies during the current funding cycle include SiF_4 , TiCl_4 , SiCl_4 and CCl_4 and its radicals, C_2F_6 and B_2H_6 , and BCl_3 and its radicals. This choice is motivated on one hand by the relevance of these species in specific etching applications (e.g. poly-Si and amorphous Si, Al and Al-Cu, and WSi_2 and TiSi_2 etching and the etching of thin magnetic films) and, on the other hand, by basic collision physics aspects (SiCl_x and CCl_x are of similar molecular structure as the species studied previously and thus complement the existing data base for these targets). The targets of choice for the neutral molecular dissociation studies include SiH_4 , $\text{Si}(\text{CH}_3)_4$ (tetramethylsilane, TMS), SiF_4 , and BCl_3 . The fragments to be probed include $\text{Si}({}^1\text{S})$, $\text{Si}({}^1\text{D})$, $\text{SiH}(\text{X } {}^2\Pi)$, $\text{BCl}(\text{X } {}^1\Sigma)$, and $\text{B}({}^2\text{P}^\circ)$.

The scientific objectives of the research program can be summarized as follows:

- (1) to provide the atomic and molecular data that are required in efforts to understand the properties of low-temperature processing plasmas on a microscopic scale
- (2) to identify the key species that determine the dominant plasma chemical reaction pathways
- (3) to measure cross sections and reaction rates for the formation of these key species and to attempt to deduce scaling
- (4) to establish a broad collisional and spectroscopic data base which serves as input to modeling codes and CAD tools for the description and modeling of existing processes and reactors and for the development and design of novel processes and reactors
- (5) to provide data that are necessary to develop novel plasma diagnostics tools and to analyze more quantitatively the data provided by existing diagnostics techniques

Recent Progress:

The main emphasis of the program up to now was on ionization processes and the targets were chosen with 2 objectives in mind, (i) relevance to the physics and chemistry of low-temperature, non-equilibrium plasmas used in current technologies and (ii) relevance from a collision physics point of view. More than 25 molecules and free radicals have been investigated and a comprehensive database of ionization cross sections and appearance energies has been compiled. Systematic trends, similarities as well as discrepancies in the data for targets of similar molecular and/or electronic structure have been established. The experimental efforts are complemented by calculations of ionization cross sections using semi-empirical and semi-classical approaches.

Specific recent accomplishments:

1. Measurement of ionization cross sections for C_2F_6

We measured the absolute partial electron impact ionization cross sections for the formation of molecular and atomic fragment ions from C_2F_6 using a time-of-flight mass spectrometer. The reliable performance of the apparatus was demonstrated by reproducing the benchmark cross

sections for the formation of fragment ions from CF_4 . The partial cross sections of C_2F_6 for the formation of the most abundant molecular fragment ions CF_3^+ , C_2F_5^+ , CF^+ , and CF_2^+ are determined along with the considerably smaller cross sections for the formation of the ions C_2F_4^+ , C_2F^+ , C_2^+ , F^+ , and C^+ . As in the case of CF_4 , no parent ion is formed for C_2F_6 , but in contrast to CF_4 no double charged fragment ions were observed in the case of C_2F_6 . Our results for the four abundant ions CF_3^+ , C_2F_5^+ , CF^+ , and CF_2^+ are in good agreement with recent results of Jiao et al. [6]. For the ions that are formed with negligible excess kinetic energy, CF_3^+ and C_2F_5^+ , our results are also in good agreement with the earlier data of Poll and Meichsner [1]. The total electron impact ionization cross section obtained as the sum of the partial cross sections is in excellent agreement with the results of the total ionization cross section measurements and the calculations of Nishimura et al. [2] and with the measured cross section of Jiao et al. [3]. Absolute ionization cross sections for C_2F_6 have now been measured using several experimental methods (TOF-mass-spectrometer, Fourier transform mass spectrometer, quadrupole mass spectrometer, parallel-plate type apparatus) and the results are in good agreement, at least for the larger partial cross sections and for the total cross section. The present results in conjunction with the results of the electron impact ionization studies of the CF_x ($x=1-3$) free radicals and C_2F_5 radical provide a reliable and comprehensive data base of ionization cross sections for the modeling of the electron impact induced ion formation in C_2F_6 -containing plasmas.

[1] H.U. Poll and J. Meichsner, *Contrib. Plasma Phys.* **27** (1987) 5, 359

[2] H. Nishimura, W. M. Huo, M. A. Ali, and Y.-K. Kim, *J. Chem. Phys.* **110** (1999) 3811.

[3] C. Q. Jiao, A. Garscadden, and P.D. Haaland, *Chem. Phys. Lett.* **310** (1999) 52

2. Measurements of ionization cross sections for NO, N_2O , and NO_2

We carried out absolute partial ionization cross section measurements for the three nitrogen-oxygen compounds NO, NO_2 , and N_2O for which the ionization cross section data base is incomplete and to some extent unreliable. These measurements are the first effort to measure absolute partial ionization cross sections for all three species in the same apparatus using the same experimental technique. Several persistent ambiguities that existed in the literature have been addressed in the course of our work. In the case of NO, our measured total single ionization cross section is in very good agreement with the data reported by Iga et al [1] and at higher impact energies above about 100 eV also with the data of Rapp and Englander-Golden [2], whereas the recent data reported by Lindsay et al. [3] and the calculated cross section of Kim and co-workers lie somewhat below our data in the energy range from threshold to 200 eV. Excellent agreement between all measured and calculated total N_2O cross sections was found with only minor discrepancies in the reported partial ionization cross sections. In NO_2 , minor discrepancies in the partial ionization cross sections result in minor discrepancies in the total ionization cross section between our data and the recent data of Lindsay et al. [3].

[1] I. Iga, M.V.V.S. Rao, and S.K. Srivastava, *J. Geophys. Res.* **101**, 9291 (1996)

[2] D. Rapp and P. Englander-Golden, *J. Chem. Phys.* **43**, 1464 (1965)

[3] B.G. Lindsay et al., *J. Chem. Phys.* **112**, 9404 (2000)

3. Measurement of ionization cross sections for B_2H_6

Measurements of ionization cross sections for this H-containing molecule with a molecular structure that is different from C_2H_6 or Si_2H_6 are currently underway. One of the more remarkable findings was the observation of a discernible ion signal attributable to the formation of H_3^+ fragment ions. The possibility of forming H_3^+ fragment ions, which were not observed in the case of C_2H_6 and Si_2H_6 , is supported by quantum chemistry calculations.

4. Neutral molecular dissociation

To date, there have been few quantitative studies of the electron-impact neutral dissociation of molecules under controlled experimental conditions. This is mainly due to the difficulty in detecting neutral ground-state species with little or no internal energy. We developed a triple-beam apparatus and use a combination of electron scattering and laser-induced fluorescence (LIF) techniques to measure absolute cross sections for the electron-impact dissociation of molecules into neutral ground-state fragments. The experimental set-up consists of a crossed electron-beam - gas-beam set-up inside a stainless steel high-vacuum chamber (base pressure of 1×10^{-7} Torr). The two beams intersect at right angles. A tunable laser beam propagates either parallel or antiparallel to the electron beam in order to maximize the overlap of the three beams. Optical detection of the fluorescence from the interaction region is made perpendicular to both the electron beam and the gas beam. We now have absolute cross sections for the final-state-specific formation of Si(¹S) atoms from SiH₄ for impact energies from 20 eV to 100 eV.

5. Incorporation of a new detector system into the fast-beam apparatus

We have received a new dual-detector system from Roentdek GmbH in Germany. One fast position-sensitive MCP detector replaces the channeltron in the fast-beam apparatus and serves as the final product ion detector. The second detector will be installed as an alternative to the Faraday cup and will serve as a monitor of the fast neutral beam and the product ion beam prior to entering the electrostatic energy analyzer. This will allow us to obtain information about the excess kinetic energy of the fragment ions. At present, the new ion detector has been installed and its performance is being tested. We anticipate resuming experiments within 2 months.

6. Supporting semi-classical ionization cross section calculations

We made significant progress in applying our semi-classical ionization cross section calculation method to singly-ionized molecular and radical targets and to highly ionized atomic targets.

Future Plans

The future work on molecular and radical ionization properties will resume after the full implementation and testing of the new detector and will concentrate on those targets listed in the section "Program Scope" that have not yet been investigated. The main immediate emphasis for the neutral molecular dissociation studies is on the measurements of the electron-impact induced neutral molecular dissociation for the target molecules listed below together with the various atomic as well as molecular neutral fragments that will be probed.

Fragment	Parent Molecule	Transition	Pump Wavelength	Detection Wavelength
BCl(X ¹ Σ)	BCl ₃	X ¹ Σ → A ¹ Π ⁺	272 nm	272 nm
B(² P ^o)	BCl ₃	(2p) ² P ^o → (3s) ² S	250 nm	250 nm
Si(¹ S)	SiH ₄ , SiF ₄ , Si(CH ₃) ₄	(3p) ² ¹ S → (4s) ¹ P	391 nm	288 nm
Si(¹ D)	SiH ₄ , SiF ₄ , Si(CH ₃) ₄	(3p) ² ¹ D → (4s) ¹ P	288 nm	391 nm
SiH(X ² Π ⁺)	SiH ₄	X ² Π ⁺ → A ² Δ	415 nm	415 nm

Application of the proposed method to some of the above listed dissociation processes requires the implementation of a frequency doubler to pump the corresponding transitions (pump

wavelengths below 350 nm). This has been successfully accomplished and data are now available for the formation of Si(¹D) formation from SiH₄ and SiF₄.

Recent publications (since 2000) and manuscripts accepted for publication

1. "Calculations of Cross Sections for the Electron Impact Ionization of Molecules", *Int. J. Mass Spectrom.* **197**, 37 (2000), with H. Deutsch, S. Matt, and T.D. Märk (Invited Topical Review)
2. "Elementary Collision Processes in Plasmas", in "Low-Temperature Plasma Physics: Fundamental Aspects and Applications", editors: R. Hippler, S. Pfau, M. Schmidt, and K.H. Schoenbach, Wiley-VCH Publishing, Berlin/New York (2001), p. 55-77
3. "Calculation of Absolute Electron-Impact Ionization Cross Sections of Dimers and Trimers", *Europ. Phys. J. D* **12**, 283-287 (2000), with H. Deutsch and T.D. Märk
4. "Calculated Cross Sections for the Multiple Ionization of N and Ar Atoms by Electron Impact Using the DM Formalism", *Plasma Phys. Controlled Fusion* **42**, 489-499 (2000), with H. Deutsch and T.D. Märk
5. "Electron-Impact Ionization of TiCl₄", *Thin Solid Films* **374**, 219-291 (2000), with R. Basner, M. Schmidt, V. Tarnovsky, and H. Deutsch
6. "Absolute Cross Section for the Formation of Si(¹S) Atoms Following Electron Impact Dissociation of SiH₄", *J. Chem. Phys.* **113**, 2250-2254 (2000), with N. Abramzon and K. Martus
7. "Calculated Absolute Electron Impact Ionization Cross Sections for AlO, Al₂O, and WO_x (x=1-3)", *J. Appl. Phys.* **89**, 1915-1921 (2001), with H. Deutsch, K. Hilpert, M. Probst, and T.D. Märk
8. "Calculations of Absolute Electron Impact Ionization Cross Sections for Molecules of Technological Relevance Using the DM Formalism", *Int. J. Mass Spectrom.* **206**, 13-25 (2001), with M. Probst, H. Deutsch, and T.D. Märk
9. "Absolute Total and Partial Cross Sections for the Electron Impact Ionization of SiF₄", *J. Chem. Phys.* **114**, 1170-1177 (2001), with R. Basner, M. Schmidt, E. Denisov, and H. Deutsch
10. "Electron Impact Ionization of the TiCl_x (x=1-3) Free Radicals" *Int. J. Mass Spectrom.* **208**, 1-5, (2001), with V. Tarnovsky, R. Basner, and M. Schmidt
11. "Calculated Cross Sections for the Multiple Ionization of Krypton and Chromium Atoms by Electron Impact", *Contr. Plasma Phys.* **41**, 73-83 (2001), with H. Deutsch and T.D. Märk
12. "Calculated Cross Sections for the K-Shell Ionization of Cr, Ni, Cu, Sc, and Va Using the DM Formalism", *J. Phys. B* **34**, 3377-3382 (2001), with B. Gstir, H. Deutsch and T.D. Märk
13. "Calculated Absolute Cross Section for the Electron-Impact Ionization of CO₂⁺ and N₂⁺", *J. Phys. B* **35**, L65-9, (2002), with H. Deutsch, P. Defrance, U. Onthong, R. Parajuli, M. Probst, S. Matt, and T.D. Märk
14. "Calculated Cross Sections for the K-Shell Ionization of Fe, Co, Mn, Ti, Zn, Nb, and Mo Atoms Using the DM Formalism", *Int. J. Mass Spectrom.* **213**, 5-8 (2002), with H. Deutsch, B. Gstir, and T.D. Märk
15. "Calculated Absolute Electron Impact Ionization Cross Sections for the Molecules CF₃X (X=H,Br,I)", *Int. J. Mass Spectrom.* **214**, 53-56 (2002), with U. Onthong, H. Deutsch, S. Matt, M. Probst, and T.D. Märk
16. "Total Electron Impact Ionization Cross Sections of CF_x and NF_x (x=1-3)", *Chem. Phys. Lett.* **358**, 328-336 (2002), with W.M. Huo and V. Tarnovsky
17. "Absolute Total and Partial Electron-Impact Ionization Cross Sections for C₂F₆", *Int. J. Mass Spectrom.* (2002), in press, with R. Basner, M. Schmidt, E. Denisov, P. Lopata, and H. Deutsch
18. "Electron Impact Ionization of NO, N₂O, and NO₂", *Int. J. Mass Spectrom.* (2002), in press, with J. Lopez and V. Tarnovsky
19. "Calculated Absolute Cross Sections for the Electron-Impact Ionization of Simple Molecular Ions", *Int. J. Mass Spectrom.* (2002), in press, with H. Deutsch, P. Defrance, U. Onthong, M. Probst, S. Matt, P. Scheier, and T.D. Märk

Polyatomic Excitation Effects in Electron-Molecule Collisions: a First-Principles Study of Electron-CO₂ Scattering

Thomas N. Rescigno

Computing Sciences

Lawrence Berkeley National Laboratory

Although the principal features of low-energy electron- CO₂ scattering have been the subject of numerous experimental and theoretical investigations, recent laboratory studies¹ of resonant vibrational excitation have been carried out with unprecedented energy resolution and have revealed subtle details in the excitation cross sections whose origin and quantitative understanding pose serious challenges for *ab initio* theory.

The electron-CO₂ system is complicated for a number of reasons. The phenomenon of ‘Fermi resonance’, ie. an accidental degeneracy that occurs between certain zero-order vibrational states, leads to strong mixing between vibrational modes and necessitates a multi-dimensional treatment of the dynamics. The problem is further complicated by the fact that the negative ion “shape” resonance, which is degenerate in linear geometries ($^2\Pi_u$), splits into two non-degenerate surfaces upon bending which are strongly coupled by non-adiabatic Coriolis effects (Renner-Teller coupling).

Our recent work in this area will be described. Ours is a first-principles computational approach, starting with fixed-nuclei variational calculations of the electronic scattering problem that provide the (complex) potential energy surfaces on which time-dependent wavepacket studies of the nuclear dynamics studies are then carried out. We have found that it is essential to consider both symmetric stretch and bending degrees of freedom to achieve even qualitatively accurate results and that details of the excitation cross sections, including subtle interference structures, are controlled by non-adiabatic coupling between the 2A_1 and 2B_1 resonance surfaces.

1. M. Allan, Phys. Rev. Letts. **87**, 033201 (2001); *Photonic, Electronic and Atomic Collisions* (ICPEAC XXII), July 18-24, 2001, Santa Fe, NM, Book of Invited Papers (Rinton Press, 2002) p. 284.

Triply Excited States in Three-Electron Ions

Patrick Richard, J. R. Macdonald Laboratory, Kansas State University
Manhattan, KS 66506 [richard@phys.ksu.edu; (785)532-6783]

[Collaborators: M. Zamkov, E.P. Benis, T.J.M. Zouros, T.G. Lee, C.D. Lin, and T. Morishita]

Theoretical and experimental investigations of triply excited states of three-electron atoms and ions are of fundamental interest to the atomic physics of the ideal four-body Coulomb system. The symmetries of preferred excited states and their decay modes are dominated by electron-electron correlation. A wealth of experimental information about these states has come from the study of Li atoms excited by synchrotron radiation. The excitation of triply excited Li by synchrotron radiation is limited to $^2P^o$ excited resonances. Laser excited $1s^22p^2P^o$ targets can be used to produce $^2S^e$, $^2P^e$ and $^2D^e$ states, but this method poses experimental challenges. Theoretical investigations of triply excited states include saddle-point complex-rotation, R-Matrix, Dirac-Fock, and a systematic classification of these states using the hyperspherical approach by Morishita and Lin.

The study of triply excited states of three electron ions with $Z > 3$ using synchrotron radiation is difficult due to insufficient fluxes of high photon energies required for the excitations. Theoretical studies of the isoelectronic sequences of such states have been done, however, by Safronova *et al.*, using the perturbative $1/Z$ -expansion method, and by Madsen *et al.*, and Conneely *et al.* using configuration interaction models.

Doubly and triply excited states of atoms and ions can be studied by ion-atom interactions. Early work by Rodbro *et al.* investigated optically inaccessible states of Li and Be by observing the forward emitted projectile Auger electron emission spectra from slow ion-atom/molecule collisions. These spectra are very rich, and are dominated by single excitation states, but contain doubly excited two- and three-electron states with $2snl$ and $2s^2nl$ configurations, respectively. Selective excitation of doubly excited two-electron states can be achieved in fast ion-atom collisions by observing the projectile Auger decay. One process that selectively excites these states is the e-ion excitation of the projectile [e.g. $F^{8+}(1s) + e^- \rightarrow F^{7+}(2p^2, ^1D^e)$]. This process has been called resonance transfer excitation. We have studied the He-like isoelectronic sequence C^{4+} , N^{5+} , O^{6+} , and F^{7+} . Measured Auger rates were obtained using the electron scattering model and compare exceedingly well with R-Matrix theory calculations.¹ We have extended the method to the excitation of Li-like triply excited states by using well characterized metastable-ion beams. For example, we can reach hollow ionic states by the reaction $F^{7+}(1s2s, ^3S) + e^- \rightarrow F^{6+}(2s2p^2, ^2D^e)$.²

The newest method that we employed to study multiply excited states is triple electron capture in high velocity bare-ion + argon collisions. We observed triple capture to $1s2l2l'$ configurations in $C^{6+} + Ar$ collisions.^{3a} At the suggestion of C. D. Lin, we looked for a favorable system for capturing to higher n-levels. We found that $F^{9+} + Ar$ provides a favorable level matching. We observed the following: $F^{9+} + Ar \rightarrow F^{6+}(2s2p^2, ^2S^e, ^2P^e, ^2D^e \text{ and } (2p)^3, ^2,4P^o \text{ and } ^2,4D^o \text{ states}) + Ar^{3+}$.^{3b} These are ideal three electron states to test existing theories. The experiments are made possible by the use of a high efficiency, high-resolution zero-degree off-axis hemispherical spectrometer.⁴ Differential cross sections, Auger energies, and Auger branching ratios are determined. The results are compared with available theoretical calculations.

1) G. Toth, P. Zavodszky, C. P. Bhalla, P. Richard, S. Grabbe and H. Aliabadi, *Physica Scripta T* **92**, 272 (2001).

2) M. Zamkov, H. Aliabadi, E. P. Benis, P. Richard, H. Tawara, and T.J.M. Zouros, *Phys. Rev. A* **65**, 032705 (2002).

3) M. Zamkov, E. P. Benis, P. Richard, T. G. Lee, and T.J.M. Zouros

a) Accepted for publication in *Phys. Rev. A.*, and b) submitted to *Phys. Rev. A*

4) E. P. Benis, T.J.M. Zouros, H. Aliabadi, and P. Richard, *Physica Scripta T* **80**, 529(1999).

Dissociation and Coulomb Explosion of Model Molecular Hydrogen Ions by Intense Short Laser Pulses

Uwe Thumm[thumm@phys.ksu.edu] and Bernold Feuerstein
Dept. of Physics
Kansas State University
Manhattan, KS 66506

In this talk I will discuss the interaction of 25 fs, 0.2 PW/cm², 780 nm pulses with H₂⁺ molecular ions within a reduced-dimensionality model that represents both the nuclear and electronic motion by one degree of freedom. We carefully adjusted the adiabatic molecular electronic potential by introducing a “soft-core function” $a(R)$ in the electron-nucleus interaction potentials $1/(x \pm R/2 + a(R))$ that depends on the internuclear distance R instead of the commonly used fixed soft-core constant a . We obtained molecular model potentials that reproduce accurate three-dimensional results for the known number of 19 vibrational states in the electronic ground state and for the dipole oscillator strength.

We solved the time-dependent Schrödinger equation on a two-dimensional numerical grid and designed a simple, but as far as we know, new method to calculate the flux of emitted electrons and protons by means of “virtual detectors” for electrons and protons. These detectors are placed outside the excursion range of the electron and at a distance R where the amplitudes of bound vibrational states have become irrelevant, respectively.

Our results reproduce the main features of measured kinetic-energy release spectra, support the “charge-resonance enhanced” ionization mechanism, and allow us to clearly distinguish between molecular dissociation (MD) into field-dressed final channels and fast, ionization-induced Coulomb explosion (CE). Both MD and CE appear as distinct peaks in the kinetic energy release spectra. We find that MD dominates for molecular ions that are prepared in the two lowest vibrational states only, while CE becomes increasingly dominating for higher vibrational states.

For two short laser pulses of variable delay, we started to resolve in time the interplay between MD and CE. We intend to further investigate the pump-probe dynamics for two short pulses of which I will discuss some first results. Motivated by new experiments in the Macdonald Laboratory, we have started to investigate the ionization of model atoms under the combined influence of a few-cycle intense laser pulse (10^{14} to 10^{15} W/cm²) and a significantly longer and less intense pulse (about 10^{12} W/cm²). I anticipate to discuss first results, including the effect of phase coherence between the two pulses.

“Quantum/Classical Atomic Interactions”

F. Robicheaux

Auburn University, Department of Physics, 206 Allison Lab, Auburn AL 36849-5311
(robicfj@auburn.edu)

Project Scope

There are two separate projects that are being investigated in this theory proposal. They are related in the sense that both explored issues of nonstandard scattering. In the first project, I study the stimulated attachment of an electron to an ion using a pulsed electric field; besides the inherent interest in understanding the physical process, it is possible that the method could be used to create high Rydberg states of complex molecules or to make anti-Hydrogen at CERN. This project has led us to study ultra-cold plasmas. In the second project, I study the interaction of quantum targets with matter beams containing some longitudinal coherence; this project addresses basic issues of scattering theory and how to use the beam coherence to extract new quantum parameters.

Recent Progress

In the first project, we recently published[1] the large version of the paper that describes how a ramped electric field can be used to stimulate the recombination of a free electron with an ion. Previous results were described in two short papers[7] before this project began. Reference [1] presents both new calculations and new experimental results. The experiments showed that the method worked in medium strength magnetic fields (60 mT) and when using trapped electrons. On the theory side, I show the regions of space that contribute to the recombination and give other parameters that cannot be directly obtained from experiment (for example, the energy distribution of the recombined electron). This method has been used in an attempt to make anti-Hydrogen at CERN in collaboration with Gabrielse's group. Calculations showed that anti-Hydrogen signal should have been observed for the parameters that were available in the experiment, but it was judged that the data did not clearly demonstrate the presence of anti-Hydrogen. The suspicion is that the $v \times B$ motional electric field was stripping the Rydberg positron from the anti-proton. I am currently performing calculations which show there really isn't a $v \times B$ motional electric field for high Rydberg states: neutral particles cross magnetic field lines in a simple way only when the internal time scales are short compared to cyclotron periods. The results of the calculations predict that highly excited anti-Hydrogen atoms were not being stripped but were not leaving the magnetic field at the rate that was originally expected.

Interest in the interaction of cold electrons with cold positive ions led us to investigate the phenomena discovered in ultra-cold, neutral plasmas. Experiments performed in S. Rolston's group (NIST), T. Gallagher's group (U of Virginia), and G. Raithel's group (U of Michigan) showed many puzzling features; these features were fundamental and showed that the basic processes were not well understood. Although these experiments did not use a strong magnetic field (like those in the anti-Hydrogen experiments), we felt this would be a good starting problem. The new project that was begun last year resulted in one publication[6]; we are

preparing a larger paper for publication which has more details of our methods. This project fits in with those originally proposed because high Rydberg states are formed in the plasma and the interaction between electrons and Rydberg atoms as well as the interaction between pairs of Rydberg atoms are important. Our calculation was able to explain most of the puzzling features in the experiments through a proper understanding of the role played by the formation of Rydberg atoms and their subsequent interaction with electrons in the plasma.

The second project (stimulated by Ref. [8]) is delayed while the experiments can begin to measure some of the phenomena that we showed could be measured. The difficulty is with a practical method for making short pulses of electrons. However, there was a recent paper from Corkum's group in Science which showed that very strong laser pulses could give rise to very short electron pulses. These electron pulses can be made to interact with the atom or molecule from which the electron was stripped. This would give rise to the situation we studied in Ref. [5]. It is possible that this source of electron pulses will help push forward studies of electron scattering with electron pulses that have longitudinal coherence.

Future Plans

The prospects for the coming year are good for the theory side of the project. The most promising project is to continue studies of the interaction between cold electrons, positive ions, and Rydberg atoms. During the next year, we will start a project to investigate the interaction of electrons, ions, and Rydberg atoms in strong magnetic fields; this system is important for the experiments that are trying to make anti-Hydrogen and it will also be studied in other experimental groups as a basic physics process. This will require a substantial effort because we will need to generalize our computer programs to work in cylindrical coordinates (we currently use the approximate spherical symmetry in the ultra-cold plasma experiments) and we will need to generate basic atomic data. As an example, we want to understand the experiments that demonstrate positron cooling of anti-protons. However, the basic collision process (cold positron + cold anti-proton in a strong magnetic field) is not understood well enough to model the cooling mechanism.

We also plan to continue studies of ultra-cold plasmas with no magnetic field. We plan to perform detailed comparisons between simulations and experiments for other key parameters. We have been working with S. Rolston's group to make comparisons between simulations and experiments at a detailed level. For example, we have compared the time dependence of the electron flux escaping the plasma. This comparison will ensure that the simulations are representing the main plasma processes. We also plan to continue investigating basic unexplained phenomena. For example, the experiment on the conversion of a Rydberg gas into an ultra-cold plasma (T. Gallagher) has not been understood: the source of the energy to convert the Rydberg atoms into free electrons plus ions is not known.

Experiments are being planned to study the interaction of a pulsed electron beam with Rydberg atoms. This will test the ideas we have proposed for the interaction of a longitudinally coherent beam with a quantum target. There is no

need for further theoretical investigations until the experiments are at a more advanced stage.

DOE Supported Publications

- [1] C. Wesdorp, F. Robicheaux, and L.D. Noordam, Phys. Rev. A **64**, 033414 (2001).
- [2] M.S. Pindzola, M. Witthoef, and F. Robicheaux, J. Phys. B **33**, L839 (2000).
- [3] F. Robicheaux, Phys. Rev. A **62**, 062706 (2000).
- [4] F. Robicheaux and L.D. Noordam, Physics Essays **13**, 496 (2000).
- [5] M. Ferrero and F. Robicheaux, Chem. Phys. **267**, 93 (2001).
- [6] F. Robicheaux and J.D. Hanson, Phys. Rev. Lett. **88**, 055002 (2002).

Other Relevant Publications

- [7] C. Wesdorp, F. Robicheaux, and L.D. Noordam, Phys. Rev. Lett. **84**, 3799 (2000); Chem. Phys. Lett. **323**, L427 (2000).
- [8] F. Robicheaux and L.D. Noordam, Phys. Rev. Lett. **84**, 3735 (2000).

Double K-photoionization of Heavy Atoms

E. P. Kanter,* R. W. Dunford, D. S. Gemmell, B. Krässig, S. H. Southworth, and L. Young
Argonne National Laboratory, Argonne, Illinois 60439[†]

With the advent of modern synchrotron radiation sources providing intense, collimated beams of tunable monochromatic x-rays, there has been increased interest in the investigation of multielectron processes. Beyond the importance of such processes in understanding electron-electron correlations in atoms, they also have significant applications in other fields. For example, they are responsible for the production of satellite structures in extended x-ray absorption fine structure (EXAFS) and x-ray absorption near-edge structure (XANES) studies of materials. The most basic multielectron process is the complete emptying of an atomic K shell in photoabsorption, thus creating a "hollow atom". As an outgrowth of our previous work on the double ionization of He, we have begun a program studying double K -ionization in heavy atoms. In addition to this fundamental interest in this subject, these studies are also a core element of our longer range program to understand strong-field x-ray interactions where multielectron processes will play a dominant role. The present studies will provide benchmark multielectron photoabsorption cross sections for hard x-rays in the weak-field limit which will be required as a basis for future strong-field work. Argonne's Advanced Photon Source (APS) is unique among U.S. synchrotron light sources for these experiments in that it provides high fluxes of hard x-rays enabling us to reach the double ionization thresholds of all elements.

We had previously demonstrated a relatively simple method to isolate the effects of electron-electron correlations in heavy atoms by simultaneous x-ray photoionization of both K-electrons in molybdenum. [1] The presence of these double-hole states was signaled by the observation of $K_{\alpha\beta}^h$ hypersatellite fluorescence detected in coincidence with the subsequent satellite transition filling the second vacancy. More recently, we were able to extend these measurements to the more interesting case of Ag ($Z=47$). Because of extensive previous studies of this atomic system using the electron capture (EC) decay of ^{109}Cd , the shakeoff contribution is well-known experimentally for the single-electron final state produced in EC [2]. Thus, our photoionization measurements isolate the effects of the dynamic electron-electron scattering term. Measurements were carried out at several energies from the double K-ionization threshold to the region of the expected maximum (from 50–90 keV) in the cross-section. Analysis of these data has confirmed the predicted rise in the double-ionization cross section throughout this region. The measured ratio (double/single ionization) in this peak region is found to agree well with the Z -dependence we had found from fitting the earlier measurements [1] and much slower than the characteristic $1/Z^2$ dependence of shakeoff expected in the asymptotic limit. We have also extended these measurements to lower Z by measuring Ne Auger hypersatellite transitions following double K -photoionization and find similarly good agreement with this Z dependence.

Our principal goal for the future is to observe this phenomenon in Au ($Z=79$). This is a case where relativistic effects should be dominant. We choose to concentrate on this specific atomic system because of our on-going work at GSI investigating 2-photon decays in Au and our plans to conduct future measurements of Au 2-photon decays at the APS. Another issue which we will investigate is the 2-electron transition in which the double vacancy is filled with the emission of a single photon. The simplest of these so-called "correlated hypersatellite" transitions are $1s^{-2} \rightarrow 2s^{-1}2p_{1/2,3/2}^{-1}$ and denoted $K_{\alpha_2\alpha_3}^h$ and $K_{\alpha_1\alpha_3}^h$ respectively. Although these have been observed in experiments using ion and electron-impact excitation, such transitions have never been observed following photoionization [3]. Åberg and co-workers have obtained a relatively simple expression for the ratio of the intensity of these correlated hypersatellites to the more probable satellite transitions [4] which, aside from trivial energy factors, is determined solely by the square of the overlap integral of the K -vacated $2s$ orbital with the relaxed $1s$ orbital. Thus, such a measurement would serve as a particularly simple test of relativistic atomic structure calculations.

-
- [1] E. P. Kanter, R. W. Dunford, B. Krässig, and S. H. Southworth, *Phys. Rev. Lett.* **83**, 508 (1999).
[2] S. K. Ko, H. J. Cho, and S. K. Nha, *Nucl. Phys. A* **641**, 49 (1998).
[3] R. Diamant *et al.*, *Phys. Rev. A* **62**, 052519 (2000).
[4] T. Åberg, K. A. Jamison, and P. Richard, *Phys. Rev. Lett.* **37**, 63 (1976).

*kanter@anl.gov

[†]This work was supported by the Chemical Sciences, Geosciences, and Biosciences Division of the Office of Basic Energy Sciences, Office of Science, U.S. Department of Energy, under Contract W-31-109-Eng-38.

Research Summaries
(multi-PI programs alphabetical by institution)

X-ray and Inner-Shell Interactions

R. W. Dunford, E. P. Kanter, B. Krässig, S. H. Southworth, L. Young
Argonne National Laboratory, Argonne, IL 60439

dunford@anl.gov, kanter@anl.gov, kraessig@anl.gov, southworth@anl.gov, young@anl.gov

We seek to establish a quantitative understanding of x-ray interactions with free atoms and molecules. We have explored a broad energy range where the dominant interaction evolves from photoabsorption to scattering, with careful attention to regions near resonances and thresholds. The focus has been on understanding the limitations of theory, in particular the validity of the independent particle approximation and the role of multipole effects. Multipole effects are studied using an apparatus with four photoelectron spectrometers to monitor multiple angles simultaneously. Complex decay pathways following inner-shell excitation are investigated using x-ray-ion coincidence techniques. Multielectron excitation is studied as a measure of electron-electron correlation in heavy atoms. Studies of forbidden transitions in few-electron ions are being shifted to address rare decay modes of neutral species using x-ray excitation to create inner-shell vacancies. Future plans are discussed individually in the following subsections. In addition, we plan to investigate two-color, optical-x-ray interactions, specifically the effect of strong-AC fields on the x-ray spectrum of a free atom.

Double K-photoionization of Heavy Atoms

E. P. Kanter, R. W. Dunford, D. S. Gemmell, B. Krässig, S. H. Southworth, and L. Young

We previously demonstrated a relatively simple method to isolate the effects of electron-electron correlations in heavy atoms by simultaneous x-ray photoionization of both K-electrons in molybdenum. The presence of these double-hole states was signaled by the observation of $K_{\alpha\beta}^h$ hypersatellite fluorescence detected in coincidence with the subsequent satellite transition filling the second vacancy. More recently, we were able to extend these measurements to the more interesting case of Ag ($Z=47$). Because of extensive previous studies of this atomic system using the electron capture (EC) decay of ^{109}Cd , the shakeoff contribution is well known experimentally for the single-electron final state produced in EC. Thus, our photoionization measurements isolate the effects of the dynamic electron-electron scattering term. Measurements were carried out at several energies from the double K-ionization threshold to the region of the expected maximum (from 50-90 keV) in the cross-section. Analysis of these data has confirmed the predicted rise in the double-ionization cross section throughout this region. The measured ratio (double/single ionization) in this peak region is found to agree well with the Z -dependence we had found from fitting the earlier measurements and much slower than the characteristic $1/Z^2$ dependence of shakeoff expected in the asymptotic limit. We have also extended these measurements to lower Z by measuring Ne Auger hypersatellite transitions following double K-photoionization and find similarly good agreement with this Z dependence. Our principal goal for the future is to observe this phenomenon in Au ($Z=79$). This is a case where relativistic effects should be dominant.

Nondipole Photoelectron Asymmetries

R. W. Dunford, E. P. Kanter, B. Krässig, S. H. Southworth, L. Young, L. A. LaJohn¹, R. H. Pratt¹, R. Guillemin², O. Hemmers², D. W. Lindle², R. Wehlitz³, N. L. S. Martin⁴

Photoionization of atoms and molecules is being studied through measurements and theoretical calculations of nondipole interactions on photoelectron angular distributions. Interference between photoionization amplitudes for electric-dipole, electric-quadrupole and higher-order terms are characterized by photoelectron asymmetries with respect to the direction of the photon propagation vector. We have measured nondipole asymmetries as functions of photon energy in studies of inner-shell photoionization using hard x rays at Argonne's Advanced Photon Source (APS) and in studies of valence-shell photoionization using VUV radiation at Wisconsin's Synchrotron Radiation Center (SRC).

At the APS, Kr 1s asymmetries were measured over 11-8000 eV kinetic energy and agree well with both full multipole relativistic calculations and nonrelativistic first-order retardation calculations. Deviations of the measured asymmetries from predictions of the point-Coulomb retardation correction confirm the importance of screening on the continuum-wave normalizations and phase shifts. The nondipole asymmetries of Br *K*-shell photoelectrons from Br₂ and BrCF₃ were measured over the 20-1000 eV kinetic energy range and compared with first-order calculations for atomic Br 1s. Only small deviations are observed between the measured asymmetries and the calculations for atomic Br, in contrast with the strong extra-atomic asymmetries measured and calculated for the N₂ *K*-shell in the soft x-ray regime. The ratio of photon wavelength to internuclear distance is identified as a factor in explaining these contrasting results.

At the SRC, nondipole asymmetries of He 1s and Xe 5s were measured over the photon energy range 30-150 eV. Even at such low photon energies nondipole asymmetries are distinctly present, particularly in spectral regions where many-electron interactions are important. In the region of the autoionizing double-excitation resonances in He, the nondipole asymmetry exhibits strong variations caused by variations in the relative contributions of the dipole and quadrupole channels, and the Fano resonance parameters of the 2p² ¹D quadrupole autoionization resonance were determined. The nondipole asymmetry of Xe 5s varies from positive to negative values in the region of the 5s Cooper minimum in qualitative agreement with recent calculations but appears to differ from the predictions in the absolute magnitude.

Plans for future experiments include use of a soft x-ray beamline at the APS to investigate extra-atomic effects on the nondipole asymmetries of molecules. To continue studies of the relatively small asymmetries measured on valence electrons, the sensitivity and stability of the spectrometer system will be optimized. Higher members of the autoionizing double-excitation series in He will then be studied at the SRC.

Threshold Krypton Charge-State Distributions Coincident with *K*-Shell Fluorescence

G. B. Armen⁵, E. P. Kanter, B. Krässig, J. C. Levin⁵, S. H. Southworth, and L. Young

Krypton ion charge-state spectra (Kr¹⁺ to Kr⁸⁺) were measured in coincidence with *K*-shell fluorescence following photoionization as a function of absorbed photon energy across the *K* edge. The partial yields for lower charge states show a resonance peak near threshold superimposed on a smoothly rising edge, while the yields for higher charge states show only the

smooth rise. The resonance effects near threshold arise from cascade decay of $[2p]np$ excited states produced by $[1s]np$ intermediate states. A simple model was developed which accounts for these features by incorporating both the threshold excitation and cascade behavior of spectator electrons. Fits to the model yield values of average "sticking probabilities" for each charge state, i.e., probabilities that an initially excited Rydberg electron survives the ionizing cascade decay steps and remains bound to the ionic core. The sticking probabilities were found to increase with increasing charge state, a result that is consistent with a decreasing number of states available for participant Auger decay.

In followup experiments on cascade decay of K-shell vacancies in Kr, Xe, and $CBrF_3$, the decay pathways were further distinguished by recording ion charge-state spectra in coincidence with specific x-ray fluorescence diagram lines.

Two-Photon Decay

R. W. Dunford, E. P. Kanter, Th. Stöhlker⁶, P. H. Mokler⁶, A. Warczak⁷

Two-photon decay provides a means for studying the entire structure of an atom since calculations require a sum over a complete set of intermediate states and both energy levels and wavefunctions must be understood. In the past we have studied this process by comparing the shapes of two-photon decay in He-like Ni ($Z=28$) and at high- Z in He-like Au ($Z=79$). The Au data are sensitive to the radiative corrections to two-photon decay. Our current plans are to study two-photon decay of inner-shell vacancy states produced by photoionization of neutral atoms. This work will be done at Argonne's Advanced Photon Source where we will be able to study the process in very heavy atoms such as gold or uranium. Two-photon decay produces a broad continuum below the transition energy of the decay. In atomic systems with one K vacancy, two-photon decay has to compete with the fast, allowed decay modes in singly ionized atoms. The wings of the characteristic lines are orders of magnitude larger and strongly interfere with two-photon decay. However, coincidence detection of the two photons provides a powerful means for picking out two-photon decay. In our measurements we plan to study the two photon transitions $2s \rightarrow 1s$, $3s \rightarrow 1s$, $3d \rightarrow 1s$ and $4s/d \rightarrow 1s$ in gold. These data can be compared to our earlier results on heliumlike gold and will provide new, much-needed tests of relativistic many-body theory in the heaviest neutral atoms.

K-shell Excitation of He-like Ions

R. W. Dunford, E. P. Kanter, Th. Stöhlker⁶, P. H. Mokler⁶, H. G. Berry⁸, S. Cheng⁹, L. J. Curtis⁹,
and A. E. Livingston⁸

Collisions between highly-charged ions and atoms are of importance in a wide range of applications from interactions of charged particles with solids to the study of radiation damage in biology. One area where more study is needed is that of state-specific projectile excitation in the intermediate energy regime where the orbital velocity of the projectile electron is similar to the velocity of the ion. We are nearing completion of a study of projectile excitation at intermediate energies at ATLAS using both foil and gas targets. The experiment measured the cross sections for excitation from the ground state of He-like Ni ions to the $n=2$ excited states. The results show that direct excitation to the triplet He-like states is important in excitation by both gas and foil

targets. This is significant since excitation to this level from the $1s2s\ ^1S_0$ ground state requires a spin flip and is forbidden in the lowest order theories currently available.

¹University of Pittsburgh, ²University of Nevada, Las Vegas, ³Synchrotron Radiation Center, Stoughton, WI, ⁴University of Kentucky, ⁵University of Tennessee, ⁶GSI, Darmstadt, Germany, ⁷Jagiellonian University, Poland, ⁸University of Notre Dame, ⁹University of Toledo

Publications 2000 – 2002

Photoexcitation of a Dipole-Forbidden Resonance in Helium, B. Krässig *et al*, Phys. Rev. Lett. **88**, 203002 (2002)

Double Electron Capture in Relativistic U^{92+} Collisions Observed at the ESR Gas-Jet Target, G. Bednarz *et al*, Physica Scripta **T92**, 429-431 (2001).

Strong Evidence for Enhanced Multiple Electron Capture from Surfaces in 46 MeV/u Pb^{81+} Collisions with Thin Carbon Foils, H. Bräuning *et al*, Phys. Rev. Lett. **86**, 991-994 (2001).

Multiple Electron Capture by 46 MeV/u Pb^{81+} Ions from Solid Targets, H. Bräuning *et al*, Physica Scripta **T92**, 43-46 (2001).

The Two-Photon Decay of the $1s2s\ ^1S_0$ -like States in Heavy Atomic Systems, P. H. Mokler and R. W. Dunford, Fizika A **10**, 105-112 (2001).

Near-Threshold Photoionization of Hydrogenlike Uranium Studied in Ion-Atom Collisions via the Time-Reversed Process, T. Stöhlker *et al*, Phys Rev Lett. **86**, 983-986 (2001).

Radiative Electron Capture Studied for Bare, Decelerated Uranium Ions, T. Stöhlker *et al*, Physica Scripta **T92**, 432-434 (2001).

Corrections to the usual x-ray scattering factors in rare gases: experiment and theory, L. Young *et al*, Phys Rev A **63**, 052718 (2001).

Nuclear Excitation by Electronic Transition in ^{189}Os , I. Ahmad *et al*, Phys. Rev. C **61**, 051304 (2000).

Evolution of Beam-Foil-Excited Rydberg States at Femtosecond Time Scales, E. P. Kanter *et al*, Phys. Rev. A **61**, 042708 (2000).

$1s$ Lamb Shift in Hydrogenlike Uranium Measured on Cooled, Decelerated Ion Beams, T. Stöhlker *et al*, Phys. Rev. Lett. **85**, 3109-3112 (2000).

Simultaneous Excitation and Ionization of He-like Uranium Ions in Relativistic Collisions with Gaseous Targets, T. Ludziejewski *et al*, Phys. Rev. A **61**, 052706 (2000).

Ultracold Atoms: Applications

R. W. Dunford, S.H. Southworth, L. Young
Argonne National Laboratory, Argonne, IL 60439

dunford@anl.gov, southworth@anl.gov, young@anl.gov

The unique properties of cooled and trapped neutral atoms enable applications in a variety of fields. The highly-localized, low-momentum spread sample of ultracold atoms provides a well-defined target for ionization studies. Extreme isotopic selectivity combined with efficient capture probability has spurred the development of an ultrasensitive trace isotope analysis technique based upon counting individual atoms, ATTA (atom trap trace analysis). In addition, ultracold atoms are ideal for precision spectroscopy as the absence of Doppler spread simplifies the lineshape. We are currently using cooled and trapped atoms in these applications.

Electron-Impact Double and Triple Ionization of Lithium

M.T. Huang, L. Zhang, S. Hasegawa¹, S.H. Southworth, L. Young

Electron-impact ionization is a fundamental collision process in atomic physics. Because of importance from both applied and theoretical viewpoints, it has been the subject of study for many years. Nevertheless, the predictive power of theory remains limited. Theoretical challenges are great, as even the simplest process, electron-impact single ionization, yields a final state with three charged particles in the continuum. Over the past decade, considerable theoretical progress has been made on electron-impact single ionization based on non-perturbative methods, where calculations in the electron + hydrogen system reproduce the observed ionization cross-sections to within experimental error bars over a wide energy range. For atoms more complex than hydrogen, the agreement between theory and experiment for total ionization cross sections is somewhat less impressive, particularly when target electrons occupy more than one shell, e.g. metastable He ($1s2s\ ^3S$) and the alkalis. For electron-impact double-ionization, an *ab initio* theoretical understanding is starting to emerge, although the emphasis has been on the observed angular correlation patterns observed in $(e,3e)$ experiments rather than the value of the absolute cross-section. To our knowledge, only one *ab initio*, fully quantal work has calculated the double-to-single ionization ratio, despite the existence of rather reliable data in, e.g., the two-electron atom helium. For triple ionization, the *ab initio* theoretical work is non-existent, and semi-empirical calculations are used for estimates. Lithium holds special interest as the simplest three-electron system and the natural progression to more complex systems.

We used lithium atoms confined in a magneto-optical trap, MOT, as a target to study electron-impact ionization by ion time-of-flight (TOF) spectrometry. The trapped atom sample combined with an ion imaging time-of-flight spectrometer offers some advantages for these measurements: 1) elimination of dimers and impurities, 2) enhanced control of ion collection efficiency and 3) reduction of background through position sensitive cuts on the data. The $\text{Li}^{2+}/\text{Li}^+$ production cross section ratio by electron impact was measured for electron energies ranging from $\approx 200\text{eV}$ to $\approx 1500\text{eV}$. The measured ratios range from ≈ 0.1 to 0.4% and appear to reach a plateau value of $\approx 0.37\%$ above 500 eV . The $2+/1+$ ratios were found to be systematically lower than the one earlier measurement and those predicted by semi-empirical formulas.

Recently we have observed the triple ionization of lithium by electron impact. The cross-section was found to be surprisingly small: two orders of magnitude smaller than the semi-empirical calculation, which predicts a factor of ten difference between Li^{3+} and Li^{2+} . Just observing the triple ionization channel required substantial improvements to the TOF spectrometer and MOT number. Here the MOT played a critical role as the H_2^+ , the wings of which form the major background interference with Li^{3+} , was reduced substantially over what is typically obtained in thermal atomic beams. The observed cross-section ratios at an electron impact energy of 1000 eV [$\text{Li}^{3+}/\text{Li}^{2+}/\text{Li}^+ \approx 4 \times 10^{-6} : 4 \times 10^{-3} : 1$] are smaller than those observed in photoionization by roughly a factor of 10. The ratio of triple-to-double ionization in lithium, $\approx 10^{-3}$, is substantially smaller than in any other atom observed to date. We hope that these results will motivate *ab initio* calculations for this relatively simple system.

Optical Production of Metastable Krypton

L. Young, D. Yang², R. W. Dunford

Metastable rare gas atoms are useful in a range of important applications such as cold collision physics, optical lattices, atom lithography, rare isotope detection and Bose-Einstein condensation. Such atoms are produced by direct extraction from DC or rf discharges or by excitation of an atomic beam via electron bombardment. Metastable fractions in such beams are typically less than 0.1% and this can be a severe limitation on the applications which utilize these beams. To address this issue, we are investigating an optical method for excitation of the 5s, J=2 metastable level of Kr ($5s[3/2]_{J=2}$) which has the potential to significantly increase the metastable fraction available. The technique will also work for other rare gases. In the scheme, an ultraviolet lamp is used to create a population of Kr atoms in the $5s[3/2]_{J=1}$ level in a gas cell. The excited atoms are then pumped to the $5p[3/2]_{J=2}$ level, using 819-nm light from a Ti:Sapphire laser, from which they decay to the metastable state with a branching ratio of 77%. We demonstrated this method by production of metastable Kr in a gas cell. The metastable atoms were identified by observing the 760 nm radiation emitted in the decay of the atoms to the metastable state. We were able to model our experiment using a Monte-Carlo simulation that accounts for the multiscattering of the uv photons in the cell. Based on these experiments and simulations, which show a conversion efficiency of UV photons to metastable atoms of $\approx 10\%$, we have designed and built an apparatus to produce an optically pumped atomic beam of metastable Kr atoms and have begun initial tests with this system. Our goal is to obtain a metastable flux of about 10^{14} metastables/second and a metastable fraction of better than 1%.

Atom Trap Trace Analysis

X. Du³, K. Bailey³, Z.-T. Lu³, I. Moore³, P. Mueller³, T. P. O'Connor³, L. Young

We have developed a new method for ultrasensitive trace isotope analysis based upon laser manipulation of neutral atoms, atom trap trace analysis (ATTA). In this method, individual atoms are counted while residing in a magneto-optical trap (MOT). With no observed contamination from neighboring isotopes, the selectivity appears to be limited only by the number of atoms that can be sorted during a finite operation time and has been demonstrated at the ppt level. Key technical features are an efficient capture rate and the ability to detect a single atom in the MOT. Applications involving ^{85}Kr and ^{81}Kr should be of particular interest to the

DOE. Trace detection of ^{85}Kr ($t_{1/2} = 10.5$ yrs) can be used to monitor nuclear fission activities. ^{81}Kr ($t_{1/2} \approx 229$ kyrs) is a cosmogenic nuclide and homogeneously distributed over the earth. Its concentration is unaltered by human activities because stable ^{81}Br shields ^{81}Kr from the neutron-rich isotopes that are produced in nuclear fission. Thus, ^{81}Kr is ideal for dating polar ice and groundwater in the 100 kyr range.

This past year, we have improved our atom-counting system with the goal of realizing ^{81}Kr -dating of ancient groundwater and polar ice. The counting efficiency initially demonstrated was 2×10^{-7} . By implementing a RF-driven discharge source of metastable krypton atoms and by adding a gas recirculation system, the counting rate was increased by one order of magnitude, and the counting efficiency by at least three orders of magnitude. These improvements will allow ^{81}Kr -dating of ancient groundwater samples. The calibration of the system is in progress. Collaborating with an international team of geologists, we plan to determine the age of water samples in Nubian Aquifer of Egypt.

In addition, an apparatus for detection of ^{41}Ca using ATTA has been commissioned, with single atom sensitivity demonstrated for the stable isotopes. The applications for ^{41}Ca ($t_{1/2} = 103,000$ years) and natural abundance of $10^{-15} - 10^{-14}$ include medical use as a tracer for osteoporosis, nuclear activity monitoring and radioisotope dating of ancient bones. A slightly modified system could be of interest to DOE as a trace analyzer for ^{90}Sr , a fission product.

¹Tokyo University, ²Peking University, ³Physics Division, Argonne National Laboratory

Publications 2000-2002

Measurements of the electron-impact double-to-single ionization ratio using trapped lithium

M.T. Huang, L. Zhang, S. Hasegawa, S. H. Southworth, L. Young

Phys. Rev. A **66**, 012715:1-7 (2002).

Optical production of metastable krypton

L. Young, D. Yang, R.W. Dunford

J. Phys. B **35**, 1-8 (2002).

A Beam of Metastable Krypton Atoms Extracted from an RF-Driven Discharge

C.Y. Chen, K. Bailey, X. Du, Y.M. Li, Z.-T. Lu, T.P. O'Connor, L. Young, G. Winkler

Rev. Sci. Instr. **72**, 271-272 (2001).

Atom Trap Trace Analysis

Z.-T. Lu, K. Bailey, C.Y. Chen, X. Du, Y.-M. Li, T.P. O'Connor, L. Young

Atomic Physics 17, Proceedings of the 17th International Conference on Atomic Physics
(Eds. E. Arimondo, P. DeNatale, M. Ingusio, copyright 2001) p.367-381.

ATTA -- a new method of ultrasensitive isotope trace analysis

K. Bailey, C.Y. Chen, X. Du, Y.M. Li, Z.-T. Lu, T. P. O'Connor, L. Young

Nuclear Instruments and Methods B**172**, 224-227 (2000).

Atom Trap Trace Analysis

K. Bailey, C.Y. Chen, X. Du, Y.M. Li, Z.-T. Lu, T.P. O'Connor and L. Young

Hyperfine Interactions **127**, 515-518 (2000).

Generation and Characterization of Attosecond Pulses

L. F. DiMauro¹, K. C. Kulander², I. A. Walmsley³ and R. W. Boyd³

¹*Chemistry Department, Brookhaven National Laboratory, Upton, NY 11973*

²*Lawrence Livermore National Laboratory, Livermore, CA 94551 and*

³*The Institute of Optics, University of Rochester, Rochester, NY 14627*

(Dated: August 28, 2002)

Introduction

High harmonic (HHG) radiation, which results from atoms interacting with an intense laser field, has the potential to produce pulses of light with unprecedented durations approaching the attosecond ($1 \text{ as} = 10^{-18} \text{ s}$) time-scale. Moreover, with high conversion efficiencies ($\approx 10^{-5}$) [1] in the XUV range and $\approx 10 \text{ \AA}$ [2] spectral content, HHG exhibits attractive traits for coherent XUV research. Within the past year, two separate confirmations [3, 4] of attosecond pulse durations from HHG have been reported. These experiments have inferred sub-femtosecond pulse durations (250 as) from modulations in photoelectron spectra. In addition, correlations measurements of HHG radiation have been performed [5, 6] using nobles gases as nonlinear media. Such elaborate techniques are a result of inadequate nonlinear materials in the VUV/XUV spectral region. These wavelength limitations can be circumvented using visible/UV harmonic radiation. By generating harmonics with an intense mid-infrared (MIR) light source, the resulting high harmonic spectrum has considerable (order ≤ 17) visible/UV content. As a result, standard temporal metrology, such as second-order-autocorrelation, can be employed to quantify harmonic pulse durations. Moreover, interferometric techniques, like spectral phase interferometry for direct electric-field reconstruction (SPIDER) [7], become feasible for complete characterization of harmonic radiation. By performing strong MIR field experiments in a scaled manner, extensions of these studies have direct analogs in the VUV/XUV regime.

Scaled Strong Field Interactions

Strong field experiments performed with different drive fields and atomic media may initially appear to have no direct correlation. However, if the experiments are carried out in a scaled manner analogies between dissimilar systems become apparent. A reasonable metric for scaling a strong field interaction is the Keldysh adiabaticity parameter (γ).

$$\gamma = (I_p/2U_p)^{1/2}, \quad (1)$$

$$U_p = 9.3[eV]I[10^{14}W/cm^2](\lambda[\mu m])^2; \quad (2)$$

The Keldysh parameter, which describes the ionization dynamics, relates the optical frequency to the electron tunneling rate as shown by (1), where I_p is the ionization potential of the atom and U_p is pondermotive (quiver) energy given by (2). In the case where $\gamma < 1$, the ionization is dominated by the tunneling of the electron through the field suppressed Coulomb potential into the continuum. This suggests either an intense or a low-frequency light source. In the alternate case of $\gamma > 1$, the ionization mechanism is multiphoton. With this view of ionization, systems that have a similar value for the Keldysh parameter should also exhibit similar dynamics. This allows "typical" HHG experiments performed with Ti:sapphire (high ω) lasers and rare gases (high I_p) to be compared to a MIR (low ω) alkali metal (low I_p) system. Table I compares our experimental conditions to those of a "typical" Ti:Sapphire study. Notice that the number of photons needed for ionization, n_i , is similar for both cases. However, the number of photons to the first excited state, n_e , and the number of photons to ionize the ionic ground state, n_i^+ , are different. Consequently, one could expect some differences due to the atomic structure. More details of such scaling have been reported in [8].

Characterizing High Harmonic Generation

As eluded to earlier, HHG from a strong MIR light source is an advantageous means for completely characterizing harmonic radiation. Our experiments are performed at nominal wavelength of $3.4 \mu m$ and intensities of approximately 2 TW/cm^2 . The linearly polarized MIR field is strongly focused to a confocal parameter of $\approx 2 \text{ mm}$ into a heat pipe containing vaporized Cs at 10 torr. We have confirmed harmonic production through order 17 (200 nm, our instrumental limit) with lower-order pulse energies nearing or exceeding a 100 pJ. Such pulse energies fulfill the minimum

TABLE I: Comparison of MIR-alkali experimental conditions to Ar-Ti:sapphire system.

Atom	λ (μm)	γ	I (TW/cm^2)	I_p (eV)	U_p (eV)	$h\nu/U_p$	n_e	n_i	n_i^+
Ar	0.8	1.0	130	15.8	8	0.20	8	11	18
Cs	3.6	1.0	1.6	3.9	2	0.18	4	11	73

TABLE II: Time-bandwidth products and scaling factors with corresponding pulse durations and bandwidths for harmonic orders 5 through 9.

Harm. order	$\Delta\tau$ (ps)	Δf (THz)	$\Delta\tau\Delta f$ TBWP	Measured Scaling	Perturb. Scaling
MIR	2.90	0.16	0.46	N/A	N/A
H5	1.35	0.74	1.00	2.11	$\sqrt{5}$
H7	1.05	0.94	0.90	2.77	$\sqrt{7}$
H9	0.88	1.16	1.02	2.86	$\sqrt{9}$

requirements (a few pJ) for second-order correlation techniques. As a result, autocorrelations measurements were achieved for harmonics 5 and 7. Since H9 is less than 400 nm, which is doubling limit of our nonlinear crystal, a cross-correlation measurement was performed between H9 and H5. These initial results were reported in [9]. More recently, harmonic pulse duration measurements coupled with bandwidth measurements have allowed for basic characterization of orders 5 through 9. We have found that H5 through H9 are all at least twice the Fourier-limit ($\Delta\tau\Delta\nu \approx 0.44$, Gaussian pulse). Nevertheless, we find that the harmonic pulse durations maintain a perturbative scaling with the fundamental drive field ($\tau_q \approx \tau_{fund}/\sqrt{q}$). These results are compiled in Table II. Following the analysis of [5], the magnitudes of the residual chirp in harmonic orders 5 through 9 were calculated from our measured results. These can be found in Table III. We compared our chirp data against that of an intensity-dependent phase which was proposed in [10] as a possible explanation. We find that this mechanism underestimates our results by 3 orders of magnitude. We have concluded that the increased harmonic bandwidths and the residual chirp are due to a blue-shift of the fundamental. A blue-shift arises from dispersion due to free electron during the ionization process. For a more complete analysis, we refer to our discussions in [11].

Enhancement of High Harmonic Generation

Due to the easy accessibility of the D_1 and D_2 transitions in alkali metals in visible light, harmonic generation from excited alkali atoms can be systematically studied. Theoretical studies [12] have predicted both an increase in yield and harmonic order from a coherently prepared superposition of ground and excited states. While our initial study is performed incoherently (fast dephasing time compared to the natural linewidth), we have quantified enhanced harmonic yields as great as 10^4 compared to the pure ground state yield. The experiment consists of pumping the D_2 (≈ 780 nm) line in a Rb jet with a stabilized diode laser. The $5S_{1/2}$ to $5P_{3/2}$ is easily saturated by our diode beam intensity of $10 \text{ mW}/\text{cm}^2$. Due to a near redundancy between the transition energies of the $5S_{1/2} \rightarrow 5P_{3/2}$ and the $5P_{3/2} \rightarrow 5D_{3/2}$, we excite approximately 1% of the Rb vapor into the $5D_{3/2}$ and/or the $6P_{1/2}$ ($5D_{3/2}$ fluoresces to $6P_{1/2}$). It appears that our measured enhancement is entirely due to one or both of these states not the $5P_{3/2}$ state. Nevertheless, the measured enhancement of 10^4 is real and very robust. Furthermore, we have measured increased harmonic bandwidths as large as a factor of 3 from the excited Rb system. If compressible, the excited system would be useful for generation of even shorter harmonic pulse durations.

Attosecond XUV Metrology

As addressed earlier, standard pulse metrology is limited to the NIR/visible/UV spectrum, a result of unsuitable optical materials below 200 nm. Therefore, characterizing XUV radiation becomes problematic. We have theorized a self-referencing, spatially encoded method, that has both attosecond sensitivity and XUV bandwidth. The technique

TABLE III: Calculated chirp values from measured pulse durations and bandwidths for harmonic orders 5 through 9.

Harmonic Order	Negative Chirp (10^{27} 1/s ²)	Positive Chirp (10^{26} 1/s ²)	Error (10^{26} 1/s ²)
H5	-3.7	14	0.8
H7	-2.2	7.4	0.6
H9	-1.4	4.3	3.1

(SEA-SPIDER, Spatially-Encoded Arrangement for SPIDER) is based on self-referencing spectral interferometry of photoelectrons produced from the simultaneously ionization of a noble gas by an XUV pulse and two spatially sheared optical pulses. The encoding of the phase information is achieved by interfering energy-shifted photoelectron wave packets in the spatial domain. The resulting electron interferogram contains information about the spectral phase structure of the attosecond pulse. The interferogram is related to the input XUV pulse field by

$$S(x, \omega) = \left| \int (E(x', \omega - \omega_0) + E(x', \omega - \omega_0 + \Omega)) e^{i\kappa x'} e^{i\frac{kx'}{2L} + i\frac{kx'}{L}x} dx' \right|^2 \quad (3)$$

where κ and k are the difference in the mean transverse wavevectors of the photoelectron wave packets and the mean deBroglie wavenumber of the electron wave packet, respectively. The resulting interferogram is processed using the same algorithms as a conventional SPIDER, except Fourier transforms are taken in the spatial coordinate. Along with the measured XUV spectrum, the pulse duration and phase can be reconstructed to within a constant phase and an arbitrary delay. The details of the device can be found in [13].

Future Plans and Considerations

Current limitations, such as relatively low harmonic pulse energies, have constrained our studies to correlation measurements for low-order harmonics. For interferometric measurements, like SPIDER, an increase in harmonic pulse energy is required. To meet this requirement, the peak MIR field power will be increased by approximately two orders of magnitude to 5 GW. This growth in field will be accomplished through two separate methods. First, the pulse duration will be decreased from the current value of ≈ 2 ps to 80 fs. Likewise, an additional amplification stage will be added to our Ti:Sapphire system (one component of MIR generation process) allowing for MIR energies nearing 400 μ J. This will be a four-fold amplification over the current MIR pulse energy. Through the increase in participating atoms, a result of the enlarged confocal parameter, harmonic production should increase by nearly 2000 times, limited only by the gas region. Furthermore, relaxing the strong focusing requirement should also enhance the phase-matching condition. With a saturation intensity of 8×10^{13} W/cm², Xe also becomes a viable harmonic medium under the new MIR field parameters. Under these conditions, the field can impart over 100 eV of energy to a free electron. This leads to a cut-off harmonic of approximately 30 \AA (water window 40 \AA) or a harmonic order greater than 1000. With this increased harmonic yield, it would be possible to construct and characterize a light field composed of the sum of different harmonic orders. Since orders 17 and below all lie in the visible/UV spectrum, characterizing these fields with a SPIDER apparatus is practical. Additionally, we plan the construction a self-referencing, spatially encoded apparatus, allowing for direct characterization of attosecond pulses.

Conclusion

Using visible/UV harmonics from a strong MIR field is a practical means for studying the physics of high harmonic generation. By employing standard pulse metrology, we have measured harmonics (orders 5 through 9) which are twice the Fourier-limit. One proposed explanation, such as an intensity-dependent, phase fails to account for the magnitude of the residual chirp, while a blue-shifted fundamental yields an accurate description. Furthermore, by generating harmonics from excited Rb atoms, we have quantified enhanced yields of the order of 10^4 . These harmonics have increased bandwidths, which should allow for shorter pulse durations compared to ground state harmonics. By performing our experiments in a scaled manner, these results have direct analogies to more widely performed HHG experiments. We foresee the systematic construction of arbitrary harmonic fields by summing various harmonic orders. Given the limitations of current metrology, we are looking for new techniques to characterize XUV attosecond

radiation. This work has facilitated the understanding of HHG radiation and its possible extensions into attosecond regime.

-
- [1] E. Constant *et al.*, Phys. Rev. Lett. **82**, 1668 (1999).
 - [2] Z. H. Chang *et al.*, IEEE J. Sel. Top. QEX, **4**, 266 (1998).
 - [3] P. M. Paul *et al.*, Science, **292**, 1689 (2001).
 - [4] M. Hentschel *et al.*, Nature, **414**, 509 (2001).
 - [5] T. Sekikawa *et al.*, Phys. Rev. Lett., **83**, 2564 (1999).
 - [6] T. Clover *et al.*, Phys. Rev. A, **63**, 023403 (2001).
 - [7] C. Iaconis and I. A. Walmsley, Opt. Lett., **23**, 792 (1998).
 - [8] B. Sheehy *et al.*, Laser Physics, **11**, 226 (2001).
 - [9] T. O. Clatterbuck *et al.*, J. Mod. Opt., *in press*.
 - [10] T. Sekikawa *et al.*, Phys. Rev. Lett., **88** 193902 (2002).
 - [11] T. O. Clatterbuck *et al.*, Phys. Rev. A, *submitted*.
 - [12] F. Gauthey *et al.*, Phys. Rev. A, **52**, 525 (1995).
 - [13] C. Dorrer *et al.*, Phys. Rev. Lett., *submitted*.

Publications resulting from this research

1. "Calculations of Strong Field Multiphoton Processes in Alkali Metal Atoms", K. J. Schafer, M. B. Gaarde, K. C. Kulander, B. Sheehy and L. F. DiMauro, in *Multiphoton Processes: ICOMP VIII*, eds. L. F. DiMauro, R. R. Freeman and K. C. Kulander (AIP, New York), 45 (2000).
2. 2000 "Strong Field Atomic Physics in the Mid-Infrared", , B. Sheehy, J. D. D. Martin, T. O. Clatterbuck, D. W. Kim, L. F. DiMauro, P. Agostini, K. J. Schafer, M. B. Gaarde and K. C. Kulander, in *Multiphoton Processes: ICOMP VIII*, eds. L. F. DiMauro, R. R. Freeman and K. C. Kulander (AIP, New York), 59 (2000).
3. "Strong Species Dependence of High Order Photoelectron Production in Alkali Metal Atoms", M. B. Gaarde, K. J. Schafer, K. C. Kulander, B. Sheehy, Dalwoo Kim and L. F. DiMauro, *Phys. Rev. Lett.* **84**, 2822 (2000).
4. "Atomic Dynamics at Long Wavelengths", B. Sheehy, J. D. D. Martin, T. Clatterbuck, Dalwoo Kim, L. F. DiMauro, K. J. Schafer, M. B. Gaarde and K. C. Kulander, in *Advances in Multiphoton Processes and Spectroscopy, Volume 14. Quantum Control of Molecular Reaction Dynamics*, eds. R. J. Gordon and A. Fujimura (World Scientific Press, Singapore), 203 (2001).
5. "Strong Field Physics in a Scaled Interaction", B. Sheehy, T. O. Clatterbuck, C. Lyngå, J. D. D. Martin, Dalwoo Kim, L. F. DiMauro, K. J. Schafer, M. B. Gaarde, P. Agostini and K. C. Kulander, *Laser Physics* **11**, 226 (2001).
6. "Absorptionless Self-Phase Modulation in a Dark-State Electromagnetically Induced Transparency System", V. Wong, R. W. Boyd, C. R. Stroud, Jr., R. S. Bennink, D. L. Aronstein, and Q.H. Park, *Phys. Rev. A* **65**, 013810, (2001).
7. "Scaled Intense Laser-Atom Physics: The Long Wavelength Regime", T. O. Clatterbuck, C. Lyngå, P. Colosimo, J. D. D. Martin, B. Sheehy, L. F. DiMauro, P. Agostini and K. C. Kulander, *J. Mod. Optics*, accepted.
8. "Self-referencing, spatially encoded spectral interferometry for the characterization of attosecond electromagnetic pulse", Christophe Dorrer, Eric Cormier, Ian A. Walmsley and Louis F. DiMauro, submitted to *Phys. Rev. Lett.* (2002).
9. "Theory of Relativistic Optical Harmonic Generation", Q-Han Park, Robert W. Boyd, J. E. Sipe and Alexander L Gaeta, accepted for publication in the *IEEE Journal of Selected Topics in Quantum Electronics*, (2002).

Structure and Dynamics of Atoms, Ions, Molecules, and Surfaces: Atomic Physics with High Velocity, Highly Charged Ion Beams

Patrick Richard, J. R. Macdonald Laboratory, Kansas State University

Manhattan, KS 66506 [richard@phys.ksu.edu; (785)532-6783]

The goals of this part of the J. R. Macdonald Laboratory, JRML, program are 1) to study double and triply excited states formed in high velocity, highly charged ion-neutral target collisions by state selective electron-ion resonances and by triple electron capture and 2) to study the dynamics of one and two electron processes in which electrons from bound neutral target states are brought to continuum and bound states of high velocity, highly-charged ions.

Doubly and Triply Excited States in High Z Few Electron Ions

H. Aliabadi, E. P. Benis, P. Richard, M. Zamkov, H. Tawara, T. G. Lee, C. D. Lin, T.J.M. Zouros (U of Crete, Greece), and Tom Gorczyca (Western Michigan U, Kalamazoo, MI)

We continue our investigation of doubly excited states of ions via electron resonant transfer and excitation in ion-atom collisions. The process is one in which a quasi-free target electron is captured into a resonant state of the projectile ion. The process is detected by observing the Auger electron emission from the resonant state at zero degrees in the laboratory frame. This process gives rise to 180° scattering when transformed to the center of mass. The projectile electron emission spectrum can be analyzed as an electron-ion collision system by including the effects of the Compton profile of the target electrons and the kinematical transformation. It can then be directly compared with electron-ion differential elastic and inelastic scattering calculations. We have successfully demonstrated that the Auger emission from C^{5+} , N^{6+} , O^{7+} , and $F^{8+} + H_2$ collisions, when analyzed in this way, gives very good agreement with R-Matrix calculations for $C^{5+}(1s) + e^- \rightarrow C^{4+}(2p^2, ^1D) \rightarrow C^{5+}(1s) + e^-$ (and similarly for N^{6+} , O^{7+} , and F^{8+}) resonance elastic scattering [Publ. #6]. We have recently extended these measurements to the complete $2nl$ manifold of resonance states for B^{4+} and B^{3+} projectiles. R-Matrix calculations are in good agreement for the $2p^2, ^1D$ state as indicated above and in less good agreement for the case of three electron resonance states (e.g. $1s2p^2, ^2D$).

We have also measured the inelastic scattering channel of the ion-electron scattering process by observing the Auger decays to the $2s/2p$ final states. The first manifold above the inelastic scattering threshold is the $3/3l'$ configuration. The states in the $3/3l'$ configuration decay primarily via the inelastic scattering channel. The experiment was done for $F^{8+}(1s) + e^- \rightarrow F^{7+}(3/3l') \rightarrow F^{8+}(2s/2p) + (e^-)$. The outgoing electrons are very low in energy in the center of mass, but in the lab frame are observed at energies above and below the projectile electron cusp energy, i. e. electrons moving with the velocity of the beam. The electron group at energies greater than the cusp energy corresponds to 180° scattering in the c.m. frame and the electron group at energies less than the cusp energy corresponds to the 0° scattering in the c.m. frame. We have recently extended the measurements to B^{4+} projectiles. The resonances in this case are poorly resolved, however the gross structural features are reproduced by R-matrix calculations. These experiments are extremely time consuming. The inelastic scattering experiments were performed in our double 45° parallel plate analyzer.

with retardation between the analyzers. The experiments could be performed much more efficiently using our high efficiency, high-resolution zero-degree off-axis hemispherical spectrometer with position sensitive detection on the image plane. Unfortunately we have encountered large electron backgrounds in the vicinity of the cusp, which have made these experiments impossible. We believe the background is from the scattering of the cusp electrons from the hemispheres of the analyzer. We are planning to solve this problem by introducing a high efficiency pre-analyzer to catch these unwanted electrons before they reach the position sensitive detector in the hemispherical analyzer.

In the process of studying these resonance states we noticed that for two-electron ion beams we could enhance the production of certain states by controlling the manner in which the beam was prepared. The effect is due to the $1s2s\ ^3S$ metastable component in the beam. We undertook a systematic study of the production of metastable ion beams, since what we discovered was that we could preferentially populate triply excited resonant states from the metastable beam component, e.g. $1s2s + e^- \rightarrow 2sn/nl'$ resonances. Below is a summary of these studies.

FIRST STUDY: The fraction of metastable ions in $B^3(1s^2\ ^1S; 1s2s\ ^3S)$ beams produced in collisions with thin-foil and gas targets has been measured as a function of the incident energy in the range of 0.85-9 MeV. This was done by comparing the electron yield of doubly excited states formed in the collision of B^{3+} with hydrogen and helium targets. Significant differences were observed in the energy dependence of the metastable fraction between production in foil and gas targets. It was shown that the production of $1s2s\ ^3S$ metastable ions in a foil yields a constant fraction over the investigated energy range, unlike the fraction of metastable $1s2s\ ^3S$ ions produced in collisions with gas targets, which strongly depends on the incident beam energy. A theoretical study of the processes contributing to the formation of the 3S metastable ions in collisions with foil and gas has been made. K-vacancy production in the ion-beam stripping process has been identified as a dominant mechanism and used to explain the observed difference in the energy dependence of the metastable fraction between production in collisions with gas and foil targets. A model is proposed for the calculation of the metastable fraction for He-like beams. [Publ. #4]

Z DEPENDENCE: Auger spectroscopy has been used to measure the fraction of metastable $1s2s\ ^3S$ ions in fast He-like B, C, N, O, F beams produced in collisions with thin carbon foils as a function of both the incident energy in the range of 0.5 to 2 MeV/u and the foil thickness in the range of 1-5 $\mu\text{g}/\text{cm}^2$. The method used for determination of the metastable fraction is based on measurements of the electron emission from the doubly excited states of Li-like ions formed in collisions of primary beams with hydrogen and helium targets. Some differences were observed both in the energy dependence and the absolute value of metastable fractions for different beams. In particular, the metastable content in C^{4+} ions produced in carbon foils was found to be significantly lower than that of other investigated beams. The observed deviation has been explained on the basis of K-vacancy sharing, which is known to have the highest probability for symmetric collisions. A model recently proposed for the calculation of the metastable fraction in He-like beams has been used to predict the metastable fraction of B^{3+} ions leading to good agreement with the experiment. [Publ. # 2]

NEW TECHNIQUE: An experimental technique for the determination of the metastable $1s2s\ ^3S$ fraction of two-electron ion beams has been reported. The method utilizes the electron

yields of the $1s2p^2\ ^2D$ and $1s2s2p\ ^4P$ doubly excited states, produced in collisions of two-electron ion beams with H_2 or He targets. The metastable beam fraction is determined in two successive measurements at the same beam energy but having different metastable fractions. The technique is applied to the case of B^{3+} ions in collisions with H_2 targets. The results are in good agreement with those from our recent paper on similar metastable fraction measurements [Publ. # 4]. The method can be safely applied in cases where the two different metastable fractions differ significantly. [Publ. # 3]

PRODUCTION OF TRIPLY EXCITED STATES: Triply excited states of three-electron ions have been produced by resonant transfer excitation (RTE) in metastable two-electron-ion-beam— H_2 collisions. Measurements of the Auger-electron emission in the direction of the ion beam is used to determine the absolute cross sections for formation of the triply excited states and the branching ratios of the corresponding elastic and inelastic electron scattering channels. The results are compared to existing theoretical calculations of the Auger decay rates. Accurate measurements of the double differential cross sections are made on the basis of the known metastable ion beam fractions and known cross sections for RTE from the ground-state component of the beam. The system investigated is $B^{3+}(1s2s\ ^3S) + H_2$ leading to the $B^{2+}(2s2p^2\ ^2D)$ resonance that decays to $B^{3+}(1s2s\ ^3S)$, the elastic scattering channel and to $B^{3+}(1s2s\ ^1S)$ and $B^{3+}(1s2p^3P)$, two inelastic scattering channels. [Publ. # 1]

At this point in our research we observed that we could readily populate doubly and triply excited states in triple capture measurements. The first experiment involved producing states of the $1s2l2l'$ manifold. A summary of this study is given below. We later figured a way to populate more exotic and interesting triply excited manifolds, in particular the $2p^3$ states. See invited abstract by P. Richard in this conference.

TRIPLE CAPTURE: Doubly excited KLL states were populated by triple electron capture in collisions of fast ($v = 4.5-6.6$ a.u.) C^{6+} ions with Ar atoms. Measurements of the Auger electron emission in the direction of the ion beam was used to determine the absolute single differential cross sections for the triple electron capture to all autoionizing KLL states. The results were compared with cross sections calculated within the independent particle model, in which the simultaneous capture of all three-target electrons was assumed. Single electron capture probabilities, employed by the model, were calculated using the two-center semiclassical close-coupling method, based on an atomic orbital expansion. In order to allow comparison of the measured zero-degree differential cross sections with calculated total cross sections, the Auger electron emission from the doubly excited KLL states was assumed isotropic. Model calculations were found to be in a good agreement with the experimental data. The adequate description of the triple electron capture by the model implies that the projectile screening and electron-electron correlation effects in multiple electron capture are significantly reduced in fast highly charged ion-atom collisions.

Study of One- and Two-Electron Processes in Ion-Atom Collisions: Single Capture and Transfer Ionization, *R. Unal, P. Richard, N. Woody, E.P. Benis, I. Ben-Itzhak, C. L. Cocke, M. J. Singh, H. Tawara, C. D. Lin, and T. G. Lee.*

We have investigated the charge state and energy dependences of Transfer Ionization (TI) and Single Capture (SC). The main emphasis of this research is to provide reliable measured cross sections that can be compared with new state of the art calculations. The collision

systems studied are $F^{(4-9)+}$ ions interacting with helium produced in a collimated supersonic jet. The measurements were made for beam energies between 0.5 and 2.5 MeV/u, which corresponds to projectile velocities between 6 and 10 au. A recoil ion momentum spectrometer was used to separate TI and SC based on the longitudinal momentum transfer as well as the time-of-flight of the recoil ions. The ratio, σ_{TI}/σ_{SC} , was accurately obtained by this method, and the individual cross-sections for the cases of bare and hydrogen-like fluorine ions were determined by using the measured ratios and the previously measured total charge exchange cross-sections.

New calculations were undertaken to compare with this accurate data set. Previous data obtained from time of flight of the recoil ions suffer from large errors and are not in agreement with the present data or previous calculations. A more consistent independent electron model, using the two-center semiclassical close coupling method was used to calculate the SC and TI cross sections. Good agreement was found between the new measurements and the new calculations.

Publications:

- 1) "Absolute Cross Sections and Decay Rates for the Triply Excited $B^+(2s2p^2\ ^2D)$ Resonance in Electron—Metastable-Ion Collisions,"
M. Zamkov, H. Aliabadi, E. P. Benis, P. Richard, H. Tawara, and T.J.M. Zouros,
Phys. Rev. A **65**, 032705-1 (2002).
- 2) "Fraction of Metastable $1s2s\ ^3S$ Ions in Fast He-like Beams ($Z=5-9$) Produced in Collisions with Carbon Foils,"
M. Zamkov, E. P. Benis, P. Richard, and T.J.M. Zouros
Phys. Rev. A **65**, 062706 (2002).
- 3) "Technique for the Determination of the $1s2s\ ^3S$ Metastable Fraction in Two-Electron Ion Beams,"
E. P. Benis, M. Zamkov, P. Richard, and T.J.M. Zouros
Phys. Rev. A **65**, 064701 (2002).
- 4) "Energy Dependence of the Metastable Fraction in $B^{3+}(1s^2\ ^1S, 1s2s\ ^3S)$ Beams Produced in Collisions with Thin-Foil and Gas Targets,"
M. Zamkov, H. Aliabadi, E. P. Benis, P. Richard, H. Tawara, and T.J.M. Zouros
Phys. Rev. A **64**, 052702 (2001).
- 5) "Two-center effect on low-energy electron emission in collisions of 1-MeV/u bare ions with atomic hydrogen, molecular hydrogen and helium.
I. Atomic Hydrogen,"
Lokesh C. Tribedi, P. Richard, L. Gulyas, M. E. Rudd, and R. Moshhammer
Phys. Rev. A **63**, 062723 (2001).
II: H_2 and He"
Lokesh C. Tribedi, P. Richard, L. Gulyás, and M.E. Rudd
Phys. Rev. A **63**, 062724 (2001)
- 6) "Electron Elastic Scattering Resonances in the Collisions of Fast Hydrogenic Ions with Molecular Hydrogen",
G. Toth, P. Zavodszky, C. P. Bhalla, P. Richard, S. Grabbe and H. Aliabadi,
Physica Scripta T **92**, 272 (2001).

Structure and Dynamics of Atoms, Ions, Molecules and Surfaces: Atomic Physics with Ion Beams, Lasers and Synchrotron Radiation

C.L.Cocke, Physics Department, J.R.Macdonald Laboratory, Kansas State
University, Manhattan, KS 66506, cocke@phys.ksu.edu

The goals of this aspect of the JRML program are (1) to explore mechanisms of ionization of atoms, ions and small molecules by intense laser pulses, (2) to investigate the dynamics of photoelectron emission from small molecules interacting with synchrotron radiation and (3) to identify and explain basic mechanisms whereby electrons are removed from simple systems in capture and ionization processes.

Recent progress and future plans:

1) Photoelectron diffraction from C_2H_2 , C_2H_4 and other small molecules, T.Osipov, C.L.Cocke (KSU), A.Landers (Western Mich.Univ.), R.Doerner, Th.Weber, L.Schmidt, A.Staudte, H.Schmidt-Boecking(U.Frankfurt), M.H.Prior(LBNL) Using beamlines 4.0 and 9.3.2 at the Advanced Light Source, we measure the correlated momentum-space distributions of photoelectrons and charged photofragments ejected when the K-shells of acetylene and ethylene, in addition to other small molecules, are photoionized. Photoions and photoelectrons are detected in coincidence. The diffraction patterns are shaped by the interaction of the electron with the instantaneous potential presented by the remaining nuclei and electrons of the molecule. The data provide an extremely comprehensive picture of the diffraction patterns, which in turn probe the overall charge density distribution within the molecule at the time of photoelectron emission. During the past year our work has centered on the analysis of diffraction patterns from C_2H_2 and C_2H_4 . Our attempt to identify in acetylene an f-wave shape resonance, well known in N_2 and CO but controversial for C_2H_n , was initially frustrated by the interesting observation that this molecule often undergoes isomerization to the vinylidene configuration before it dissociates. The separation of decays from the acetylene and vinylidene channels proved challenging, but has finally been resolved, with the following conclusions:

(1) Using only molecules decaying approximately along the polarization vector, the acetylene channel shows the expected f-wave structure near the predicted resonant energy (Fig. 1a). (2) The vinylidene channel shows that this structure is considerably washed out (Fig. 1b). This can only occur because the molecule rotates the bond angle after the photoelectron departs (a fast process) but before the dissociation is complete. This rotation angle provides information on the isomerization time: if the proton realignment occurs slowly, the correlation between axial dissociation and photoelectron emission will be entirely lost. Analysis of the data reveals that the rotation of the bond angle is very close to the minimum value consistent with the mass redistribution if the proton travels peripherally around the molecule to its new home. We deduce that the time scale for isomerization is no longer than approximately 100 fs.

For the case of C_2H_4 , no such complication occurs, and full photoelectron angular distributions have been taken as a function of photoelectron energy spanning the range of the expected shape resonance; a partial wave analysis is in progress. This work is part of the Ph.D.work of Timur Osipov. In addition to the completion of the analysis of this data, future plans include the experimental studies at the ALS of ionization-excitation of

D_2 below the double ionization threshold, photo double ionization of D_2 far enough above threshold (>150 eV) that interference between photoelectron waves from the two centers might be observable, and coincident high-resolution-Auger/photoelectron/KER experiments for which the limits of the validity of the two-step picture of Auger and dissociation process may be probed.

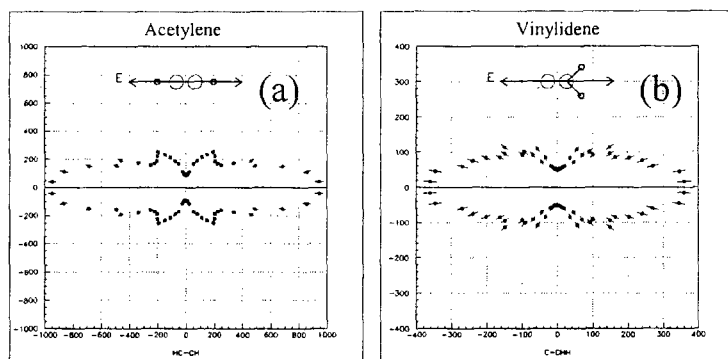


Fig.1. Angular distributions of photoelectrons from acetylene photoionized by 309 eV photons, for decay into the CH^+/CH^+ channel (a) and CH_2^+/C^+ channel (b). The electron emission angle is measured relative to the dissociation axis, which is required to lie near the polarization axis.

2) COLTRIMS measurements of electron capture from and low energy ionization of atomic H *E. Edgu-Fry and C. L. Cocke* The goal of this project is to establish an atomic hydrogen source compatible with use in a COLTRIMS experiment. It will be used to identify and characterize as cleanly as possible the process whereby a slow charged projectile promotes into the continuum an electron from a neutral target. For this case, the projectile velocity is sufficiently low that direct kinematic ionization is forbidden, and saddle-point electron promotion, in some form, is expected to be the major process. In addition, electron capture from atomic hydrogen by multiply charged ions will be studied. The use of the true one-electron target removes uncertainties associated with the comparison of one-electron dynamics calculations with data from multielectron targets. The major difficulty of this project has been to develop a COLTRIMS-compatible atomic hydrogen target. We finally have a working microwave discharge source which provides a jet of atomic hydrogen with an acceptable momentum spread. Using this target, electron capture from atomic hydrogen by Ar^{8+} projectiles has been studied, differential in both the Q-value of the reaction and the transverse momentum transfer. These data are under analysis. Preliminary data have been taken for the ionization of atomic H by protons. It is expected that the performance of this ion source will be adequate to enable the completion of this project. This project is the Ph.D. thesis work of Erge Edgu. The major future plan for this project is to complete the investigation of the mechanism for low energy ionization from atomic hydrogen over as extended a range of proton energies and as highly differential as possible.

3) Electron capture from D_2^+ by doubly charged projectiles *I. Reiser, H. Braeuning(U. Giessen), C.D. Lin, E. Sidky and C.L. Cocke*. The dependence of the cross section for electron capture from H_2^+ by the doubly charged projectiles He^{2+} , N^{2+} and Ar^{2+} on the angle between the beam axis and the molecular axis has been measured. The purpose of this experiment was to seek evidence for a "two-slit" interference of amplitudes for capture from the two centers. This description is meaningful to the extent that the target state can be described as a grade linear combination of 1s atomic orbitals centered on the two nuclei of D_2^+ , a good approximation in this context. Previous

experiments of this nature have been always clouded by the fact that the target was a multielectron target, and required a multielectron transition to reach a dissociating state of the molecule whereby the alignment of the molecule could be ascertained. The price one pays for the clean nature of the present experiment is that it is an ion-ion collision with the attendant low count rates and ion-optics difficulties. The experiment has now been completed. The results show a clear tendency for the capture to optimize for molecules aligned perpendicular to the beam axis. This result is qualitatively consistent with the expectations of the "two-slit" interference picture and is also confirmed by a model calculation based on a coherent combination of calculated atomic scattering amplitudes. This work was the thesis work of Ingrid Reiser and is being prepared for publication. No further work on this project is planned.

4) Identification of a rescattering mechanism in the double ionization of D₂ by intense laser pulses, T.Osipov, M.Benis, A.Weck, C.Wyant, B.Shan, Z.Chang and C.L.Cocke. It is now well established that so-called "non-sequential" ionization of neutral atoms by fs laser pulses with intensities in the range 10^{14} - 10^{15} watts/cm² can occur through a rescattering mechanism whereby the electron liberated in the single ionization process returns to the ion with sufficient energy to further ionize the singly charged ion through an (e,2e) process. The equivalent process in the ionization of molecules has not been seen until very recently, partially due to the fact that charge-resonance-enhanced ionization is usually the dominant process for multiple ionization. Two recent experiments have shed the light on this issue: 1) Evidence for rescattering in electron-H₂ collisions has been reported by Niikura et al. [Niikura, et al., *Nature* **417**, 917 (2002)], deduced from the detection of high energy protons emitted in a singles experiment from molecules aligned perpendicular to the laser polarization. (2) A high energy group of deuterons was seen for the double ionization of D₂ by Staudte et al.[ref.1, below], who, however, did not attribute this particularly to a rescattering process. Using the newly installed fs light source in the JRM laboratory, we have established, using linearly and circularly polarized light, that the high energy group reported by Staudte et al. is caused by a rescattering process (fig. 2). The energy distribution of the resulting deuterons is consistent with the picture that the vibrational wave packet created in the single ionization of the D₂ molecule, trapped in the gerade potential well of the D₂⁺ ion, is further ionized by the returning electron. This second step must itself proceed through excited states of the D₂⁺ ion, however, since the returning electron lacks sufficient energy to ionize the molecular ion in a single step. The observed deuteron energy distribution extends between limits consistent with the reflected energies from the turning points of the vibrational wave packet in the D₂⁺ gerade potential well.

Future plans in this area include:

(1) Continuing investigation of the rescattering process for molecules, including theoretical modeling of the process in collaboration with KSU and other theorists, with an eye to exploiting the generation of short electron bursts in the first step to explore the dynamics of the outgoing vibrational wave packet on a fs time scale. (2) Construction of a special ultra-high-vacuum COLTRIMS chamber suitable for investigating correlated momentum spectra of both electrons and heavy fragments from laser ionization of atoms and molecules; use of this chamber to carry out kinematically complete ionization studies of neutral targets. (3) Investigation of the ionization of H₂⁺ and singly charged noble gas beams from the KSU ECR source by intense laser pulses (with I. Benlitzhak).

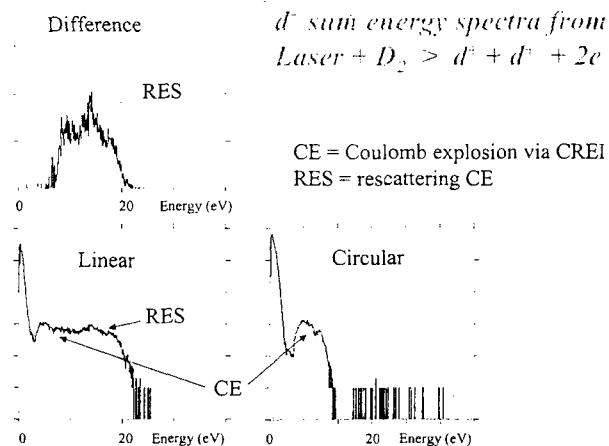


Fig. 2. Energy distributions of coincident d^+ ion pairs from double ionization of D_2 by 35 fs pulses with a peak intensity of 1.1×10^{14} watts/cm² for linearly and circularly polarized light.

PUBLICATIONS APPEARING IN 2001-2002 NOT PREVIOUSLY CITED

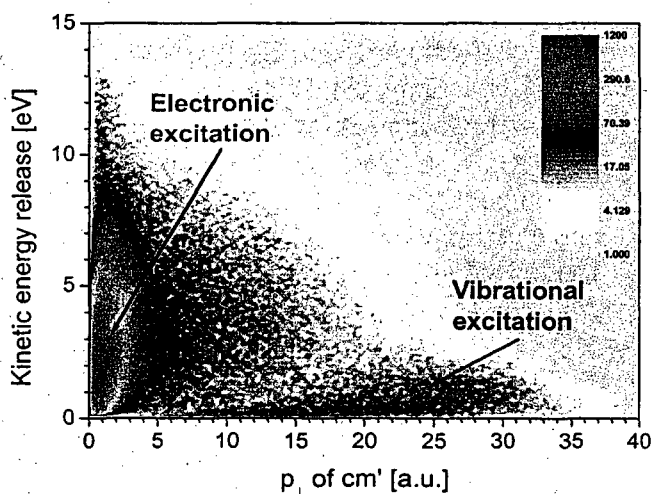
- 1) Observation of a nearly isotropic, high-energy Coulomb explosion group in the fragmentation of D_2 by short laser pulses, A. Staudte, C. L. Cocke, M. H. Prior, A. Belkacem, C. Ray, H. W. Chong, T. E. Glover, R. W. Schoenlein, and U. Saalmann, *Phys. Rev. A* **65**, 020703 (2002).
- 2) Intermediate energy ionization of helium by proton impact, E Edgü-Fry, C L Cocke, E Sidky, C D Lin and M Abdallah, *J. Phys. B: At. Mol. Opt. Phys.* **35** No 11 (14 June 2002) 2603-2612.
- 3) Mechanisms of Photo Double Ionization of Helium by 530 eV Photons, A. Knapp, A. Kheifets, I. Bray, Th. Weber, A. L. Landers, S. Schössler, T. Jahnke, J. Nickles, S. Kammer, O. Jagutzki, L. Ph. H. Schmidt, T. Osipov, J. Rösch, M. H. Prior, H. Schmidt-Böcking, C. L. Cocke, and R. Dörner, *Phys. Rev. Lett.* **89**, 033004 (2002).
- 4) Comparative study of the ground-state dissociation of H_2^+ and D_2^+ induced by ionizing and electron-capture collisions with He^+ at velocities of 0.25 and 0.5 a.u., W. Wolff, I. Ben-Itzhak, H. E. Wolf, C. L. Cocke, M. A. Abdallah, and M. Stöckli, *Phys. Rev. A* **65**, 042710 (2002).
- 5) Circular Dichroism in K-Shell Ionization from Fixed-in-Space CO and N_2 Molecules, T. Jahnke, Th. Weber, A. L. Landers, A. Knapp, S. Schössler, J. Nickles, S. Kammer, O. Jagutzki, L. Schmidt, A. Czasch, T. Osipov, E. Arenholz, A. T. Young, R. Díez Muiño, D. Rolles, F. J. García de Abajo, C. S. Fadley, M. A. Van Hove, S. K. Semenov, N. A. Cherepkov, J. Rösch, M. H. Prior, H. Schmidt-Böcking, C. L. Cocke, and R. Dörner, *Phys. Rev. Lett.* **88**, 073002 (2002).
- 6) Atomic dynamics in single and multi-photon double ionization: An experimental comparison, Th. Weber, M. Weckenbrock, A. Staudte, M. Hattass, L. Spielberger, O. Jagutzki, V. Mergel, H. Schmidt-Böcking, G. Urbasch, Harald Giessen, H. Bräuning, C. L. Cocke, M. Prior, and Reinhard Dörner D-79104 *Opt. Express* **8**, 368, (2001).
- 7) K-shell photoionization of CO and N_2 : is there a link between the photoelectron angular distribution and the molecular decay dynamics? Th Weber, O Jagutzki, M Hattass, A Staudte, A Nauert, L Schmidt, M H Prior, A L Landers, A Bräuning-Demian, H Bräuning, C L Cocke, T Osipov, I Ali, R Díez Muiño, D Rolles, F J García de Abajo, C S Fadley, M A Van Hove, A Cassimi, H Schmidt-Böcking and R Dörner, *J. Phys. B* **34**, 3669 (2001).

**Structure and Dynamics of Atoms, Ions, Molecules, and Surfaces:
Molecular Dynamics with Ion and Laser Beams**

*Itzik Ben-Itzhak, J. R. Macdonald Laboratory, Kansas State University
Manhattan, Ks 66506; ibi@phys.ksu.edu*

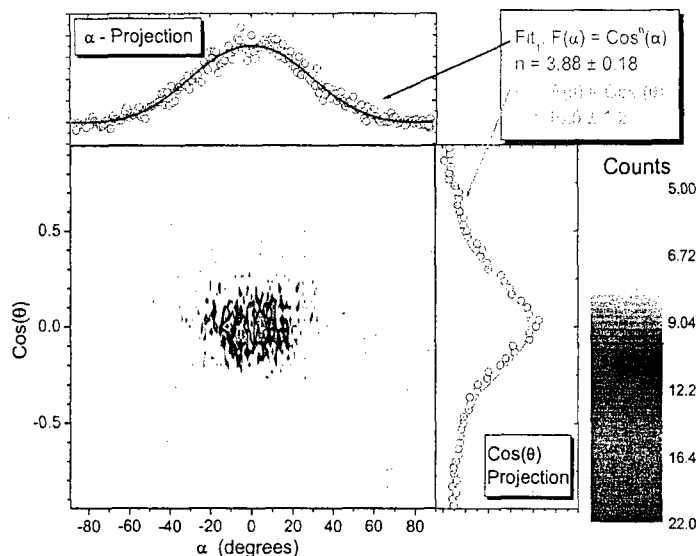
The goals of this part of the JRML program are to study the different mechanisms leading to molecular dissociation and charge exchange following fast collisions, slow collisions, or interactions with an intense short laser pulse.

Molecular dissociation imaging of collision-induced dissociation and dissociative capture in slow $H_2^+ + Ar$ (He) collisions, *D. Hathiramani, I. Ben-Itzhak, J.W. Maseberg, A.M. Saylor, M.A. Smith, and K.D. Carnes.* The dissociation of hydrogen molecular ions following a slow collision (keV) is studied by 3D momentum imaging of the fragments. The two main processes at this collision energy, collision-induced dissociation (CID, e.g. $H_2^+ + Ar \rightarrow H^+ + H + Ar$) and dissociative capture (DC, e.g. $H_2^+ + Ar \rightarrow H + H + Ar^+$), are experimentally separated in the method we recently developed. Using an electric field in the target region followed by a field free region, we managed to separate the CID from the DC in time. Thus, it is possible to evaluate the relative importance of these two processes, because both CID and DC are measured simultaneously. The same is true for the ratio of the two possible CID channels for heteronuclear molecules, i.e. $A^+ + B$ or $A + B^+$. Moreover, this method allows one to distinguish experimentally between two different mechanisms of CID as shown in the figure, and thus study each one of them in detail. The two mechanisms are (i) CID caused by an electronic excitation to a repulsive state, and (ii) CID caused by a vibrational/rotational excitation. These mechanisms differ in the kinetic energy release upon dissociation (KER) and the momentum transfer to the projectile (labeled as P in the figure). For the first the KER is relatively large while the momentum transfer to the projectile is very small. In contrast the latter is associated with small KER and very large momentum transfer. This distinguishes the present work from previous studies [1], in which no such separation was possible.



The electronic excitation to a repulsive state (mostly the first excited state of H_2^+) is the dominant CID mechanism for 3 keV $H_2^+ + Ar$ collisions. The angular dependence of this CID mechanism indicates that the dissociating fragments align along the beam direction for “short” molecular ions and perpendicular to the beam for “long” ones, as predicted by Green and Peek [2].

The vibrational/rotational dissociation mechanism shows very strong alignment effects, as shown in the figure. First, molecular ions aligned perpendicular to the beam velocity (i.e. $\theta = 90^\circ$) are much more likely to dissociate by this mechanism. Second, the dissociation velocity is preferentially aligned along the momentum transfer (i.e. $\alpha = 0^\circ$, where α is the angle between the dissociation velocity in the x-y plane and the direction of the transverse momentum transfer). The angular distribution in θ is much narrower than in α , as indicated by the much higher power of the \cos^n fit to the data. Further analysis of the DC and CID processes as well as model calculations of the vibrational CID mechanism are underway.



Recently we have conducted studies of CID of HD^+ in similar collisions in search of the isotopic effects observed previously for this molecular ion [see, for example, Refs. 3,4], namely, that *the dissociation into $\text{H} + \text{D}^+$ was favored over $\text{H}^+ + \text{D}$* . Preliminary results indicate that such effects, if they exist, are much smaller than those reported in previous work. These results will be presented as an invited talk in the CAARI 2002 meeting.

Future plans: Systematic studies of DC and CID caused by either electronic or vibrational excitation will be conducted focusing on the effect of the target species and the collision energy. Our preliminary results indicate significant differences in vibrational CID between Ar and He targets. Furthermore, we plan to investigate both these processes for a few additional simple molecular ions, such as HeH^+ , He_2^+ and H_3^+ . While conducting these studies on the existing system, an improved setup, which includes a cold jet target, will be assembled and tested. This will enable the simultaneous measurement of the recoil ion momentum for DC reactions, thus providing kinematically complete information about the process.

1. J. Los and T.R. Govers, in *Collision Spectroscopy* (ed. R.G. Cooks, Plenum Press, NY 1978) p-289
2. T.A. Green and J.M. Peek, *Phys. Rev.* **183**, 166 (1969)
3. T.A. Lehman et al. *Int. J. Mass Spectrom. Ion Proc.* **69**, 85 (1986)
4. R.W. Rozett and W.S. Koski, *J. Chem. Phys.* **49**, 2691 (1968)

Isotopic effects and asymmetries in bond-rearrangement and bond-breaking processes in water ionized by fast proton impact. A.M. Saylor, Z.S. Casey, J.W. Maseberg, D. Hathiramani, K.D. Carnes, B.D. Esry, and I. Ben-Itzhak. Studies of ionization and fragmentation of water molecules by fast protons and highly charged ions have revealed an interesting isotopic preference for H-H bond rearrangement. Specifically, the dissociation of $\text{H}_2\text{O}^+ \rightarrow \text{H}_2^+ + \text{O}$ is about twice as likely as $\text{D}_2\text{O}^+ \rightarrow \text{D}_2^+ + \text{O}$, with $\text{HDO}^+ \rightarrow \text{HD}^+ + \text{O}$ in between. Further investigations of this isotopic effect lead us to discover a similar isotopic effect following double ionization of water,

i.e. in $\text{H}_2\text{O}^{2+} \rightarrow \text{H}_2^+ + \text{O}^+$, although these results are preliminary. In addition, we have observed large asymmetries in bond breaking in the HDO isotope. For example, $\text{HDO}^+ \rightarrow \text{H}^+ + \text{OD}$ is more likely than $\text{HDO}^+ \rightarrow \text{D}^+ + \text{OH}$ by about a factor of 1.5, suggesting that it is easier to break the O-H bond than the O-D bond. This preference is even larger in the dissociation of HDO^{2+} . Calculations are underway to determine the relative production rates for the different isotopes from the overlap of the initial and final vibrational wave functions and the time evolution of the final wave function. In addition, we determined the relative cross sections of all dissociation channels including $\text{H}^+ + \text{H}^+ + \text{O}$ which typically are not measured by TOF techniques. These results were presented by Max Saylor as an invited talk in the undergraduate research session of DAMOP 2002.

Future plans: The isotopic enhancement in the $\text{H}_2\text{O}^{2+} \rightarrow \text{H}_2^+ + \text{O}^+$ dissociative double ionization channel requires further investigation to determine if it is similar in magnitude to that found in single ionization. We also intend to study ionization and fragmentation of water by fast highly charged ions and compare them to fast proton impact.

High intensity laser interactions

1. Evidence for pondermotive-gradient field-ionization in an intense focused laser beam, E. Wells (UVA), I. Ben-Itzhak, and R.R. Jones (UVA). We have measured the Rydberg ion population produced during intense laser ionization in Xe, Kr, and Ar. The branching ratio for production of Rydberg ions, $\text{A}^{(q-1)+*}$, to ions A^{q+} has been measured as a function of laser intensity and polarization. Using 100 fs, 790 nm laser pulses, singly and double charged Rydberg ions are observed in Xe, but in Kr and Ar only singly charged Rydberg ions are seen. Model calculations of ionization by the gradient of the pondermotive potential (∇U_p) of the focused laser beam suggest that the Rydberg population is inversely proportional to the ionization potential of the ion species. These calculations are in agreement with our data except for the $\text{Xe}^{2+*}/\text{Xe}^{3+}$ ratio, which is anomalously large, approximately a factor of two higher than the $\text{Xe}^{+*}/\text{Xe}^{2+}$ ratio.

2. Photo ionization and photo dissociation of H_2^+ by an intense short pulse laser, I. Ben-Itzhak, J.W. Maseberg, A.M. Saylor, M.A. Smith, K.D. Carnes, Z. Chang, C. Fehrenbach, and C.L. Cocks. We have recently begun measurements of ionization and dissociation of a few keV H_2^+ beam crossed by an intense short-pulse laser beam using 3D molecular dissociation imaging on a newly installed apparatus employing techniques similar to those described in 3.1. Only a couple of previous measurements have been reported so far [1,2].

Future plans: We plan to measure the dependence of ionization and dissociation of H_2^+ , and other simple molecular ions, on the duration of the intense laser pulse. It has been predicted that the ratio of ionization to dissociation will change with increasing number of laser cycles, i.e. pulse width [3].

1. K. Sändig, H. Figger, and T.W. Hänsch, Phys. Rev. Lett. **85**, 4876 (2000)
2. I.D. Williams *et al.* J. Phys. B **33**, 2743 (2000)
3. Kulander *et al.* Phys. Rev. A **53**, 2562 (1996)

Formation and decay mechanisms of ${}^4\text{He}_2^{2+}$ dimers, I. Ben-Itzhak, and A. Bar-David, I. Gertner, and B. Rosner (*Technion*). We have measured the decay rate and kinetic energy release upon dissociation of ${}^4\text{He}_2^{2+}$ dimers formed in $\text{He}_2^+ + \text{Ar}$ charge stripping collisions. The measured mean lifetime indicates that He_2^+ molecular ions are preferentially formed with high angular momentum, i.e. high l values, as suggested by our previous measurements of ${}^3\text{He}{}^4\text{He}^{2+}$. For the ${}^4\text{He}_2^{2+}$ isotope low l -states as well as high l -states are within the high sensitivity range of our experimental setup.

Publications:

1. "A comparative study of the ground state dissociation of H_2^+ and D_2^+ induced by ionizing and electron capture collisions with He^+ at velocities of 0.25 and 0.5 a.u.", W. Wolff, I. Ben-Itzhak, H.E. Wolf, C.L. Cocke, M.A. Abdallah, and M. Stöckli, *Phys. Rev. A* **65**, 042710 (2002).
2. "A kinematically complete charge exchange experiment in the $\text{Cs}^+ + \text{Rb}$ collision system using a MOT target", X. Flechard, H. Nguyen, E. Wells, I. Ben-Itzhak, and B.D. DePaola, *Phys. Rev. Lett.* **87**, 123203 (2001).
3. "Charge exchange and elastic scattering in very slow $\text{H}^+ + \text{D}(1s)$ "half" collisions", E. Wells, I. Ben-Itzhak, K.D. Carnes, and B.D. Esry, *Phys. Rev. Lett.* **86**, 4803 (2001).
4. "Transfer Ionization to Single Capture Ratio for Fast Multiply Charged Ions on He", R. Ünal, P. Richard, H. Aliabadi, H. Tawara, C.L. Cocke, I. Ben-Itzhak, M.J. Singh, and A.T. Hasan, **Application of Accelerators in Research and Industry**, edited by J.L. Duggan and I.L. Morgan (AIP press, New York 2001), p-36.
5. "Velocity Dependence of Electron Removal and Fragmentation of Water Molecules Caused by Fast Proton Impact", A.M. Saylor, E. Wells, K.D. Carnes, and I. Ben-Itzhak, **Application of Accelerators in Research and Industry**, edited by J.L. Duggan and I.L. Morgan (AIP press, New York 2001), p-33.
6. "Double and Single Ionization of hydrogen molecules by fast proton impact", I. Ben-Itzhak, E. Wells, D. Studanski, Vidhya Krishnamurthi, K.D. Carnes, and H. Knudsen, *J. Phys. B* **34**, 1143 (2001).
7. "Measurements of the mean lifetime and kinetic energy release of metastable CO^{2+} ," J.P. Bouhnik, I. Gertner, B. Rosner, Z. Amitay, O. Heber, D. Zajfman, E.Y. Sidky, and I. Ben-Itzhak, *Phys. Rev. A* **63**, 032509 (2001).
8. "Charge exchange in slow $\text{H}^+ + \text{D}(1s)$ collisions", B.D. Esry, H.R. Sadeghpour, E. Wells, and I. Ben-Itzhak *J. Phys. B* **33**, 5329 (2000).
9. "Asymmetric branching ratio for the dissociation of $\text{HD}^+(1s\sigma)$ ", E. Wells, I. Ben-Itzhak, K.D. Carnes, and B.D. Esry, *Phys. Rev. A* **62**, 622707 (2000).
10. "Symmetry breakdown in ground state dissociation of HD^+ ," I. Ben-Itzhak, E. Wells, K.D. Carnes, Vidhya Krishnamurthi, O.L. Weaver, and B.D. Esry, *Phys. Rev. Lett.* **85**, 58 (2000).
11. "The "Foil-Mesh" method for mean lifetime measurements of long lived molecular ions", A. Bar-David, I. Ben-Itzhak, J.P. Bouhnik, I. Gertner, Y. Levy, and B. Rosner, *Nucl. Instrum. Method B* **160**, 182 (2000).

Ultrafast X-ray Source and Detector

Z. Chang

J. R. Macdonald Laboratory, Department of Physics,
Kansas State University, Manhattan, KS 66506, chang@phys.ksu.edu

The goals of this aspect of the JRML program are (1) to develop a high repetition rate, high intensity laser for laser-atom interaction studies at KSU, (2) to study the x-ray source based on high order harmonic generation from laser/OPA-atom/molecule interactions, and (3) to develop an ultrafast x-ray streak camera for time-resolved x-ray studies at synchrotron facilities.

Recent progress and future plans:

1) Development of the *Kansas Light Source*, a high repetition rate and high intensity laser system, *Bing Shan, Chun Wang, Shambhu, Ghimier and Zenghu Chang*

The new inhouse-built femtosecond laser laid the foundation for the initiative to study high intensity laser-atom interactions at KSU. It is a high repetition rate laser to reduce data acquisition time and to avoid space charge effects. It can operate at a 1 to 2 kHz repetition rate to accommodate the data acquisition electronics of the COLTRIMS and other time-of-flight spectrometers. A strong optical field (about 1 atomic unit) can be achieved with a moderate focusing lens. The laser oscillator and amplifier are pumped with diode pumped solid-state lasers to assure shot-to-shot and long time stabilities. The laser has been used by six users from the JRML and from outside, which include:

1. Zenghu Chang: high harmonic generation (one paper submitted).
2. C. Lew Cocke: laser-molecule interactions in a COLTRIMS.
3. Brett DePaola: laser-atom interactions in a MOTRIMS.
4. Patrick Richard and Zenghu Chang: laser-atom interactions using imaging detector.
5. Jin Wang (Argonne National Laboratory): streak camera testing (one paper submitted).
6. Itzik Ben-Itzhak: Laser-molecular ion beam interactions.

We are building a high intensity optical parametric amplifier that will produce 10^{15} W/cm² intensity in the 1-1.6 μm wavelength range. We also plan to build a hollow-core fiber compressor that will produce high intensity pulses with less than a 10 fs duration.

2) High harmonic cutoff extension with molecules, *Bing Shan, Mahendra Shakya and Zenghu Chang*

Since the early discovery of HHG at the end of the 1980s, most of the studies have been concentrated on rare gas atoms. There have been a number of experimental studies of HHG from molecules. In an earlier experiment, it was found that "the harmonic spectra from molecular gases are very similar to those obtained in the atomic gases, with a plateau and a cutoff whose location is strongly correlated to the value of the ionization potential". As an example, the HHG spectra of O₂ are close to that of Xe. Their ionization potentials are comparable (~12 eV). Compared to the preliminary studies of HHG from molecules, the ionization of molecules has been studied more extensively. Recently, it

was found that the ionization of O_2 is suppressed by about one order of magnitude when comparing with Xe. However, there is no ionization suppression for N_2 when comparing with Ar, which has nearly the same ionization potential as N_2 . As is known, the HHG is closely related to the ionization in the intense laser. The suppressed ionization of O_2 should lead to a significant extension of harmonic spectra, which was not observed in the previous HHG measurements. Stimulated by such a controversy and the desire to further explore the relationship between the HHG and ionization, we studied the HHG cutoff behavior for molecules and their companion atoms, for cases with a strong ionization suppression (O_2 , Xe), and for cases with no ionization suppression (N_2 , Ar).

The experiment was carried out with the newly established high intensity laser facility at the J. R. Macdonald laboratory. We compared Ar and N_2 which have nearly the same ionization potentials, at 15.76 eV and 15.58 eV, respectively, and we found they have nearly the identical harmonic cutoff (The cutoff positions for Ar and N_2 are $q_c = 63$ and $q_c = 57$, respectively). On the other hand, while Xe and O_2 have nearly the same ionization potentials, at 12.13 eV and 12.06 eV, respectively, the harmonic cutoff for O_2 ($q_c=53$) is much higher than for Xe ($q_c=29$). The spectra are shown in figure 1. We attributed this to the O_2 molecule being much harder to ionize than the Xe although they have the same ionization potential. Therefore, the harmonic cutoff extension and the ionization suppression are strongly correlated. The cutoff extension caused by the ionization suppression provides another avenue for obtaining energetic x-ray photons.

In the future, we will generate high harmonic radiation from molecules with two laser pulses. The first pulse is to align the molecules and the second pulse generates high harmonic radiation from them.

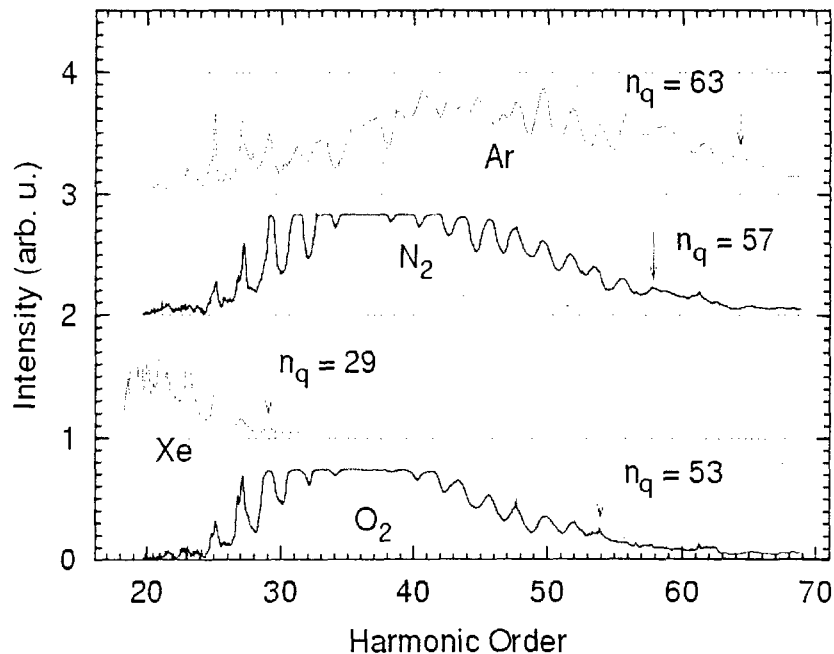


Fig. 1 The comparison of harmonic cutoff between atoms and their companion molecules. O_2 's cutoff photon energy is two times higher than Xe's though their ionization potentials are almost identical.

3) High harmonic generation by using a long wavelength field from an optical parametric amplifier. Bing Shan, A. Cavalieri(U. M.), and Zenghu Chang

We demonstrated that by using a long wavelength ($\sim 1.5 \mu\text{m}$) infrared pump pulse with 10^{14} W/cm^2 from an optical parametric amplifier, the cut-off photon energies of Ar and Xe atoms were increased by a factor of two or more compared to that by a conventional 800nm pump laser. For Xe gas, the cutoff is $\sim 40 \text{ eV}$ with an 800nm pump and is $\sim 80 \text{ eV}$ with a $1.5 \mu\text{m}$ pump (Fig.2). It also shows that a harmonic wavelength can be easily tuned to cover any wavelength from the 5th order to the cutoff by changing the OPA wavelength.

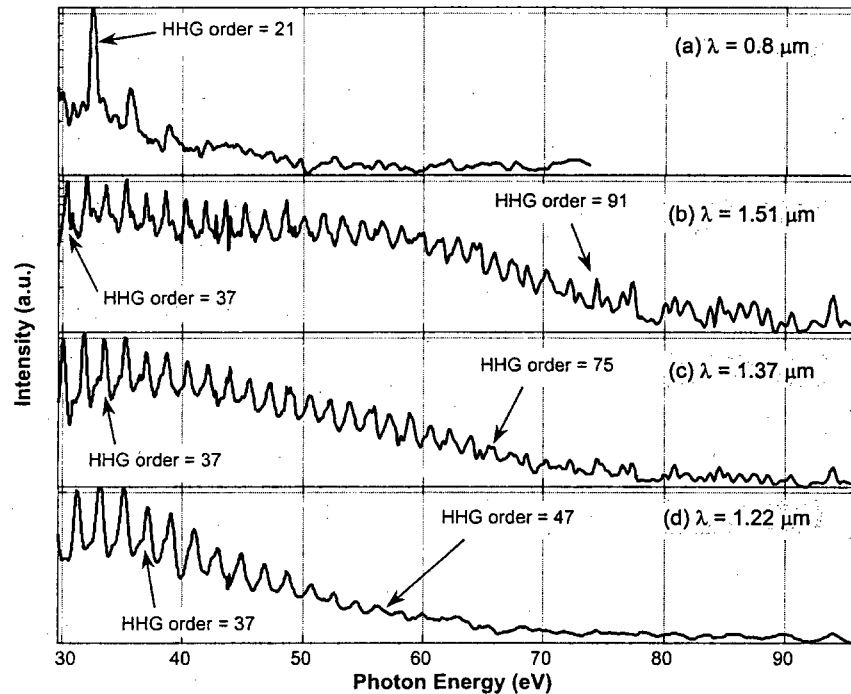


Fig. 2: Harmonic spectrum using different pump wavelengths, constant pulse energy and focal point size.

4) Ultrafast X-ray streak camera development, Bing Shan, Jinyuan Liu(ANL), Andrew MacPhee(LBL), Jin Wang (ANL) and Zenghu Chang

When a streak camera operates in the accumulation mode, the dominating factor that limits the time resolution is the timing jitter. While the response time of the photoconductive switch to the triggering laser may be instantaneous, the timing jitter is not zero unless the laser pulse is absolutely stable. At the present time, the lasers used in synchrotron facilities for time-resolved x-ray studies are Ti:Sapphire lasers operating at kilohertz repetition rates. The same laser is used to pump the sample under investigation and to trigger the photoconductive switch. The pulse energy fluctuation is on the order of 1 % RMS. This energy fluctuation causes the output amplitude of a photoconductive switch to change from shot to shot, which in turn produces timing jitter. When the switch responds to the laser energy linearly, the timing jitter is inversely proportional to the rise time of the ramp voltage for given ramp slope. Therefore, the jitter can be reduced by decreasing the rise time.

In our previous camera, the rise time is limited to 300 ps by the bandwidth of the deflection plates. The jitter-limited resolution is 2ps. The photoconductive switch and deflection plates are redesigned so that the response time is improved to 150 ps. The measured response time of the switch and the deflection system are shown in Figure 3a. We expected the two-fold reduction of the response time to result in a two-fold timing jitter, which was confirmed by the measurement shown in Figure 3b. This confirmation is important because it points us in the right direction for future work. Compared to other approaches such as improving laser pulse energy fluctuation in order to reduce timing jitter, our method is much easier to implement.

We plan to further reduce the time jitter. This will be accomplished by improving the response time of the photoconductive switch and the deflection plates by a factor of three (from 150 ps to 50 ps).

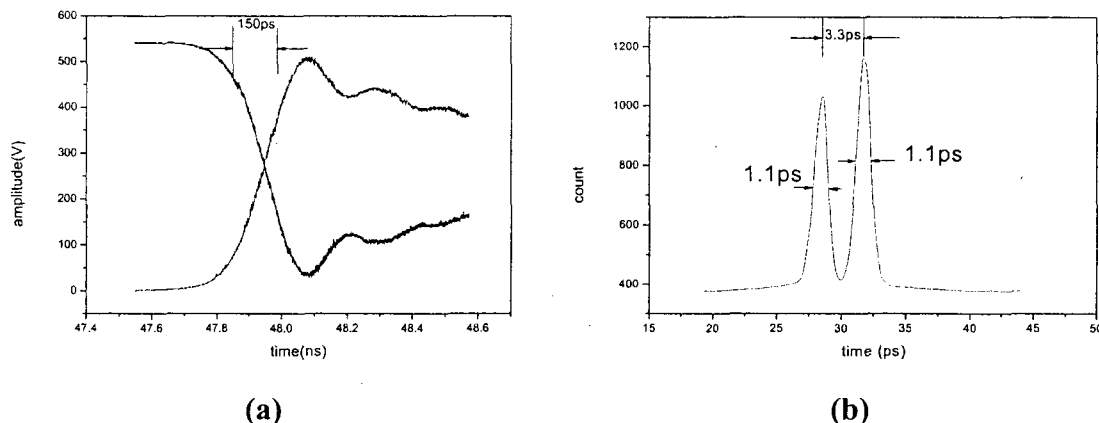


Fig 3. (a). The combined response time of the photoconductive switch and the deflection plates. (b). The temporal resolution measured with the switch and the deflection plates.

PUBLICATIONS

- 1).B. Shan, Z. Chang, "Dramatic extension of the high-order harmonic cutoff by using a long-wavelength pump", *PHYS. REV. A*, Vol.65, 011804(R) (2002).
- 2).A. M. Lindenberg, I. Kang, S. L. Johnson, R. W. Falcone, P. A. Heimann, Z. Chang, R. W. Lee, J. S. Wark, "Coherent control of phonons probed by time-resolved x-ray diffraction", *OPTICS LETTERS*, Vol.27, 869 (2002).
- 3).PA Heimann, AM Lindenberg, I Kang, S Johnson, T Missalla, Z Chang, RW Falcone, RW Schoenlein, TE Glover, HA Padmore, "Ultrafast X-ray diffraction of laser-irradiated crystals", *NUCLEAR INSTRUMENTS & METHODS IN PHYSICS RESEARCH SECTION A-ACCELERATORS SPECTROMETERS DETECTORS AND ASSOCIATED EQUIPMENT*, Vol. 467, Part 2, 986-989 (2001).
- 4).Wark-JS; Allen-AM; Ansbro-PC; Bucksbaum-PH; Chang-Z; DeCamp-M; Falcone-RW; Heimann-PA; Johnson-SL; Kang-I; Kapteyn-HC; Larsson-J; Lee-RW; Lindenberg-AM; Merlin-R; Missalla-T; Naylor-G; Padmore-HA; Reis-DA; Scheidt-K; Sjoegren-A; Sondhauss-PC; Wulff-M, "Femtosecond X-ray diffraction: experiments and limits", *PROCEEDINGS OF THE-SPIE—THE INTERNATIONAL SOCIETY FOR OPTICAL ENGINEERING*. Vol.4143; p.26-37 (2001).
- 5).B. Shan, A. Cavalieri, and Z. Chang, "Tunable High Harmonic Generation With an OPA", *APPL. PHYS. B*, accepted for publication.

Ion and Photon Interactions with Laser Cooled Targets

B. D. DePaola, Physics Department, J.R. Macdonald Laboratory, Kansas State University, Manhattan, KS 66506, depaola @phys.ksu.edu; (785)532-1623

1) **Capture cross sections, differential in scattering angle**, *B. D. DePaola, C. W. Fehrenbach, X. Flechard (CNRS, Caen, France), R. Bredy, H. Camp, and H. Nguyen.* The use of a laser cooled and trapped target in charge transfer studies has many advantages over conventional techniques such as COLTRIMS (COLd Target Recoil Momentum Spectroscopy). In new methodology, MOTRIMS (Magneto-Optical Trap Recoil Ion Momentum Spectroscopy) the target can be made colder than in the coldest COLTRIMS by several orders of magnitude. Thus, momentum spread in the target can be completely neglected; limitations in momentum resolution are now set by detector spatial resolution, limitations in flight time resolution, projectile beam energy spread, and deviations in recoil ion trajectories caused by stray magnetic fields. Thus, even for massive targets such as ^{87}Rb , the resolution in momentum is factors of 3 to 10 better than the best COLTRIMS results in the kinematically favorable low mass He targets.

Perhaps more important than this modest improvement in resolution is that MOTRIMS allows the use of targets which can be laser-excited. (Generally speaking, pre-cooling and expanding

in a supersonic jet results in molecule or cluster formation in atomic species having optically active electrons. Thus, COLTRIMS is not suitable for use with atomic species which can be readily laser-excited.) We have exploited both advantages of the MOTRIMS techniques to study charge transfer cross sections which are differential in initial state of the target, final state of the projectile, and projectile scattering angle. The target in all cases was ^{87}Rb , trapped and cooled to roughly 130 K. In most experiments the Rb was in a mixture of the ground and first excited states (5s and 5p) due to the effects of the trapping lasers. However, in some cases, an additional laser at 1.5 μm was used to excite the transition from 5p to 4d. Projectiles studied thus far include Cs^+ and Na^+ at collision energies between 2 and 7 keV. Figure 1 shows a typical Q-value spectrum for 7 keV Na^+ incident on Rb in a mixture of 5s, 5p, and 4d states. Because the ion source currently in place on the MOTRIMS apparatus is of the thermionic type (chosen so as to have a very small spread in projectile velocity) the initial experiments

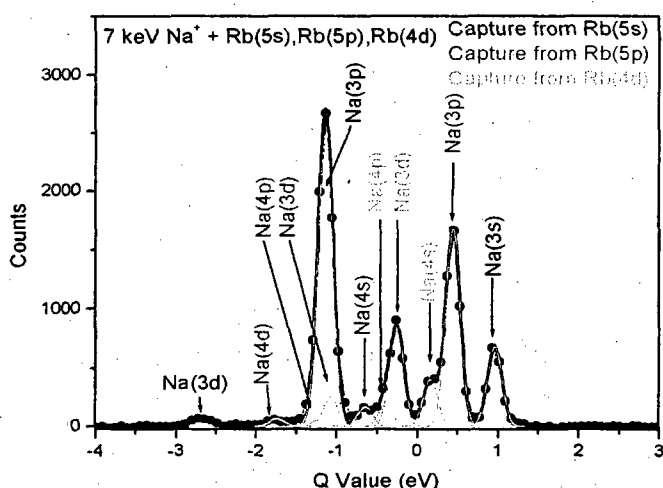


Figure 1 Q-value spectrum for $\text{Cs}^+ + \text{Rb}$

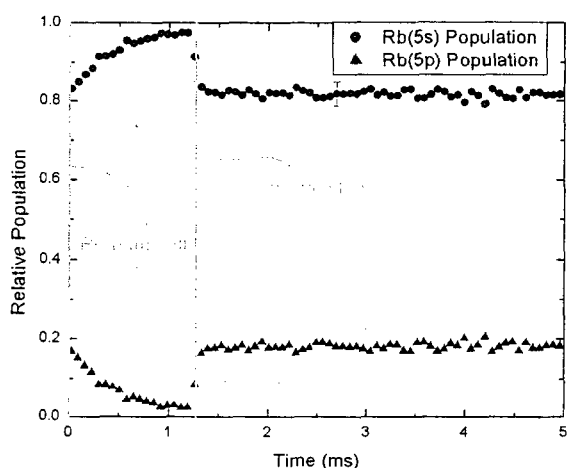
are limited to singly charged alkali and alkali earth projectiles. In the coming year, the alkali and alkali earth cross section measurements will be completed.

In order to measure relative cross sections for capture from Rb(5p) and Rb(5s), one must know the fraction of atoms in the excited state. The extremely high Q-value resolution – and with it the capability of separating even closely spaced collision channels – allows us to determine the ratio of these cross sections without relying on model-dependent fluorescence measurements. This is accomplished by chopping trapping and re-pump lasers and measuring changes in the areas of the peaks in the Q-value spectra corresponding to various capture channels. Because the atoms are cold, the time it takes for them to drift out of the ion beam is very long compared to the excited state lifetime. Thus the same atoms are examined with lasers on and off. The excited state fractions obtained in this manner have uncertainties of less than 7%, while conventional methods, which rely on fluorescence from a MOT, are closer to 200%. The technique can be generalized to n-level systems, and will therefore be instrumental in our measurements of charge transfer cross sections from Rydberg targets.

In addition to initiating the measurements of these cross sections, quite a bit of effort has been spent on enabling the fast chopping of the MOT's quadrupole B-field. Based on numerical simulations of ion trajectories in an idealized quadrupole B-field, it is believed that at least a threefold improvement in scattering angle resolution will be achieved once this upgrade is implemented. During the coming year, we will try to implement the B-field chopping electronics and use the expected enhancement in scattering angle resolution to look for structure in $d\sigma/d\Omega$, as predicted by theory for certain selected collision systems.

2) Use of charge exchange as a diagnostic of population dynamics, B. D. DePaola, C. W. Fehrenbach, R. Bredy, X. Flechard(CNRS, Caen, France), H. Camp, and H. Nguyen.

We have explored the capabilities of the MOTRIMS apparatus for measuring excited state fractions in the MOT. An important test case was to measure cross section ratios (as



described in the preceding section) while deliberately varying excited state fraction by adjusting the detuning of the trapping laser. While the excited state fraction was measured to vary by a factor of 2 (from 15% to 30%) the cross section ratios remained constant – as they should for fixed collision energy. A second important test was the measurement of the *time dependence* of the excited state fraction in the MOT as the re-pump laser was chopped on and off as shown in Figure 2.

Figure 2 Relative 5s and 5p populations in Rb MOT as a function of time. The trap laser is always on.

The experiment confirmed what is already known: the excited state fraction falls to zero when the re-pump laser is blocked, since the trapping laser optically pumps the target atoms to the “dark”, optically inaccessible lower hyperfine level. The success of these experiments opens the door to studies of population dynamics in the MOT caused by a variety of processes, including stimulated Raman adiabatic passage (STIRAP), dimer formation due to 3-body collisions, and photo-association. With the MOTRIMS apparatus, excited state dynamics can be studied with a temporal resolution of a few nanoseconds, over a time span of up to a few milliseconds. Unlike the use of an optical probe, the ion beam interacts so weakly with the target that the measurements may be viewed as non-perturbative.

3) Ion spatial imaging to measure above threshold ionization rates, B. D. DePaola, Z. Chang, C. W. Fehrenbach, R. Bredy, X. Flechard (CNRS, Caen, France), H. Camp, and H. Nguyen. A long-time problem in the measurement of ionization rates in interaction of intense laser pulses with atomic and molecular gasses and vapors, is in the accurate determination of the laser intensity which caused the ionization. The difficulty is that intensity variation in a focused laser beam can vary over more than an order of magnitude. Thus, ions extracted from the interaction region were produced by a field whose value has large uncertainty. A possible solution to this problem has been explored by using ion optics to image the laser interaction region onto a 2D-PSD (Figure 3).

The apparatus consisted of the MOTRIMS momentum spectrometer, to which potentials were applied which were appropriate to spatial, rather than momentum, imaging. With two dimensions provided by the PSD, and the third dimension provided by the ion the time-of-flight, a 3-D image of the ionization region was built up, event by event. The spatial variation of the laser beam intensity was separately measured with a scanning CCD

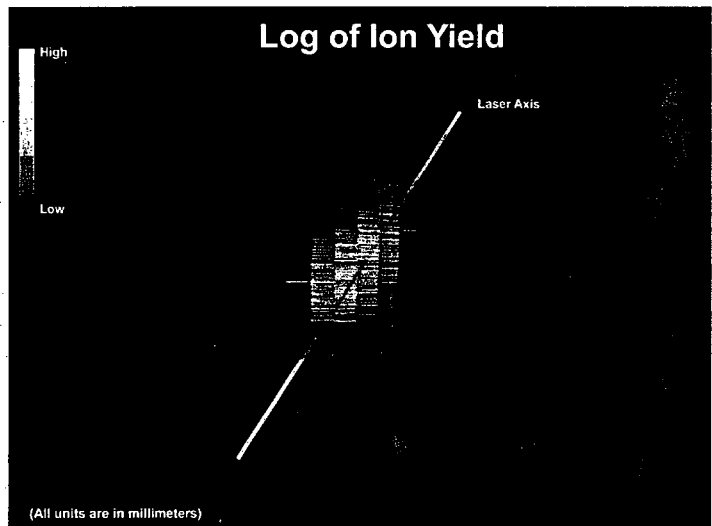


Figure 3 Photo-ion yield from a Rb target as a function of position. The log of the yield is represented in false color. The red line indicates the path of the ionizing laser.

camera. Thus, with knowledge of the target thickness, one could deduce, through a single image of thousands of events, the absolute ionization rate as a function of laser intensity, for a range of intensities. In principle, one could introduce any number of atomic or molecular gasses or vapors into the chamber for ionization studies. In this test case, ionization of Rb atoms in vapor supplied by the “getter” source used in MOT experiments was studied. The target thickness was directly measured from absorption studies which made use of one of the diode lasers normally tuned for trapping. Laser pulses of approximately 25 fs were used to ionize the Rb. The various parts of the

technique (ion imaging, target thickness measurement, and laser profiling) were each found to work beautifully. In the future, all three components will be combined in a single measurement of absolute ionization rates for Rb in the ground state. We also plan to use our trapping lasers to optically pump the Rb into a particular orientation; ionization rates will then be measured as a function of the angle between the orientation axis of the atoms and the polarization axis of the ionizing laser.

Publications Appearing in 2001-2002 Not Previously Cited

- 1) “Kinematically complete charge exchange experiment in the Cs^+ +Rb collision system using a MOT target, X. Flechard, H. Nguyen, E. Wells, I. Ben-Itzhak, and B. D. DePaola, *Phys. Rev. Lett.* **87**, 123203 (2001).
- 2) “Energy transfer in ion-Rydberg-atom charge exchange”, D. S. Fisher, S. R. Lundeen, C. W. Fehrenbach, and B. D. DePaola, *Phys. Rev. A* **63**, 052712 (2001).
- 3) “Experimental study of L distribution from charge capture by Si^{3+} on Rydberg atoms”, S. R. Lundeen, R. A. Komara, C. W. Fehrenbach, and B. D. DePaola, *Phys. Rev. A* **64**, 052714 (2001).
- 4) “Stark-induced x-ray emission from high Rydberg states of H-like and He-like silicon ions”, M.A. Gearba, R.A. Komara, S.R. Lundeen, W.G. Sturru, C.W. Fehrenbach, B.D. DePaola, X. Flechard, *Physical Review A* (accepted).

Structure and dynamics of atoms, ions molecules and surfaces:

Atomic physics with ion- and electron beams

*S. Hagmann, Physics Dept. J. R. Macdonald Lab., KSU, Manhattan, Kansas 66506 and
Inst. für Kernphysik, Universität Frankfurt, Frankfurt, Germany*

The projects presented in this section cover advances in spectroscopy of few electron very heavy ions, a new access to (e,3e) spectroscopy of atoms, and delta electron spectroscopy for heavy ions traversing condensed matter.

Recent progress and future plans :

1. Electron spectroscopy of relativistic ions in the ESR storage ring

S. Hagmann(KSU and IKF, Frankfurt), Th. Stöhlker(IKF, Frankfurt), J. Ullrich, R. Moshhammer(MPI, Heidelberg), Ch. Kozhuharov(GSI, Darmstadt)

We have designed a new electron spectrometer to be used in the ESR storage ring; its purpose is twofold: a) investigate the role of strong ($E \geq 10^{16}$ V/cm) and rapidly varying ($\tau \leq 10^{-18}$ sec) electromagnetic fields active in the fragmentation of ions and atoms during relativistic collisions using high resolution projectile electron spectroscopy; b) investigate (e,2e) spectroscopy of ions in inverse kinematics using a combination of the electron spectrometer with the reaction microscope.

The instrument is designed as a forward electron spectrometer for electrons emitted near 0° around the beam direction with $v_e \approx v_{\text{Proj}}$. The spectrometer consists of a 60° dipole magnet followed by a quadrupole triplet and second 60° dipole. After momentum analysis, electrons will be detected by a 2D position sensitive detector. We will make use of the advantages offered by relativistic kinematics, which allows for $\beta \approx c$ very high resolution spectroscopy of high lying autoionizing Rydberg states (e.g. with $n \geq 100$ in few electron U ions) in such collisions. We can thus study coherent states via anisotropies of Rydberg states and the corresponding asymmetry¹ of ELC and ECC Cusp peaks. For kinematically complete experiments, i.e. when jointly operated with the reaction microscope, the optical design D-QT-D allows us to reconstruct the scattering plane for (e,2e) experiments on ions performed in inverse kinematics. This latter type of experiment will be feasible after implementation of a new reaction microscope in the ESR, until then we will use the forward electron spectrometer to study ELC and ECC Cusps.

In relativistic collisions a large flood of secondary products is generated besides electrons ionized from the collision partners; as the current 2D position sensitive detector in the electron spectrometer is not measuring the energy of the detected particles, it is imperative to show first that the spectrometer is suppressing the intense beam-induced background and is only transmitting electrons of selected momenta onto the detector.

In the commissioning phase of the instrument we have for this reason temporarily replaced the 2D position sensitive detector with an energy analyzing Si(Li) and studied the reaction $392 \text{ MeV/u } U^{89+} + N_2 \rightarrow U^{90+} + \text{fragments} + \text{electrons}$. We could verify that the spectrometer very efficiently suppresses the flood of secondary products generated in the collision; the spectrometer was operated at a current for which, according to optics calculations, it only transmits electrons with a momentum of a Cusp electron, i.e. with a velocity $v_e \approx v_{\text{Proj}}$. Virtually all electrons detected with the Si(Li) appeared in coincidence with the charge exchanged projectile U^{90+} ; the energy loss measured for these electrons is

in accordance with that calculated for Cusp electrons traversing the Fe exit window of the spectrometer.

An interesting first application after completion of this phase of commissioning will be a combined study of the shape of the ECC Cusp in coincidence with the Radiative Electron Capture into Continuum, RECC, photons- a process which is closely related to the elementary process of bremsstrahlung.

At least one new Ph.D student will be joining our group in fall 2002 to work on this topic.

1. J. Burgdörfer, Phys. Rev. A33(1986) 1578

2. Two-electron Lambshift in high-Z He-like Ions

A. Gumberidze, Th. Stöhlker, F. Bosch, Ch. Kozhuharov(GSI, Darmstadt) X. Ma(IMP Lanzhou), S. Hagmann(KSU and IKF, Frankfurt), Y. Zou(Fudan Univ, Shanghai)

We are using radiative recombination (RR) into the 1s state of bare and H-like U to investigate 2-electron contributions to the ground state of He-like U and thus gain access to 2-electron QED effects. In RR electrons undergo direct transitions to bound states of ions via emission of photons carrying $\Delta E = E_{\text{kin}} + E_{\text{bind}}$. The difference in the energies for RR transitions into a vacant shell of a bare or H-like ion is equal to the difference in the associated ionization potentials of the respective H- and He-like ions created in the collision. This directly provides the two-electron contribution to the ground state energy of He-like ions. The different energies of these photon transitions will be measured for bare and H-like $U^{92+,91+}$ beams in the ESR cooler region with an intended accuracy of below 5 eV. Since 2-electron QED effects are calculated to contribute 7eV such an experiment would provide the first test of higher order QED corrections for high-Z ions.

The experiment will be conducted in the electron cooler region of the ESR storage ring and is taking advantage of the deceleration technique where the beam energy of the bare and H-like U ion is taken from 400 MeV/u - where bare and H-like ions can be produced very efficiently - to 43.5 MeV/u. At such low collision energies bremsstrahlung intensity is much attenuated and Doppler corrections are strongly reduced. A preliminary analysis for a test run determined the splitting with an accuracy of 9 eV; this is to be compared with a QED contribution of 7 eV to a total 2-electron contribution of 2.2 keV. As a next step we plan a production run with the same collision system to achieve an experimental accuracy of below 5 eV

3. He-double ionization via electron impact: (e,3e) spectroscopy

A. Knapp, L. Schmidt, R. Dörner, O. Jagutzki, H. Schmidt-Böcking(IKF, Frankfurt), S. Hagmann(KSU and IKF, Frankfurt)

The COLTRIMS technique has established itself as an immensely powerful technique to study the dynamics of atomic and molecular collision processes, as it provides in a natural way reconstruction of vector momenta of all collision partners involved in a collision. We have undertaken to construct a COLTRIMS type spectrometer which will allow us to measure kinematically complete 5-fold differential ionization cross sections for double ionization of He under electron impact. Scattered electrons which have ionized the target are energy analyzed following the target zone using a 127° electrostatic analyzer equipped with a 2D position sensitive electron detector while the direct beam not having suffered an energy loss will leave the spectrometer through a slit in the outer

section of the 127° spectrometer. An electric extraction field in the target zone perpendicular to the primary electron beam guides slow ionized electrons with an energy of up to 10 eV with a 4π solid angle onto a large 2D position sensitive delay line detector. The same electric field will guide recoiling He ions from the target zone onto another 2D position sensitive detector with a momentum resolution of 0.53 a.u./mm. Flight-time and detection location on the respective detectors provides the charge state and the momentum of the particles. For double ionization of He the momentum of the fast ionized electron- if not detected - can be reconstructed via momentum and energy conservation. At present the ion- and electro-optical properties of the entire spectrometer are mapped. First experiments will focus on single ionization of He, followed by studies of double ionization for low collision energies, where the projectile electron's energy loss is significant. Here discrepancies with theory are large. The coincidence rates are estimated to be a factor of 100 higher than in traditional configurations. This is the Ph.D. project of A. Knapp

4. An electrostatic toroidal electron energy analyzer for delta electrons excited in collisions of heavy ions up to relativistic collision velocities

S. Dreuil, G. Kraft(GSI, Darmstadt) S. Hagmann(KSU and IKF, Frankfurt), H. Rothard(CIRIL, Caen)

In radiotherapy with relativistic heavy ions the success in cell deactivation and thus an effective treatment is largely based on understanding the details of the mechanism of energy deposition in the intracellular medium leading to double strand breaks of DNA.

For relativistic ion beams the energy deposition in a cellular environment is dominated by creating free electrons from the ionization of molecules; these electrons in turn will ionize other molecules and thus produce a high concentration of chemically active radicals.

The biological effective dose optimization, at the core of inverse treatment planning¹ codes, thus depends – as a key part of it – on the electron emission pattern observed for swift heavy ions passing through dense matter. Such electron emission cross sections differ depending on the proximity to the primary track. For regions more distant from the primary projectile track model calculations appear to be in sufficient agreement with experiment. However, a serious lack of precise data is found to exist for electron emission for the inner track ($< 10^{-7}$ cm). Here a large number of biologically active electrons with energies $E < 100$ eV is created but important details are not known. The extrapolation of data from gas targets is not adequate because density effects on production and transport are not of any importance as in solids. Our goal is a systematic measurement of doubly differential cross sections DDCS for electron emission and of electron transport for a variety of condensed matter targets, emphasizing variations in solid state density and electron density to assess their respective influence on creation and transport of continuum electrons. Two additional Ph.D. students are expected to join this project later this fall.

1. W. K. Weyrather *et al.*, Int. J. of Radiation Biology 75(1999) 1357

5. Laser Spectroscopy of Hyperfine Transitions in very heavy H- and Li-like ions in the ESR

Th. Kühl, W. Nörtershäuser, A. Dax, M. Tomaselli, R. Sanchez , (GSI-Darmstadt), S. Hagmann(KSU and IKF, Univ. Frankfurt), Th. Stöhlker(IKF, Univ. Frankfurt)

The simplest and most basic magnetic interaction in atomic physics is the hyperfine splitting of the 1s ground state of a one-electron ion or atom. For very heavy ions, around Pb and Bi, QED effects - which amount to just 10^{-6} for protons - rise to several percent; theory thus can be subject to very sensitive tests in this region. Recently discrepancies have been found¹ between high-resolution optical spectroscopy of hyperfine transitions and calculated wavelengths, for $^{207}\text{Pb}^{81+}$ and $^{209}\text{Bi}^{82+}$. In the case of lead, optical spectroscopy in the infrared range on 200 MeV/u $^{207}\text{Pb}^{81+}$ was performed. Of two rotating bunches of ions in the ESR ring the ions in one bunch were excited by a frequency doubled Nd:YAG laser. While ions were excited in one of the straight sections, fluorescence light detection occurred in the other in an array of mirrors equipped with 3 photomultipliers. Fluorescence detection was synchronized with the bunches: light from one bunch was beam related background, while light from the other also contained the signal. Wavelength tuning was affected by changing the electron coolers acceleration voltage, thus changing the beam velocity. The resulting wavelength for the M1 hyperfine transition was found to be 1019.7 nm, i.e. a disagreement of 4.5 nm with respect to theory. In order to address questions with respect to a possible nuclear origin of the observed discrepancy we plan to improve the experimental setup by increasing the light detection efficiency in a new design of the fluorescence detection assembly and then measure Li-like 2s and H-like 1s hyperfine transitions for $^{209}\text{Bi}^{82+}$.

1. P. Seelig *et al.*, Phys. Rev. Lett **81**, 4824 (1998).

Theoretical studies of interactions of atoms, molecules and surfaces

C. D. Lin

J R Macdonald Laboratory
Kansas State University
Manhattan, KS 66506
e-mail: cdlin@phys.ksu.edu

In this abstract we report progress and future plans in the theoretical developments in three areas: (1) Interactions of intense laser fields with atoms and molecules. (2) Hyperspherical approach for ion-atom collisions at low energies. (3) Classification of intershell triply excited states of atoms. Computations carried out in conjunction with new ion-atom collision experiments are also summarized.

1. Interaction of intense laser fields with atoms and molecules

Background.

In conjunction with the new experimental initiative in the JR Macdonald Laboratory we have also started a theoretical program studying the interaction of atoms and molecules with intense lasers. After surveying the literature, we decided to take on the theory of ionization of molecules by an intense laser. There are a number of puzzling experimental observations where even a simple qualitative interpretation is not available.

The ionization of atoms, especially of rare gas atoms, by femtosecond Ti:Sapphire lasers has been well studied experimentally and the ionization yield has been found to be well-described by the tunneling ionization model, or the so-called ADK model. In this model the ionization by an intense laser field is calculated from the ionization rate of a static electric field which can be approximately expressed in analytic form. The ADK model has been widely used by experimentalists for the ionization of atoms.

When comparing the ionization of molecules vs. atoms with similar ionization potentials, it was found that there were irregularities. For N_2 vs. Ar, where the potentials are nearly the same, their ionization rates were found to be about the same too. On the other hand, O_2 and Xe also have nearly identical ionization potentials, but the ionization rates for O_2 are significantly smaller than Xe. Thus O_2 ionization is suppressed.

The origin of ionization suppression of O_2 has been controversial. It has been "explained" in terms of many-electron effect [Guo, PRL85,2276,(2000)], or in terms of interference from the two atomic centers [Muth-Bohm et al PRL, 85, 2280(2000)].

Progress in the last year

We have succeeded in extending the ADK model to describe tunneling ionization of molecules. The basic idea is rather simple. Since the ADK model was derived for the one-center atoms, to apply it to molecules, one needs to extract the one-center parameters from the two-center (for diatomic molecules) molecular wavefunctions. By fitting the asymptotic electronic wavefunction of a molecule in proper form, we derived the parameters needed for the ADK model for molecules. With these parameters the tunneling ionization rates for each molecule can be calculated for any pulse shape, laser intensity and pulse duration, in analytical form. Our theory also accounts for the dependence on the alignment of molecules.

We have completed two manuscripts on molecular tunneling ionization so far. The theoretical paper [#A1] which detailed the theory has been submitted for publication. In this paper we also calculated the ratio of the ionization yield of the molecule with its companion atom, as a function of the peak laser intensity. The molecular tunneling model results are compared to the experimental data from Bob Jones' group in Virginia. We found generally good agreement with their data.

The molecular tunneling model predicts that most molecules would show ionization suppression if its valence electron is a π orbital. This is the case for O_2 . Since ionization suppression means a higher saturation intensity to ionize the molecule, this implies that the cutoff for the harmonic generation would be greater for the molecule than for its companion atom. This has been shown to be true by Z. H. Chang's group in their first experiment at the J. R. Macdonald Laboratory. Indeed the cutoff for O_2 was found to be much higher than for Xe, but N_2 and Ar have an essentially identical cutoff. A combined experimental and theoretical paper on this work has been submitted for publication [see #A2].

Future Plans

Our molecular tunneling ionization model also predicts the dependence of ionization rates on the alignment of molecules. In the coming year we will calculate the ionization yields for molecules that are aligned. It is well known that molecules exposed to a short pulse laser will be found partially aligned at each "revival" time. We will calculate the ionization rates of molecules in the short interval near the revival period which can be tested experimentally. We expect the dependence for O₂ and N₂ to be quite different.

Our tunneling model has been applied to molecules near the equilibrium internuclear distance so far. To understand the dissociation of molecules we need to obtain the ionization rates of molecules and molecular ions at all internuclear distances. We hope to extend the present tunneling model to all internuclear distances, to account for the so-called charge resonance enhancement effect in the tunneling model as well.

2. Hyperspherical approach to ion-atom collisions at low energies

Background

Ion-atom collisions at low energies are usually carried out using the close-coupling expansion with molecular orbitals. This is the so-called Perturbed Stationary State (pss) approximation. While the pss model is widely used, this "standard" approach has serious fundamental difficulties since the theory is not Galilean invariant. In the past few decades translational factors were introduced in an ad hoc manner to account for such a deficiency. The validity of such an approach is difficult to assess. It is well-known that the problems associated with the pss model can be avoided if the collision theory is formulated using hyperspherical coordinates. However, the hyperspherical approach has not been used for ion-atom collisions so far since one has to sum over thousands of partial waves to obtain a converged scattering cross section. However, in previous studies, we have shown that simplified calculations are possible.

Progress in the last year

In the last two years, we have developed the computer codes needed to perform close-coupling calculations for ion-atom collisions in hyperspherical coordinates. We formulated the theory in the body-frame of the quasi-molecule. To avoid calculating the nonadiabatic coupling terms directly we adopted the slow discretized variable approach. From the S-matrix the differential as well as total inelastic scattering cross sections can be extracted.

In the last months, we finally have all the programs developed and a first calculation has been carried out. We calculated the charge transfer cross sections for He⁺⁺ on H from 500 eV down to about 10 eV in the center-of-mass frame. In this energy region, the cross section drops by a factor of about 10⁶. We have found that our results differ significantly from calculations based on the molecular orbitals with translational factors. At higher energies the discrepancy becomes smaller. There are no experimental data available for comparison but our results at low energies agree with another calculation that uses expansion of the wavefunction in two sets of Jacobi coordinates. It is difficult to generalize the latter method to other systems.

Future plans

Our goal for this project is to provide benchmark results for simple ion-atom collision systems. We intend to explore the energy region from subdegree Kelvins up to about a few keV's where the semiclassical approach can be used. We expect to study basic systems such as H⁺+H for the excitation and charge transfer at low energies, electron capture of H by multiply charged ions where some experiments are available from the merged-beam experiments at ORNL. By treating atoms or ions using model potentials we expect to be able to study their collisions at low energies as well.

In the future, we can also extend the newly developed hyperspherical code for collisions involving atom and diatom, to test how well this package compares to other reactive scattering codes.

3. Classification of Intershell triply excited states of atoms

Background

In the previous years we have succeeded in classifying the 2/21'21'' and 3/31'31'' intrashell triply excited states of atoms. The states are classified in terms of the bending vibrational normal modes of an XY₃ molecule with X being the nucleus and Y the electron. These normal modes have been abbreviated as A, B and C and they are to distinguish the different modes of angular correlations.

Progress in the last year

In the last year we made an effort to classify the intershell triply excited states. Specifically our goal was to classify the 49 $2l2l'3l''$ triply excited states. There are eight $2l2l'2l''$ intrashell states, and thus only eight of the 49 states can be classified as radially excited from the $2l2l'2l''$ intrashell states. The other 41 of them have to be classified separately.

For the $2l2l'3l''$ intershell states, the first two electrons have the same principal quantum number so that the radial motion of these two electrons corresponds to "+", since the two-electron states would belong to intrashell doubly excited states. A new radial quantum number has to be added to describe the "+" or "-" of the radial motion of the third electron with respect to the first two. To incorporate such radial correlations, the states that have intrashell states as the first member of the Rydberg series are designated as A^{++} , B^{++} and C^{++} . For the others we would have A^{+-} , B^{+-} and C_s^{+-} and C_h^{+-} . Such states have been identified. There are only a few other states that are not easily classified. They belong to the high-energy states and are probably difficult to treat as similar to the rovibrational motion of a rigid body.

Future plans

Once we have classified the intershell triply excited states, we are not planning to pursue the more complicated higher states in view of the lack of any experimental work. Instead we plan to start looking into quadruply excited states. The calculations and the understanding of such a 4-electron system will be complicated and slow. On the other hand, there are intriguing questions to address. Since a 4-electron system can have two possible equilibrium configurations—a square with all the four electrons and the nucleus on a plane, or a tetrahedron where the four electrons occupy the corners with the nucleus at the center. What would happen to the other normal modes? For such an investigation we need to build up all the necessary programs so we can do some preliminary calculations. Exploratory calculations in the limited subspace are underway.

4. Ion-atom collisions

Progress in the last year

We undertook two projects involving ion-atom collisions last year. We have performed careful studies of the differential and integral charge transfer cross sections for Na^+ on the ground and the excited states of Rb. The experiment was carried out in *Brett DePaola's* group. We have been able to reproduce their experimental results quite well, except that the predicted oscillatory structures in the differential cross sections were not reproduced by the experiment due to the limited angular resolution. At the lowest energy point where the cross section is rather small, we noticed some discrepancies between the calculation and the experiment. We will use the hyperspherical quantum calculation (see #2) to look at the low-energy region in the future.

In the last year we also revisited the shakeoff theory. The motivation of this study is from an experiment carried out at Stockholm. In that experiment, they measured the ratio of a transfer ionization cross section to single electron capture cross section of He as a function of the proton collision energy. By determining the momentum of the recoil ion, they were able to show that for the so-called kinematic transfer ionization (KTI) process, this ratio is very similar to the ratio of double ionization to single ionization by high energy photons in He. Intuitively the similarity points out that both processes could be understood in terms of the shakeoff theory where the first electron is ejected with a different mechanism but the ejection of the second electron is the result of shakeoff. The shakeoff theory in the literature assumes that the first electron escapes with an infinite velocity, thus the inability to predict the energy dependence of the ratios mentioned. We have performed the correct shakeoff calculations using correlated He wavefunctions and confirmed that the experimental results are in good semiquantitative agreement with the shakeoff theory.

Publications including preprints (2000-2002)

A. Interactions of intense lasers with atoms and molecules

A1. X. M. Tong, Z. X. Zhao and C. D. Lin, "Theory of molecular tunneling ionization", submitted to PRA(2002).

A2. Bing Shan, X. M. Tong, Z. X. Zhao, Z.H. Chang and C. D. Lin, "High Harmonic cutoff extension of molecules due to ionization suppression", submitted to PRA (2002)

- A3. Z. X. Zhao, B. D. Esry and C. D. Lin " Boundary-free scaling calculation of the time-dependent Schroedinger equation for laser-atom interactions ", Phys. Rev. A **65**, 023402 (2002)
- A4. Xiaoxin Zhou, Baiwen Li and C. D. Lin "Linear-least-squares-fitting procedure for the solution of time-dependent wavefunction of a model atom in a strong laser field in the Kramers-Henneberger frame ", Phys. Rev. A **64**, 043403 (2001)

B. Triply excited states of atoms

- B1. Toru Morishita and C. D. Lin, " Identification and visualization of the collective normal modes of intrashell triply excited states of atoms", J. Phys. **B34**, L105 (2001).
- B2. C. D. Lin and Toru Morishita, "Few-body problems: the hyperspherical way", Physics Essays, **13**, 367 (2001).
- B3. Toru Morishita and C. D. Lin "Classification and rovibrational normal modes of 3l3l'3l triply excited states of atoms", Phys. Rev. A **64**, 052502 (2001)

C. Ion-atom and Ion-molecule collisions

- C1. T. G. LEE, H. NGUYEN, X. FLECHARD, B. D. DEPAOLA AND C. D. LIN, "Differential charge-transfer cross sections for $\text{Na}^{\{+\}}$ with Rb collisions at low energies", submitted to Phys. Rev. A (2002)
- C2. T. Y. Shi and C. D. Lin, " Double photoionization and transfer ionization of He: Shakeoff theory revisited", submitted to PRL(2002)
- C3. Emil Y. Sidky and C. D. Lin " cross section calculations on proton-impact ionization of hydrogen", Phys. Rev. A **65**, 012711 (2002)
- C4. C. D. Lin and Ingrid Reiser, "Alignment-dependent Atomic Model for Electron Transfer in Ion-Molecule collisions", Int. J. Mol. Sci. **3**, 132-141 (2002)
- C5. C. D. Lin and F. Martin, *Fast and Slow Collisions of Ions, Atoms and Molecules*, a chapter in *Encyclopedia of Scattering*, Academic Press. (2001) p. 1025.
- C6. Emil Sidky, Clara Illescas and C. D. Lin, "The role of potential Saddle in $\alpha + \text{H}$ impact ionization", J. Phys. B. Lett. **B34**, L163 (2001)
- C7. A. Amaya-Tapia and H. Martínez, R. Hernández-Lamoneda and C. D. Lin, "Charge transfer in $\text{H}^+ + \text{Ar}$ collisions from 10 to 150 keV", Phys. Rev. A **62**, 052718 (2000).
- C8. B.B. Dhal, Lokesh C. Tribedi, U. Tiwari, P.N. Tandon, T. G. Lee, C.D. Lin and L. Guly'as, "Single K-K electron transfer and K-ionization cross sections in collisions of highly charged C,O,F,S,Cl ions with Ar and Kr", Phys. Rev. A **62**, 022714 (2000)
- C9. B. B. Dhal, L. C. Tribedi, U. Tiwari, P. N. Tandon, T. G. Lee, C. D. Lin and L. Gulyas, " Strong double K-K transfer channel in near symmetric collision of $\text{Si} + \text{Ar}$ ", J. Phys. **B33**, 1069 (2000)
- C10. T. G. Lee, H. C. Tseng and C. D. Lin, " Evaluation of antiproton impact ionization of He atoms below 40 keV", Phys. Rev. A **61**, 062713(2000)
- C11. H. C. Tseng and C. D. Lin, "Total and State-selective Electron Capture Cross Sections for $\text{B}^{4+} + \text{H}$ collisions", Phys. Rev. A **61**, 034701 (2000)
- C12. Emil Sikdy, Clara Illescas and C. D. Lin, "Electrons ejected with half the projectile velocity and the saddle point ionization mechanism", Phys. Rev. Lett. **85**, 1634 (2000)

D. Others

- D1. B. D. Esry, C. D. Lin, C. H. Greene and D. Blume
" Comments on "Efimov states for ^4He trimers?" Phys. Rev. Lett **86**, 4189 (2001)
- D2. Chien-Nan Liu, Ming-Keh Chen, and C.D. Lin " Radiative Decay of Helium Doubly Excited States", Phys. Rev. A **64**, 01050(R), 2001 [Rapid Commu.]

THEORETICAL STUDIES OF INTERACTIONS OF ATOMS, MOLECULES, AND SURFACES: DYNAMICS OF FEW-BODY SYSTEMS

B.D. Esry

*J. R. Macdonald Laboratory
Kansas State University
Manhattan, KS 66506
esry@phys.ksu.edu*

Program Scope

This research program will explore the three- and four-body problem under a variety of circumstances ranging from bound states to collisions, both with and without an external field. A major component of this program is to develop the novel theoretical tools — both analytical and numerical — required for this effort. The ultimate goal is to understand the dynamics of these strongly coupled systems in quantum mechanical terms.

Charge exchange in $\alpha + \text{H}_2^+$ collisions

Recent progress My graduate student, Shu-chun (Amy) Cheng, has recently been working on solving the time-dependent Schrödinger equation for electron capture from H_2^+ by an ion. The calculations were motivated by an experiment carried out by C.L. Cocke's group in our lab. The essential physics is that when the electron is captured from H_2^+ , the molecule will dissociate. Amy is propagating the Schrödinger equation in three-dimensions for the electronic wave function. The projectile is assumed to move along a straight line trajectory, and the molecular nuclei are assumed stationary. At the collision energies relevant to the experiments, both assumptions are quite good.

To help her understand the propagation methods, Amy started working on a one-dimensional model of the system. In the model, the molecule is in line with the trajectory of the incoming ion. The approaching ion comes within some minimum distance of the molecular center of mass, then recedes along its entrance direction. We used this model to test both the propagation code and a masking function that damps all of the electron wave function save that on the molecular ion. Since we are only interested in the total electron capture, this approach is both sufficient and efficient. Amy has obtained the capture probability in this model as a function of the distance of closest approach and presented the results at a poster at DAMOP.

Future plans Amy is in the process of developing the three-dimensional code, and no problems are expected. Once the total electron capture probability is obtained for this case, the dissociation probability is known since they are the same. The angular and energy distributions of the molecular nuclei are then known as well. We can thus obtain a quantity that is directly comparable to experiment. We plan to begin generating the data soon. It will take some time, though, since the capture probability depends on five parameters: the impact parameter b , the orientation of the molecule θ and ϕ , the distance between the nuclei R , and the velocity of the incident ion v . In the end, we will integrate over b , ϕ , and R , weighting the integrals with the appropriate nuclear wave function. As long as only one electron is active, there is, in principle, no difficulty to include a polyatomic target, or even a molecular projectile. These cases will, of course, require careful modelling to reduce them to one active electron, but they could be quite interesting to study.

Ionization in ion-atom collisions

Recent progress We have worked on applying the scaled coordinate method to the time-dependent Schrödinger equation for ionization in ion-atom collisions. The advantage of the scaling method is that it analytically removes much of the known behavior of the ionized wave function, leaving only a smooth, stationary envelope to propagate. In particular, it alleviates the need for the absorbing boundaries normally used in such calculations.

The primary effort on this project came from my postdoc, Wei Guo. He arrived in August 2001 and worked to apply the scaling method to a one-dimensional model of the collision. Using this model gave us the opportunity to explore the scaling method for ion-atom collisions in an efficient manner since the one-dimensional model already contains all of the elements peculiar to the scaling method. Wei eventually got the code working and began to generate data for the one-dimensional problem, but was unable to complete the project. Wei left at the end of May, 2002; a replacement, Vladimir Roudnev, has been hired and is scheduled to arrive in October 2002.

Future plans While the numerical aspects of this method require care, there appear to be no fundamental difficulties in extending the scaling to the three-dimensional ion-atom collision problem. My plans for the near future, however, do not include this project since other efforts appear more timely.

Protonium formation in $\bar{p}+H(1s)$ collisions

Recent progress The low-energy, less than roughly 10 eV, collision of \bar{p} with hydrogen is one of the most asymmetric systems one can consider. The difficulty lies in the fact that \bar{p} and p can form bound states with a ground state energy of approximately -459 a.u. By comparison, the energy in the incident channel is -0.5 a.u. The formation of protonium, Pn or $\bar{p}p$, occurs when the proton is captured by the antiproton, ionizing the electron in the process. Based on simple energy arguments, the most likely Pn states produced are in the $n=30$ manifold. The extreme change in length and energy scales — going from truly quantum mechanical in the initial state to nearly classical in the final state — makes the problem extremely difficult to treat theoretically. Not surprisingly, the experiment is also difficult to do. Nevertheless, the ASACUSA collaboration at CERN predicts that they will make preliminary measurements of Pn formation within the next year. Unfortunately for us, the target will likely be hydrogen molecules rather than atoms since the Pn formation cross section is predicted to be larger from classical calculations.

It is tempting to apply the Born-Oppenheimer approximation to this problem, and many people have. The Born-Oppenheimer curves, however, do not allow for the formation of Pn; the united atom limit is a free electron. In collaboration with Hossein Sadeghpour at ITAMP, I have instead used the adiabatic hyperspherical approach to generate potentials that do indeed correlate to the $\bar{p}+H(1s)$ limit as well as all of the $Pn(n\ell)+e^-$ channels. Unfortunately, about 450 potential curves are required to cover the energy range of interest. This multitude of channels and the strong coupling between them is at the heart of the problems with asymmetric systems. To gain some insight into the physics, we have artificially reduced the masses of p and \bar{p} and carried out the scattering calculations with these simpler systems. By examining several values of the mass, we could identify the important channels. This work has been submitted for publication and has so far resulted in two invited talks: one at an ITAMP workshop and the other at an ECT* workshop in Trento, Italy.

Future plans I want to combine the physical insight gained in our scaled-mass calculations with a diabatic representation in order to reduce the number of channels in the full-mass problem. While we have recently completed the manuscript describing our split diabatic approach, another

adiabatic approach will likely be needed. The split diabatic representation requires one to identify all of the curve crossings by hand — an unreasonable task with 450 channels. We will thus seek alternative diabatization schemes that can be applied more automatically. I anticipate that any method successful for this system can be profitably applied to other collision systems, allowing quantum mechanical calculations where none are now possible.

Low-energy Ps+Ps collisions

Recent progress Roman Krems, a very capable Predoctoral Fellow at ITAMP who is soon to be a postdoc there, recently spent two weeks at Kansas State to begin implementing my formulation of an adiabatic hyperspherical approach for the low-energy collision of two Ps (e^+e^-) “atoms”. The only four-body adiabatic hyperspherical treatments that have been done to date are for three electron atoms (see C.D. Lin’s report). With an infinitely heavy nucleus, this system has a natural center about which to define approximately good angular momentum quantum numbers. In fact, four electrons can be treated in the adiabatic hyperspherical approach for this same reason. The equal mass problem that we are considering, however, does not have such a natural center, making the necessary expansion over partial waves more slowly converging.

Because the adiabatic equation for the four-body problem in the center-of-mass (CM) frame requires eight coordinates, we must expand the wave function using partial waves. There is one spherical harmonic associated with each of the three relative position vectors in the CM frame, accounting for six coordinates. The other two coordinates are our hyperangles. In principle, then, coupled two-dimensional partial differential equations must be solved. This route very quickly becomes too computationally demanding. Instead, we are diagonalizing the adiabatic equation for a fixed set of $\{\ell_1, \ell_2, \ell_3\}$, then coupling these together to obtain the final result. Even though the $\{0,0,0\}$ curve by itself recovers more than 90% of the asymptotic Ps+Ps energy, we are finding that the last few percent require many partial waves.

Future plans The code seems to be nearly complete, but we are still struggling to achieve convergence in the partial wave expansion. Roman will continue to work on this problem as a postdoc, trying to determine whether our current difficulties are due to lingering bugs in the program or to actual physics. Successful completion of this project will be an exciting accomplishment since few other methods could similarly treat equal mass four-body systems for both bound and collisional states.

Publications

- “Boundary-free scaling calculation of the time-dependent Schrodinger equation for laser-atom interactions,” Z.X. Zhao, B.D. Esry and C.D. Lin, *Phys. Rev. A* **65**, 042725 (2002).
- “Charge transfer and elastic scattering in very slow $H^+ + D(1s)$ half collisions,” E. Wells, K.D. Carnes, B.D. Esry, and I. Ben-Itzhak, *Phys. Rev. Lett.* **86**, 4803 (2001).
- “Helium trimer has no bound rotational excited states,” T.G. Lee, B.D. Esry, B.C. Gou, and C. D. Lin, *J. Phys. B* **34**, L203 (2001).
- “Charge exchange in slow $H^+ + D(1s)$ collisions,” B.D. Esry, H.R. Sadeghpour, E. Wells, and I. Ben-Itzhak, *J. Phys. B* **33**, 5329 (2000).
- “Asymmetric branching ratio for the dissociation of $HD + (1s\sigma)$,” E. Wells, B.D. Esry, K.D. Carnes, and I. Ben-Itzhak, *Phys. Rev. A* **62**, 062707 (2000).

- “Boundary-free propagation with the time-dependent Schrödinger equation,” E.Y. Sidky and B.D. Esry, *Phys. Rev. Lett.* **85**, 5086 (2000).
- “Symmetry breakdown in ground state dissociation of HD^+ ,” I. Ben-Itzhak, E. Wells, V. Krishnamurthi, K.D. Carnes, O.L. Weaver, and B.D. Esry, *Phys. Rev. Lett.* **85**, 58 (2000).

Interactions of Ions and Photons with Atoms, Surfaces, and Molecules

Uwe Thumm [thumm@phys.ksu.edu, (785) 532-1613]

1. Neutralization of Negative Hydrogen Ions near Metal Surfaces (T. Niederhausen, H. Chakraborty, U. Thumm)

We have applied wave-function propagation techniques to charge-transfer processes in ion-surface interactions, using self-consistent potentials to represent the electron-surface interaction. Apart from contributing to the qualitative understanding of the interaction mechanism through computer animations, this project has led to the quantitative assessment of charge transfer and to the characterization of surface resonances in terms of level shifts and decay widths as functions of the ion-surface distance. Using the split-operator Crank-Nicholson propagation technique in conjunction with carefully adjusted absorbing potentials near the numerical grid edges, we have performed 3D propagation calculations for the decay of negative hydrogen ions near metal surfaces.

In particular, we have completed calculations for the neutralization of negative hydrogen ions near two copper surfaces of different symmetries, Cu(100) and Cu(111). In these (adiabatic) calculations, we kept the ion-surface distance D fixed and propagated the electronic wave function. To start with, we used a 1D propagation scheme where the active electron is restricted to move along the surface normal. To model the electron-surface interaction, we used suitable parametrizations of self-consistent LDA potentials. For numerical convenience, we performed these calculations for 100 monolayer thick Cu films and extended the numerical grid 200 atomic units on the vacuum side. In order to test the accuracy of our Cu potentials, we diagonalized the effective one-electron Hamiltonian and were able to reproduce the experimentally known energies of the upper and lower limits of the surface projected L-band gap, the surface-state energy, and the energies of the few lowest image states.

We obtained resonance positions and widths by first propagating the initial negative hydrogen state (one-electron approximation) for fixed D . Next, we calculated the projected density of states (PDOS) by Fast Fourier Transformation of the autocorrelation function, i.e., the overlap of the electronic wave function at time t with the initial electronic state. We repeated this calculation for various D and identified peaks in the PDOS as resonance states that asymptotically (for large D) correspond to the affinity level of the negative hydrogen ion, to image states, surface states, and bulk states of the 100 layer thick film. The lifetimes of those resonance states were extracted from the line widths of the corresponding peaks in the PDOS. We compared our results for the Cu(100) and Cu(111) surfaces with results for a structureless Cu-jellium potential.

By plotting the level shifts and widths for Cu(100), Cu(111), and Cu(jellium) as a function of D , we noticed several avoided crossings between image-state, surface-state and affinity-level resonances (Fig.1). Interestingly, the detailed behaviour of both level widths and shifts differs strongly for decay into Cu(100) and Cu(111). Qualitatively, we

understand this difference in terms of the different energetic location of image states, surface state, and surface band gap.

We plan to extend this 1D adiabatic propagation calculations to two and three dimension. We will try to quantify to what degree the inclusion of the active electron's motion in the surface plane affects resonance widths, and shifts. Next, we intend to include the motion of the projectile in order to provide neutralization probabilities for the scattering of negative ions near surfaces and to understand the interplay of elementary processes at different time scales (decay into surface states, decay of surface states, effects of the electron's motion parallel to the surface, the role of lifetimes and interaction times).

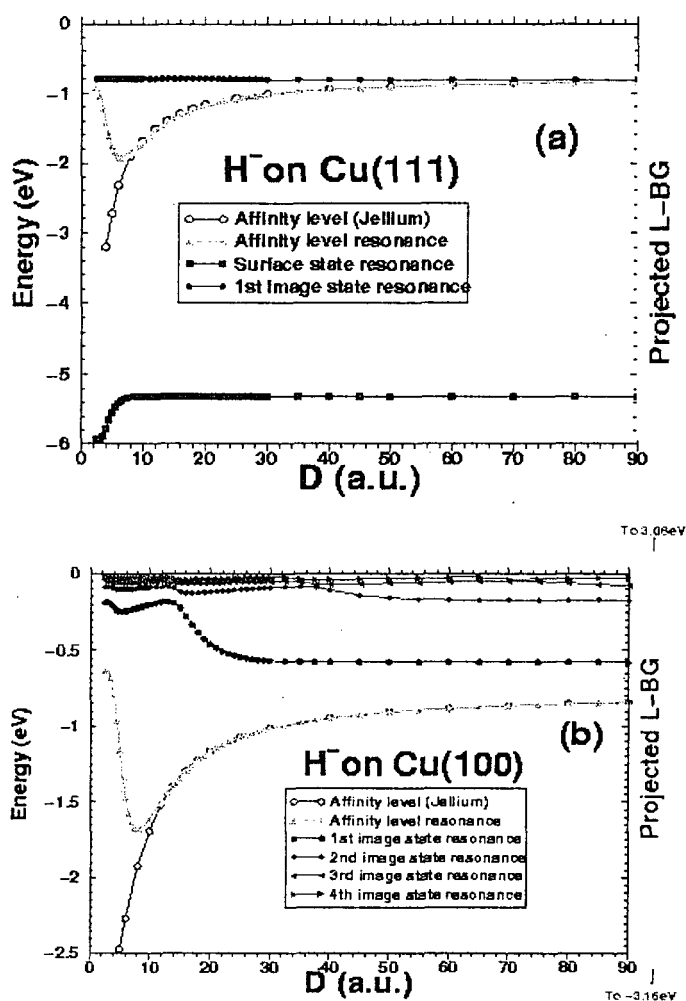


Fig.1: Affinity level, surface state, and image state peak position as a function of the ion-surface distance D . Results obtained from the projected density of states for a Cu(111) surface (a) and a Cu(100) surface (b).

2. Laser-Matter Interactions (M. Alcantara Ortigoza, B. Feuerstein, U. Thumm).

We have investigated the interaction of 25 fs, 0.2 PW/cm^2 , 780 nm pulses with H_2^+ and D_2^+ molecular ions within a reduced-dimensionality model that represents both the nuclear and electronic motion by one degree of freedom. We carefully adjusted the adiabatic molecular electronic potential by introducing a „soft-core function“ $a(R)$ in the electron-nucleus interaction potentials $1/(x \pm R/2 + a(R))$ that depends on the internuclear distance R instead of the commonly used fixed soft-core constant a . We obtained molecular model potentials that reproduce accurate three-dimensional results for the known number of 19 vibrational states in the electronic ground state and for the dipole oscillator strength.

We solved the time-dependent Schrödinger equation on a two-dimensional numerical grid and designed a simple, but as far as we know new, method to calculate the flux of emitted electrons and protons by means of „virtual detectors“ for electrons and protons. These detectors are placed outside the excursion range of the electron and at a distance R where the amplitudes of bound vibrational states have become irrelevant.

Our results reproduce the main features of measured kinetic-energy release spectra, support the „charge-resonance enhanced“ ionization mechanism, and allow us to clearly distinguish between molecular dissociation (MD) into field-dressed final channels and fast, ionization-induced Coulomb explosion (CE). Both MD and CE appear as distinct peaks in the kinetic energy release spectra. We find that MD dominates for molecular ions that are prepared in the two lowest vibrational states only, while CE becomes increasingly dominating for higher vibrational states (Fig.2).

For two short laser pulses of variable delay, we started to resolve in time the interplay between MD and CE. We intend to further investigate the pump-probe dynamics for two short pulses (Fig.3). We will explore the possibility of adding a further dimension to the electronic motion. Motivated by new experiments in the Macdonald Laboratory, we have stated to investigate the ionization of model atoms under the combined influence of a few-cycle intense Laser pulse (10^{14} to 10^{15} W/cm^2) and a significantly longer and less intense pulse (about 10^{12} W/cm^2). The two pulses may or may not be phase coherent.

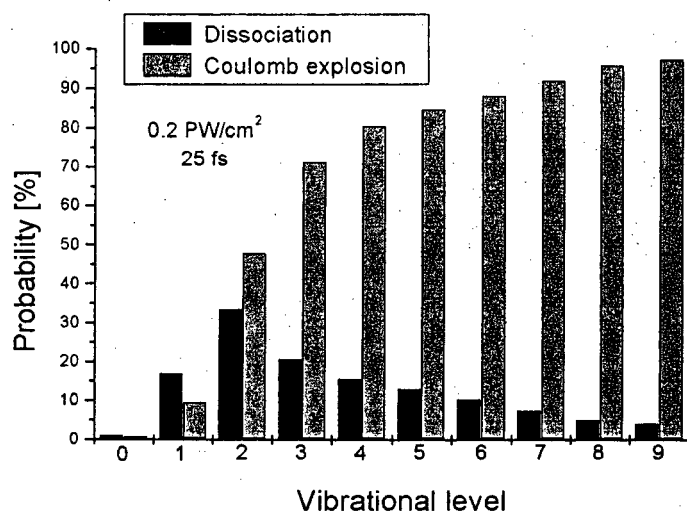


Fig.2: Dissociation and Coulomb explosion fractions for H_2^+ and 25 fs, 0.2 PW/cm^2 Laser pulses as a function of the initial vibrational state of the molecular ion.

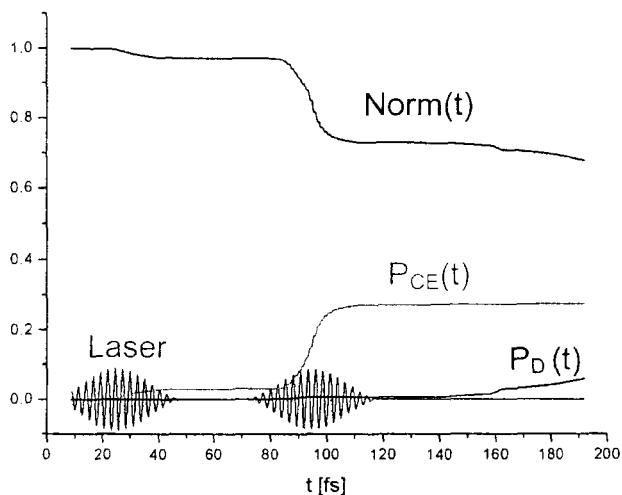
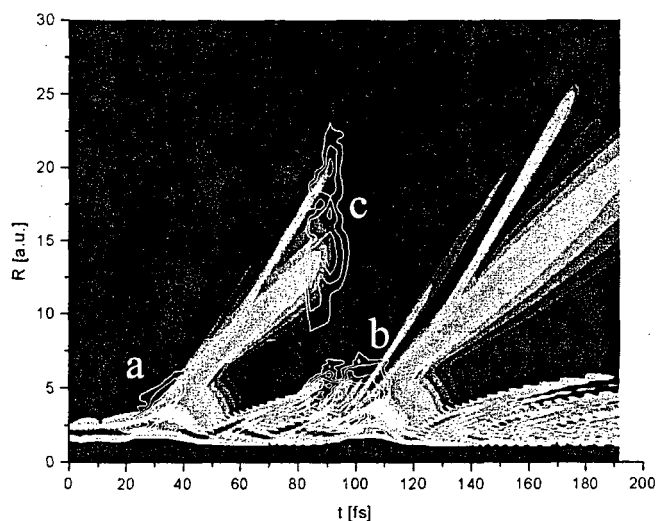
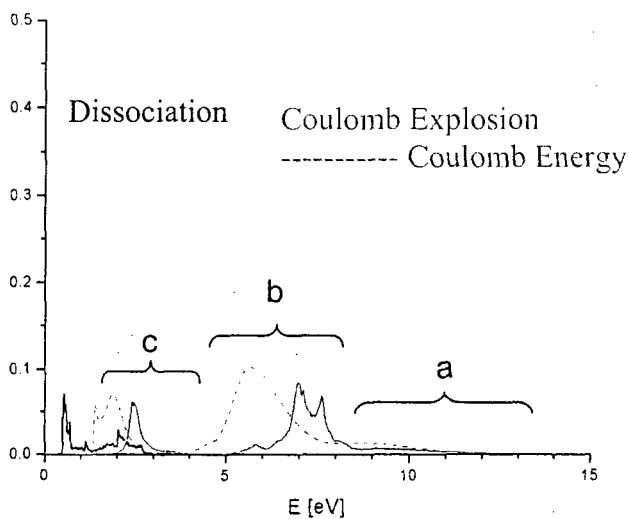


Fig.3: Pump-probe results for D_2^+ molecular ions, initially in the vibrational ground state ($v=0$), and two 25fs, $0.3PW/cm^2$ pulses with a delay of 70fs.

Top: Norm of the molecular wave function on the numerical grid, laser pulses, and probabilities for Coulomb explosion (P_{CE}) and dissociation (P_D) versus time.



Middle: Probability density of the molecular wave function, integrated over the electronic coordinate x . The jets correspond to dissociation. The contour lines represent the rate of Coulomb explosion (a,b) and dissociation followed by Coulomb explosion (c).



Bottom: Kinetic energy release spectrum corresponding to the middle graph. The dashed line shows Coulomb explosion results where the initial kinetic energy of the nuclei is neglected.

Inner-Shell Photo-ionization of Atoms and Small Molecules

A. Belkacem and M. Prior

Chemical Sciences Division
Lawrence Berkeley National Laboratory
Berkeley, CA 94720

Objective and Scope

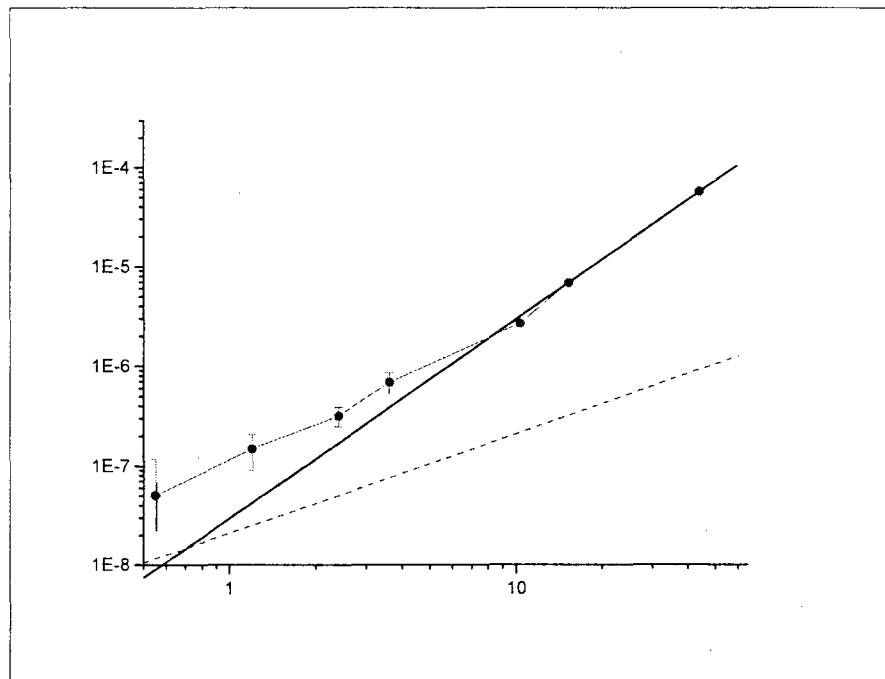
The goal of this part of the LBNL AMOS program is to understand the structure and dynamics of atoms and molecules using photons as probes. The current research carried out at the Advanced Light Source is focused on studies of inner-shell photo-ionization and photo-excitation of atoms and molecules, as well as breaking new ground in the interaction of x-rays with atoms and molecules dressed with femto-second laser fields. These studies can be divided into three complementary parts, a) dynamics of x-ray ionization of atoms and molecules, b) intense-field, two-color (x-ray + laser) inner-shell photo-ionization, (*this part is included in the abstract of Ali Belkacem's talk*) c) inner-shell photo-ionization at high energies. The low-field photo-ionization work seeks new insight into atomic and molecular processes and tests advanced theoretical treatments by achieving new levels of completeness in the description of the distribution of momenta and/or internal states of the products and their correlations. The intense-field two-color research is designed to provide new knowledge of the evolution on a femto-second time scale (ultimately atto-second) of atomic and molecular processes as well as the relaxation of atomic systems in intense transient fields. This very exciting new area draws from and brings together two very fertile tools of research of AMO physics (synchrotron radiation and high power lasers). The third part of this research seeks to expand the knowledge of atomic physics into new frontiers in the relativistic regime and very strong fields where the negative energy continuum plays a major role in photo-ionization and charge transfer processes.

A. Photo-ionization Studies - Low Field (single photon)

The LBNL AMOP program has been active in studies of the photo-ionization of simple atoms and molecules at the Advanced Light Source (ALS) since 1995. This work is collaborative with groups from U. Frankfurt, Kansas State and Western Michigan Universities, and occasionally with members of other institutions. Initial work concentrated upon the double ionization of He, a prototype system for study of the single photon double ionization process. These measurements have stimulated advanced theoretical treatments. Although He continues to be studied (see below), we have also addressed the H₂ (or D₂) molecule and, most recently the study of core electron ionization of simple molecular targets. For the latter, the inter-nuclear axis alignment or orientation is determined, a posteriori, from the anti-parallel molecule fragment ion momenta, and the distribution of photo-electrons is referenced to this axis as if the molecule were "fixed-in-space" (a term now prevalent in the literature).

In February 2001, we utilized the circularly polarized photons at the ALS undulator beamline 4.0.2 to make detailed measurements of circular dichroism in the K-shell photo-ionization of oriented CO and aligned N₂ molecules. Circular dichroism refers to modifications in photo-induced processes that depend upon the handedness of the incident photons. A random collection of chiral molecules, such as many naturally occurring biomolecules, can exhibit dichroism in simple absorption. However to observe circular dichroism in the angular distribution (CDAD) of photo-electrons from a diatomic molecule, the experiment must define the momentum vector of the photon, the molecular axis and the photoelectron momentum. The experimental approach used was the same as in our earlier COLTRIMS studies of core photoelectron distributions using linear polarized photons. The photon energies covered the same range,

We set up an experiment at the ESRF in Grenoble France to measure vacuum-assisted photoionization in an energy domain where this process is expected to dominate over Compton scattering and the photo-electric effect. The high energy photon beam is produced at the GRAAL beamline through back-scattering of a cw laser beam on the electrons of the ESRF storage ring. We produce approximately 10^5 photons per second in the GeV energy range.



The figure above summarizes some of the data and shows the probability of producing a K-vacancy in Ag in coincidence with the production of an electron positron pair as a function of the target thickness. The solid line represents a calculated dependence of the probability with the target thickness for a two-step process. In a two-step process the pair is created on one atom and the pair creates a K-vacancy through collision with a different atom. The two-step probability varies as the square of the target thickness and is well reproduced by theoretical calculations. More interesting is the very clear departure from the quadratic behavior for the thin targets. This departure from a quadratic to a linear behavior is a signature of the contribution of vacuum-assisted photo-ionization. This contribution is at least one order of magnitude larger than a combination of the photoelectric effect and Compton scattering. This measurement confirms the theoretical prediction that vacuum-assisted photo-ionization is the most probable ionization mechanism at very high energies.

Future Plans

Further study of the Auger electron emission from fixed-in-space molecules will include a wider range of photon energies for the case of CO, C and O K-shell excitation. We are also measuring (August 2002) the photoelectron and Auger electron emission patterns from fixed-in-space hydrogen and deuterium molecules ionized to dissociating states. Analysis of this data will be completed in FY2003. We also plan to explore extensions of momentum spectroscopy to the study of electron molecule collision processes. This would establish an LBNL experimental accompaniment to the theoretical program in electron molecule collisions conducted by LBNL PI's C.W. McCurdy and T.N. Rescigno. This work will focus upon dissociative electron attachment and ion-pair formation.

yielding photo-electron energies of 0-30 eV, i.e. from below to above the σ shape resonances. Measurements with both linear and circularly polarized photons are necessary to completely determine the relative phase of the complex amplitudes for electron emission in the molecular frame. The new CDAD results together with the linear polarization measurements form the most complete description of the core photoelectron emission from a free diatomic system. The CDAD measurements are compared with state-of-the-art one-electron multiple scattering and partially-correlated random phase approximation calculations done by theoretical colleagues. These calculations are in good agreement with many, but not all aspects of the measurements. This work has been published in PRL **88**, 073002 (2002). (A figure from this work appeared on the journal cover.)

Also during February 2001 at the ALS, in a continuation of our studies of He, we measured the fully differential cross sections for single photon double ionization of He at photon energies 450 eV above the threshold for this process ($\cong 80$ eV). We found an extremely asymmetric energy sharing distribution between the two photo-electrons, i.e. a strong preference for one electron to have most of the energy available. The angular distributions showed large anisotropy ($\beta \approx 2$) for the high energy electron and near isotropy ($\beta \approx 0$) for the low energy electron. The measurements covered the energy range 0-50eV for the slow electron. The triply differential distributions of the electrons (differential in the energy partition, and the solid angle of emission of each electron) show a dominance of the shake-off mechanism when the low energy electron has 2 eV (of the total 450 available). This changes to that characteristic of an inelastic electron-electron scattering when the low energy electron is above about 20 eV kinetic energy. In this case the fast electron's emission is peaked parallel to the linear polarization of the photons and the slow electron is distributed broadly with a weak preference for emission opposite the fast electron. At higher energies of the slow electron (e.g. 30 eV) the distributions favor 90 degrees between the two electron momenta as if the low energy electron were scattered in a binary encounter with the fast electron. Theoretical calculations by collaborators A. Kheifets and I. Bray using their convergent close coupling (CCC) approach are in excellent agreement with these new measurements. This work was published in PRL **89**, 033004 (2002).

K-shell photo-ionization of an atom in a molecule yields a photo-electron followed by at least one Auger electron and the fragmentation of the molecule. The photo-emission and Auger processes are thought to be independent so that, e.g. the Auger electron angular distribution in the molecular frame should not depend on the photon energy or the orientation of the photon's linear polarization. However, a recent report claims that there is a marked difference in the Auger emission patterns following K-shell ionization of C in CO by photons polarized parallel vs. perpendicular to the molecular axis. This unexpected observation is reported to depend strongly on the particular Auger transition, and is strongest for photon energies (305 eV) near the peak of the σ shape resonance in CO. In February 2002 we used a modified COLTRIMS setup to measure energy resolved Auger electron emission patterns from oriented CO molecules at the ALS Beam-line 4.0. The Auger electron was measured with improved collection efficiency; the C^+ and O^+ fragments were collected with 4π efficiency and their kinetic energy measurement resolved the different CO^{++} final channels. The result is a much more complete study of the correlation between the Auger emission and the photon polarization in the molecular frame. Our measurements are consistent with the independence of the Auger and photo-electron emission and hence contradict the recent report claiming the contrary. This work is in preparation for publication.

B. Inner-shell photo-ionization at high energies

This part of the program performs detail studies of atomic collision processes that involve large momentum transfer during the interaction. The goal of these studies is to expand the knowledge of atomic physics into new frontiers in the relativistic regime of atomic collisions and strong fields.

Research with Cold Molecules and Cold Atoms

Harvey Gould,

MS 71-259, Lawrence Berkeley National Laboratory, Berkeley, CA 94720 (gould@lbl.gov)

Molecular Synchrotron Feasibility Shown by Modeling

Hiroshi Nishimura, Glen Lambertson, Juris Kalnins, and Harvey Gould

Storing large numbers of neutral molecules for long times, essential for evaporative cooling, moved a step closer to realization with the successful modeling of a synchrotron storage ring for neutral polar molecules. Ammonia molecules with velocity spread, angular spread, and position spread, traveling 90 m/s, were mathematically tracked for four hundred turns (15 s flight time) through bending sections, longitudinal bunching elements, transverse focusing lenses and drift sections. All of these elements used realistic fields, including fringe fields and gravity.

Storage rings, unlike traps, can confine large numbers of molecules with kinetic energies that are higher and largely independent of temperature. Simple toroidal storage rings can store a single pulse of molecules but have no means to keep it from spreading and becoming too diffuse to observe. Bunching the molecules, storing, or extracting multiple bunches, changing their velocity,

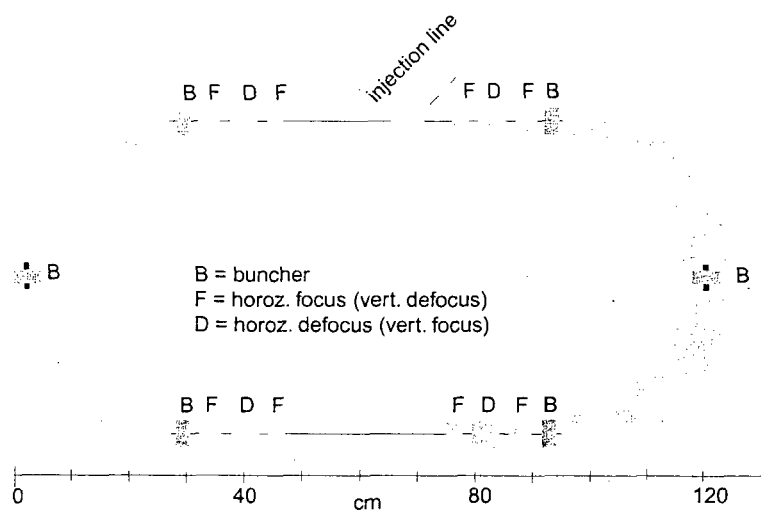


Figure 1 - Desk-top molecular synchrotron storage ring: Up to 52 bunches can be independently loaded and stored for over 400 turns and their velocity synchronously varied from 90 m/s to 60 m/s. The straight sections are for experiments where other beams, lasers, synchrotron light, and other diagnostics can be introduced. This ring with its high intensity, fine energy scan, and very low losses is well suited for elastic scattering and reactive scattering experiments. A modified design can store lower velocity molecules.

continued on next page

New Measurement of Cs Dipole Polarizability

Jason Amini* and Harvey Gould

A new technique, developed at LBNL, has been used to measure the static dipole polarizability of cesium to an uncertainty of about 0.25%. This is the most accurate measurement of the static polarizability of any non-noble element, and improves upon the previous Cs measurement of 2% uncertainty.

In alkali atoms most of the polarizability arises from the dipole matrix element between the $nS_{1/2}$ ground state and the nearby $nP_{1/2}$ and $nP_{3/2}$ states, with a small contribution from core polarizability. The contribution of the core polarizability, which is a challenging part of the polarizability calculation, increases with alkali atomic number reaching about four percent in Cs (Fig. 3). Testing the core polarizability portion of the calculation requires using a high-Z atom and performing a precise measurement. Previous measurements in alkali atoms have tested the calculation of the core contribution to an uncertainty about 50%. This measurement reduces that uncertainty to 6.25 percent or less.

continued on third page

We plan to continue the measurements of photo-ionization at high energies in FY2002. We will make use of the COLTRIMS detection technique to discriminate between the two vacuum-assisted photo-ionization mechanisms. The momentum transfer to the nucleus during the process of pair creation is of order of mc , where m is the mass of the electron and c the speed of light. This translates into an uncertainty in the localization of the electron-positron pair of the order of the Compton wavelength. However what's relevant for the particular mechanism of vacuum-assisted photo-ionization, in which the pair is created in the nuclear field, is the *initial relative* distance between the electron and the positron. Since the K-shell orbit of a high-Z atom is very small, the K-electron has a very high probability to be within a Compton wavelength or less from the nucleus when the process of pair creation occurs in the nuclear field. The interaction of this K-shell electron with the electron-positron pair will depend on the nature of the pair in the first 10^{-20} s of its creation

Recent Publications

A. Staudte, C.L. Cocke, M.H. Prior, A. Belkacem, C. Ray, H.H.W. Chong, T.E. Glover and R.W. Schoenlein, "Observation of a nearly Isotropic, High Energy Coulomb Explosion Group in the Fragmentation of D_2 by Short Laser Pulses." Physical Review A (Rapid Communication), **65**, 020703(R) (2002)

T. Jahnke, Th. Weber, A.L. Landers, A. Knapp, S. Schössler, J. Nickles, S. Kammer, O. Jagutski, L. Schmidt, A. Czasch, T. Osipov, E. Arenholz, A.T. Young, R. Díez Muiño, D. Rolles, F.J. Garacia de Abajo, C.S. Fadley, M.A. Van Hove, S.K. Semenov, N.A. Cherepkov, J. Rösch, M.H. Prior, H. Schmidt-Böcking, C.L. Cocke and R. Dörner, "Circular Dichroism in K-shell Ionization from Fixed-in-Space CO and N_2 Molecules" Physical Review Letters, **88**, 073002 (2002) [Figure on journal cover]

A. Knapp, A. Kheifets, I. Bray, Th. Weber, A. L. Landers, S. Schössler, T. Jahnke, J. Nickles, S. Kammer, O. Jagutski, L. Ph. H. Schmidt, T. Osipov, J. Rösch, M. H. Prior, H. Schmidt-Böcking, C. L. Cocke, and R. Dörner, " Mechanisms of Photo Double Ionization of Helium by 530 eV Photons" Physical Review Letters, **89**, 033004 (2002).

D.C. Ionescu and A. Belkacem
"Dynamics of ionization mechanisms in relativistic collisions involving heavy and highly charged ions"
Eur. Phys. J. D18, 301-307 (2002). LBNL - 48642

D. Ionescu, A. Belkacem, A. Sorensen
"Photo-ionization at relativistic energies"
Physica Scripta Volume T92, R. Swedish Acad. Sci, 330, (2001) – LBNL-48648

molecular synchrotron - continued

and providing access for experiments, requires a more advanced design such as a synchrotron.

In our model synchrotron storage ring, the molecules are deflected, focused and bunched using the interaction between the electric dipole moment of the polar molecule and static and time-varying electric field gradients. Our design (Fig 1) is a racetrack type lattice consisting of two 180-degree arcs, three pairs of focusing electrodes, six sets of bunchers, and long straight sections for experiments and for evaporative cooling. The molecular beam, in this case $^{14}\text{N}^2\text{H}_3$ molecules are injected at a velocity of 90 m/s, but can be synchronously lowered to 60 m/s. Up to 52 independent bunches may be loaded into the ring, greatly increasing the circulating intensity.

The synchrotron is modeled for molecules in a weak-field seeking state. Except for the rotational state $J=0$ state (which is always strong-field seeking), rotational levels are degenerate in zero field, containing weak-field seeking and strong-field seeking m_j components. Molecules that repeatedly enter regions of weak and rapidly changing electric field direction, can undergo transitions between the m_j components leading to a rapid loss of the molecule. In the bend section, which uses electrodes with zero electric field near their center, the centripetal force keeps the molecules in a strong electric field. However in the straight sections, gravity is not sufficient to keep the molecules away from the center region of the electrodes. Therefore the focusing elements, which are of our own new design (Fig. 2), add a strong dipole field. These elements focus in only one transverse direction while defocusing in the other, and are in an alternating gradient configuration. Regardless of the gradient direction, *all electric fields in the synchrotron are in the same direction*. In

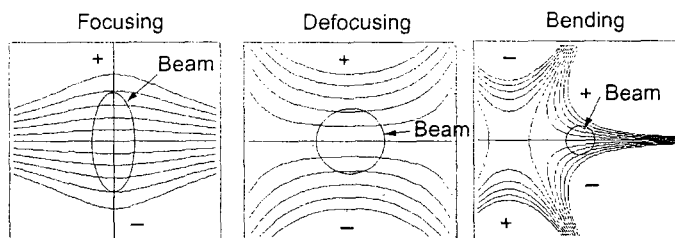


Figure 2- Equipotentials for focusing, defocusing and bending elements for the molecular synchrotron storage ring. The squares are ± 20 mm in each direction and the approximate beam size is indicated. A focusing element focuses in the horizontal direction and defocuses in the vertical direction and the defocusing element focuses in the vertical direction while defocusing in the horizontal. (See publication 1.)

addition we add a weak bias electric field in the otherwise field free regions of the straight sections to maintain the quantization axis.

The overall size of the ring is chosen to balance easily attainable electric fields and good transverse acceptance (high intensity) with desk-top size. The bending radius is chosen to produce nearly zero dispersion in the long straight sections. Otherwise, strong synchrotron coupling develops from bunching and the momentum acceptance is reduced.

The transverse acceptance of this synchrotron is 35 mm-mr in the horizontal direction and 71 mm-mr in the vertical direction (equivalent to the beam from a 1 mm source passing through a 70 mm by 142 mm aperture located one meter downstream.) The energy acceptance is $> \pm 1\%$. These figures are for the surviving beam after 400 turns and *include* slowing the molecules from a jet source using a linear slower of our own design (ammonia seeded in xenon gas at a reservoir temperature of 300 K).

The design and modeling of this synchrotron uses the same methods and procedures as are used in other accelerator design projects such as the ALS super bend. Subject to unknowns about low energy molecular scattering, vibrational excitation by black body radiation, etc. a working synchrotron could be engineered from this design.

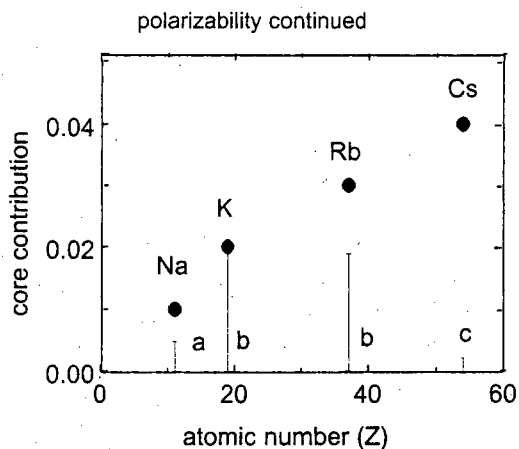


Figure 3 - Contribution of core polarizability to the static dipole polarizability of some alkali atoms (dots) and the experimental uncertainty in the total polarizability measurement. (a) is Eckstrom et. al, PRA 51 3882 (1995), (b) is Molof et. al, PRA 10, 1131 (1974); Hall & Zorn, PRA 10, 1141 (1974), and (c) is this work.

Static polarizability is related to van der Waals interaction and to the $nP_{1/2,3/2}$ lifetimes. With some help from theory, each can be a check on the others (but not an independent determination).

Our new measurement technique, measures the acceleration of the atom entering an electric field. The polarizability (induced electric dipole moment of the atom) interacts with the electric field gradient at the entrance producing an accelera-

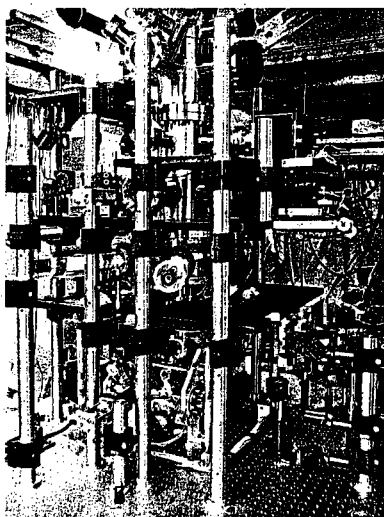


Figure 4 - Cold atom fountain polarizability apparatus at the conclusion of the experiment. The cables and heating tapes have been removed.

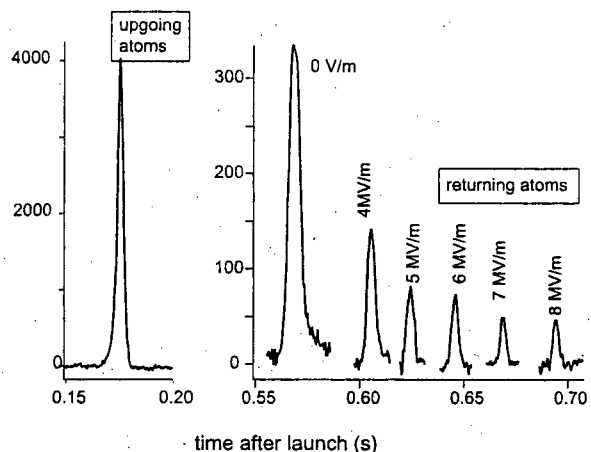


Figure 5 - Detected signal as a function of time after launch. The upgoing atoms pass the probe at about 0.17s and return after 0.57s - 0.695s depending on the electric field.

All ground state atoms are strong-field seeking and accelerate into an electric field. Conservation of energy requires that the change in kinetic energy upon entering the electric field be equal to the change in potential energy (Stark effect) and independent of the gradient.

In the experiment, which uses a fountain of very cold Cs atoms (Fig. 4), the atoms, traveling at 3 m/s enters an electric field of up to 8 MV/m. The change in the round trip flight time due to the acceleration of the field is the measured quantity (Fig. 5).

The largest systematic effects in the measurement arises from velocity - and position dependent losses of atoms in the electric field plates, especially in the fringe fields. To deal with this we calculate and measure the evolution of the phase space of the beam in the actual fields of the experiment and compare calculated and measured arrival time distribution and intensity. Our preliminary result is $\alpha_{Cs} = 6.607 (0.017) \times 10^{-39} \text{ J}/(\text{V/m})^2$ ($[59.38 \pm 0.15] \times 10^{-24} \text{ cm}^3$).

Our work on slowing, cooling, and now polarizability measurements have lead to new insights about slowing, cooling, focusing and storing neutral polar molecules, some of which appear in other places in this abstract.

* Jason Amini is partially supported by the NSF and NASA

Future Work

Synchrotron storage ring: Molecules in weak-field seeking states can collisionally deexcite. This, limits their storage times in imperfect vacuum and, more importantly for evaporative cooling, their storage densities. The $J = 0$ rotational level is the lowest rotational level, is not degenerate at zero field, and is far less subject to collisional excitation, especially if the temperature of the molecules is less than the rotational spacing. Thus the $J = 0$ state is the best state to use for to evaporative cooling. However molecules in $J = 0$ are strong-field seeking and are far more difficult to focus, and deflect than molecules in weak-field seeking states.

Having developed improved focusing elements for molecules in strong field seeking states, we will be using this new knowledge and our understanding of end field effects to model a synchrotron storage ring for the $J = 0$ state. Once we have demonstrated it's feasibility we expect to go on to construct and operate the synchrotron.

Molecular slower: We are presently designing a molecular beamline for experiments on slowing, focusing, and deflecting polar molecules in the $J = 0$ state. The beamline will evolve into a linear

slower for injecting a molecular synchrotron storage ring. A simple extension of the slower will be used to reach very low energies (independent of a synchrotron). We expect to use the extension for initial molecule-helium scattering experiments at mK energies.

Publications

Manuscripts describing our work on the molecular synchrotron storage ring and on the Cs polarizability measurement are in preparation..

1. J. Kalnins, G. Lambertson, and H. Gould, "Improved alternating gradient transport and focusing of neutral molecules," *Rev. Sci. Instr.* **73**, 2557 (July 2002).
2. J. A. Maddi, T.P. Dinneen, and H. Gould, "Slowing and cooling molecules and neutral atoms by time-varying electric-field gradients," *Phys. Rev. A* **60**, 3882 (Dec. 1999).

Acknowledgments

This work is supported by the U.S. Department of Energy under Contract DE-AC03-76SF00098. The Cs polarizability experiment was partially supported by NASA.

Electron-Atom and Electron-Molecule Collision Processes

C. W. McCurdy and T. N. Rescigno

Computing Sciences, Lawrence Berkeley National Laboratory, Berkeley, CA 94720

cwmccurdy@lbl.gov, tnrescigno@lbl.gov

Program Scope: This project seeks to develop theoretical and computational methods for treating electron collision processes that are currently beyond the grasp of first principles methods, either because of the complexity of the targets or the intrinsic complexity of the processes themselves. We are developing methods for treating low energy electron collisions with polyatomic molecules, complex molecular clusters and molecules bound to surfaces and interfaces, for studying electron-atom and electron-molecule collisions at energies above that required to ionize the target and for calculating detailed electron impact ionization probabilities for simple atoms and molecules.

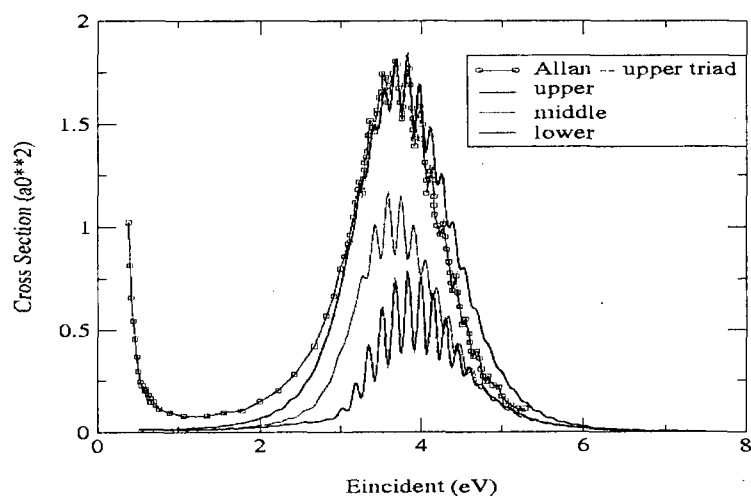
Recent Progress and Future Plans: We can report significant progress in the two distinct areas covered under this project, namely electron-polyatomic molecule collisions and electron impact ionization.

1. Electron-Molecule Collisions

A major goal of our research in the area of electron-polyatomic molecule scattering is to explore the mechanisms that control the flow of energy from electronic to nuclear degrees of freedom in such collisions. To this end, we have been studying the electron-CO₂ system, exploring resonant vibrational excitation in the 4 eV energy region. The first phase of our attack on this problem was aimed at treating the fixed-nuclei electronic scattering problem and calculating, from first principles, accurate electronic cross sections for a number of target nuclear geometries. These calculations provided the complex resonance potential energy surfaces on which time-dependent wavepacket studies of the nuclear dynamics could be carried out. For these studies, we use a novel and highly efficient suite of codes that employ the multi-configuration time-dependent Hartree (MCTDH) approach developed in Heidelberg by Prof H. Dieter-Meyer and coworkers. Last summer, we reported results of wavepacket calculations on the ²A₁ resonance surface at the Santa Fe ICPEAC (and subsequently published in *Phys. Rev. A*) that conclusively demonstrated the importance of considering both the bending and symmetric stretch degrees of freedom, which are strongly coupled by a Fermi resonance. We have since extended these studies to include motion on the ²B₁ resonance surface. The two resonance states, which are degenerate in linear geometry, behave differently as the molecule bends and are strongly coupled by non-adiabatic (Renner-Teller) forces. Our calculations have produced vibrational excitation cross sections that are in excellent agreement with experiments and reveal the origin of the subtle interference effects observed in the most recent experimental studies. This study represents the first time that all aspects of an electron-polyatomic collision, including not only the determination of the fixed-nuclear electronic cross sections, but a treatment of the nuclear dynamics in multiple dimensions on coupled resonance surfaces, has been carried out entirely from first principles.

Cross sections for excitation of the [(2,0,0)/(1,2,0)/(0,4,0)] Fermi triad in CO₂ by electron impact. *Ab initio* results are compared with recent experiment.

Fermi Triad -- SCF ground state



Several interesting questions arise from an examination of the *ab initio* results which would be difficult to address with large-scale first-principles calculations. To gain further insight into the nature of low-energy electron-CO₂ scattering, we examined several model problems whose analytic structure could be studied in detail and which are expected to reflect key aspects of the true physical problem. We used these models to study the pole trajectories of both resonances and virtual states, both of which figure prominently in low-energy electron-CO₂ scattering, in the plane of complex momentum. The connection between resonant and virtual states was found to display a different topology in the case of a polyatomic molecule than it does in diatomic molecules. In particular, these states may have a conical intersection and consequently acquire a Berry phase along closed paths in two-dimensional vibrational motion. The analytic behavior of the S-matrix is further modified by the presence of a geometry dependent dipole moment. The model results, which have been accepted for publication in Phys. Rev. A, may help to explain the nature of threshold vibrational excitation in the virtual state region, far from the resonance region, and will hopefully suggest possible directions for further *ab initio* work.

The principal tool we have developed for studying electron-molecule scattering has become known as the Complex Kohn Variational method, which allows for the inclusion

of accurate target electronic states as well as the complete treatment of correlation between the incident electron and those of the target. As part of our current development plans, we are building a new interface between the Complex Kohn scattering codes and a modern suite of electronic structure codes. We have chosen to carry out that development with NWCHEM, which was designed to run on distributed memory platforms. The initial phases of that new interface have now been completed. Our future plans include a complete study of electron-impact excitation dynamics – as we have carried out for CO₂ – in a polyatomic that undergoes *dissociation* following resonant electron attachment. To this end, we have initiated work on the electron-H₂O system.

2. Electron-Impact Ionization

The computational approach we have developed to study electron impact ionization, which has provided the only *complete* solution to the quantum mechanical three-body Coulomb problem at low collision energies to date, relies on a mathematical transformation of the Schrödinger equation called *exterior complex scaling* (ECS) that allows us to solve for the wave function without detailed specification of complicated asymptotic boundary conditions. Our efforts over the past year have focused on developing scalable extensions of the ECS method that will allow us to study ionization of target atoms with two active electrons. Specifically, we have developed a time-dependent version of the basic approach that does not require the solution of large systems of complex linear equations. This is accomplished by constructing the scattering wave function from the Fourier transform of an initial wave function that is time-propagated on an exterior-scaled complex grid using a discrete variable representation in conjunction with finite elements. The basic method, along with some proof-of-principle demonstrations on model 3D problems, was outlined in a paper we published in *Phys. Rev. A*. We have since obtained preliminary results on electron-helium ionization after an extensive series of calculations on the NERSC IBM-SP. Our plans are to continue these investigations and to carry out a complete study of electron-helium ionization within the Temkin-Poet model. This work is being carried out by UC Berkeley graduate student Dan Horner as part of his doctoral research. We have also begun to investigate alternative methods for carrying out the time-propagation, including higher-order Crank-Nicolson methods, as well as Lanczos techniques that may obviate the need for the split-operator approximations that we are currently employing.

The extraction of breakup amplitudes from multi-electron wave functions is considerably more difficult than what we previously encountered in two-electron systems; this is also a topic of ongoing research in our group.

Publications (2000-2002):

1. T. N. Rescigno and C. W. McCurdy, “Numerical Grid Methods for Quantum Mechanical Scattering Problems”, *Phys. Rev. A* **62**, 032706 (2000).
2. C. W. McCurdy and T. N. Rescigno, “Practical Calculations of Quantum Breakup Cross Sections”, *Phys. Rev. A* **62**, 032712 (2000).
3. C. W. McCurdy, D. A. Horner and T. N. Rescigno, “Practical Calculations of Amplitudes for Electron Impact Ionization”, *Phys. Rev. A* **63**, 022711 (2001).

4. M. Baertschy, T. N. Rescigno, W. A. Isaacs, X. Li and C. W. McCurdy, "Electron Impact Ionization of Atomic Hydrogen", *Phys. Rev. A* **63**, 022712 (2001).
5. W. A. Isaacs, M. Baertschy, C. W. McCurdy and T. N. Rescigno, "Doubly Differential Cross Sections for the Electron Impact Ionization of Hydrogen", *Phys. Rev. A* **63**, 030704 (2001).
6. M. Baertschy, T. N. Rescigno, C. W. McCurdy, J. Colgan and M. S. Pindzola, "Ejected-Energy Differential Cross Sections for the Near Threshold Electron-Impact Ionization of Hydrogen", *Phys. Rev. A* **63**, 050701 (2001).
7. M. Baertschy, T. N. Rescigno and C. W. McCurdy, "Accurate Amplitudes for Electron Impact Ionization", *Phys. Rev. A* **64**, 022709 (2001).
8. T. N. Rescigno, "The Three-Body Coulomb Problem", in "Yearbook of Science and Technology", (McGraw Hill, New York, 2001).
9. T. N. Rescigno, W. A. Isaacs, A. E. Orel, H.-D. Meyer and C. W. McCurdy, "Theoretical Studies of Excitation in Low-Energy Electron-Polyatomic Molecule Collisions", in *Photonic, Electronic and Atomic Collisions, Invited Papers, Proceedings of the XXII International Conference on Photonic, Electronic and Atomic Collisions*, Santa Fe, NM 2001 (Rinton Press, Princeton 2002).
10. C. W. McCurdy, M. Baertschy, W. A. Isaacs and T. N. Rescigno, "Reducing Collisional Breakup of a System of Charged Particles to Practical Computation: Electron-Impact Ionization of Hydrogen", in *Photonic, Electronic and Atomic Collisions, Invited Papers, Proceedings of the XXII International Conference on Photonic, Electronic and Atomic Collisions*, Santa Fe, NM 2001 (Rinton Press, Princeton 2002).
11. T. N. Rescigno, W. A. Isaacs, A. E. Orel, H.-D. Meyer and C. W. McCurdy, "Theoretical Study of Resonant Vibrational Excitation of CO₂ by Electron Impact", *Phys. Rev. A* **65**, 032716 (2002).
12. C. W. McCurdy, D. A. Horner and T. N. Rescigno, "Time-dependent approach to collisional ionization using exterior complex scaling", *Phys. Rev. A* **65**, 042714 (2002).
13. W. Vanroose, C. W. McCurdy and T. N. Rescigno, "On the Interpretation of Low Energy Electron-CO₂ Scattering", *Phys. Rev. A* (accepted for publication).

Femtosecond X-ray Beamline for Studies of Structural Dynamics

Robert W. Schoenlein

Materials Sciences Division
Lawrence Berkeley National Laboratory
1 Cyclotron Rd. MS:2-300
Berkeley, CA 94720
email: rwschoenlein@lbl.gov

Background and Program Scope

Modern synchrotrons providing high-brightness, tunable x-ray beams, have driven rapid advances in our understanding of the structure of condensed-matter on the atomic scale via x-ray diffraction and spectroscopy techniques such as EXAFS and XANES. However, the structure of condensed matter is not static, and the fundamental time scale for atomic motion is the time scale of a vibrational period, ~ 100 fs. This is the limiting time scale for structural changes that determine the course of phase transitions in solids, the kinetic pathways of chemical reactions, and even the function and efficiency of biological processes. The direct study of structural dynamics is a frontier research area in physics, chemistry, materials science and biology. However, the development of this research area has been limited by the lack of suitable tools for probing structural dynamics on the femtosecond time scale. A significant limitation of synchrotron sources is the pulse duration (~ 100 ps) as determined by the duration of the stored electron bunch. Advanced femtosecond laser technology now enables the measurement of dynamic processes on time scales shorter than 10 fs. However, femtosecond lasers probe the extended electronic states of condensed matter (using low-energy visible photons) and such states are only indirect indicators of atomic structure.

Our research group has pioneered the development of a novel technique (illustrated in Fig. 1) for generating femtosecond x-ray pulses from a synchrotron storage ring by using femtosecond optical pulses to modulate the energy (and time structure) of a stored electron bunch[1]. A simple bend-magnet beamline, incorporating this technique, has recently been constructed at the Advanced Light Source. The beamline will provide ~ 100 fs x-ray pulses over an energy range of 0.1-12 keV with an average brightness approaching 10^8 ph/s/mm²/mrad²/0.1% BW and an average flux in the range of 10^5 ph/s/0.1% BW.

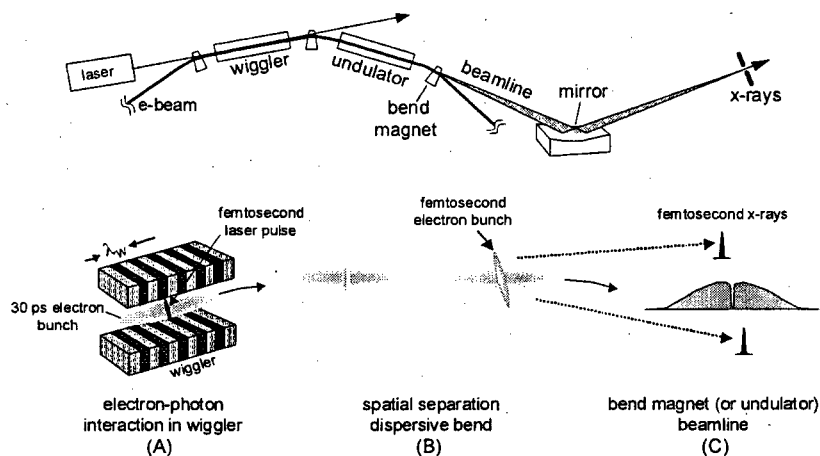


Figure 1. Schematic of method for generating femtosecond synchrotron pulses. (a) laser acceleration/deceleration of a short slice of the stored electron bunch via co-propagation in a resonantly-tuned wiggler. (b) separation of the modulated electrons in a dispersive section of the storage ring, (c) generation of femtosecond x-rays from a bend-magnet, using an imaging optic and slit to isolate the femtosecond x-rays.

The scope of this research program includes the development and characterization of a unique synchrotron bend-magnet beamline for generating 100 fs x-ray pulses based on laser modulation of the stored electron beam. In addition to providing for the development of femtosecond x-rays, this beamline will be a state-of-the-art user facility for time-resolved x-ray science incorporating femtosecond laser systems and endstations suitable for time-resolved x-ray diffraction, EXAFS, XANES, and photoionization measurements. Finally, this research program seeks to develop scientific applications and associated measurement techniques including pump-probe with femtosecond visible and x-ray pulses, ultrafast x-ray streak camera detectors, and dispersive measurement schemes. Initial research will focus on ultrafast solid-solid phase transitions in crystalline solids, light-induced structural changes in molecular crystals, and x-ray interactions with atoms in the presence of strong laser fields.

Recent Progress

The bend-magnet beamline has been commissioned, including the double-crystal monochromator for tunable hard x-ray measurements, and the ruled grating spectrometer for dispersive soft x-ray spectroscopy. In addition, a cryogenically-cooled laser system with parallel amplifiers (~500 nsec relative delay) has been constructed and provides >7 W total output power in two beams with TM₀₀ mode quality. One amplifier provides pulses for modulating the electron beam and generating femtosecond x-rays. The second amplifier provides pulses for sample excitation which are absolutely synchronized to the pulses from the first amplifier, and therefore to the femtosecond x-rays. The entire laser system is synchronized to the storage ring to within a few percent of the electron bunch duration.

Since the femtosecond x-rays are generated in the transverse spatial tails of the main x-ray beam, an important consideration for effective isolation of the femtosecond x-rays from the long synchrotron pulse is the x-ray beam profile. The expected flux in the femtosecond pulse is $\sim 10^{-4}$ of the long synchrotron pulse. This is based on the ratio of the pulse durations (100 fs/70 ps) and the fact that $\sim 10\%$ of the electrons interacting with the laser pulse receive the maximum energy modulation. The x-ray beam profile, originating from the electron beam source and imaged by the toroidal mirror, has been measured and is shown in Fig. 2. The image quality is quite good, exhibiting only minor deviation from the $\sigma_x=0.1$ mm size of the electron beam. The non-Gaussian tails of the profile are due primarily to non-specular scattering from the toroidal optic. The background level ($\sim 3 \times 10^{-4}$ at 0.5 mm) allows for effective isolation of the femtosecond x-rays.

Figure 3 shows the measured femtosecond x-ray flux at 10 keV, relative to the long-pulse background level as a function of transverse displacement. At 500 μm displacement (corresponding to ~ 13 MeV modulation of the electron beam) the signal/background ratio is nearly one. For spectroscopy experiments, such background levels are easily eliminated using differential measurement techniques.

Figure 4 shows time-resolved measurements of synchrotron pulses of ~ 150 fs duration. These measurements are made by cross-correlating visible light from the beamline with femtosecond pulses from the second laser amplifier. Since the time structure of the bend-magnet radiation is determined by the time structure of the electron bunch, it is invariant over the entire emission spectrum (extending from the infrared to the x-ray range). These are the shortest pulses ever generated from a synchrotron.

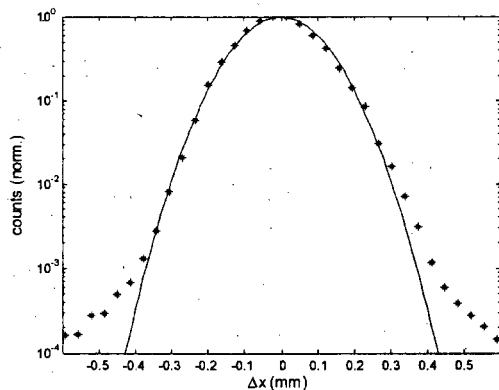


Figure 2. Profile of the long-pulse x-ray beam at 10 keV at the image plane (focus) of the beamline. The solid line is a Gaussian fit ($\sigma_x=0.1$ mm) and reflects the transverse size of the electron beam in the bend magnet.

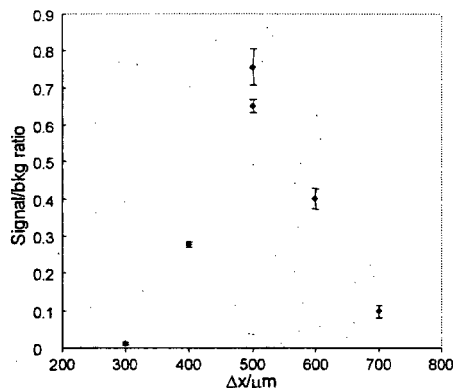


Figure 3. Femtosecond x-ray flux (measured relative to the background flux) as function of transverse displacement. Measurements are made at 10 keV using 100 μm slits and integrating over the ~ 70 ps synchrotron pulse.

In addition to the femtosecond x-ray development work, preliminary results have been achieved by beamline users in several experiments. Absorption spectra of laser heated carbon and silicon foils, have been measured on the picosecond time scale (Falcone Group, U.C. Berkeley). Initial measurements have been made of the thermally-driven solid-solid phase transition in VO_2 , and of the photo-induced spin-crossover transition in $\text{Fe}[\text{tpen}]^{3+}$ molecular crystals (Shank/Schoenlein Group, LBNL). Preliminary evidence of laser perturbation of the Ar photoionization spectra near threshold has been observed (Belkacem Group, LBNL).

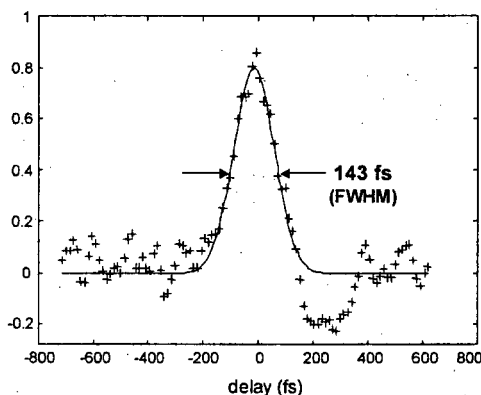


Fig. 4. Cross-correlation measurements of femtosecond synchrotron pulses from ALS beamline 5.3.1. The pulse duration is deconvolved from the measured duration of the up-converting laser pulse.

Future Plans

Recent changes to the ALS storage ring lattice (to accommodate superconducting bend magnets) now require stronger modulation of the electron beam in order to generate femtosecond x-rays during normal user operation. Continued development of the femtosecond x-ray source will focus on increasing the energy modulation. We will develop advanced diagnostics such as detection of coherent IR synchrotron radiation as a monitor of laser/electron beam interaction. In addition, gated x-ray CCD cameras and photodetectors will be employed for isolating single synchrotron pulses. The time resolution of the ultrafast x-ray streak camera will be improved by incorporating the latest design advances from collaborator, Z Chang (Kansas State). Planned modifications by the Falcone Group at U.C. Berkeley include a dual photoconductive switch to minimize trigger jitter, and faster deflection voltage ramping.

The development and support of scientific applications and experiments in time-resolved x-ray science will be expanded. Studies of Si and C foils excited to the warm dense matter regime (~1 eV) via laser heating will be made via time-resolved dispersive XANES measurements on the picosecond time scale using the streak camera in combination with a soft-x-ray spectrometer. Time-resolved XANES and EXAFS measurements in VO₂ will investigate changes in short-range order and bonding following laser excitation. VO₂ is a correlated electron system which is an insulator at room temperature (rutile structure), and undergoes an insulator-metal transition at ~340 K (monoclinic structure). Previous time-resolved optical and x-ray (Bragg) measurements indicate that the phase transition can be induced electronically on a sub-picosecond time scale. Measurements on the V L-edge will provide complementary information about the electronic dynamics (XANES) and the short-range structural dynamics (EXAFS), and may elucidate the role of the V-O bonding on the phase transition.

Time-resolved x-ray absorption (EXAFS/XANES) measurements in molecular crystals of the [Fe(tpen)]²⁺ complex will address fundamental questions about the role of structural dynamics in the ultrafast spin-crossover transition in these molecules. This research builds on previous time-resolved optical studies and static x-ray studies. Optical measurements indicate a sub-picosecond transition from the metal-to-ligand charge-transfer (¹MLCT) state to the high-spin ligand-field state (⁵T₂). Static x-ray measurements indicate a ~15% dilation of the metal-ligand bond distance in the high-spin state, and it has been suggested that this structural change may facilitate the spin-crossover transition.

X-ray photoelectron and ion spectroscopy will be used for initial measurements of two-photon (visible plus x-ray) ionization of core levels in Ar gas. This will provide new knowledge about the physics underlying two-photon processes in atoms, and will provide the basis for future experiments of x-ray ionization in the presence of a strong laser field.

Publications from DOE Sponsored Research (since 2000)

- R.W. Schoenlein, S. Chattopadhyay, H.H.W. Chong, T.E. Glover, P.A. Heimann, C.V. Shank, A. Zholents, and M. Zolotarev, "Femtosecond x-rays from a synchrotron: A new tool for ultrafast time-resolved x-ray spectroscopy," *Science*, **287**, 2237, (2000).
- R.W. Schoenlein, S. Chattopadhyay, H.H.W. Chong, T.E. Glover, P.A. Heimann, C.V. Shank, A. Zholents, and M. Zolotarev, "Generation of x-ray pulses via laser-electron beam interaction," *Appl. Phys. B*, **71**, 1, (2000).
- R.W. Schoenlein, H.H.W. Chong, T.E. Glover, P.A. Heimann, C.V. Shank, A.A. Zholents, and M.S. Zolotarev, "Femtosecond x-ray pulses from a synchrotron," **Ultrafast Phenomena XII**, T. Elsaesser, S. Mukamel, M.M. Murnane, N.F. Scherer, Eds., Springer-Verlag, 271, (2000).
- P.A. Heimann, A.M. Lindenberg, I. Kang, S. Johnson, T. Missalla, Z. Chang, R.W. Falcone, R.W. Schoenlein, T.E. Glover, H.A. Padmore, "Ultrafast x-ray diffraction of laser-irradiated crystals," *Nuclear Inst. and Methods A*, **467**, 986, (2001).
- R.W. Schoenlein, H.H.W. Chong, T.E. Glover, P.A. Heimann, W.P. Leemans, H.A. Padmore, C.V. Shank, A. Zholents, M. Zolotarev, and J.S. Corlett, "Femtosecond x-rays from relativistic electrons: New tools for probing structural dynamics," *Comptes Rendus de l'Académie des Sciences IV Physique Astrophysique*, **2**, 1371, (2001).

References

- [1] A.A. Zholents and M.S. Zolotarev, *Phys. Rev. Lett.*, **76**, 912, (1996).

**ATOMIC AND MOLECULAR PHYSICS RESEARCH
AT
OAK RIDGE NATIONAL LABORATORY**

David R. Schultz, Group Leader, Atomic Physics
ORNL, Physics Division, P.O. Box 2008
Oak Ridge, TN 37831-6372

Principal Investigators

M. E. Bannister [bannisterme@ornl.gov]
C. C. Havener [havenercc@ornl.gov]
H. F. Krause [krausehf@ornl.gov]
J. H. Macek [macek@utk.edu]
F. W. Meyer [meyerfw@ornl.gov]
C. Reinhold [reinhold@ornl.gov]
D. R. Schultz [schultzd@ornl.gov]
C. R. Vane [vanecr@ornl.gov]

OVERVIEW

The ORNL atomic physics program has as its overarching goal the understanding and control of interactions and states of atomic-scale matter. The scientific objective is to enhance progress toward development of detailed understanding of the interactions of multicharged ions, charged and neutral molecules, and atoms with electrons, atoms, ions, surfaces, and solids. Towards this end, a robust experimental program is carried out by our group centered at the ORNL Multicharged Ion Research Facility (MIRF) and as needed at other world-class facilities such as the ORNL Holifield Radioactive Ion Beam Facility (HRIBF) and the CRYRING heavy-ion storage ring in Stockholm. Closely coordinated theoretical activities support this work as well as lead investigations in complementary research. Specific focus areas for the program are broadly classified as particle-surface interactions, atomic processes in plasmas, and manipulation and control of atoms, molecules, and clusters, the latter focus area cross cutting the first two.

Low-Energy Multicharged Ion-Surface Interactions – F. W. Meyer, H. F. Krause, and C. R. Vane

This section deals with investigations at the ORNL MIRF studying the interactions of slow, highly charged ions with metal, semiconductor, and insulator surfaces. Our goal is to improve fundamental understanding of neutralization and energy dissipation occurring in such interactions, and subsequently to apply the knowledge gained to probe and modify the surfaces of single crystals, thin films, and nanostructures. This year, we have extended our earlier studies^{1,2} of site-specific neutralization of multicharged projectile ions in large angle (120°) quasi-binary collisions from solid surfaces to a RbI(100) target. This alkali-halide crystal is an ionic solid, both of whose constituents are sufficiently heavy to backscatter low-Z multicharged projectiles with not more than 50% energy loss, thus permitting measurements with incident energies as low as a few keV. At the same time, the two constituents, i.e., Rb and I, are sufficiently different in mass, that the different energy loss from the two sites is clearly resolvable with our TOF setup, thus permitting unambiguous identification of the collision partner with which the hard collision occurs. Our earlier Au(110) measurements^{1,2} have shown that grazing interactions with neighboring lattice sites on the receding trajectory, i.e., after the hard collision, can play an important role in projectile neutralization, which depends sensitively on target azimuthal orientation. With the RbI(100) target, the identity of this second, grazing collision partner can be selected by suitable azimuthal orientation. Thus, for measurements along the $\langle 100 \rangle$ direction, interactions of the type a-b, or b-a are selected, while along the $\langle 110 \rangle$ direction the interactions are of the type a-a, or b-b, with a and b denoting the two constituents of the RbI lattice. In this manner, both the hard, first collision, and the second, grazing collision, that results in little additional energy loss can be uniquely selected and identified. Their effect on

the overall projectile neutralization can then be assessed by measuring the final charge-state distribution resulting from each of these interactions. Crucial to this approach is that the projectiles approach the surface at normal incidence, so that, by virtue of the RbI (100) crystal structure, only the surface layer is seen by the approaching projectile, i.e., the deeper layers are blocked or shadowed.

We have used the approach described above to make measurements for 5 keV F^+ , F^{6+} , F^{7+} , Ne^{8+} , Ne^{9+} , and Ar^{11+} incident on RbI(100). Scattered charge-state distributions were determined as functions of polar incidence angle and azimuthal target orientation. For the F^{q+} projectiles, negative-ion formation was studied as well. In all cases, significant variations of the measured distributions were seen as functions of target azimuthal orientation and of incidence angle. While the incidence angle dependence is most likely the result of deeper layer contributions as the incidence angle is changed from normal, as implied above, the azimuth variations, seen even at normal incidence angle, provide information about neutralization as well as negative-ion formation efficiencies of Rb vs. I. Detailed analyses of the measurement results coupled with MARLOWE³ trajectory simulations are underway to extract this information from our data.

1. V. A. Morozov and F. W. Meyer, Phys. Rev. Lett. **86**, 736 (2001).
2. V. A. Morozov and F. W. Meyer, Phys. Scripta **T92**, 31 (2001).
3. M T. Robinson, Rad. Effects and Defects in Solids **130**, 3 (1994); Phys. Rev. B **40**, 10717 (1989).

Electron-Molecular Ion Fragmentation – M. E. Bannister and C. R. Vane

A program of electron-molecular ion interaction research is being developed, which will be complementary to our continuing studies of zero-energy dissociative recombination (DR) being pursued in collaboration with Mats Larsson and colleagues at the CRYRING heavy-ion storage ring at Stockholm. At ORNL, we will experimentally investigate at low to moderate energies the electron-molecular ion-collision processes of dissociative excitation (DE), ionization (DI), and recombination (DR). The studies will concentrate on systems of particular relevance to fusion energy research, plasma processing applications, and aeronomy. These measurements will be carried out utilizing the unique capabilities of the ORNL MIRF, especially after implementation of a new ECR source and a high-voltage platform upgrade, which will provide ion beams at energies up to 250 keV \cdot q. Also, a novel source of cold molecular ions is being developed for use in collision studies with well-characterized initial-state ions. The studied interactions will be primarily with electrons, but also with atoms, neutral molecules, and surfaces. This source, known as a surfajet, is based on the expansion of a surface-wave-sustained discharge through a supersonic nozzle to adiabatically relax the vibrational and rotational modes of the extracted ions. Hydrodynamic and spectroscopic diagnostics are being developed in parallel to measure the degree of cooling given by the source, providing initial-state characterization of the target molecular ions.

Electron-molecular ion experiments performed at MIRF and at CRYRING will be coordinated to enable inter-comparisons of results from these complementary experimental approaches. For example, the coordination will help characterize electronic and rovibronic-state distributions of molecular ions extracted from the ECR source at MIRF, where ions too heavy for routine measurements at CRYRING will be investigated. A current area of ongoing research at CRYRING involves developing a reliable base of accurate data on fragmentation of cold triatomic di-hydride ions in DR at zero energy. DR results from recombination of a molecular ion with a free electron, leading to disintegration of the molecular ion into several neutral fragments. A complete analysis of measured DR cross sections, fragmentation fractions, and dynamics for vibrationally cold H_2O^+ ions has recently been completed and is now being published.¹ Analyses of similar measurements for DR of vibrationally cold NH_2^+ and CH_2^+ are proceeding, and new experimental studies of DR of H_2S^+ (and possibly BH_2^+) are planned for the fall of this year at CRYRING. Studies of more complex molecular ion systems, e.g., heavier hydrocarbons, will also be initiated using existing techniques, modified to accept heavier ions and more channels of decay. The scientific goal is to develop a systematic base of reliable state-specific data for relatively simple molecular ions, sufficient to support progress toward a fundamental understanding of DR, and especially of the roles of initial internal state populations on the routes of mass and energy dissipation in fragmentation.

1. Richard Thomas et al., Phys. Rev. A (2002).

We are continuing studies of neutralization of hollow ions moving in Al, Al₂O₃, and Si, using stable energetic heavy-ion beams from the Holifield Radioactive Ion Beam Facility (HRIBF) tandem to produce slowly recoiling ions from Cl and Ar atoms implanted in the solids. The characteristic Cl and Ar target X rays emitted when K-vacancy ions are produced contain information on the electronic properties of the excited target atoms and on the surrounding material environment. The ORNL von Hamos broad band, high-resolution X-ray spectrometer is being employed in these measurements. These measurements are based on our previous studies on chemical sensitivity of X rays excited by heavy ions,¹⁻³ and are directly related to our ongoing research on particle-surface interactions at the MIF. The spectral information obtained is being used to extract electron transfer (ion neutralization) rates and electron densities for the specific collision systems and target materials being examined. The energies and intensities of satellite X rays emitted depend on the specific electronic states of the target ions populated as they recoil in the substrate. A multiply ionized recoil ion can be partially neutralized in flight by transfer of electrons from the surrounding material. The degree of neutralization prior to fast (femtosecond – in third row elements) radiative filling of an inner-shell vacancy depends on the availability of nearby weakly bound electrons, their density of states, and the relevant transfer mechanism rates. These aspects depend on the vacancy states populated in the recoiling ion and on the local and global electronic environments provided by the specific targets. In the last year, we have implanted Cl and Ar at several densities ($1 - 10 \times 10^{16} / \text{cm}^2$) in thin targets of Al, Al₂O₃, and Si using beams from the MIF. We have subsequently measured X rays emitted under impact by 200-MeV Ti ions at HRIBF, and are presently analyzing these recently obtained data. It appears that, as noted previously for Ar implanted in Ni, Ar^{q+} recoil neutralization occurs more slowly than for Cl^{q+}, possibly indicating that Ar forms bubbles of dense gas under implantation beyond about $10^{16} / \text{cm}^2$ in Al. Comparisons of these data with X rays emitted from HCl and Ar thin gas targets will permit extraction of refilling rates for Cl and Ar ions moving in the various conductive, insulating, and semiconducting solids.

It is anticipated that these neutralization rates and the resultant variations in X-ray spectra will also be sensitive to the limited number and modified conduction electron states available in nanosized structures, such as quantum dots and carbon nanotubes. Measuring the modifications in X-ray spectra as functions of size and electronic character (conducting versus insulating and/or semi-conducting) of the targets will give rather unique information on rapid electron response characteristics of these new structures.

In the last year, we have begun measurements of the transport and energy loss of Ti ions in 100-nm-diameter channels in 60- μm -thick Al₂O₃ formed by anodization of Al. This is a first step toward forming sufficiently aligned, arrayed, parallel carbon nanotubes through which heavy ions may be channeled. Measurements of channeled bare ion scattering, energy loss, and radiative electron-capture X rays will provide the means to determine the electron densities and Compton profiles inside of carbon nanotubes grown in these channels. This research is in collaboration with members of the ORNL Solid State and Chemical Technology Divisions characterizing and supplying the carbon nanotubes and other nano-structured targets.

1. S. Raman et al., Nucl. Instrum. Meth. Phys. Res. B 3, 71-103 (1984).
2. C. R. Vane et al., Contributed Abstracts, XX ICPEAC, Vienna, Austria, July 23-29, 1997, p. FR 130.
3. C. R. Vane, M. S. Smith, and S. Raman, ORNL Report ORNL/TM-10658.

Near-Thermal Collisions of Multicharged Ions with H and Multi-Electron Targets – C. C. Havener, H. F. Krause, and C. R. Vane

The merged-beams technique¹ is being used to explore near-thermal collisions of multicharged ions with neutral atoms and molecules, providing benchmark measurements for comparison with state-of-the-art theories. Electron capture by multicharged ions from neutrals is important in many technical plasmas including those used in materials processing, lighting, ion-source development, and for spectroscopic diagnostics and modeling of core, edge, and divertor regions of magnetically confined fusion plasmas.

Cross-section measurements of electron capture for Ne²⁺ + H and Ne⁴⁺ + H have just been completed. Improvements in the neutral detector and calibration have increased the reliability of the secondary electron efficiency measurement and hence the cross section. The measurements for Ne²⁺ show a sharply decreasing cross section that is almost a factor of two below previous measurements² at 200 eV/u. In

contrast, the measured Ne^{4+} cross section shows a relatively flat-energy dependence from 1000 eV/u to below 1 eV/u, extending previous measurements¹ two orders-of-magnitude lower in energy. Theoretical analysis of these results is underway.

This last year, the capability of the ORNL ion-atom merged-beams apparatus to perform collision studies with multi-electron targets was first demonstrated. nA beams of Li were produced and used in electron-capture measurements with Ar^{4+} at 60 eV/u. The absolute cross section shows good agreement with previous measurements.³ This new capability of the merged-beams apparatus will allow measurements with a variety of neutral beams, such as Li, B, Na, Al, P, K, Ca, Cr, Fe ..., and molecular beams such as O_2 , CH_2 , Modifications of the de-merge section are planned which will allow measurements with $\text{He}^{2+} + \text{Li}$ to try to observe the expected shape resonances formed due to the strong ion-induced dipole attraction between reactants.

1. R. A. Phaneuf, C. C. Havener, G. H. Dunn, and A. Muller, Rep. Prog. Phys. **82**, 1143 (1999).
2. W. Seim, A. Muller, I. Wirkner-Bott, and E. Salzborn, J Phys. B: At. Mol. Phys. **14**, 3475 (1981).
3. S. L. Varghese, W. Waggoner, and C. L. Cocke, Phys. Rev. A **29**, 2453 (1984).

Theoretical Atomic Physics – C. Reinhold, J. Macek, D. R. Schultz, S. Ovchinnikov, T. Minami, and J. Burgdörfer

The internal state of a fast hydrogenic ion traversing a solid represents a simple open quantum system whose dynamics can be analyzed theoretically and experimentally in great detail. As the ion traverses the foil, the coherence of the internal state of the ion is destroyed due to the interaction with the environment, which is given by particles in the foil and the electromagnetic field. The former leads to multiple collisions whereas latter leads to the radiative decay of the ion. We study this system as a prototype of open quantum systems. One of our ultimate goals is to be able to simulate the decoherence of “open” excited states of atoms as exactly as possible. We describe such systems using a Monte Carlo or test-particle discretization approach in which the density matrix is obtained as an average of a large but finite number of density matrices of quantum trajectories (pure states) whose dynamics is governed by a stochastic nonlinear Schrödinger equation.

We are exploring new avenues for steering and probing Rydberg wave packets by subjecting stationary Rydberg states to designer pulses. One objective of the investigation is to develop unitary control protocols leading to the production of localized wave packets in phase space. We have found that dynamics can be used to enhance the phase-space coherence of a wave packet, and that the ideal time of transient coherence can be optimized by analysis of the coarse-grained entropy. Such localized states can be “trapped” for extended periods using a train of subsequent “kicks.” The most transiently coherent states are obtained following the dynamics of Rydberg wave packets produced by the application of a single “kick” to strongly polarized quasi-one-dimensional atoms (created by photo-excitation in the presence of a weak *DC* field).

In other work, the Sturmian theory of ion-atom collisions has been constructed for arbitrary (non-zero) impact parameters. The approach is essentially nonperturbative, and has wide range of applicability from low velocities, provided that quantum motion of heavy particles can be neglected, to high velocities, as long as the relativistic effects are not important. The theory has been applied to calculation of electron spectra at low and high-collision velocities of two zero-range potentials. For slow collisions, we have described Fermi oscillations in the spectra of ejected electrons. At higher velocities, our theory confirms the possibility of cusp formation even when the heavy particles are neutral in the final state.

We are also undertaking a many-body simulation to study the neutralization of highly charged ions near insulator surfaces. Such simulations follow the projectile dynamics, electron transfer between the ion and the surface, the dynamics of the heavy particles in the crystal, and the hopping of the holes produced by the impinging ion. Since the HCI is repelled by the positive holes, the evolution and redistribution of the microscopic charge-up of the surface is important for understanding the neutralization dynamics. The dynamics of all the heavy particles and the electronic dynamics determining the transfer rates from/to the ion are obtained using a classical trajectory approach. Using recent developments for molecular Auger rates, we have devised a model to evaluate interatomic Auger rates as well. The hole mobility is treated as a random diffusive process with a hole velocity distribution obtained from the band structure of the solid.

Finally, over the past several years, a new approach for treating strongly interacting, few-body atomic problems has been developed and applied that utilizes the power of contemporary computational platforms and techniques to solve the time-dependent Schrödinger equation on a numerical lattice (LTDSE). Several

fundamental problems have previously been addressed that sought to go beyond existing theoretical approaches. In the past year, two projects have been completed that have extended the basic method two new regimes of interest: the ejected electron spectrum and fully correlated two-electron systems. In the first, we have used the LTDSE approach to address challenges posed by recent measurements of the momentum distribution of electrons in ionizing collisions in coincidence with recoil-ion momenta via the COLTRIMS technique. Evolution of the electronic wave function to sufficiently large times in such collisions necessitated development of new methods in LTDSE and a number of insights were obtained. This first study also resulted in strategies for improving it to allow a full, well-converged treatment of ionization. In the second new study, a four-dimensional, planar model of helium was developed and tested in order to allow a computationally tractable LTDSE calculation of collisions involving more than one electron. The model was applied to compute the single ionization cross section in antiproton-helium collisions.

References to Publications of DOE Sponsored Research from 2000-2002 (decending order)

Year 2002 publications

"Electromagnetically Induced Nuclear-Charge Pickup Observed in Ultrarelativistic Pb Collisions," C. Scheidenberger, I. A. Pshenichnov, T. Aumann, S. Datz, K. Sümmerer, J. P. Bondorf, D. Boutin, H. Geissel, P. Grafström, H. Knudsen, H. F. Krause, B. Lommel, S. P. Möller, G. Münzenberg, R. H. Schuch, E. Uggerhøj, U. Uggerhøj, C. R. Vane, Ventura, Z. Z. Vilakazi, and H. Weick, *Phys. Rev. Lett.* **88**, 042301 (2002).

"*Photonic, Electronic, and Atomic Collisions*," *Proceedings of the Invited Talks, XXII ICPEAC*, Editors, J. Burgdörfer, J. S. Cohen, S. Datz, and C. R. Vane (Rinton Press, Princeton, NJ, 2002).

"Laboratory Measurements of Charge Transfer on Atomic Hydrogen at Thermal Energies," C. C. Havener, C. R. Vane, H. F. Krasue, P. C. Stancil, T. Mrozkowski, and D. Savin, *Proceedings, NASA Laboratory Astrophysics Workshop*, NASA-Ames Research Center, CA May 2002.

"Ejected-Electron Spectrum in Low-Energy Proton-Hydrogen Collisions," D. R. Schultz, C. O. Reinhold, P. S. Krstic, and M. R. Strayer, *Phys. Rev. A* **65**, 052722 (2002).

"Exact Electron Spectra in Collisions of Two Zero-Range Potentials with Non-Zero Impact Parameters," S. Yu. Ovchinnikov, D. B. Khrebtukov, and J. H. Macek, *Phys. Rev. A* **65**, 032722 (2002).

"Evidence of Collisional Coherences in the Transport of Hydrogenic Krypton Through Amorphous Carbon Foils," T. Minami, C. O. Reinhold, M. Seliger, J. Burgdörfer, C. Fourment, B. Gervais, E. Lamour, J. P. Rozet, and D. Vernhet, *Nucl. Instrum. Meth. Phys. Res.* **193**, 79 (2002).

"Time Dependent Dynamics of Atomic Systems," M. S. Pindzola, F. J. Robicheaux, J. Colgan, D. M. Mitnik, D. C. Griffin, and D. R. Schultz, p. 483 in *Photonic, Electronic & Atomic Collisions, Proceedings of the XXII ICPEAC*, J. Burgdörfer, J. S. Cohen, S. Datz, and C. R. Vane, eds. (Rinton Press, Princeton, 2002).

"Recent Advances and Applications of Lattice, Time-Dependent Approaches: Fundamental One- and Two-Electron Collision Systems," D. R. Schultz, P. S. Krstic, C. O. Reinhold, M. R. Strayer, M. S. Pindzola, and J. C. Wells, in *Photonic, Electronic & Atomic Collisions, Proceedings of the XXII ICPEAC*, J. Burgdörfer, J. S. Cohen, S. Datz, and C. R. Vane, eds. (Rinton Press, Princeton, 2002), p. 536.

"Comparative Study of Surface-Lattice-Site Resolved Neutralization of Slow Multicharged Ions During Large-Angle Quasi-Binary collisions with Au(110): Simulation and Experiment," F. W. Meyer and V. A. Morozov, *Nucl. Inst. Methods Phys. Res.* **B193**, 530 (2002).

“Large-Angle Backscattering of Ar^{q+} ($q = 1 - 13$) During Quasi-Binary Collisions with $\text{CsI}(100)$ in the Energy Range $10 \text{ eV}/q - 2.8 \text{ keV}/q$: Energy Loss Analysis and Scattered Charge-State Distributions,” W. Meyer, V. A. Morozov, J. Mrogenda, C. R. Vane, S. Datz, *Nucl. Instrum. Meth. Phys. Res.* **B193**, 508 (2002).

“Quantum Transport of Kr^{35+} Ions through Amorphous Carbon Foils,” T. Minami, C. O. Reinhold, M. Seliger, J. Burgdörfer, C. Fourment, B. Gervais, E. Lamour, J.-P. Rozet, and D. Vernhet, *Phys. Rev. A* **65**, 032901 (2002).

“Transient Phase Space Localization,” C. L. Stokely, F. B. Dunning, C. O. Reinhold, and A. K. Pattanayak, *Phys. Rev. A* **65**, 021405 (2002).

“Absolute Cross Sections for Electron-Impact Excitation of the $3d^2 \ ^3F \rightarrow 3d4p \ ^3D, \ ^3F$ Transitions in Ti^{2+} ,” *Phys. Rev. A* **65**, 034704/1-4 (2002).

“Three-Body Recombination of Ultracold Atoms Near a Feshbach Resonance,” *Few-Body Systems* **31**, 249 (2002).

Year 2001 publications

“Path-Dependent Neutralization of Multiply Charged Ar Ions Incident on Au (110),” V. A. Morozov and F. W. Meyer, *Phys. Rev. Lett.* **86**, 736 (2001).

“Target Orientation Dependence of the Backscattered Intensities and Charge Fractions Observed for Large-Angle Quasi-Binary Collisions of Ar^{q+} Ions with Au(110),” A. Morozov and F. W. Meyer, *Phys. Scripta* **T92**, 31 (2001).

“Electrostatic Trap for keV Ion Bemas,” H. F. Krause, C. R. Vane, and S. Datz, in *Proceedings, 16th Intl. Conf. On Application of Accelerators in Research and Industry*, Editors – J. L. Duggan and I. L. Morgan, AIP Press, New York, AIP Conference Series **576**, 126-129 (2001).

“Charge Transfer Experiment,” C. C. Havener, in *Spectroscopic Challenges of Photoionized Plasmas*, Editors, G. Ferland and D. Savin, ASP Conference Series, 2001.

“Charge Fraction Measurements for 2.4 – 35 keV Ar^{q+} ($q = 2-13$) Projectile Backscattered from Au(110),” F. W. Meyer, V. A. Morozov, S. Datz, and R. Vane, *Phys. Scripta* **T92**, 182 (2001).

“Adiabatic Limit of Inelastic Transitions,” P. Krstic, C. O. Reinhold, and J. Burgdörfer, *Phys. Rev. A* **63** 032103 (2001).

“Autoionization of Doubly and Triply Excited States of Li^+ and Li Produced in Li^{3+} Ion Collision with C_{60} , Ar, and Xe,” D. V. Lukic, P. R. Focke, C. Koncz, V. A. Morozov, F. W. Meyer, and I. A. Sellin, *Physica Scripta* **T92**, 174 (2001).

“Relativistic Electron Transport Through Carbon Foils,” M. Seliger, K. Tökesi, C. O. Reinhold, J. Burgdörfer, Y. Takabayashi, T. Ito, K. Komaki, T. Azuma, and Y. Yamazaki, *Physica Scripta* **T92**, 211 (2001).

“Low-Energy Electron Capture by Cl^{7+} from D Using Merged Beams,” J. S. Thompson, A. M. Covington, P. S. Krstic, Marc Pieksma, J. L. Shinpaugh, P. C. Stancil, and C. C. Havener, *Phys. Rev. A* **63**, 012727 (2001).

“Dynamics of Dissociative Recombination of Molecular Ions: Three-body Breakup of Triatomic Di-Hydrides,” S. Datz, *J. Phys. Chem. A* **105**, 2369 (2001).

"Electron Capture and Ionization of 33-TeV Pb Ions in Gas Targets," H. F. Krause, C. R. Vane, S. Datz, P. Grafström, H. Knudsen, U. Mikkelsen, C. Scheidenberger, R. H. Schuch, and Z. Vilakazi, *Phys. Rev. A* **63**, 032711 (2001).

"Random and Channeled Energy Loss of 33.2-TeV Pb Nuclei in Silicon Single Crystals," S. Pape Møller, V. Biryukov, S. Datz, P. Grafström, H. Knudsen, H. F. Krause, C. Scheidenberger, U. I. Uggerhøj, and C. R. Vane, *Phys. Rev. A* **64**, 032902 (2001).

"Inelastic Transitions in Slow Heavy-Particle Atomic Collisions," P. S. Krstic, C. O. Reinhold, and J. Burgdörfer, *Phys. Rev. A* **63**, 052702 (2001).

"Designing Rydberg Wave Packets Using Trains of Pulses," C. O. Reinhold, J. Burgdörfer, S. Yoshida, B. E. Tannian, C. L. Stokely, and F. B. Dunning, *J. Phys. B* **34**, L551 (2001).

"Probing Coordinates of Rydberg Wave Packets," B. E. Tannian, C. L. Stokely, F. B. Dunning, C. O. Reinhold, and J. Burgdörfer, *Phys. Rev. A* **64**, 021404 (2001).

"Transport of Kr³⁵⁺ Inner-Shells through Thin Carbon Foils," D. Vernhet, C. Fourment, E. Lamour, J.-P. Rozet, B. Gervais, L. J. Dube, F. Martin, T. Minami, C. O. Reinhold, M. Seliger, and J. Burgdörfer, *Physica Scripta* **T92**, 233 (2001).

"Vertical Incidence of Slow Ne¹⁰⁺ Ions on a LiF Surface: Suppression of the Trampoline Effect," L. Wirtz, C. Lemell, J. Burgdörfer, L. Hagg, and C. O. Reinhold, *Nucl. Instrum. Meth. Phys. Res.* **182**, 36 (2001).

"Siegert-Pseudostate Representation of Quantal Time-Evolution: A Harmonic Oscillator Kicked by Periodic Pulses," S. Tanabe, S. Watanabe, N. Sato, M. Satsuzawa, S. Yoshida, C. O. Reinhold, and J. Burgdörfer, *Phys. Rev. A* **63**, 052721 (2001).

"Relativistic Electron Transport through Carbon Foils," M. Seliger, L. Tokesi, C. O. Reinhold, and J. Burgdörfer, *Physica Scripta* **T92**, 211 (2001).

"Time-Dependent Treatment of Electron-Hydrogen Scattering of Higher Angular Momenta ($L > 0$)," D. O. Otero, J. L. Peacher, D. R. Schultz, and D. H. Madison, *Phys. Rev. A* **63**, 022708 (2001).

"On Quantum-Classical Correspondence in Classical Studies of Atomic Processes," M. Rakovic, D. R. Schultz, P. C. Stancil, and R. K. Janev, *J. Phys. A* **34**, 473 (2001).

"Classical/Quantal Correspondence in State-Selective Charge Transfer for Partially-Stripped Ion Impact on Atomic Hydrogen: Improvements to the CTMC Method," D. R. Schultz, P. C. Stancil, and M. J. Rakovic, *J. Phys. B* **34**, 2739 (2001).

"Excitation of He⁺ to the 2²S and 2²P States by Electron Impact," A.C.H. Smith, M. E. Bannister, Y.-S. Chung, N. Djuric, G. H. Dunn, A. Neau, D. Popovic, M. Stepanovic, and B. Wallbank, *J. Phys. B* **34**, L571 (2001).

Year 2000 Publications

"Curve Crossing Analysis for Potential Sputtering of Insulators," L. Wirtz, G. Hayderer, C. Lemell, J. Burgdörfer, L. Hagg, C. O. Reinhold, M. Schmid, P. Varga, H.-P. Winger, and F. Aumayr, *Surface Science* **451**, 197 (2000).

"Multiple Ionization in Fast Ion-Atom Collisions: Simultaneous Measurement of Recoil Momentum and Projectile Energy Loss," M. A. Abdallah, C. R. Vane, C. C. Havener, D. R. Schultz, H. F. Krause, N. Jones, and S. Datz, *Phys. Rev. Lett.* **85**, 278 (2000).

"Radiative Electron Capture at Ultrarelativistic Energies: 33-TeV Pb⁸²⁺ Ions," C. R. Vane, H. F. Krause, S. Datz, P. Grafström, H. Knudsen, C. Scheidenberger, and R. H. Schuch, *Phys. Rev. A* **62**, 010701 (2000).

- “Electrons Emitted from 33-TeV Pb Ions during Penetration of Solids,” C. R. Vane, U. Mikkelsen, H. F. Krause, S. Datz, P. Grafström, H. Knudsen, S. Møller, E. Uggerhøj, C. Scheidenberger, R. H. Schuch, and Z. Vilikazi, *Proceedings, Intl. Conf. on the Physics of Electronic and Atomic Collisions*, Sandei, Japan, July 22-27, 1999, American Institute of Physics (AIP), Editor, Y. Itikawa, No. 500, pp. 709-714 (2000).
- “Atomic Collision Processes in Solids and Gases at Ultrarelativistic Energies,” S. Datz, *Nucl. Instrum. Meth. Phys. Res. B* **164-165**, 1 (2000).
- “Dynamics of Three-Body Breakup in Dissociative Recombination: H_2O^+ ,” S. Datz, R. Thomas, S. Rosen, M. Larsson, A. Derkatch, F. Hellberg, and W. van der Zande, *Phys. Rev. Lett.* **85**, 5555 (2000).
- Three-body Breakup Dynamics in Dissociation Recombination,” S. Datz, S. Rosen, A. Al-Khalili, A. Derkatch, W. Shi, R. Thomas, L. Vikor, R. Peverall, M. Larsson, and W. van der Zande, pp. 210-213 in *Dissociative Recombination: Theory, Experiment, and Application*, Editor, M. Larsson, World Scientific Publishing, Singapore 2000.
- “Low-Energy Electron Capture by Cl^{7+} from D using Merged-Beams,” J. S. Thompson, A. M. Covington, P. S. Krstic, Marc Pieksma, J. L. Shinpaugh, P. C. Stancil, and C. C. Havener, *Phys. Rev. A* **63**, 012727 (2000).
- “De-Excitation X Rays from Resonant Coherently Excited 390-MeV/u Hydrogen-like Ar Ions,” T. Ito, Y. Takabayashi, K. Komaki, T. Azuma, Y. Yamazaki, S. Datz, E. Takada, and T. Murakami, *Nucl. Instrum. Meth. Phys. Res. B* **164-165**, 69-79 (2000).
- “Quantum Localization of the Kicked Rydberg Atom,” S. Yoshida, C. O. Reinhold, and J. Burgdörfer, *Phys. Rev. Lett.* **84**, 3602 (2000).
- “Enhanced Population of High-l States due to the Interplay Between Multiple Scattering and Dynamical Screening in Ion-Solid Collisions,” C. O. Reinhold, D. G. Arbo, J. Burgdörfer, B. Gervais, E. Lamour, D. Vernhet, and J. P. Rozet, *J. Phys. B* **33**, L111 (2000).
- “Collisions Near Threshold in Atomic and Molecular Physics,” H. R. Sadeghpour, J. L. Bohn, M. J. Cavagnero, B. D. Esry, I. I. Fabrikant, J. H. Macek, and A. R. P. Rau, *J. Phys. B* **33**, R93 (2000).
- “Time-Dependent Treatment of Electron-Hydrogen Scattering for Higher Angular Momenta ($L>0$),” D. O. Otero, J. L. Peacher, D. R. Schultz, and D. H. Madison, *J. Phys. B* (2000).
- Kicked Rydberg Atom: Response to Trains of Unidirectional and Bidirectional Impulses,” B. E. Tannian, C. L. Stokely, F. B. Dunning, C. O. Reinhold, S. Yoshida, and J. Burgdörfer, *Phys. Rev. A* **62**, 043402 (2000).
- Exponential and Non-Exponential Localization of the One-dimensional Periodically Kicked Rydberg Atom,” S. Yoshida, C. O. Reinhold, P. Kristöfel, and J. Burgdörfer, *Phys. Rev. A* **62**, 023408 (2000).
- “Quantum Evolution and Atomic States During Transmission Through Solids,” D. G. Arbó, C. O. Reinhold, S. Yoshida, and J. Burgdörfer, *Nucl. Instrum. Meth. Phys. Res.* **164-165**, 495 (2000).
- “Collisions of Ground-State Hydrogen Atoms,” M. J. Jamieson, A. Dalgarno, B. Zygelman, P. S. Krstic, and D. R. Schultz, *Phys. Rev. A* **61**, 014701 (2000).
- “ECR-Based Atomic collision Physics Research at ORNL MIRF,” F. W. Meyer, pp. 117-164 in *Trapping Highly Charged Ions: Fundamentals and Applications*, Editor, J. D. Gillaspay, Nova Science Publishers, 2000.
- “Effective Range Analysis for Positron-Hydrogen Collisions,” S. J. Ward and J. H. Macek, *Phys. Rev. A* **62**, 052715 (2000).

Research Summaries
(single-PI grants alphabetical by PI)

Properties of Transition Metal Atoms and Ions

D. R. Beck
Physics Department
Michigan Technological University
Houghton, MI 49931
e-mail: donald@mtu.edu

Program Scope

Transition metal atoms are technologically important in plasma physics (e.g. as impurities in fusion devices), Atomic Trap Trace Analysis (detection of minute quantities of radioactive species), astrophysical abundance (e.g. Fe II) and atmospheric studies, deep-level traps in semiconductors, hydrogen storage devices, etc. The more complicated rare earths which we are beginning to study are important in lasers, high temperature superconductivity, advanced lighting sources, magnets, etc.

Because of the near degeneracy of nd and $(n+1)s$ electrons in lightly ionized transition metal ions and the differing relativistic effects for d and s electrons [1], any computational methodology must simultaneously include the effects of correlation and relativity from the start. We do this by using a Dirac-Breit Hamiltonian and a Relativistic Configuration Interaction (RCI) formalism to treat correlation. Due to the presence of high- l (d) electrons, computational complications are considerably increased over those in systems with just s and/or p valence electrons. These include the following: (1) larger energy matrices (5-10 times larger) because the average configuration can generate many more levels [2]. Multi-root calculations with matrices of order 20-30 000 are becoming common, (2) increased importance of interactions with core electrons (d 's tend to be more compact, and there can be more of them), (3) a significant variation of the d radial functions with level (J), which requires the presence of second order effects. Methodological improvements are most needed in the treatment of second order effects.

We desire to develop the methodology to a point where properties of $(d+s)^n$ states can be treated accurately and efficiently. To date, this is only possible for $n < 5$. A systematic knowledge of which basis functions are crucial to a physical property can allow us to limit basis set sizes, while retaining accuracy. To this end, contributions to properties are generated at all computational stages. These are particularly helpful in determining where the saturation of radial basis sets may need further exploration.

Recent Progress

[A] Tc I f values

The most complex project undertaken during this period was to obtain accurate f values for $(d+s)^7 \rightarrow (d+s)^6p$ Tc I f values. No prior *ab initio* results exist. The specific goal was to find a strong transition involving just two levels (absorption and emission). One such was found $-4d^65s\ ^6D_{9/2} \rightarrow 4d^65p\ ^6F_{11/2}$ with $f \sim 0.3$, with the $^6D_{9/2}$ having a long lifetime (decays by an E2 process). It should be a relatively easy matter to modify the data files to treat the homologous Fe II case, which is of great interest to astrophysicists.

Even using our most powerful algorithms [4], as of last year, we were only able to produce

average energy errors of 500 cm^{-1} for the odd states, and $\sim 1500 \text{ cm}^{-1}$ for the even states. For some of the energetically higher levels this accuracy could give rise to configurational and LS labels in significant disagreement with those in Moore [5]. Large second order effects are present, and they are difficult to handle directly due to the complexity of the configurations involved, e.g. $(d+s)^3 p^2 f^2$.

At the end of the last project year, we submitted this work for publication [6]. In responding to the referee's comments, we have undertaken a lengthy recalculation of the even parity states, which has managed to reduce the energy error 40% in some cases. This has brought our results in to much better agreement with Moore [5]. We did this by using REDUCE [4] to produce a second order basis, using first order REDUCE reference functions. This greatly decreases the total number of second order basis functions (from as many as 20 500 to as few as 2000).

[B] Lifetimes of $np^5(n+1)s J=2$ Rare Gas States

Our attention was drawn [7] to a factor of 2 discrepancy [8] between theory and experiment for Magnetic Quadrupole (M2) lifetimes in $np^5(n+1)s J=2$ states. The discrepancy grew worse as correlation effects were added to the states [7]. This was an attractive problem, because it potentially involved $np^5(d+s)$ mixing. We were able to identify the problem with missing second order effects associated with the $np^5 nd$ basis function. The $np^5 nd$ and $np^5(n+1)s$ basis functions must be treated on an equal footing with respect to correlation. The work is complete, and has been accepted for publication [9].

[C] K II $3p^6 \rightarrow 3p^5(4s+3d) J=1 f$ values

Ab initio f values for K II are in poor agreement with experiment [10]. The problem lies with the near degeneracy of the levels (as close as $\sim 1300 \text{ cm}^{-1}$) and the great variation of the d radial function with level (3P vs 3D vs 1P). A thorough *ab initio* treatment involves the presence of considerable second order effects – matrices of order $\sim 10\,000$ are utilized. Agreement with 2 of the 3 measured f values is excellent, with the 3rd it is fair. F values to the two uppermost levels are newly predicted. The work has been submitted for publication [11].

[D] Zr III $(5s+4d)^2 J=0 \rightarrow (4d5p+5s5p) J=1 f$ values

The Zr III f values are of astrophysical interest. Three of the levels have been greatly revised by Reader and Acquista [12] who also obtained semi-empirical wavefunctions for the levels, and from them f values. Two other model/semi-empirical f value calculations exist, the most recent by E. Charro *et al* [13]. Some of these results differ by 20%. We have completed f value calculations [14] for all 15 transitions, using our “one-shot” algorithm [2] which calculates all possible transitions at the cost of one. The average gauge difference is 4.6% for f 's > 0.01 , and we agree best with Reader and Acquista [12].

[E] $\text{Er}^{3+} 4f^{11} 4S_{3/2} \rightarrow 4I_{15/2}$ Transition Energy

Eventually, we want to be able to treat correlation and relativistic effects in the even more difficult open f subshell species (rare earths). Here, we make a beginning by calculating the Er^{3+} transition energy, which in GaN, is important in high temperature optoelectronic

device applications [15]. Correlation effects contribute $\sim 5000 \text{ cm}^{-1}$ to this transition, and I have accounted for most of them [16]. N.B. The GaN host has little impact on energy differences, but greatly impacts this transition probability.

[F] Miscellaneous

The work on Ta II f values [2] has now been published [17], and a stand alone relativistic continuum algorithm has now been published [18]. This is essential for the completion of a relativistic correlation continuum properties suite we have under development [19]. Several software improvements have been made to the bound state codes to improve computer/human efficiency, and a new 73GB hard drive added. The M2 option was added to the oscillator strength algorithm. During the 2000-2 period, DOE supported work that has been published or accepted for publication includes items 9, 16, 17, 18 as well as work on Fe v f values [20] and Au⁶⁶⁺ lifetimes [21].

Future Plans

Near future applications include finishing Tc I and Fe II f values. The continuum algorithms [19] will be completed, and we will begin to apply them.

References

- [1] R. L. Martin and P. J. Hay, J. Chem. Phys. **75**, 4539 (1981).
- [2] D. R. Beck, 2001 AMOP Research Meeting Abstracts.
- [3] C. Y. Chen, Y. M. Li, K. Bailey, T. P. O'Connor, L. Young, and Z.-T. Lu, Science **286**, 1139 (1999).
- [4] The RCI program suite consists of 3 unpublished programs written by D. R. Beck over a period of years. RCI calculates the bound state wavefunctions, hyperfine structure, and Landé g values. RFE uses RCI wavefunctions and computes E1, E2, M1 and M2 f values, including the effects of non-orthonormality. REDUCE minimizes the number of eigenvectors needed for a correlation manifold by rotating the original basis to maximize the number of zero matrix elements involving the reference functions; only rotated vectors having non-zero reference interactions are retained.
- [5] C. E. Moore, Atomic Energy Levels, Volume II, NSRDS-NBS 35, US GPO, Washington D.C., Reissued Dec. 1971.
- [6] S. M. O'Malley and D. R. Beck, "Lifetimes of Tc I States", Phys. Rev. A, submitted for publication (under revision).
- [7] Yong-Ki Kim, private communication, April 2002.
- [8] M. Walhout, A. Witte, and S. L. Rolston, Phys. Rev. Letts. **72**, 2843 (1994).
- [9] D. R. Beck, "Magnetic Quadrupole Lifetimes of $np^5(n+1)s$ $J = 2$ States of Rare Gases", Phys. Rev. A, accepted for publication.
- [10] M. Henderson, L. J. Curtis, R. Matulioniene, and D. G. Ellis, Phys. Rev. A **55**, 2723 (1997).
- [11] D. R. Beck, "Oscillator Strengths for K II $3p^6$ to $3p^5(4s+3d)$ $J = 1$ Transitions", J. Phys. B, submitted for publication.
- [12] J. Reader and N. Acquista, Phys. Scr. **55**, 310 (1997).
- [13] E. Charro, J. L. Lopez-Ayuso, and I. Martin, J. Phys. B **32**, 4555 (1999).

- [14] D. R. Beck and L. Pan, Zr III f values, to be submitted.
- [15] M. Thaik, U. Hommerich, R. N. Schwartz, R. G. Wilson, J. M. Zavada, Appl. Phys. Lett. **71**, 2641 (1997).
- [16] D. R. Beck, "Important Correlation Effects for the $\text{Er}^{3+} 4f^{11} {}^4S_{3/2} \rightarrow {}^4I_{15/2}$ Laser Transition Energy", Int. J. Quant. Chem. **90**, 439 (2002) (in press).
- [17] P. L. Norquist and D. R. Beck, J. Phys. B **34**, 2107 (2001).
- [18] M. G. Tews and W. F. Perger, Comp. Phys. Commun. **141**, 205 (2001). Tews was an MS student of the PI's and was DOE supported.
- [19] Program RAUTO computes the matrix elements for the Dirac, electrostatic, and Breit operators between bound and continuum states of the same J and parity, including non-orthonormality effects. Program RPI computes photoionization E1, E2, M1 and M2 f values, including non-orthonormality effects, D. R. Beck, unpublished.
- [20] S. M. O'Malley, D. R. Beck and D. P. Oros, Phys. Rev. A **63**, 032501 (2001).
- [21] D. R. Beck and P. L. Norquist, Phys. Rev. A **61**, 044504 (2000).

PROBING DYNAMICS AND STRUCTURE IN ATOMS, MOLECULES AND NEGATIVE IONS USING THE ADVANCED LIGHT SOURCE

Nora Berrah

Physics Department, Western Michigan University, Kalamazoo, MI 49008

e-mail:Berrah@wmich.edu

Program Scope

The objective of the research program is to advance fundamental understanding of the interaction between vuv/soft x-ray photons and gas-phase targets as well as to achieve a better understanding of the dynamics and electronic structure of atoms, molecules, clusters and negative ions. These studies allow an understanding, at the atomic and molecular level, of many processes important to the understanding of the properties of complex materials and of strongly correlated systems. We use photons from the Advanced Light Source as our probe because they provide the photon energy range that accesses inner-shells as well as tunability and resolution, necessary to obtain detailed knowledge with an impressive degree of precision. We have also developed and improved experimental techniques to achieve high detection efficiency and high precision measurements. We present here results completed and underway this past year and plans for the immediate future.

Recent Progress

1) Development of Inner-Shell Photodetachment Studies of Negative Ions

We have been planning these past 11 years and developing these past six years a new program of inner-shell photodetachment studies of negative ions to investigate the correlation and dynamics between a core and valence electrons in a situation where one electrons is very loosely bound to the atoms.

Investigation of electrons dynamics through photodetachment studies of negative ions provides valuable insights into the general problem of the correlated motion of electrons in many-particle systems such as heavy atoms, molecules, clusters and solids. Photoexcitation and photodetachment processes of negative ions stand out as an extremely sensitive probe and theoretical test-bed for the important effects of electron-electron interactions because of the weak coupling between the photons and the target electrons. Therefore, these target ions constitute excellent systems for studying dynamics and for testing the ability of theoretical calculations to incorporate electron-correlation effects. In addition, negative ions present a severe theoretical challenge since the independent-electron model is inadequate for even a qualitative description of their properties. Previously, many calculations only took the electron-correlation contributions from the valence shell into account. However, new theoretical work including core-valence and core-core effects has lead to much better agreement with experiments than just a few years ago. Although negative ions usually exist only in a single bound configuration, it is known that numerous resonances exist in the detachment cross section originating from short-lived excited states above the first detachment limit [a]

Numerous experimental and theoretical studies of valence-shell photodetachment have been conducted using lasers [b]. However, studies of the correlation between a core and valence electrons, through inner-shell photodetachment studies, is a largely unexplored territory; Li^- , the simplest multishell negative ion has been investigated, only last year, independently by us and by the Danish group [1,c]. With the advent of 3rd generation synchrotron light sources with higher flux, brightness, tunability and resolution, it is now possible to investigate experimentally inner-shell processes in tenuous negative ion targets. Our studies were facilitated by the purchase of two negative ion sources last year; a cesium sputtering source (SNICS II) used for the production of several negative ions and of an RF charge exchange ion source (Alphatross) for the production of He^- and H^- . Motivated by a recent theoretical calculations [d], we have carried out an experimental K-shell photodetachment study of Li^- , giving rise to doubly photoionized Li^{2+} ions, using a collinear photon-ion beam apparatus built (through an Instrumental-Facilities- Initiative collaboration between WMU and UNR) at Reno Nevada by R. Phaneuf's group.

Briefly, the first comparison between a high-resolution experimental and sophisticated theoretical [1,d] K-shell study of a negative ions was undertaken. The data revealed dramatic structure qualitatively and quantitatively unlike K-shell photoabsorption of atoms and positive ions which are characterized by structureless, monotonically decreasing $1s$ photoionization cross-section. The comparison of the data with calculations [1, c, d] shows good agreement over some of the photon energy range, but also reveals some puzzling discrepancies. Two shape resonances were predicted but only one of them was observed by us and also independently by [c]. The first predicted shape resonance, $1s2s^2$ (2S) around 57 eV, is not observed in addition to two other structures between 63 and 64 eV, even though we were able to measure the second weaker shape resonance, $1s(2s2p(^3P))(^2P)$ around 60 eV, and narrow structure at 62.6 eV. One of the possible reasons for not observing the first shape resonance is that it may decay primarily to the ground state and valence excited states $1s^22p$, $1s^23p$ of neutral He which we didn't measure with the present experimental system, aimed at measuring positive ion. If it autoionized to a core excited state of neutral Li, and then Auger decay to the ground state of Li^+ , we will have observed it, as we did for the other structures. In fact, the calculation included $1s^22p$ and $1s^23p$ but not the higher levels $1s^2nl$, which may be the reason for not predicting that the decay should be toward neutral Li and not toward Li^+ [1, c, d]. This discrepancy reveals the complexity of this dynamical problem, even though we are dealing with only a four electrons system. Theoretical efforts are underway by our collaborators to understand the discrepancy. From the experimental side, measuring the neutral atoms will allow us to determine if the decay is mostly to the neutral atoms channel as opposed to the positive ion channel as predicted. This test will infer the importance of higher valence excited levels needed to be included in the calculation, in addition to pointing out to the sensitivity of using accurate thresholds values to locate resonances positions.

2) Vibrational Structure and Partial Rates of Resonant Auger Decay of the N $1s \rightarrow 2\pi$ Core Excitation in Nitric Oxide.

Auger-electron spectroscopy is a valuable tool for investigating the electronic structure and potential-energy surfaces of molecules [e]. An accurate interpretation of a molecular resonant Auger spectrum requires a thorough understanding of the core-excitation process and a characterization of the numerous final ionic states of the decay process. We have been motivated by recently reported *ab-initio* calculations [f] to carry out high-resolution measurements of resonant Auger decay of the 2π excitations of the nitrogen $1s$ edge of NO. We have then compared the vibrationally resolved resonant Auger-electron spectra from the decay of the ${}^2\Delta$, ${}^2\Sigma^-$, and ${}^2\Sigma^+$ states of the $N\ 1s^{-1}2\pi^2$ core-excited configuration of NO, with the results of *ab-initio* calculations [f]. Good agreement was found between the experimental and theoretical vibrational progressions of the $X\ {}^1\Sigma^+$ band, indicating that the calculated potential-energy curves adequately describe a ground and core-excited electronic states. The agreement was further improved by a least-squares optimization procedure, resulting in slight modifications of the Morse potential of the ${}^2\Delta$ core-excited state and also yielding an estimate of 130 (10) meV for its lifetime width. In the higher binding energy region, the spectra were decomposed into partial contributions from the decay to different final ionic states. Here, the primary objective was to compare the calculated partial Auger decay rates with the experiment. A good agreement was found in the decay from the lowest levels of the core-excited to the Σ^+ , Σ^- , and Δ states of the $2\pi^0$, $5\sigma^{-1}2\pi^1$ and $1\pi^{-1}2\pi^1$ ionic configurations. The largest discrepancies were found in the case of the ${}^{1,3}\Pi$ Auger final states, for which the calculated intensities tend to be underestimated relative to the other bands in the Auger electron spectra. In addition, a new value of the adiabatic ionization energy of the ${}^1\Delta$ ionic state was obtained from least-squares analysis of the spectra.[2]

3) Dynamical Relativistic Effects in Photoionization: Spin-Orbit Resolved Angular Distribution of Xe 4d Photoelectrons near the Cooper Minimum.

Two decades ago, it was predicted by Y. S. Kim et al. [g] that relativistic effects should alter the dynamics of the photoionization process in the vicinity of Cooper minima. Our experimental study of the angular distribution of Xe $4d_{3/2}$ and $4d_{5/2}$ photoelectrons demonstrate the predicted effects for the first time. New calculations performed by one of us [3] corroborate the previous prediction. Our results clearly imply that relativistic effects are likely to be important for intermediate-Z atoms at most energies.

Future Plans.

The principal areas of investigation planned for the coming year are: (1) Build a neutral detector to measure the neutral decay channel in the photodetachment experiments of negative ions; Li^- , He^- , B_2^- . In addition, we plan to measure the absolute cross section since our measurements were relative. (2) Analyze our spin resolved data of the $2p$ photoionization of OCS. 3) Carry out and analyze high-resolution measurements of inner-shell photodissociation dynamics in diatomic molecules.

Publications from DOE sponsored research.

- [1] N. Berrah, J. D. Bozek, A. A. Wills, G. Turri, H. -L. Zhou, S. T. Manson, G. Akerman, B. Rude, N. D. Gibson, C. W. Walter, L. VoKy, A. Hibbert, and S. Fergusson, "K-shell photodetachment of Li: Experiment and Theory", *Phys. Rev. Lett.* **87**, 25002 (2001).
- [2] E. Kukk, J. D. Bozek, W. T. Cheng, G. Snell, and N. Berrah "Vibrational structure and partial rates of resonant Auger decay of the N 1s \rightarrow 2 π core excitations in nitric oxide", *Phys. Rev. A* **63**, 062702 (2001).
- [3] H. Wang, G. Snell, O. Hemmers, M. M. Sant'Anna, I. Sellin, N. Berrah, D. Lindle, P.C. Desh-mukh, N. Haque, and S. T. Manson "Spin-orbit resolved angular distribution of xenon 4d photoelectrons in the photon energy range of 100-250 eV: Experiment and theory", *Phys. Rev. Lett.* **87**, 123004 (2001).
- [4] G. Snell, M. Martins, E. Kukk, W. T. Cheng, and N. Berrah "High-resolution electron spectroscopy of a strongly correlated system: atomic barium" *Phys. Rev. A* **63**, 062715 (2001).
- [5] O. Nayandin, E. Kukk, A. A. Wills, B. Langer, J. D. Bozek, S. Canton-Rogan, M. Wiedenhoef, D. Cubaynes, and N. Berrah, "Angle-resolved two-dimensional mapping of electron emission from the inner-shell 2p excitations in Cl₂" *Phys. Rev. A* **63**, 062719 (2001).
- [6] K. J. Borge, L. J. Saethre, T. D. Thomas, T. X. carol, N. Berrah, J. D. Bozek, and E. Kukk, "Vibronic Structure in the Carbon 1s Photoelectron Spectra of HCCH and DCCD", *Phys. Rev. A* **63**, 012506-1 (2001).

References:

- [a] S.J. Buckman and C.W. Clark, *Rev. Mod. Phys* **66**, 539 (1994); C. W. Walter, *et al*, *Phys. Rev. A* **50**, 2257 (1994) and references therein.
- [b] T. Andersen *et al*, *J. Phys. Chem. Ref. Data* **28**, 1511 (1999) and references therein.
- [c] H. Kjeldsen, P. Andersen, F. Kristensen and T. Andersen, *J. Phys. B* **34**, L353 (2001).
- [d] H. L. Zhou, S. T. Manson, L. VoKy. N. Feautrier and A. Hibbert, *Phys. Rev. Lett.* **87**, 023001 (2001)
- [e] W. Eberhart, J.-E. Rubensson, K. J. Randall, J. Feldhaus, A. L. D. Kilcoyne, A. M. Bradshaw, Z. Xu, P. D. Johnson and Y. Ma, *Phys. Scr.* **T41**, 143 (1992).
- [f] R. Fink, *J. Chem. Phys.* **106**, 4038 (1997).
- [g] Y. S. Kim, A. Ron, R. H. Pratt, B. R. Tambe and S. T. manson, *Phys. Rev. Lett.* **46**, 1326 (1981).

Coherent Control of X-rays

Principal Investigator: P.H. Bucksbaum; Co-PI: D.A. Reis
FOCUS Center, Physics Department, University of Michigan, Ann Arbor, MI 48109-1120
pbb@umich.edu. Grant DEFG02-00ER15031

Program Scope

The Advanced Photon Source at Argonne National Laboratory provides tunable x-rays for research in physics, chemistry, biology, and engineering. Most spectroscopic or imaging problems at this third-generation synchrotron make use of its high average spectral brightness, which can exceed 10^{12} x-rays per second within a 10^{-4} fractional energy band, with beam divergence below $100\mu\text{r}$. Still more impressive is the peak spectral brightness, which can approach 10^4 monoenergetic hard x-rays per picosecond. This is high enough for diffraction or absorption measurements on the time scale of atomic motion in molecules and condensed media.

The x-ray pulse duration from the synchrotron is on the order of 100 ps . To resolve motion on the 0.1 ps - 1 ps scale of molecular dynamics, ultrafast x-ray gates or x-ray detectors are needed. We have an experimental program to modulate the synchrotron x-ray beam by ultrafast laser excitation of x-ray diffractive optics, such as Bragg mirrors. Pump-probe techniques are used to study ultrafast dynamics on the 100 ps – 1 msec time scale, and x-ray streak cameras are used for 1 - 100 psec experiments. We are studying techniques to switch x-rays so that they can be used to study dynamics down to 0.1 psec . These studies have helped to establish the field of ultrafast x-ray science at synchrotrons, and they form the foundation for ultrafast x-ray studies at future fourth-generation x-ray free electron lasers or novel linac-based femtosecond x-ray sources such as SLAC's SPPS (sub-picosecond photon source).

Most of our work is done in conjunction with the MHATT-CAT collaboration, on Sector 7 of the APS, and at the NSF FOCUS Physics Frontier Center at the University of Michigan. The hutch housing our experiment is at the end of the undulator insertion device (ID) beam line. We have approximately four 7-10-day periods of access to x-rays per year. We also have several collaborations, which give us access to other x-ray sources at ESRF, ALS, and soon at the SLAC SPPS. We have also held a workshop for potential future collaborators and users of our ultrafast beam line at the APS. Workshop participants came from physics, chemistry, materials science and biology groups in the US and Europe.

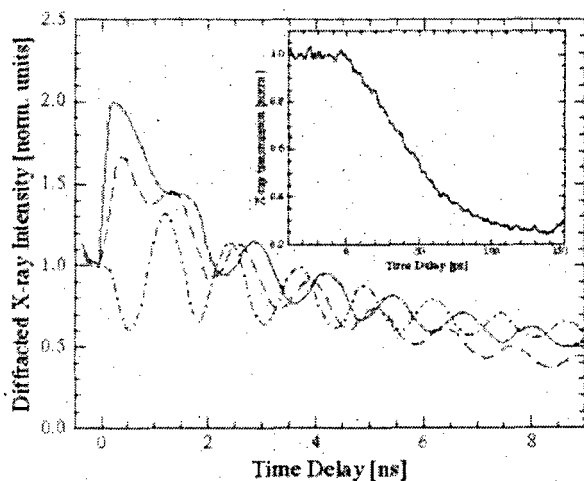
Recent progress

Improvements to the instrumentation: The laser that we have installed in the 7ID-D hutch at APS is a Ti:Sapphire multipass chirped-pulse amplified design, with the following output characteristics: 50 - 100 fsec pulse duration; 840 - 790 nm central wavelength; 1 kHz repetition rate; 0.5 - 1 mJ pulse energy. The laser pulse is synchronized to the x-rays to better than the x-ray pulse duration. In the past, this was accomplished by slaving the laser oscillator cavity round-trip period to the synchrotron accelerator RF signal. This year we improved this synchronization to about 3 psec , and eliminated long-term drift between the x-rays and the laser, by employing a beam position monitor in the x-ray ring to supply us with the timing of the electron bunch. We also replaced the optics in the amplifier, which doubled the output power and improved the laser stability.

We have begun construction of our own x-ray streak camera, which will eventually replace the need to borrow the Falcone/Chang x-ray streak camera and transport it half-way across the country from Berkeley for our experiments. The camera construction was made possible by instrumentation money from the FOCUS center and from the University of Michigan. This camera will have a similar design to the Berkeley camera, but will be more compact, and will employ external focusing and UHV vacuum components.

One major improvement in experimental capabilities was an extension of the timing dynamic range. We can now vary the delay between the laser pump and x-ray probe by up to one millisecond with a precision of 19 psec. This critical improvement permits us to observe transient dynamics in thin crystals over many acoustic impulse returns. We also improved the x-ray beam path so that we can use the pink beam (i.e. the non-monochromatized undulator beam).

Transmission switching in Ge. Our major experimental progress this year was further studies of acoustic phonon switching via the laser-induced Pendellösung effect in x-ray transmission in Ge. We observed that an impulsively generated acoustic pulse in a thick crystal modulates the coherent transmission of x-rays propagating many x-ray incoherent absorption depths through the material (a combination of the Borrmann effect and the Pendellösung effect). The excitation was observed to transfer energy between two x-ray beams in a time shorter than the synchrotron pulse width. Different arrangements were studied, including a switch made from two counter-propagating acoustic pulses that collide deep inside the crystal. This effectively halves the Pendellösung period, and also provides one means to observe a localized transient strain inside an otherwise opaque material. The initial report of these studies was published in *Nature*, and has also been featured in news articles in *Physics Today*, *Chemical and Engineering News*, and *Nature News and Views*.



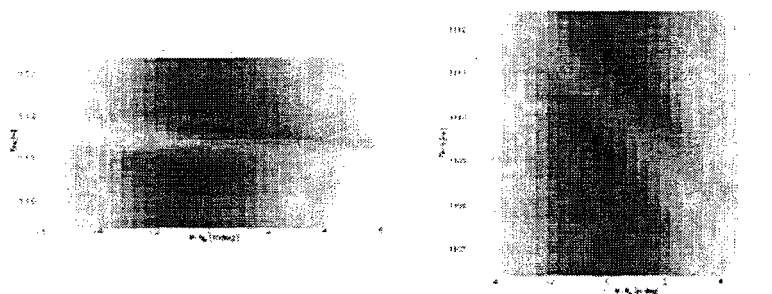
One of the most interesting aspects of the work reported in *Nature* was a rapid transient switch, much faster than a Pendellösung period, following excitation. We followed up on preliminary x-ray streak camera measurements of the rapid transient switching effect in Ge. We found that the initial coherent acoustic pulse front propagates into the crystal at supersonic speeds. Further studies and modeling suggest that the cause is rapid ambipolar diffusion of the dense electron-hole plasma created by the laser. The switching speed is ultimately limited only by the motion of atoms, and could be much less than a picosecond for optical phonon excitation.

The figure shows time-resolved anomalous transmission. The time dependent intensity of the deflected diffracted beam is shown at three different optical fluences, which correspond to formation of electron-hole plasmas with different initial densities. Both the phase and amplitude of the oscillations are affected. The initial transient is shown with higher time resolution in the inset, which was obtained with an x-ray streak camera. This shows that the transient switch

occurs in about 40 psec, much less than the duration of the x-ray pulse at the APS. This work is in preparation for submission in the immediate future.

Studies of coherent acoustic strain. Our work on x-ray switching is giving us new information on coherent acoustic strain in materials. Using pump-probe time-resolved x-ray diffraction at a synchrotron, we are able to follow the generation and propagation of a picosecond coherent acoustic pulse in an ultrafast laser-strained single crystal. Comparison of the data with dynamical diffraction simulations allows for the quantitative determination of both the surface and bulk components of the associated strain. This technique is scalable to femtosecond and shorter time-scales as x-ray pulses become shorter in duration.

We studied phonon dispersion and attenuation directly using time-resolved x-ray diffraction in Ge. By changing the diffraction angle, the x-rays can probe either the compression or expansion components of the crystal lattice. After twenty reflections (total propagation distance of ~ 5.5 mm) the arrival time of the compression and the expansion components are significantly different, as shown in the figure below.



In another work, performed in a collaboration at ESRF we studied time-dependent rocking curves of laser-irradiated asymmetrically cut single InSb crystals. Coherent acoustic phonons were excited in the crystals, and the induced time-dependent strain profiles corresponding to the coherent phonons were monitored. Recording of the diffracted radiation with a fast low-jitter X-ray streak camera resulted in an overall temporal resolution of better than 2 ps.

Future plans

We propose to continue to develop the new field of ultrafast x-ray coherent control. The research plan has three main goals:

1. First we want to improve the quality of ultrafast x-ray modulators. This means developing methods to increase the speed, contrast, and efficiency, and also finding new methods that make these novel devices more accessible to other researchers at the APS and elsewhere.
2. Second, we want to develop the science of laser excitation and x-ray coherent scattering in solids that makes these switches possible in the first place. We are particularly interested in two research topics begun in the previous grant cycle: the partitioning of laser-deposited energy in semiconductors; and the rapid transport of energy into the crystal following initial surface excitation, by electron-hole plasma diffusion or other means. Our x-ray streak camera will aid this effort by increasing our x-ray temporal resolution by two orders of magnitude with existing technology. Future insertion devices or other sub-picosecond x-ray sources will also give us new opportunities as they come on line.

3. Third, we want to discover and develop new applications of ultrafast x-rays in atomic, molecular, chemical, or materials science. This will help to foster increased interest and activity in this new field, in advance of new x-ray sources developed in the coming years. This year we began collaborative experiments to study the structure of water, and phase transitions in nanocrystal bundles. These activities will expand in the future.

In the coming year, we plan to start a new series of experiments on folded acoustic phonons excited in multilayer epitaxial crystals. These excitations are capable of oscillation frequencies in excess of 1 THz, and wave vectors comparable to optical phonons, so they are interesting materials for potential new switches.

A major new activity of the coming year is our plan to participate in the first series of experiments at the SPPS under construction at SLAC. We are particularly interested in two areas of research that will mesh well with the capabilities of this 100 fsec high brightness low rep rate source: We would like to study optical phonons excited in Bi films, to see the structural changes that we have already observed indirectly in optical reflection experiments. We would also like to build diagnostics to probe the structure of the novel compressed electron beam as it exits the undulator. Our idea is to probe the strong THz radiation emitted by the relativistic electron bunch, using electro-optic sampling techniques. Both of these experiments will involve a synchronized CPA laser on the beam line, and we will be working to help install this facility in the next 6-12 months.

Publications, 2000-2002:

- [1] M. F. DeCamp, D. A. Reis, P. H. Bucksbaum, B. Adams, J. M. Caraher, R. Clarke, C. W.S. Conover, E. M. Dufresne, R. Merlin, V. Stoica, and J. Wahlstrand, "Coherent Control of Pulsed X-ray Beams," **413**, 825-828(2001).
- [2] M. F. DeCamp, D. A. Reis, P. H. Bucksbaum, and R. Merlin. Dynamics and coherent control of high amplitude optical phonons in bismuth. *Phys. Rev. B* **64**, 092301 (2001).
- [3] D. A. Reis, M. F. DeCamp, P. H. Bucksbaum, R. Clarke, E. Dufresne, M. Hertlein, R. Merlin, R. Falcone, H. Kapteyn, M. M: Murnane, J. Larsson, Th. Missalla, and J. S. Wark. Probing impulsive strain propagation with x-ray pulses. *Phys. Rev. Lett.*, **86**(14):3072-3075, 2001.
- [4] J. S. Wark, et al. Femtosecond x-ray diffraction: experiments and limits. In D. M. Mills, H. SchulteSchrepping, and J. R. Arthur, editors, *X-ray FEL Optics and Instrumentation*, SPIE International Symposium on Optical Science and Technology, San Diego, CA, 2000, **4143**, 26-37. Proceedings of the SPIE, 2001.
- [5] J. Larsson, A. Allen, P.H. Bucksbaum, R.W. Falcone, A. Lindenberg, G. Naylor, T. Missala, D.A Reis, K Scheidt, A. Sjögren, P. Sondhauss, M. Wulff, and J.S. Wark, "Picosecond X-ray diffraction studies of laser-excited acoustic phonons in InSb," *Appl. Phys. A* **75**, 467-478 (2002).
- [6] B. A. Adams, M. F. DeCamp, E. M. Dufresne, and D. A. Reis. Picosecond laser pump, x-ray probe spectroscopy of GaAs. *Submitted to J. Synch. Rad.*, 2002.
- [7] D.A. Reis, M. DeCamp, P.H. Bucksbaum, R. Clarke, R. Merlin, E.M. Dufresne, B. "Time-resolved studies of acoustic phonons" *In preperation*, 2002.
- [8] M. F. DeCamp, D.A. Reis, P.H. Bucksbaum, J. Wark, et al. Time-resolved diffraction measurements of ambipolar diffusion. *In preperation*, 2002.
- [9] M. F. DeCamp et al. Acoustic phonon dispersion measured with time-resolved x-ray diffraction. *QELS Technical Digest, Long Beach, CA*, 2002.
- [10] D. A. Reis, M. F. DeCamp, et al. Time-resolved x-ray Pendellösung oscillations in impulsively strained crystals,(invited). *QELS Technical Digest, Long Beach, CA*, 2002.
- [11] M. F. DeCamp et al. Time-resolved anomalous transmission of x-rays in laser heated germanium. *QELS Technical Digest, Baltimore, MD*, 2001.
- [12] D. A. Reis, M. F. DeCamp, et al. Time-resolved Pendellösung oscillations. *DAMOP technical digest, London, Ontario, Canada*, 2001.
- [13] M.F. DeCamp, "Seeing sound: dynamical effects in ultrafast x-ray diffraction," Ph.D. Thesis, University of Michigan, 2002 (unpublished).
- [14] D.A. Reis, et al. Picosecond Dynamics Probed by X-ray Diffraction, *APS Forfront*, **1**, 134 (2001).

Low-energy ion-surface and ion-molecule collisions

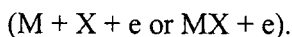
R. L. Champion
Department of Physics
College of William and Mary
Williamsburg, VA 23187-8795
champion@physics.wm.edu

Program Scope The principal thrust of the present experimental research program is upon low-energy, ion- surface and ion- molecule collisions. In the case of the ion- surface collisions, it has been observed that the secondary electron emission depends markedly upon the surface condition. The goal of the present studies has been to examine and understand the effects of adsorbates upon the secondary emission properties of both metallic and semiconductor substrates. Secondary emission is induced by positive and negative ion impact, the adsorbates studied thus far are oxygen and chlorine, and the substrates have included both crystalline and amorphous samples of Al, Mo, W, Si, Cu and Mg. In the case of Mg(0001), the sample has been studied for oxygen exposures ranging from none up to the point where the resulting MgO crystal is effectively an insulator. The adsorbate coverage is indirectly determined and ranges from none up to a few monolayers. In the ion- molecule experiments we have measured absolute cross sections for various reactive collisions involving the reactants CF_3^+ and CHF_3 . The idea here is to use these measured cross sections to model and understand the salient features of the popular etching discharge which utilizes CHF_3 . In both the ion- surface and ion- molecule collision studies, "low energy" implies collision energies ranging from a few up to 500 eV. Other experiments underway involve determining the effect of adsorbates on the field-emission of electrons from Mo substrates. Brief examples of these experimental projects will be presented in what follows.

Recent Progress

Surface studies - Negative ion projectiles. We have completed a series of experiments which have incorporated a new ion source to study anion-induced secondary emission from metallic substrates and the effects of adsorbates upon those processes. One of the principal motivations for studying *negative-ion* - induced emission was to completely eliminate the role of potential energy (such as the recombination energy associated with the neutralization of an impacting positive ion) as a precursor for the secondary emission processes. An example of the results of these experiments is shown in Fig. 1 in which the probability of secondary electron emission is shown for O^- impacting a Cu(110) surface with various amounts of adsorbed oxygen. These observations are very similar to those observed for impacting alkali cations and support the notion that the underlying mechanism for adsorbate-altered secondary electron emission has essentially nothing to do with the recombination energy of the impacting particle. We have also measured the kinetic energy distributions of the secondary electrons (and secondary anions) and the results are consistent with our model developed for ion-induced, adsorbate-altered secondary emission. The proposed mechanism involves electronic excitation of a metal(M)-adsorbate(X) complex, e.g. MX^- , to a higher, repulsive potential, $(\text{MX}^-)^*$. This excitation

can result in anion desorption into the vacuum, ($M + X^-$), or decay of the system to yield a free electron:



Surface studies - MgO. By exposing a pristine Mg crystal to oxygen it is possible to alter the substrate from metallic to approximately insulator conditions in a controlled manner. Exposing Mg(0001) to about 8 Langmuir ($1 \text{ L} = 10^{-6} \text{ torr-sec}$) of oxygen results in roughly one monolayer of oxygen adsorbed on the Mg surface. Subsequent exposure of the Mg to oxygen can result in an oxide build-up approximating that of a vapor-deposition grown Mg-oxide crystal. The latter is an insulator and, as such, has considerably different electronic

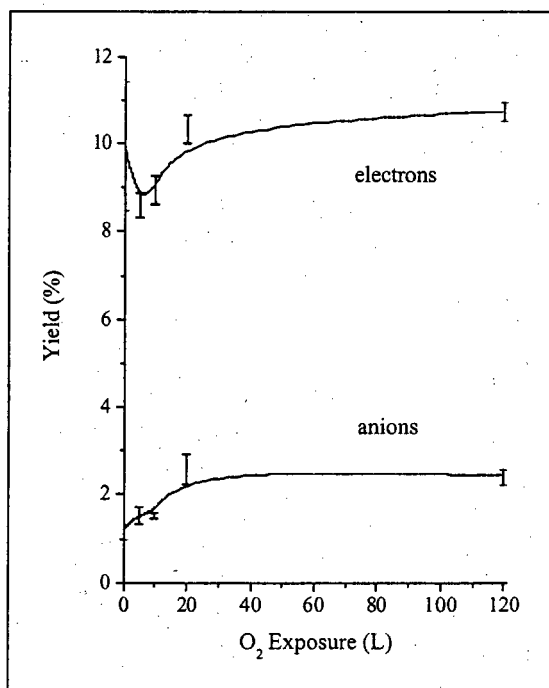


Figure 2 The secondary yields of electrons and O^- which result from Ar^+ (270 eV) impacting Mg(0001) as a function of oxygen exposure are shown.

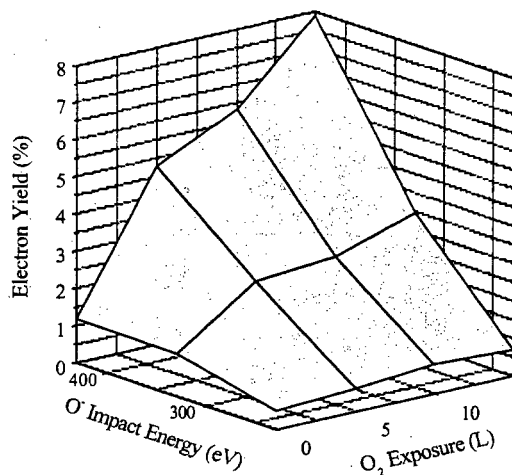


Figure 1 The probability of secondary electron emission for $O^+ + Cu(110)$ is shown as a function of the O^+ impact energy and adsorbed oxygen on the metallic substrate. (One monolayer of oxygen corresponds to an O_2 exposure of about 10 L.)

properties near the surface. Our goal in these experiments is to monitor the secondary emission properties as the oxide “grows” to ascertain if there are subsequent changes in the emission characteristics as the metallic/insulator transition occurs. The results for 270 eV Ar^+ impacting Mg are shown in Fig 2. Aside from initial changes in the emission - undoubtedly related to the severe change in the surface work function upon initial oxidation - there is relatively little alteration in the electron emission as the oxidation progresses. Once again, this observation is compatible with the notion that the underlying mechanism for emission is similar to that described in the previous paragraph.

Reactive collisions relevant to a CHF₃ discharge

Trifluoromethane (CHF₃) is used in semiconductor plasma processing chambers to achieve high etch selectivity of an oxide layer over a silicon substrate. Such surface etching is governed by the ion and molecule fluxes near the surface, the concentrations of which are dependent upon species interactions in and their transport through the plasma. In order to assist in the interpretation of ion flux measurements and to provide fundamental data required for plasma modeling, we measured total cross sections for significant ion-molecule reactions occurring in CHF₃ discharges. The reactions studied included collision induced dissociation for CF₃⁺ on CHF₃, dissociative charge transfer for CF₃⁺ and F⁺ on CHF₃, and electron detachment from F⁻ on CHF₃. Collision energies range from a few to a few hundred electron volts. A myriad of ions and neutrals are formed from the reactants studied here; the results for collisions of F⁺ with CHF₃ are shown in Fig. 3. A few general conclusions may be drawn from the experimental observations. Large cross sections for electron detachment, ~14 Å², dissociative charge transfer for ionized fluorine, ~25 Å², and collision induced dissociation, ~6 Å², indicate that neutral fluorine, one of the most important radicals in semiconductor etching, is a dominant species in CHF₃ discharge environments. The cross section for the production of the CF₃ radical is substantial as well, viz. ~26 Å², for higher collision energies.

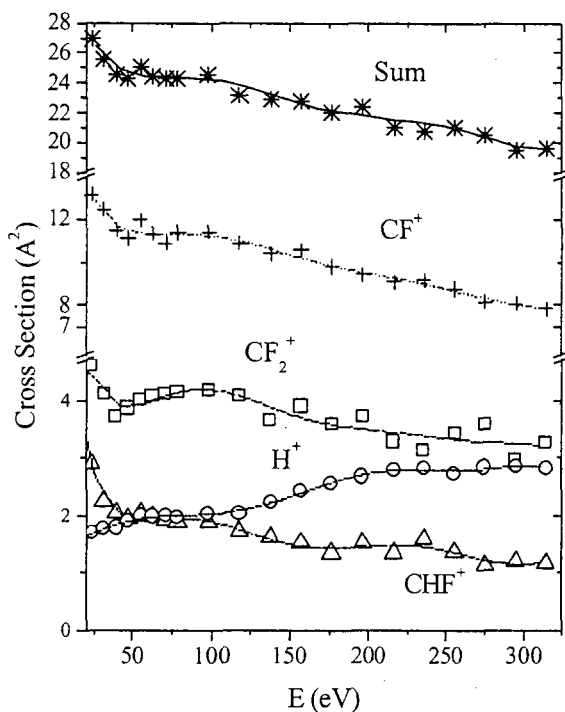


Figure 3 Dissociative charge transfer cross sections for collisions of F⁺ with CHF₃ are presented for four product channels as a function of relative collision energy.

Field Emission - Mo field emitter arrays - The effect of adsorbates on field emission can be anticipated to be substantial as the barrier through which near-surface electrons must tunnel to reach the vacuum is altered considerably by the presence of an adsorbate. The effects of various gas adsorbates on the emission characteristics of Spindt-type molybdenum field emission cathode arrays have been examined. Sputter cleaning with an argon-ion (Ar⁺) beam was used in an attempt to remove adsorbed molecules from the surface of the field emitter (i.e., the molybdenum tips). It was anticipated that surface alteration by way of adsorbate removal would alter the emission characteristics, possibly reducing field emission. The re-introduction of an adsorbate to a sputter-cleaned surface was precisely controlled with the gas-handling system. It was our goal to correlate the field emission with the amount of adsorbate on the surface and compare the results with that predicted for field emission from an adsorbate-free surface as described in the seminal work of Fowler and Nordheim. The sputter-cleaning scheme consisted of

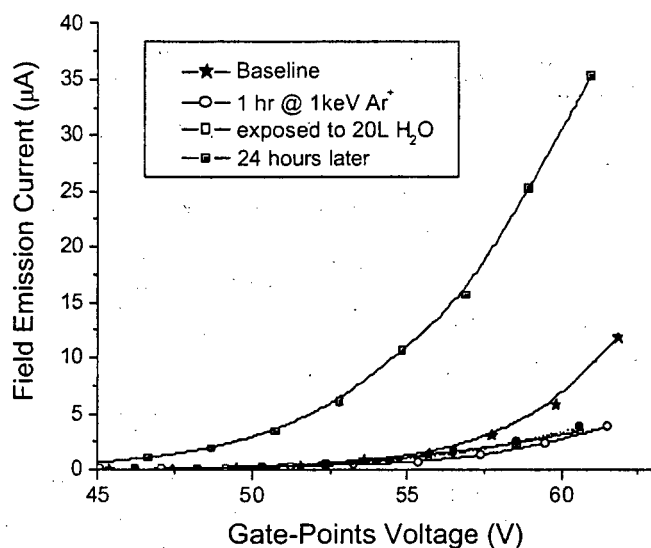


Figure 4 Field emission current is plotted as a function of voltage, which is directly related to the magnitude of the extraction field. The four scenarios are defined in the inset box

presence of surface adsorbates.

Future directions During the coming contract period we will focus principally upon ion-induced secondary emission processes on surfaces. We will continue to examine the effect of adsorbates on these processes and will employ a host of impacting ions to probe the surface. We will investigate the role of adsorbates on field emission by a variety of means. One of the main difficulties with these field emission studies is ascertaining surface cleanliness. Toward that end we will subject the Mo field-emitter array to both electron and photon impact in an effort to create a relatively adsorbate-free surface through photon- and electron-stimulated desorption.

Recent Publications

The role of O and Cl adsorbates on the secondary emission properties of tungsten.

W. S. Vogan, S. G. Walton and R. L. Champion
Surface Science **459**, 14 (2000).

Collisional decomposition of the sulfur hexafluoride anion (SF₆⁻)

R. L. Champion, I.V. Dyakov, B.L. Peko, and Y. Wang
Journal of Chemical Physics **115**, 1765 (2001).

Oxygen adsorption on a Si(100) substrate: Effects on secondary emission properties

W.S. Vogan and R.L. Champion
Surface Science **492**, 83 (2001).

Measured cross sections and ion energies for a CHF₃ discharge

B. L. Peko, R. L. Champion, M. V. V. S. Rao and J. K. Olthoff
Journal of Applied Physics **92**, xxxx (2002).

directing a 1 keV, 1 nanoampere Ar⁺ ion beam to the tips for one hour. Such cleaning invariably reduced field emission as illustrated in Fig. 4. Adsorbates were then reintroduced to the surface in an attempt to "restore" the emission. Of the adsorbates studied (O₂, CO₂, CH₄, and H₂O) none appeared to clearly and consistently return the emission level of the field emitter array to the pre-cleaning levels. Instead, the only way to return field emission to baseline levels was to let the emitter relax for a period of about twenty-four hours. A slow thermal diffusion process may account for the steady increase in field emission after cleaning. Clearly, much remains to be done to fully understand the dynamics of field emission in the

August 2002

Theoretical Investigations of Atomic Collision Physics

A. Dalgarno

Harvard-Smithsonian Center for Astrophysics
Cambridge, MA 02138
adalgarno@cfa.harvard.edu

Our research effort develops and applies theoretical methods for the quantitative predictions of atomic, molecular and optical phenomena. The program is responsive to experimental advances and influences them. A particular emphasis has been the study of collisions in ultracold atomic and molecular gases.

A considerable effort has been given to calculations of long range interactions. We have provided many estimates of van der Waals coefficients for simple systems. We are now attempting to apply density functional theory which suitably generalized may provide a procedure for reliable predictions for complex atoms.

We are also exploring the long range interactions between atoms and molecules. Estimates are available for spherical symmetric atoms with homonuclear molecules and we have obtained improved values of the isotropic and angle-dependent coefficients for the alkali metal atoms interacting with molecular hydrogen. The methods are being extended to the interactions between excited atoms and molecules for which the necessary formalism has not been written down.

The van der Waals coefficients are critical to reliable predictions of collisions at ultralow temperatures. We extended our calculations of the quenching of rotation and vibration of CO in collisions with ^3He and ^4He atoms and demonstrated that significant isotope effects occur. We carried out a comprehensive investigation of the quenching of the $v = 2$ vibrational level of CO and demonstrated that the $v = 2 \rightarrow 0$ transition is minor compared to the single quantum $v = 2 \rightarrow 1$ transition, a result that is likely to be typical of atom-molecule collisions at low temperatures.

In earlier calculations we had found that the chemical reaction $\text{F} + \text{H}_2 \rightarrow \text{FH} + \text{H}$ proceeds quite rapidly even at zero temperature. We suggested that the reaction proceeds by tunneling, enhanced by the long duration of collisions at very low velocities. There was some indication that a virtual state plays a role. We are attempting to find a more explicit description of the mechanism. We carried out calculations for the reaction $\text{F} + \text{D}_2 \rightarrow \text{FD} + \text{D}$. We found no evidence of a virtual state and a much reduced rate coefficient, due presumably to the greater mass and smaller tunneling probability of the heavier deuterium atom. This picture is supported by further calculations, still in progress, on the reaction of F with HD.

We have also considered low temperature ion-atom and ion-molecule collisions which are dominated by the influence of long range polarization force.

Calculations are in progress on rotational, vibrational and fine-structure transitions in collisions of helium with molecules of calcium hydride to compare with laboratory measurements

carried out at a temperature of 400 mK. Vibrational quenching is four to five orders of magnitude less efficient than rotational quenching. Our preliminary results differ from experiment. We are exploring the sensitivity to the interaction potential.

We had found earlier that in the collisions of a pair of metastable hydrogen atoms, double excitation transfer and not Penning ionization, is the main quenching process at low temperatures. We have now included the effects of the Lamb shift and fine-structure splitting with the same conclusion. Our quenching rate coefficients differs by a factor of two to three from a preliminary experimental value. We are continuing the calculations.

We have been involved in studies of the collisions of hydrogen and antihydrogen and we are now examining excitation transfer when either the hydrogen or the antihydrogen is in a Rydberg state.

The same kind of formalism and methods developed for atom-molecule collisions can be applied to collisions of atoms in states of non-zero angular momentum and we are examining the quenching of fine-structure levels in carbon and oxygen atoms. We have shown that the rate coefficient for the quenching of carbon 3P_1 atoms vanishes in the limit of zero temperature so that the atoms are candidates for trapping in magnetic fields.

Publications 2000-2002

- M. J. Jamieson, A. Dalgarno and L. Wolniewicz, Calculation of Properties of Two-Center Systems, *Phys. Rev. A.* 61, 042705, 2000.
- R. Côté, M. J. Jamieson, Z-C. Yan, N. Geum, G-H. Jeung and A. Dalgarno, Enhanced Cooling of Hydrogen Atoms by Lithium Atoms, *Phys. Rev. Lett.* 84, 2806, 2000.
- P. Froelich, S. Jonsel, A. Saenz, B. Zygelman and A. Dalgarno, Hydrogen-Antihydrogen Collisions, *Phys. Rev. Lett.* 84, 4577, 2000.
- R. Coté and A. Dalgarno, Ultracold atom-ion collisions, *Phys. Rev. A.* 62, 012709, 2000.
- N. Balakrishnan, A. Dalgarno and R. C. Forrey, Vibrational Relaxation of CO by Collisions with ^4He at Ultracold Temperatures, *J. Chem. Phys.* 113, 621, 2000.
- S. B. Bayram, M. Havey, M. Rosu, A. Sieradzan, A. Derevianko and W.R. Johnson, $5p\ ^2P_j \rightarrow 5d\ ^2D_{3/2}$ Transition Matrix Elements in Atomic ^{87}Rb , *Phys. Rev. A.* 61, R050502-1, 2000.
- A. Derevianko, Reconciliation of the Measurement of Parity Nonconservation in Cs with the Standard Model, *Phys. Rev. Lett.* 85, 1618, 2000.
- A. Derevianko and A. Dalgarno, Long-range Interaction of Two Metastable Rare-gas Atoms, *Phys. Rev. A.* 62, 062501-1, 2000.
- C.M. Dutta, P. Nordlander, M. Kimura and A. Dalgarno, Charge-transfer Cross Sections in Collisions of Ground-state Na Atoms with H^+ at Low-eV Collision Energies, *Phys. Rev. A.* 65, 0022709, 2001.
- N. Balakrishnan and A. Dalgarno, On the Quenching of Rovibrationally Excited Molecular Oxygen at Ultracold Temperatures, *J. Phys. Chem. A.* 105, 2348, 2001.

Femtosecond photon echo techniques for manipulation of quantum states and computation

Progress Report Grant No. DE-FG02-01ER15143 Coherent Control with Four-Wave Mixing

Marcos Dantus

Department of Chemistry and Department of Physics, Michigan State University, East Lansing MI 48824
dantus@msu.edu

1. Program Scope

Our DOE supported project is aimed at exploring the coherent manipulation of multiple quantum mechanical states. This work has proceeded in two different directions. We have carried out a number of gas phase three-pulse four wave mixing (FWM) measurements to improve our ability to load information using shaped laser pulses and to read the information stored in the quantum mechanical wave packets coherently [1]. The second line of experiments deals with the coherent control in condensed phases. We have made a breakthrough in the understanding of the underlying requirements for coherent control of nonlinear optical processes in condensed phases and have shown control of two- and three-photon excitation in large molecules including proteins [2,3].

2. Coherent control with Four-Wave Mixing

Earlier this year we published our first results on the manipulation of quantum states in iodine vapors with an ultimate goal of demonstrating molecule-based computation. In those experiments we used three beams that were crossed in the Forward-Box geometry. Beam A was used to launch a wave packet in the excited electronic state, beam B is a shaped 800 nm pulse that controls the stimulated Raman transition to high vibrational levels of the ground state ($v \sim 22-24$). The beam C brings the wave packet back to the excited state where it emits the FWM signal, which is spectrally dispersed, and time integrated.

Fig. 1

Experimental Data Obtained with the Virtual Echo Setup

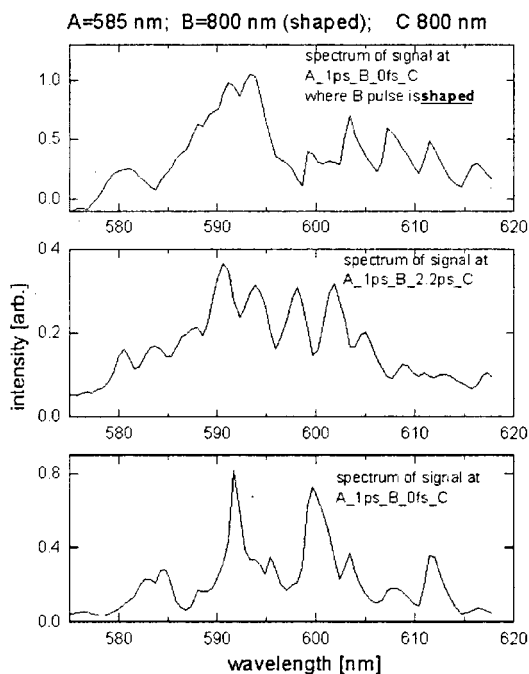
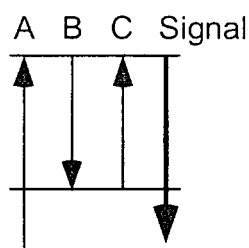


Fig. 1. Fig. 3. Experimental data for a VE setup. The *pump* (A) was centered at 585 nm, the *Stokes* beam (B) was shaped and centered at 800 nm, the *probe* beam (C) was centered at 800 nm, and the signal was centered near 590 nm. The signal beam was frequency dispersed. Three different spectra resulting from different conditions are shown. The variables for each spectrum are indicated in the upper right corner. Clearly the time between the pulses and shaping of the Stokes beams changes the outcome in the observed signal.

We have made a number of measurements regarding the electronic decoherence rate in iodine vapor. These measurements are required to determine the ratio between the time it takes for coherence to be lost through random collisions and the time it takes to coherently manipulate information (write, compute, read). Our measurements have

- V. Kharchenko and A. Dalgarno, Refractive Index for Matter Waves in Ultracold Gases, *Phys. Rev. A.* **63**, 023615, 2001.
- A. Derevianko, J.F. Babb and A. Dalgarno, High-precision Calculations of van der Waals Coefficients for Heteronuclear Alkali-metal Dimers, *Phys. Rev. A.* **63**, 052704, 2001.
- B. Zygelman, A. Saenz, P. Froelich, S. Jonsell and A. Dalgarno, Radiative Association of Atomic Hydrogen with Antihydrogen at Subkelvin Temperatures, *Phys. Rev. A.* **63**, 052722, 2001.
- A. Derevianko, R. Côté, A. Dalgarno and G.-H. Jeung, Enhanced Cooling of Hydrogen by a Buffer Gas of Alkali-Metal Atoms, *Phys. Rev. A* **64**, 011404(R), 2001.
- N. Balakrishnan and A. Dalgarno, Chemistry at Ultracold Temperatures, *Chem. Phys. Lett.* **341**, 652, 2001.
- R.C. Forrey, N. Balakrishnan, A. Dalgarno, M.R. Haggerty and E.J. Heller, Effect of Quasi-Resonant Dynamics on the Predissociation of van der Waals Molecules, *Phys. Rev. A.* **64**, 022706-1, 2001.
- C. Zhu, N. Balakrishnan and A. Dalgarno, Vibrational Relaxation of CO in Ultracold ^3He Collisions, *J. Chem. Phys.* **115**, 1335, 2001.
- N. Geum, G.-H. Jeung, A. Derevianko, R. Cote and A. Dalgarno, Interaction Potentials of LiH, NaH, KH, RbH and CsH, *J. Chem. Phys.* **115**, 13, 2001.
- A. Dalgarno, P. Froelich, S. Jonsell, A. Saenz and B. Zygelman, Collisions of H and $\bar{\text{H}}$, in *New Directions in Antimatter Chemistry and Physics*, Eds. C.M. Surko and F. A. Gianturco (Kluwer, The Netherlands) 2001.
- M. Bouledroua, A. Dalgarno and R. Côté, Diffusion and Excitation Transfer of Excited Alkali Metal Atoms *Phys. Rev. A.* **65**, 012701, 2001.
- S. Jonsell, A. Saenz, P. Froelich, B. Zygelman and A. Dalgarno, Stability of Hydrogen-antihydrogen Mixtures at Low Energies, *Phys. Rev. A.* **64**, 052712, 2001.
- S. Jonsell, A. Saenz, P. Forelich, R.C. Forrey, R. C. Forrey, R. Côté and A. Dalgarno, Long-range Interactions between Two $2S$ Excited Hydrogen Atoms, *Phys. Rev. A.* **65**, 042501, 2002.
- A. Belyaev, A. Dalgarno and R. McCarroll, The Dependence of Nonadiabatic Couplings on the Origin of Electron Coordinates, *J. Chem. Phys.* **116**, 5395, 2002.
- E. Bodo, F. A. Gianturco and A. Dalgarno, Quenching of Vibrationally Excited $\text{CO}(v=2)$ Molecules by Ultra-cold Collisions with ^4He Atoms, *Chem Phys. Lett.* **353**, 127, 2002.
- C. Zhu, A. Dalgarno and A. Derevianko, van der Waals Interactions between Molecular Hydrogen and Alkali-metal Atoms, *Phys. Rev. A.* **65**, 034708, 2002.
- E. Bodo, F. A. Gianturco and A. Dalgarno, The reaction of $\text{F} + \text{D}_2$ at Ultra-Cold Temperatures: The Effect of Rotational Excitation, *J. Phys. B* **35**, 2391, 2002.
- R. Krems and A. Dalgarno, Electronic and Rotational Energy Transfer in $\text{F}(^2P_{1/2}) + \text{H}_2$ Collisions at Ultracold Temperatures *J. Chem. Phys.* **117**, 118, 2002.
- X. Chu and A. Dalgarno, Molecular Transition Moments at Large Internuclear Distances, *Phys. Rev. A* in press.
- E. Bodo, F. A. Gianturco and A. Dalgarno, $\text{F} + \text{D}_2$ Reaction at Ultra-Cold Temperatures, *J. Chem. Phys.* in press.

led to measurements of the fundamental decoherence cross section in the presence of different buffer gasses. The electronic dephasing cross sections are extremely large even compared to Van der Waals radii. Systematic measurements of the rate of decoherence were made as a function of buffer gas. From a number of such measurements, we calculated experimental cross sections for the long-range interactions. These values range from 144 \AA^2 for Helium to 1370 \AA^2 for I_2 . We find that the cross sections can be modeled by dispersion interactions and show no dependence on the number of degrees of freedom in the buffer gas molecules. We reviewed the theory of electronic coherence dephasing and obtained an expression that can be reduced to the gas phase and the liquid phase limits [4]. Despite the large values for electronic dephasing cross section, we find that even at room temperature we can obtain a coherence ratio in excess of 10^4 , and using a molecular beam in excess of 10^7 .

We are preparing a new series of experiments that will use two NOPA systems to provide three different color lasers. This will allow us to detect background free signal. Independent control on each of the pulses will also allow us to implement simple algorithms to demonstrate coherent manipulation of individual vibronic states.

3. Coherent control in condensed phases

Multi-photon transitions are optimized when the central bandwidth of the laser pulse, ω_0 , is some fraction (half for two-photon, a third for three-photon etc.) of the total energy of the transition. The effect of pulse shaping on the probability amplitude for two-photon absorption (2PA) can be calculated as follows assuming sharp transitions [5],

$$A_2(\Delta) \propto \int_{-\infty}^{\infty} E(\Omega)E(\Delta - \Omega) \exp[i\{\phi(\Omega) + \phi(\Delta - \Omega)\}] d\Omega \quad (1)$$

For three-photon absorption (3PA) a similar formula can be derived [6],

$$A_3(\Delta) \propto \int_{-\infty}^{\infty} \int_{-\infty}^{\infty} E(\Omega_1)E(\Omega_2)E(\Delta - \Omega_1 - \Omega_2) \exp[i\{\phi(\Omega_1) + \phi(\Omega_2) + \phi(\Delta - \Omega_1 - \Omega_2)\}] d\Omega_1 d\Omega_2 \quad (2)$$

where amplitudes and phases are introduced for two different detuning values Ω_1 and Ω_2 , and $\Delta = \omega - n\omega_0$. The signal resulting from an n-photon absorption process is calculated using the equation

$$S_n \propto \int_{-\infty}^{\infty} g(\Delta) |A_n(\Delta)|^2 d\Delta, \quad (3)$$

which convolves the spectral amplitude of the laser pulse with the absorption spectrum of the molecule $g(\Delta)$. A rational approach to introduce intrapulse interference in multiphoton transitions of large molecules requires phase functions that are comparable to the homogeneously broadened absorption spectrum and the spectral width of the pulse. Conversely, in the time domain, the shaped pulse should be comparable to the relaxation dynamics of the material. We have been using a formula for defining the phase function that has a limited number of parameters,

$$\varphi(\Omega) = \alpha \cos(\gamma\Omega - \delta) + \frac{1}{2} \beta \Omega^2, \quad (4)$$

where α is the phase amplitude, β is the quadratic chirp, γ is the modulation in the frequency domain $2\pi N/(\Omega_{\max} - \Omega_{\min})$ with period N , and δ is the position of the phase mask with respect to the center of the pulse spectrum.

The results in Figure 2 show the changes in two- and three-photon induced fluorescence as a function of scanning the chirp parameter β and the mask position δ . The data were obtained using a femtosecond laser system producing 810 nm, ~ 50 fs pulses, were shaped using a spatial light modulator at the Fourier plane of a zero-dispersion stretcher. The shaper was calibrated so that only phase delays are introduced without changes to the output spectrum, intensity, or polarization. The pulses 0.5-1 μJ were focused onto quartz cells with a 200 mm focal length lens.

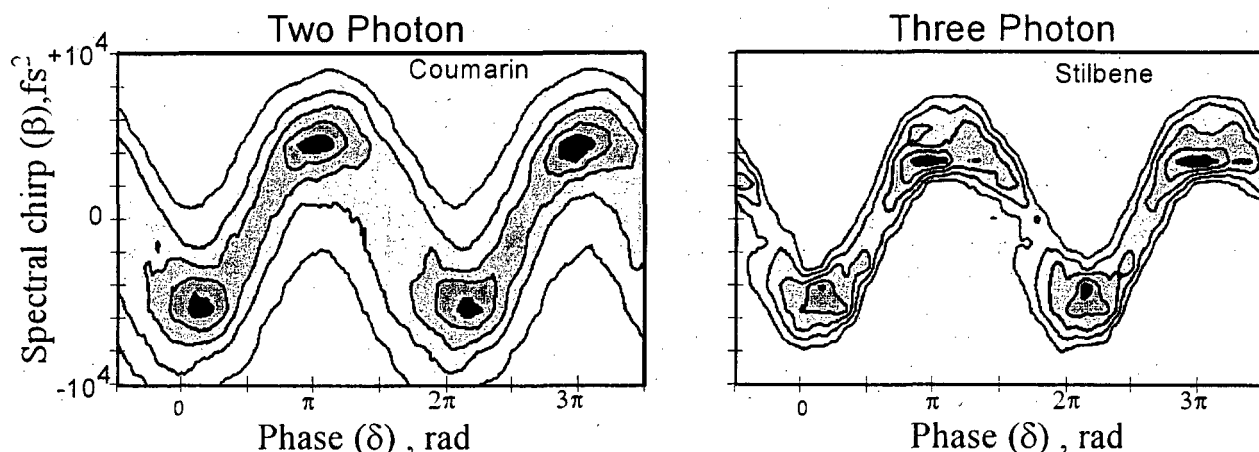


Fig. 2. Experimental measurement of the two- and three-photon induced fluorescence as a function of spectral chirp and phase mask position.

The data in Fig. 2 indicates that this concept of phase modulation originally proposed for controlling atomic transitions, is useful for controlling large molecules in condensed phases. Although the dependence of two- and three-photon induced fluorescence on the phase mask parameters is similar, there are some differences. The differences allow one to design a phase mask that can enhance one process while the other is suppressed. We have demonstrated control of multiphoton processes including continuum generation using this rational approach towards pulse shaping. We have tested this method on large organic molecules including green fluorescent protein, and concanavalin A protein.

4. Conclusions and Future Work

A. Coherent control in the gas phase:

From an experimental point of view the proposed scheme has close analogies with NMR based quantum computation [7]. As pointed out by Warren, the NMR quantum computer has two problems [8]. The first is low clock frequency, approximately 10-100 Hz. In our case, using optical frequencies, the clock rates are on the order of 10^{11} - 10^{12} Hz. The second is that NMR operates in the high temperature limit. The NMR ratio between the photon energy and temperature is $h\nu/k_B T < 10^{-6}$ for a 10 spin system. Echo sequences, analogous to the multiple pulse NMR, operate in the low temperature limit $h\nu/k_B T > 10^3$. This difference makes the optical experiments much less susceptible to quantum noise.

From a mathematical point of view, the proposed VE and SPE processes can perform the following functions: write, store in memory, read, sum, scalar product, direct products, matrix product between matrices and vectors, and can be used to construct circuits and networks. The large Hilbert space and the freedom to construct complex quantum gates give us the possibility to operate with massive coherent quantum information even within a single three-pulse sequence.

We are very encouraged by our first data for a number of reasons. Most importantly, the signal level is relatively strong and can be separated easily from background scattered light. We are looking forward to the purchase of two additional pulse shapers and the adaptation of our supersonic jet machine to finalize the full implementation. We hope to secure the funds for the additional equipment in the near future.

B. Coherent control in condensed phases:

The ability of controlling nonlinear optical processes in condensed phases opens up a number of applications in a variety of fields such as medicine and communications technology. We plan to further pursue the theory of multiphoton intrapulse interference for controlling nonlinear optics. We plan to demonstrate a number of applications, in the near future. We expect some applications will eventually be funded by other agencies.

Publications Resulting from this Grant:

I. Grimberg, V. V. Lozovoy, M. Dantus and S. Mukamel, "Femtosecond three pulse spectroscopies in the gas phase: density matrix representation," *J. Phys. Chem. A*, Feature 106, 5, 697 (2002). Our results featured in the cover.

V. V. Lozovoy and M. Dantus, "Four-Wave Mixing and Coherent Control," in *Laser Control and Manipulation of Molecules*, A.D. Bandrauk, Y. Fujimura, R.J. Gordon Editors, ACS Publishing, Washington, p. 61 (2002).

I. Pastirk, M. Comstock, and M. Dantus, "Femtosecond ground state dynamics of N_2O_4 and NO_2 investigated by degenerate four-wave mixing," *Chem. Phys. Letters*, 349, 71 (2001).

V. V. Lozovoy and M. Dantus, "Photon echo pulse sequences with femtosecond shaped laser pulses as a vehicle for molecule-based quantum computation," *Chem. Phys. Letters*, 351, 213 (2002).

K. A. Walowicz, I. Pastirk, V. V. Lozovoy, and M. Dantus, "Multiphoton intrapulse interference I; Control of nonlinear optical processes in condensed phase," *J. Phys. Chem. A*, to appear in September (2002). Our results will probably be featured in the cover.

M. Comstock, E. Sudachenko, V. V. Lozovoy and M. Dantus' "Femtosecond photon echo measurements of electronic coherence relaxation between the $X(^1\Sigma_g^+)$ and $B(^3\Pi_{0u^+})$ states of I_2 in the presence of He, Ar, N_2 , O_2 , C_3H_8 ," *J. Chem. Phys.* Submitted (2002)

V. V. Lozovoy, I. Pastirk, K. A. Walowicz, and M. Dantus, "Multiphoton intrapulse interference II; Control of nonlinear optical processes in condensed phase," *J. Chem. Phys.* Submitted (2002)

M. Comstock, V. V. Lozovoy, and M. Dantus, Rotational Wavepacket Revivals for Phase Modulation of Ultrafast Pulses, Submitted to *Chem. Phys. Letters* (2002).

References:

1 V. V. Lozovoy and M. Dantus, "Photon echo pulse sequences with femtosecond shaped laser pulses as a vehicle for molecule-based quantum computation," *Chem. Phys. Letters*, 351, 213 (2002).

2 K. A. Walowicz, I. Pastirk, V. V. Lozovoy, and M. Dantus, "Multiphoton intrapulse interference I; Control of nonlinear optical processes in condensed phase," *J. Phys. Chem. A*, to appear in September (2002). Our results will probably be featured in the cover.

3 V. V. Lozovoy, I. Pastirk, K. A. Walowicz, and M. Dantus, "Multiphoton intrapulse interference II; Control of nonlinear optical processes in condensed phase," *J. Chem. Phys.* Submitted (2002).

4 M. Comstock, E. Sudachenko, V. V. Lozovoy and M. Dantus' "Femtosecond photon echo measurements of electronic coherence relaxation between the $X(^1\Sigma_g^+)$ and $B(^3\Pi_{0u^+})$ states of I_2 in the presence of He, Ar, N_2 , O_2 , C_3H_8 ," *J. Chem. Phys.* Submitted (2002).

5 D. Meshulach, Y. Silberberg, *Nature* Vol. 396, 239, 2001.

6 K. A. Walowicz, I. Pastirk, V. V. Lozovoy, and M. Dantus, *J. Phys. Chem.* submitted 2002.

7 C.H. Bennet, D.P. DiVincenzo, "Quantum information and computation," *Nature* **404**, 247-255 (2000).

8 W.S. Warren, "The usefulness of NMR quantum computing," *Science* **277**, 1688-1689 (1997).

Chemistry with Ultracold Molecules

Bretislav Friedrich and Dudley R. Herschbach
Department of Chemistry and Chemical Biology
Harvard University
Cambridge, MA 02138

This project aims to develop simpler and more versatile means of generating slow and cold molecules in order to pursue collision dynamics with "nanomatter waves" having deBroglie wavelengths of the order of 1-100 nm. Our current work carried out in collaboration with Professor Doo Soo Chung (on sabbatical from Seoul University, Korea), Bum Suk Zhao (visiting graduate student from Korea), and Sunil Sheth (an undergraduate at Harvard) deals chiefly with 2 aspects described briefly below:

(1) **Counter-rotating surface.** The capability of rotating a surface at molecular velocity provides a means to markedly lower the velocity distribution of molecules described from a surface moving contrary to the ejected molecules. As a variant of this technique, we are studying ways of producing molecules by laser ablation. In particular, we ablate a molecular precursor upstream from a nozzle orifice. The gaseous plume produced by the ablation pulse then serves as a carrier to drive a supersonic expansion of the target species seeded in it. Such a seeded supersonic expansion is likely to endow the target molecules with the velocity of the carrier and cool its internal degrees of freedom. The miniature nozzle can be housed in a counter-rotating arm, with the result that the molecules would emerge slow in the laboratory frame.

The molecule of choice for this experiment is CaF which can be easily produced by laser-ablating CaF₂ with a Nd:YAG with an intensity of up to 10¹² W/cm². The CaF molecules are detected by laser absorption spectroscopy in the X-A band at about 600 NM and their translational temperature is determined from the Doppler-broadened line profiles. In the next stage, we'll implement laser-induced fluorescence to boost the sensitivity of the spectroscopic measurement. CaF is well suited for this, due to Franck-Condon factors that allow to separate the excitation and fluorescence wavelengths.

This work [J. Phys. Chem. A **105**, 1626 (2001)] and previous work, we have reported the early stages in developing a counter rotating nozzle apparatus which provides a means to shift the velocity distribution of a molecular beam markedly downwards. We have now been able to greatly improve the gas feed into the rotating nozzle by adding an extra differentially pumped chamber to the gas input system. It has

proved possible to feed-in up to an atmosphere of gas while maintaining the pressure in the chamber housing the nozzle below 5 microtorr. That's a huge improvement - before we had a pressure of 100 microtorr in the nozzle chamber at an inlet pressure of 20 torr! This means that, with the centrifugal enhancement, we can now reach an effective stagnation pressure of 10-50 atmospheres (depending on the molecular mass of the gas) without scattering away the slow (and cold) molecules. Before, at a 100 microtorr background pressure, the scattering was so bad that it was in fact defeating the purpose of the whole exercise; moreover, at those low inlet pressures, there wasn't much of a supersonic expansion and cooling. We expect soon to take advantage of this major improvement to obtain much slower molecular beams than was previously feasible.

2. Silver-surface imaging detector. Much of the history of molecular beams is a story of detectors. Having experienced the difficulty of determining velocity distributions of very slow molecules (bedeviled by "rap-around" problems with time-of-flight) we decided to explore the possibilities of modernizing a venerable method. We tested whether it's true (as Otto Stern had claimed) that cigar smoke can turn vacuum-deposited silver into jet-black silver sulfide. IT CAN! This resulted in the following cigar dream which is quickly becoming a reality: Take a sulfur containing molecule (such as H₂S, a thiol, etc.), cool and decelerate it in the counter-rotating nozzle, diffract it on a grating or crystal, and hit a vacuum-deposited silver surface with it. Read the "jet-black" diffraction pattern by a microscope backed by a CCD camera. This should yield a spatial resolution of μm wide and an angular resolution of about 10 microradians. Repulsed by the smell of thiols, we quickly discovered that "sulfur-containing compounds" are not needed - because, for instance, HBr works like a charm as well.

Currently we are able to create and read-off images 50 μm wide and are about to begin diffracting the HBr beam by a transmission grating (with a lattice constant of 100 nm). Note that the detector is endowed with the Fellgett advantage, has a demonstrated sensitivity of several monolayers of HBr, and a dynamic range of about 100:1.

In the next step, we will apply the detector in our cold-molecule work to determine velocity distributions of slow/cold molecules. These are convoluted in the diffraction pattern and can be extracted with high accuracy from the diffraction image.

Theoretical Studies of Atomic Transitions

Charlotte Froese Fischer

Department of Electrical Engineering and Computer Science, Box 1679B
Vanderbilt University, Nashville, TN 37235

Email: Charlotte.F.Fischer@Vanderbilt.edu OR cff@vuse.vanderbilt.edu

Program Scope and Definition

The atomic structure project is concerned with the accurate determination of wave functions from which atomic properties can be predicted. Of particular importance are properties associated with energy transfer mechanisms such as transition probabilities, where relativistic effects are essential. Light elements have been investigated primarily in the Breit-Pauli approximation, but for heavier elements our methodology relies on variational Dirac-Hartree-Fock methods that include correlation, the Breit correction, and the effect of a finite nucleus.

Recent Progress

1. Breit-Pauli Studies

We have continued to refine and improve our "spectrum" calculations where all the energy levels up to a certain excitation level are computed along with all transitions between these levels, thus making it possible to determine lifetimes for excited states as well as branching ratios. Codes have been ported to the most advanced parallel computer at NERSC, namely the IBM SP "seaborg" computer. The transition data results are being made available for ready access on the internet :

(See http://www.vuse.vanderbilt.edu/~cff/mchf_collection).

We have published the evaluation of all sequences from Be- to Oxygen-like [3, 13, 15]. Calculations for F-like to Al-like have been completed but not yet critically evaluated, Si-like is in progress. We have implemented a web-based search facility that displays requested data. For energy levels, the error in the excitation energy and ionization energy (in some cases) is displayed so that accuracy may be judged. In the case of transition data, the error in the transition energy along with the discrepancy in the length and velocity gauges (when appropriate) are also displayed so that the *ab initio* data can be evaluated. This web site is part of a GENeral Internet search Engine for Atomic Data (GENIE).

2. Relativistic Multiconfiguration Dirac-Hartree-Fock Calculations

It is known that the Breit-Pauli approximation will be inadequate for highly ionized or heavy atoms. For transitions in the Na-like sequence, calculations were done also in the multiconfiguration Dirac-Hartree-Fock (MCDHF) approximation to assess the difference. The Breit-Pauli calculation for the $3s - 3p$ transition energy, in a core-polarization model, starts with an error of 0.88% in Na I, an error that decreases to 0.21% for Al III and then increases rapidly to 2.8% for Fe XVI. In contrast, MCDHF calculations in the same model,

had a similar error at Al III, but the error decreased rapidly to a stable 0.04%. The latter included QED corrections which explains some, but not all the improvement in the MCDHF results.

Many questions remain about how multiconfiguration Dirac-Hartree-Fock calculations can be performed accurately and efficiently, particularly for heavy atoms. In the case of Lr ($Z=103$) and Rf ($Z=104$), ground states have been determined only by coupled cluster theory and resonance transitions are unknown. We recently reported results for the ground state of Lawrencium (Lr) [16] validating the coupled cluster energies, but to do so, we first investigated Lu ($Z=71$) where experimental energy level data is available for comparison. Our studies showed the importance of correlation in the core, an effect often neglected in lighter atoms. By systematically, including more and more core effects, we obtained stable results in better agreement with experiment than the coupled cluster energies. Applying the same strategy to Lr ($Z=103$) we confirmed that the ground state is indeed $6d7s^2$ rather than ns^2np as in the homologous series. Wave function expansion sizes of over 330,000 were involved in this work, the largest ever encountered to date.

3. Splines and a non-orthogonal interactions

The Goddard High Resolution Spectrograph (GHRS) aboard the Hubble Space Telescope is providing quality data which include lines in the spectra for C I with a signal-to-noise ratio greater than 100-200, and relatively weak, optically thin lines are readily seen. From this data, astrophysicists have derived oscillator strengths for transitions from the $2s^22p^2\ ^3P$ ground state to high-lying levels of $2pnl$ LSJ, where $nl = nd$, $n \leq 5$ and ns , $n \leq 6$. In collaboration with O. Zatsarinsky, a spline, non-orthogonal configuration interaction, close-coupling calculation was applied to this problem using 11 target functions [18]. States up to $2p9d$ and $2p10s$ were obtained with ionization energies deviating from observed by $1-4\text{ cm}^{-1}$. Most length and velocity oscillator strengths differed by less than 1%. f -values ($\times 10^3$) for transitions from the $2s^22p^2\ ^3P$ ground state to $2s^22pnl$ LSJ are compared with those from astrophysical observation and NIST tabulated data below:

nl	LS	$J - J'$	ZzFZ ^a	FZs ^b	NIST	spline
6s	$^3P^o$	1 - 0		1.90		1.55
		2 - 2		5.91		1.74
		0 - 1		13.7		6.80
5d	$^3D^o$	2 - 2		3.53	3.66	5.28
		1 - 1	1.90	6.97	6.09	3.98
6s	$^3P^o$	1 - 2		17.8	2.32	10.5
5d	$^3D^o$	2 - 3	6.41	34.0	20.5	15.6
		0 - 1	7.63	40.5	24.4	21.2
		1 - 2	5.71	9.36	18.3	8.64
	$^3P^o$	1 - 1	3.45		1.53	2.28
1 - 0		4.60		2.02	2.50	
0 - 1		3.04		6.05	4.93	

^a Zsargo *et al* *Ap. J* **484**, 820 (1997)

^b Federman and Zsargo, *Ap. J* **555** 1020 (2001)

Photodetachment cross sections of the He $1s2s2p\ ^4P^o$ metastable state in the region of the $1s$ threshold (38 – 52 eV) have been calculated using a modified R-matrix method based on a B-spine representation of the scattering orbitals [17]. An accurate representation of initial state and target state wave functions has been obtained using a basis of non-orthogonal orbitals. The 17 bound ($1s2l, 1s3l$) and autoionizing ($2l2l', 2l3l'$) states of He have been included in the close-coupling expansion. The convergence of the close-coupling expansion has been checked by inclusion of additional $1s4l, 1s5l$ and $3l3l'$ target states. Close agreement was found with recent high-resolution K-shell photodetachment measurements of He⁻ giving rise to He⁺ ions (Berrah *et al Phys.Rev.Lett.* 88 93001 (2002)), except for the threshold maximum above the first $1s$ detachment threshold $2s2p\ ^3P^o$ at 38.88 eV, where the theoretical cross section is a factor of two larger than experiment. Our results show $1s$ photodetachment cross sections with numerous structures which have been analyzed in detail. A set of triply-excited resonances are also found, and their energy positions, widths and decay branching ratios were determined.

Future Plans

Our spectrum codes perform well for lower members of a spectrum and we plan to extend our collection to include most of the spectra up to argon-like. Calculations for Rydberg series, in many respects, are more like continuum calculations. Since the spline approach was shown to be effective for neutral carbon we plan to extend calculations for other neutral systems to more highly excited states. Of crucial importance will be the inclusion of some non-orthogonal orbitals as well as Breit-Pauli effects.

Heavy atoms continue to be of interest.

Recent Publications from DOE supported research)

1. *The use of basis splines and non-orthogonal orbitals in R-matrix calculations: application to Li photoionization*, O. Zatsarinny and Charlotte Froese Fischer, *J. Phys. B: Atom. Molec. Phys.* **33**, 313-341, (2000).
2. *REOS99: A revised program for transition probability calculations including relativistic, correlation, and relaxation effects*, S. Fritzsche, Charlotte Froese Fischer, and C.Z. Dong, *Comput. Phys. Commun.* **124**, 340-352 (2000).
3. *Breit-Pauli energy levels, lifetimes, and transition data: boron-like spectra*, G. Tachiev and Charlotte Froese Fischer, *J. Phys. B: Atom. Molec. Phys.* **33** 2419-2435 (2000).
4. *The MCHF atomic-structure package*, Charlotte Froese Fischer, *Comput. Phys. Commun.* **128**, 635-6 (2000).
5. *Core-polarization effects in the cadmium isoelectronic sequence*, E. Biémont, C. Froese Fischer, M.R. Godefroid, P. Palmeri, and P. Quinet, *Phys. Rev. A* **62**, 032512 (2000).
6. *Multiconfiguration Dirac-Hartree-Fock calculations for Be-like Intercombination Lines Revisited*, Charlotte Froese Fischer, *Physica Scripta* **62**, 458-462 (2000).

7. *Predictive data-based exposition of $5s5p\ ^{1,3}P_1$ lifetimes in the Cd isoelectronic sequence*, L.J. Curis, R. Matulioniene, D.G. Ellis, and C. Froese Fischer, Phys. Rev. A **62** 052513 (2000).
8. *Multiconfiguration Dirac-Hartree-Fock optimization strategies for $3s^2\ ^1S_0 - 3s3p\ ^3P_1$ transition rates for $Al^+ - S^{4+}$* , Yu Zou and C. Froese Fischer, Phys. Rev. A **62** 062505 (2000).
9. *Landé g factors for $2p^4(^3P)3p$ and $2p^4(^3P)3d$ states of Ne II*, Charlotte Froese Fischer and P. Jönsson, J. Mol. Struct. (THEOCHEM) **537**, 55-62 (2001).
10. *Measurements and prediction of the $6s6p\ ^{1,3}P_1$ lifetimes in the Hg isoelectronic sequence*, L. J. Curtis, R. E. Irving, M. Henderson, R. Matulioniene, C. Froese Fischer, and E. H. Pinnington, Phys. Rev. A **63** 042502 (2001).
11. *Multiconfiguration Dirac-Hartree-Fock calculations of forbidden transitions between $3s^2\ ^1S_0$, $3s3p\ ^3P_{0,1,2}$, 1P_1 states for Mg-like ions.*, Yu Zou and Charlotte Froese Fischer, J. Phys. B: Atom. Molec. Phys. **34**, 915-931 (2001).
12. *Non-relativistic variational calculations of atomic properties in Li-like ions: Li I to O VI*, M. Godefroid, Charlotte Froese Fischer and P. Jönsson, J. Phys. B: Atom. Molec. Phys. **34** 1079-1104 (2001).
13. *Breit-Pauli energy levels, lifetimes, and transition data: carbon-like spectra*, G. Tachiev and Charlotte Froese Fischer, Can. J. Phys. **79** 955-976 (2001).
14. *Magnetic dipole transitions between the lowest $3d^4\ J=2-3$ transitions in highly charged Titanium-like ions*, Charlotte Froese Fischer and S. Fritzsche, J. Phys. B: Atom. Molec. Phys. **34** L767-L722 (2001).
15. *Breit-Pauli energy levels, lifetimes, and transition data: nitrogen-like and oxygen-like sequences*, G. Tachiev and Charlotte Froese Fischer, Aston. Astrophys. **385** 716-723 (2002).
16. *Resonance transition energies and oscillator strengths in Lutetium and Lawrencium*, Y. Zou and Charlotte Froese Fischer, Phys. Rev. Lett. **88** 183001 (2002).
17. *Photodetachment of the $He^- 1s2s2p\ ^4P^o$ in the region of the $1s$ threshold*, O. Zatsarinny, T. W. Gorczyca, and Charlotte Froese Fischer, J. Phys. B: Atom. Molec. Phys. (accepted) (2002).
18. *Oscillator strengths for transitions of high-lying excited state of carbon*, O. Zatsarinny and Charlotte Froese Fischer, J. Phys. B: Atom. Molec. Phys. (submitted).

Studies of Autoionizing States Relevant to Dielectronic Recombination

T.F. Gallagher
Department of Physics
University of Virginia
P.O. Box 400714
Charlottesville, VA 22901
tfg@virginia.edu

The scope of this program includes primarily phenomena which exist in two valence electron atoms but not in single valence electron atoms. The central focus has been dielectronic recombination (DR), the major source of recombination in high temperature plasmas. Ironically, the same physical processes which are important for DR are also important for ZEKE spectroscopy, and ideas developed under this program have been shown to be useful for ZEKE spectroscopy. In addition to the work on DR we have also worked on inner electron ionization (IEI).

In the past year we have studied IEI from high ℓ states of Sr and DR from a continuum of finite bandwidth in the presence of magnetic, microwave, and combined static and microwave fields.

The initial IEI measurements were done with Ba 6s_{nd} atoms. When a Ba 6s_{nd} Rydberg atom is exposed to a laser pulse of duration shorter than the Kepler orbit time of the Rydberg electron it is possible to eject the inner electron while leaving the outer electron bound to the ion.^{1,2} When the pulse is so short, in some of the atoms the outer Rydberg electron does not come near the ion core and cannot absorb the photon, while the inner electron easily absorbs the photon and leaves the atom. The outer electron is then simply projected onto the ionic Rydberg states.

The original experiments were done with Ba 6s_{nd} atoms in which the Rydberg electron comes near the core once on each orbit. Consequently, if the laser pulse is longer than the Kepler period the Rydberg electron is certain to be ionized. If the nd electron comes near the core during the laser pulse it is ionized. If, however, the Rydberg electron is in a high ℓ state, it never comes near the core, so even if the Kepler period is short compared to the laser pulse, only the inner electron should be ionized. In the past year we have completed a study of IEI from Sr 5s16 ℓ states, for which the Kepler period is short compared to the laser pulse. The point was to determine the value of ℓ at which IEI starts to occur. Although one might naively expect that IEI would begin as soon as the inner turning point of the orbit exceeds the size of the Sr⁺ core, such is not the case. IEI begins to occur for $\ell = 5$, for which the inner turning point is 15a₀, a factor of three greater than the radius of the Sr⁺ core. This observation suggests that IEI is governed by the long range electrostatic interaction between the Rydberg electron and the ion core, just as in autoionization. In this connection we note that the autoionization lifetime of the Sr 5p n ℓ states begins to exceed the Kepler orbit time for $\ell = 5$. In other words, IEI and the autoionization rate exhibit related ℓ dependences.

DR, the recombination of an ion and an electron through an intermediate doubly excited autoionizing state, is the dominant electron-ion recombination mechanism in high temperature fusion plasmas. Since Rydberg autoionizing states play a central role in the process, it is not surprising that small electric fields, either macroscopic fields or the microscopic fields from ions and electrons, can have a significant effect.³ Electric fields mix low angular momentum

character into high angular momentum states so that more states contribute to DR, which tends to raise the total DR rate. On the other hand, electric fields also depress the ionization limit, reducing the number of available states, which tends to lower the DR rate. Taking both effects into account, the energy integrated DR rate for singly charged ions and electrons can be increased by a factor of two by an electric field of ~ 1 V/cm. Until recently magnetic fields were ignored, but Robicheaux and Pindzola have pointed out that relatively small fields, ~ 100 G, can be important, because they can mix the m levels, with a similar result as mixing ℓ levels.⁴ Finally, the effects of time varying fields have not, until recently, been explored at all.

We have completed our investigations of DR from a continuum of finite bandwidth in the presence of linearly and circularly polarized microwave fields. The continuum of finite bandwidth is the broad Ba $6p_{3/2}11d$ state which straddles the $Ba^+ 6p_{1/2}$ limit. We excite Ba atoms to the $6p_{3/2}11d$ state, at a well defined energy. The quasi continuous $11d$ electron can be captured into $6p_{1/2} n\ell$ state, which decays radiatively to the bound $6s_{1/2} n\ell$ state, which we detect by field ionization. Here n , ℓ , and m , denote the principal, orbital angular momentum, and azimuthal angular momentum quantum numbers. We observe a clear resonant enhancement of DR when the microwave frequency matches the $\Delta n = 1, 2$, or 3 spacing of the autoionizing Rydberg states.⁵ We have verified that the effect is resonant by changing the microwave frequency from 4 to 12 GHz and observing that the enhancement in DR occurs at the energy for which the Δn spacing matches the microwave frequency. The origin of the resonant enhancement is easily understood. When the microwave frequency matches the Δn separation the microwave field couples high ℓ states differing in both ℓ and n by one. In other words, it is resonant ℓ mixing analogous to that produced by a static electric field.

One of the most puzzling features of our observations is the similarity of results obtained with linearly and circularly polarized microwaves, and in the past year we have done calculations which remove some of the mystery. Specifically, we have calculated the $\Delta n = 1 \Delta \ell = \pm 1$ radial matrix elements, and the $\Delta \ell = -1$ matrix elements fall very rapidly with ℓ and probably play a minor role in the state mixing. As a result, there is effectively no difference between the effects of linear and circular polarization of the microwave field.

Using these matrix elements we were able to construct a model which gives a reasonable representation of our data. The widths of the resonant enhancements are a reflection of how many n states are coupled, and there is a threshold field for enhancement due to the requirement of mixing low ℓ states with non zero quantum defects.

We have taken extensive data for DR in combined \bar{E} and \bar{B} fields. We previously reported the enhancement of DR for $\bar{B} \perp \bar{E}$ and the absence of enhancement for $\bar{B} \parallel \bar{E}$.⁶ In the former case there is m mixing while in the latter there is not. We are now trying to understand some of the finer points of DR in combined $\bar{E} \times \bar{B}$ fields. For example in the experiment of Bartsch et al.⁷ a decrease in the DR rate was observed as B was increased from 200-690 gauss, while we saw increasing DR rates in our experiments at lower B fields. After a careful analysis of their experiment and ours we have realized that they are always in the weak electric field regime, in which the B field should suppress the DR rate. In contrast, we are always in the strong E field regime, because of the nd entrance channel.

In this year we have begun to explore DR in combined static and microwave electric fields. The most surprising observation is that we see DR far above the classical limit for ionization in the static field alone, and the effect is far more striking for the microwave field perpendicular to the static field than parallel to it. In other words m mixing is crucial, as has been recently reported by Zeibel and Jones.⁸

Plans for the coming year include several topics.

First, we plan to finish the experiments in combined static and microwave fields. The basic experimental effect, vastly increased DR rates through m charging transitions is clear, but we need to see how many of the details can be explained with reasonably simple models.

As mentioned above, we have carried out an extensive analysis of both our DR experiment and the storage ring experiments. We are virtually certain that only high ℓ states are important in the storage ring experiments, where as low ℓ states are in ours. We plan to do DR experiments from a continuum of finite bandwidth in which we have a high ℓ , nearly hydrogenic, state as the entrance channel. While we could do optical excitation from the 6s 8g state, a more versatile approach is to use microwaves to resonantly mix 6p_{1/2} nd and 6p_{1/2} ng states. The Ba 6p_{1/2} ng states are very nearly hydrogenic, and it should be possible to see enhancement of DR at much smaller E fields, allowing B field effects to become dominant more easily, as in the storage ring experiments.

Finally, we would like to do the DR experiments in high frequency microwave fields, with no static fields. Can we see resolved enhancement of the DR signal? Can we do microwave resonance spectroscopy on the autoionizing states? To our knowledge this has never been done, and it would be a powerful new tool.

References

1. H. Stapelfeldt, D.G. Papaioannou, L.D. Noordam, and T.F. Gallagher, Phys. Rev. Lett. 67, 3223 (1991).
2. R.R. Jones and P.H. Bucksbaum, Phys. Rev. Lett. 67, 32315 (1991).
3. V.L. Jacobs, J. Davis, and P.C. Kepple, Phys. Rev. Lett. 37, 1390 (1976).
4. F. Robicheaux and M.S. Pindzola, Phys. Rev. Lett. 79, 2237 (1997).
5. V. Klimenko and T.F. Gallagher, Phys. Rev. Lett. 85, 3357 (2000).
6. V. Klimenko, L. Ko, and T.F. Gallagher, Phys. Rev. Lett. 83, 3808 (1999).
7. T. Bartsch, S. Schippers, A. Muller, C. Brandan, G. Gwinner, A.A. Saghir, M. Beutelspader, M. Grieser, D. Schwalm, A. Wolf, H. Danared, and G.H. Dunn, Phys. Rev. Lett. 82, 3779 (1999).
8. J.G. Zeibel and R.R. Jones, Phys. Rev. Lett. 89, 093204 (2002).

Publications 2000-2002

1. V. Klimenko and T.F. Gallagher, "Resonant Enhancement of Dielectronic Recombination by a Microwave Field", Phys. Rev. Lett. 85, 3357 (2000).
2. H. Maeda, W. Li, and T.F. Gallagher, "Observation of Inner Electron Ionization from Radial Rydberg Wave Packets in Two-Electron Atoms," Phys. Rev. Lett. 85, 5078 (2000).
3. H. Maeda and T.F. Gallagher, "Inner-electron ionization for wave packet detection," Phys. Rev. A 64, 013415 (2001).
4. H. Maeda and T.F. Gallagher, "Inner electron ionization of Sr 5s16 ℓ states," Phys. Rev. A 65, 053405 (2002).
5. V. Klimenko and T.F. Gallagher, "Resonant enhancement of dielectronic recombination from a continuum of finite bandwidth," Phys. Rev. A 66, 023401 (2002).

Experiments in Ultracold Collisions

Phillip L. Gould
Department of Physics U-3046
University of Connecticut
2152 Hillside Road
Storrs, CT 06269-3046
<gould@uconnvm.uconn.edu>

Program Scope:

The techniques of laser cooling and trapping continue to lead to exciting new advances in atomic, molecular, and optical (AMO) physics. These methods make possible the generation of high density (e.g., $n > 10^{11} \text{ cm}^{-3}$) and ultracold (e.g., $T < 100 \text{ } \mu\text{K}$) samples of atoms, which are the starting point for many applications. Such applications include Bose-Einstein condensation (BEC) and atom lasers, degenerate Fermi gases, improved atomic clocks, photoassociative spectroscopy, ultracold molecule production, optical lattices, quantum computing, ultracold Rydberg atoms and plasmas, and fundamental atomic and nuclear physics experiments with radioactive isotopes. In many of these research areas, ultracold collisions can play an important role. For example, many applications require high atomic densities, and at these high densities, inelastic collisions can cause the loss of atoms from traps and/or increase their temperature. In general, improved knowledge of these collisional interactions, and their possible control, will significantly benefit studies involving ultracold atoms. The main motivation of our experimental program is to improve our understanding of ultracold collisions, especially those which occur in a typical laser trap environment.

Beyond the relevance of our experiments to applications of laser-cooling, there is significant fundamental interest in these extremely low energy (e.g., $\sim 10^{-8} \text{ eV}$) collisions. Although various collisional channels are available, the collisional kinetic energy is essentially zero, so only exoergic processes are allowed. Since the collisions usually involve low angular momentum, quantum effects can be important. In contrast to the situation at higher energy, the collision dynamics for laser-excited atoms can be dominated by the long-range (e.g., $R \sim 100 \text{ nm}$) potentials, i.e., the colliding atoms begin to "feel" each other at extremely long range. This allows the possibility of laser control of the collision dynamics. Finally, the long range of the potential, combined with the low collisional velocity, yields a collisional time scale which can exceed the excited-state radiative lifetime. Therefore, the atomic excitation can spontaneously decay during the course of a slow collision, dramatically affecting the outcome.

Our ultracold samples of rubidium are generated in a magneto-optical trap (MOT) operated with diode lasers at 780 nm. The choice of rubidium is based on three factors: 1) the fortuitous match of its resonance lines with readily available diode lasers; 2) the existence of two isotopes (^{85}Rb and ^{87}Rb) which allows investigation of isotopic effects in collisions; and 3) the popularity of ^{87}Rb in BEC experiments. Atoms are loaded into the MOT from either a laser-generated slow beam or a room-temperature vapor. Measurements of inelastic collisions are carried out by monitoring the loss rate of atoms from the trap. Specific processes which can cause loss of atoms from the trap include: radiative escape (RE), where the excited-atom pair emits a less energetic photon than it absorbed; fine-structure-changing (ΔJ) collisions; and hyperfine-changing (ΔF) collisions.

Recent Progress:

During the past year, we have: 1) investigated ultracold collisions of atoms in the highly-excited Rb 5D level; 2) made significant progress in experiments involving ultracold collisions induced by frequency-chirped laser light; and 3) started the construction of the apparatus needed for studies of mixed-isotope collisions. We briefly describe each of these advances below.

The highly-excited 5D level in Rb is interesting from the point of view of ultracold collisions. Collisions involving the first excited (5P) level have been extensively studied by us and others. In this case, the excitation often takes place at long range and, because of the relatively short radiative lifetime, there is a good chance that the excitation does not “survive” to short range where the observable inelastic process occurs. For the 5D level, the corresponding potential curves (R^{-5}) are much shorter range than those involved in 5P collisions (R^{-3}). Also, the radiative lifetime (240 ns) of the 5D level is much longer than that of the 5P (27 ns). The combination of these factors yields an interesting contrast to the 5P situation: for 5D collisions, the excitation should easily “survive” to short range. The experiments were performed by exciting cold atoms with two-photon two-color diode-laser excitation: $5S\gamma 5P\gamma 5D$, and measuring the density-dependent loss rate due to collisions. In addition, the competing density-independent loss rate due to 5D photoionization (caused by both excitation lasers) was determined. We previously determined this photoionization cross section by trap loss measurements.

In a previous experiment, we observed ultracold collisions in real time by using two pulses, delayed with respect to each other in a pump-probe configuration. The first pulse, tuned close to the atomic resonance, excites the colliding atom pair at very long range. The atoms accelerate towards each other on the attractive excited-state potential, decaying back to the ground state as they approach short range. A second pulse, detuned significantly below the atomic resonance, re-excites this enhanced collisional flux, causing an observable inelastic process at short range. If instead of applying temporally separated pulses at different frequencies, we use a frequency chirp, we can exert a higher degree of control over the collisions. With a blue-to-red chirp, we can maintain resonance during the course of the collision. With a sufficiently intense red-to-blue chirp, the population can be adiabatically inverted over a significant range of internuclear separations, thereby enhancing the collision rate. This type of active control may eventually prove useful in increasing the rate of cold molecule formation via photoassociation, a process which occurs at relatively short range. We have achieved diode laser chirp rates exceeding 1 GHz in 100 ns, which is well matched to the temporal dynamics of the collisions. Preliminary measurements of collisions induced by chirped light at low power are promising. We have also shown that we can injection lock a higher-power (slave) laser with a frequency-chirped lower-power (master) laser and have the frequency of the slave follow that of the master, even under conditions of rapid chirping. This should allow us to achieve sufficient intensities for adiabaticity.

We have begun to assemble the apparatus necessary to study mixed-isotope (^{85}Rb - ^{87}Rb) collisions. An additional set of lasers for the second isotope has been constructed, and a new detection scheme to resolve the fluorescence from the two isotopes has been developed. Since their resonance fluorescence wavelengths differ by only ~ 2.5 ppm, it would be difficult to spectrally resolve them. Instead, we will use rapidly alternated excitation of the two isotopes and gated detection (with an avalanche photodiode) of the fluorescence.

Future Plans:

We have two main experiments in ultracold collisions planned for the coming year. First, we will continue our work with frequency-chirped collisions, building on the promising preliminary results we have obtained and incorporating our higher-power injection-locked chirped laser. These studies will involve characterizing the collisions as a function of the rate, range, and direction of the frequency chirp, as well as the intensity of the laser. In addition to our collisional investigations, we need to understand the effects of the chirped light on atomic excitation, since these can result in perturbations of the atomic cloud.

In our second planned experiment, we will trap both isotopes (^{85}Rb and ^{87}Rb) and study collisions involving both species. This is of interest because the long-range nature of the potentials depends on whether the two atoms are really identical. Also, experiments with mixed-species BEC's depend critically on their collisional properties. The measurements will be carried out by measuring how the trap loss rate of one species is modified by the presence of the other species.

Recent Publications:

“Ultracold ^{87}Rb Ground-State Hyperfine-Changing Collisions in the Presence and Absence of Laser Light”, S.D. Gensemer, P.L. Gould, P.J. Leo, E. Tiesinga, and C.J. Williams, *Phys. Rev. A* **62**, 030702(R) (2000).

“Measurement of the $\text{Rb}(5D_{5/2})$ Photoionization Cross Section Using Trapped Atoms”, B.C. Duncan, V. Sanchez-Villicana, P.L. Gould, and H.R. Sadeghpour, *Phys. Rev. A* **63**, 043411 (2001).

“A Frequency-Modulated Injection-Locked Diode Laser for Two-Frequency Generation”, R. Kowalski, S. Root, S.D. Gensemer, and P.L. Gould, *Rev. Sci. Instrum.* **72**, 2532 (2001).

Physics of Correlated Systems

Chris H. Greene

Department of Physics and JILA
University of Colorado at Boulder

1. Coherent control of rotational wave packets

A recent collaboration has emerged between our group and the experimental group of Kapteyn and Murnane at JILA. Using femtosecond laser pulses they are able to form coherent rotational wave packets of CO₂ molecules. At regular intervals, signatures in the spectral data from subsequent "probe" pulses have been identified as indications of periodic revivals of the coherent wave packets. Using a simple rigid rotor model we have been able to reproduce this spectrum in detail. The main point of this study is the fact that the rapidly-varying index of refraction increases the frequency bandwidth of the probe pulse when it propagates through the gas. That bandwidth increase is associated with a chirp that can be exploited by simply passing the transmitted probe beam through a transparent window, in order to produce a temporal shortening of the final pulse. In the experiment with CO₂, the probe pulse was compressed by nearly an order of magnitude, from 270 fs down to about 30 fs duration.

Since our initial joint experimental and theoretical paper on the subject appeared,[1] we have extended our studies to molecules other than CO₂ to look for different species that appear to be promising for future experiments. Moreover, additional studies have been carried out to see whether the molecular rotational alignment can provide a way to coherently control the phase-matching in a third-harmonic generation experiment.[2]

2. Extending closed-orbit theory to include nonclassical pathways

Some encouraging progress transpired this past year along the lines of the PhD dissertation of Brian Granger, which rederived closed-orbit theory within the context of a semiclassical approximation to quantum defect theory. That derivation resulted in a deeper level of understanding of those standard semiclassical approximations, and in particular, it identified a previously overlooked cancellation effect that occurs for atomic hydrogen. The main new physics to emerge from this work, which has been submitted for publication to Physical Review Letters,[3] is a new interpretation of the nonclassical "ghost orbits" that have been observed in scaled-variable spectroscopy of diamagnetic Rydberg states. A new method has been proposed for implementing closed-orbit theory for any atom possessing more than one nonzero quantum defect (for the relevant symmetry of interest), a key example being the rubidium atom. Previous methods have exhibited an unphysical divergence of the recurrence spectrum, but with the new techniques, a convergent cross section and recurrence spectrum emerge. Moreover, the results show reasonably good agreement with large-scale quantum calculations performed independently, using quantum defect and R-matrix techniques. These methods were also used to develop a qualitative understanding of a class of ultra-long-range Rydberg molecules.[4]

3. Atoms in an intense laser field

In this project we are studying the double ionization of a helium atom by a short, intense laser pulse in order to understand more about the specific mechanisms leading to double photoionization. We have been solving the time-dependent Schrodinger equation for a two dimensional model atom that has physical properties similar to those of helium. Based on our work and that of others, it is becoming clear that the mechanism proceeds by a recollision, in which the second ionization event is caused by electron-impact from the first electron to be ionized rather than by a second photoionization. However, some issues remain unclear about this mechanism, such as whether the assisting effect of the laser field on the inner electron plays a crucial role, or if instead this is a simple (e,2e) process in which the laser acts only to eject the outer electron first and then accelerate it back toward the He⁺ ion. A first publication on this subject has already appeared,[5] and we hope to push this study through to another, during the coming year.

4. Correlations between the electronic and nuclear motions in an electron-molecule collision

We have begun a new arm of research supported by this project in recent months, aimed at implementing a recently-proposed theoretical method that can handle the dissociative recombination of triatomic molecules, including the full three-dimensional dissociation dynamics of the nuclear degrees of freedom. The initial work on H_3^+ dissociative recombination pinpointed the vital role of the Jahn-Teller coupling mechanism. Our work on this grant will primarily focus on heavier linear triatomics such as HCO^+ or NO_2^+ , which are more important in terrestrial applications. The immediate goal will be to ascertain whether Renner-Teller coupling can play a vital role, akin to that of the Jahn-Teller coupling that surprisingly turned out to be the dominant recombination mechanism for H_3^+ . The latter molecule is an important prototype for these methods, since it is the simplest triatomic and it has also received the most detailed experimental study that can be used to test the theory. However, our main focus in the long term for this DOE grant will be the study of species more relevant in atmospheric science or plasma etching.

5. Scattering amplitudes for electron-impact ionization

This project has continued to support some efforts by postdoctoral associate Mark Baertschy to produce accurate triply-differential cross sections (TDCS) for electron-impact of atomic hydrogen. The TDCS represents the probability distribution of electron emission among the scattering angles and energies possible for two outgoing electrons, following a collision between an electron and the atom. The most significant accomplishment in this project, carried out in a collaboration between M. Baertschy, W. McCurdy, and T. Rescigno, has been the development and implementation of a new formalism for extracting ionization information from a wave function. That work was described in a recent paper[6], while the applications are presented in other publications.[7-12] This formalism gives an integral expression for the ionization amplitude that provides a more accurate and widely applicable means of generating differential cross sections than does the original method, which was based on an analysis of the escaping electron flux.

These studies have focused primarily on energies within a few eV above the ionization threshold, where correlation and entanglement of the two outgoing electrons is most significant. In that regime, formalisms based on separable expansions, such as convergent close-coupling (CCC) and various R-matrix hybrids, have had difficulty calculating the energy-distribution for collision energies within about 30 eV of threshold. Much of the controversy that previously existed with these methods appears to be getting resolved, based in part on the success of these benchmark calculations.

Papers published or submitted recently that were supported at least in part by this grant

[1] *Phase modulation of ultrashort light pulses using molecular rotational wave packets*, R. A. Bartels, T. C. Weinacht, N. Wagner, M. Baertschy, C. H. Greene, M. M. Murnane, and H. C. Kapteyn, Phys. Rev. Lett. **88**, 013903-1 to 013903-4 (2002).

[2] *Phase matching conditions for nonlinear frequency conversion using aligned molecular gases*, R.A. Bartels, N. Wagner, M. Baertschy, J. Wyss, M.M. Murnane, and H.C. Kapteyn, submitted to Optics Letters,

[3] *Semiclassical theory for spectra of diamagnetic atoms: a surprise cancellation and a convergent result*, B. E. Granger and C. H. Greene, submitted to Physical Review Letters.

[4] *Quantum and semiclassical analysis of long-range Rydberg molecules*, B. E. Granger, Edward L. Hamilton, and C. H. Greene, Phys. Rev. A. **64**, 042508-1 to 042508-9 (2001).

[5] *Multiphoton processes in a two-dimensional model of helium, in Correlations, Polarization, and Ionization in Atomic Systems*, C. H. Greene, M. Baertschy, A. L. Young, and B. E. Granger, in , AIP Conference Proceedings, **604**, pp.1-5, (2002),. edited by D. H. Madison and M. Schulz.

[6] *Accurate amplitudes for electron-impact ionization*, M. Baertschy, T.N. Rescigno, and C.W. McCurdy, Phys. Rev. A **64**, 002709 (2001).

[7] *Ejected-energy differential cross sections for the near threshold electron-impact ionization of hydrogen*, M. Baertschy, T.N. Rescigno, C.W. McCurdy, J. Colgan, and M.S. Pindzola, Phys. Rev. A **63**, 050701R (2001).

[8] *Doubly differential cross sections for the electron-impact ionization of hydrogen*, W.A. Isaacs, M. Baertschy, C.W. McCurdy, and T.N. Rescigno Phys. Rev. A, **63**, 030704R (2001).

[9] *Electron-impact ionization of atomic hydrogen*, M. Baertschy, T.N. Rescigno, W.A. Isaacs, X. Li, C.W. Phys. Rev. A **63**, 022712 (2001).

[10] *Time-dependent close-coupling calculations of the triple-differential cross section for electron-impact ionization of hydrogen*, J. Colgan, M. S. Pindzola, F. J. Robicheaux, D. C. Griffin, and M. Baertschy, Phys. Rev. A **65**, 042721 (2002).

[11] *Ionization of atomic hydrogen by 17.6 eV electrons*, J. Roeder, M. Baertschy, and I. Bray, submitted to Physical Review A.

[12] *Electron-Impact Ionization of Atomic Hydrogen at the Incident Electron Energy of 17.6 eV*, J.G. Childers, K.E. James, M. Hughes, Igor Bray, M. Baertschy, and M.A. Khakoo, submitted to Physical Review Letters.

Quantum Theory of Collective Effects in the Atom Laser

Murray J. Holland

JILA, Campus Box 440, University of Colorado, Boulder, CO 80309-0440

Murray.Holland@Colorado.EDU

I. Overview of research activity

During the past year, we continued our research into the many-body theory of dilute quantum atomic gases. We concentrated our efforts on describing resonances in the individual binary interactions. This topic connects with many of the future research goals of the field; e.g. the production of molecular condensates, the demonstration of high temperature superfluidity in fermion gases, the realization of low dimensional systems, and the investigation of a broad range of strongly-correlated phenomena with analogy to strongly-correlated electron systems in condensed matter physics. At first glance, it is remarkable that the collective phenomena of atomic gases could make any contact with strongly-correlated physics or high-temperature superfluidity. The gases are extremely dilute—the range of the interatomic potential is typically two to three orders of magnitude smaller than the spacing between particles. This means that the interactions are generally considered to be weak and that perturbation theory at low order is expected to provide an accurate description of the quantum kinetics. Such simplistic considerations, however, are incomplete since they neglect the complex internal structure of the atoms. In particular, there exists the possibility for Feshbach resonances which can be controlled experimentally via an external magnetic field (see Fig. 1).

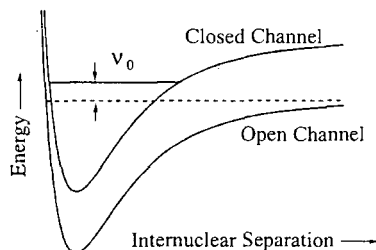


Figure 1. Illustration of a Feshbach resonance. A bound state of a closed potential is in close proximity (with detuning ν_0) to the scattering threshold (dashed line).

Such resonances are important because they allow experimentalists to control the microscopic interactions, switching from attractive to repulsive, or from weak to strong. Our theoretical study of them over the past year included the following research highlights:

- providing a quantitative theory of the Ramsey fringes observed by the Wieman group at JILA and thereby showing that they had produced a molecular condensate,
- making a quantitative proposal for ‘high-Tc superfluidity’ in fermion gases,
- predicting that a simple signature of the fermion superfluidity is found in the direct observation of the density profile of a trapped gas, and
- completing the development of a detailed second-order quantum kinetic theory needed to describe the damping of collective excitations and the frequencies of linear response.

We now briefly describe some of these topics. Further details can be found in our published work which is listed at the end.

II. Ramsey fringes in a BEC between chemically distinct species

We have recently been able to quantitatively evaluate the resonance theory we have developed over the past few years by comparison with a recent experiment (Donley *et al.* Nature **417**, 529 (2002)). The experiment involved a Feshbach resonance in bosonic ^{85}Rb . In direct analogy with a Ramsey fringe experiment in atomic physics, a time-dependent magnetic field was used to create two intervals of strong coupling (i.e. near resonance) separated by a waiting interval t_{evolve} which could be varied in duration. In the strong coupling regions the scattering length was positive and many thousands of Bohr radii in magnitude (the highest values of the dimensionless parameter na^3 , where n is the density and a is the scattering length, approach unity). This is typically considered to be a very challenging regime to explore theoretically. After applying the pulse sequence the experimenters observed three components; a residual condensate, a burst of atoms at higher energy with distinct spatial profile, and a missing fraction. As the time interval t_{evolve} was varied they observed oscillations in the proportion of atoms in each component.

Since the microscopic parameters are known to high precision for ^{85}Rb , we were able to model the dynamic experiment completely with no adjustable parameters. We calculated evolution trajectories for each value of t_{evolve} by solving the time-dependent Hartree-Fock-Bogoliubov equations appropriately renormalized to remove the ultraviolet divergences which would otherwise arise. We thereby predicted occupations in the atomic condensate, molecular condensate, and atomic non-condensate components (Fig. 2).

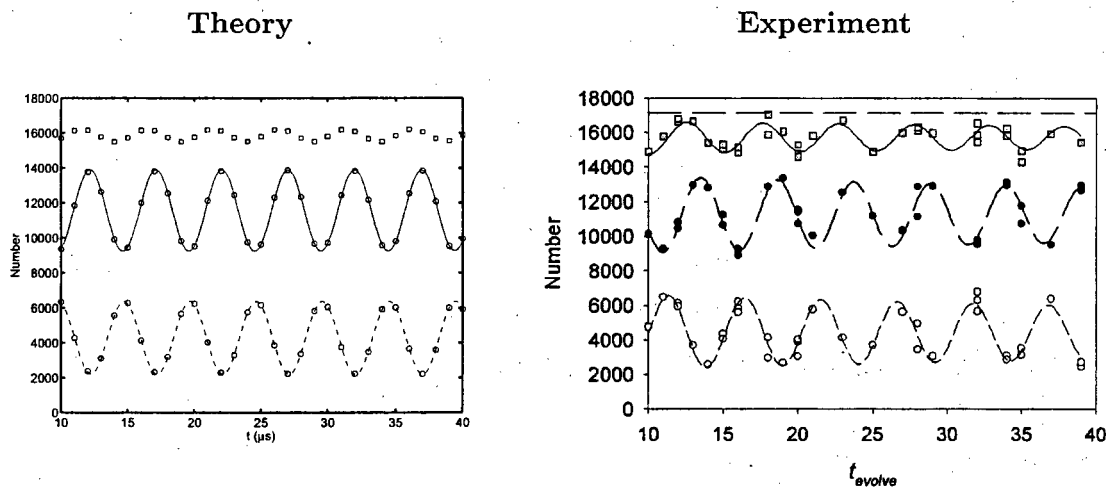


Figure 2. Ramsey fringe oscillations between the atomic condensate (theory-solid line) and the atomic noncondensate (theory-dashed line). These two components sum to the total number of recovered atoms (theory-squares), which excludes the molecular component. The experimental plot illustrates the directly analogous quantities for comparison.

The agreement with the experimental observation is striking and therefore the observed components can be unambiguously identified. Some of the properties which are correctly accounted for include the fringe frequency at the one percent level (which is a direct measure of the binding energy of the molecule in the 100 kHz scale), and the visibility and position of the fringes for each component. A phase offset in the oscillations is noted in the experimental data and reproduced in the theory.

III. Resonance superfluidity in a Fermi gas

There is currently a significant experimental effort to achieve superfluidity in a dilute Fermi gas by utilizing Feshbach resonance interactions. The direct application of the Bardeen-Cooper-Schrieffer (BCS) theory of superconductivity to a dilute Fermi alkali gas in this situation is incomplete because it involves the treatment of the interatomic interactions by the scattering length a . The requirement to have a high critical temperature in close proximity to the Fermi temperature in order for the superfluid transition to be achievable experimentally means that the theory cannot involve just the scattering length and must account for the resonance state explicitly.

We therefore developed a theory of the critical temperature for the formation of the fermion superfluid state which takes this into account. We studied the behavior of the critical temperature in the crossover region in a path integral formulation. We were able to consider the important role of fluctuations in the resonance regime (by performing the path integral calculation in the beyond saddle-point approximation) and utilized the same renormalization procedure described above for the Ramsey fringe studies. The characteristic dependence of the critical temperature on detuning is shown in Fig. 3. Note that these calculations interpolate between the BEC limit at large negative detuning, and the BCS superfluidity limit at large positive detuning.

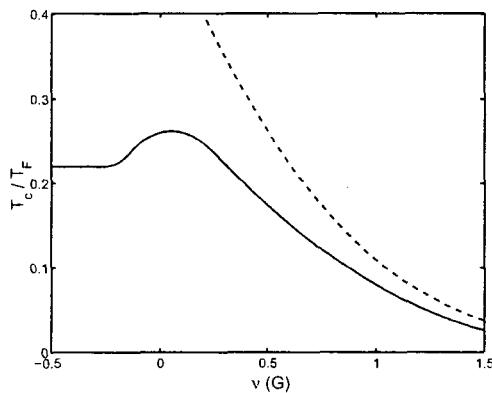


Figure 3. Ratio of the critical temperature T_c to the Fermi temperature T_F as a function of the magnetic field detuning ν across a Feshbach resonance for ^{40}K (solid line). At large negative detuning the transition is characterized by strongly bound composite pairs which Bose condense. At large positive detuning the prediction of the Bardeen-Cooper-Schrieffer theory emerges (dashed line).

We solved the resonance theory in the local density approximation and discovered that there was a direct and observable signature of the superfluid phase transition in the density behavior. As shown in Fig. 4, we predicted a density bulge to emerge in the trap center which can be seen directly by the usual methods of absorption imaging. The appearance of the bulge is due to the change in compressibility of the gas in the superfluid state. A key finding was that the compressibility remains positive and the gas therefore would be mechanically stable to collapse.

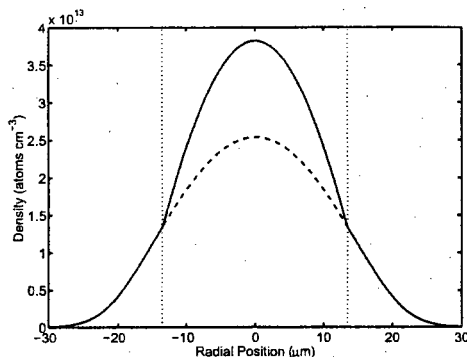


Figure 4. Density profile of a superfluid gas of ^{40}K in a harmonic trap in close proximity to a Feshbach resonance (solid line). The density bulge is a signature of the superfluid transition. In the absence of the transition the density profile would be smooth (dashed line).

Publications on DOE supported research

- [1] S.J.J.M.F. Kokkelmans and M.J. Holland, *Ramsey fringes in a Bose-Einstein condensate between atoms and molecules*, submitted to Phys. Rev. Lett. (2002); available on xxx.lanl.gov as cond-mat/0204504.
- [2] S.G. Bhongale, R. Walser, and M.J. Holland, *Microscopic nonequilibrium dynamics of an inhomogeneous Bose gas beyond the Born approximation*, submitted to Phys. Rev. A (2002); available on xxx.lanl.gov as cond-mat/0203415.
- [3] J. Milstein, S.J.J.M.F. Kokkelmans, and M.J. Holland, *A resonance theory of the crossover from Bardeen-Cooper-Schrieffer superfluidity to Bose-Einstein condensation in a dilute Fermi gas*, to be published in Phys. Rev. A (2002); available on xxx.lanl.gov as cond-mat/0204334.
- [4] M.L. Chiofalo, S.J.J.M.F. Kokkelmans, J.N. Milstein, and M.J. Holland, *Signatures of Resonance Superfluidity in a Quantum Fermi Gas*, Phys. Rev. Lett. **88**, 090402 (2002).
- [5] S.J.J.M.F. Kokkelmans, J.N. Milstein, M.L. Chiofalo, R. Walser, and M.J. Holland, *Resonance Superfluidity: Renormalization of Resonance Scattering Theory*, Phys. Rev. A **65**, 053617 (2002).
- [6] M. Holland, S.J.J.M.F. Kokkelmans, M.L. Chiofalo, and R. Walser, *Resonance Superfluidity in a Quantum Degenerate Fermi Gas*, Phys. Rev. Lett. **87**, 120406 (2001).
- [7] M. Holland, J. Park, and R. Walser, *Formation of pairing fields in resonantly coupled atomic and molecular Bose-Einstein condensates*, Phys. Rev. Lett. **86**, 1915 (2001).
- [8] R. Walser, J. Cooper, and M. Holland, *Reversible and irreversible evolution of a condensed bosonic gas*, Phys. Rev. A **63**, 013607 (2001).
- [9] M. Holland, J. Cooper, and R. Walser, *Quantum kinetic theory for a Bose-Einstein condensed alkali gas*, Proceedings of the 10th International Conference on Recent Progress in Many-Body Theories, (World Scientific, Eds. R. Bishop, K. Gernoth, N. Walet, and Y. Xian, pp 357-366, 2001).
- [10] S. Kokkelmans, M. Chiofalo, R. Walser, and M. Holland, *Resonance superfluidity in a quantum degenerate Fermi gas*, Proceedings of the XV International Conference on Laser Spectroscopy, (World Scientific, Eds. S. Chu, V. Vuletić, A. Kerman, & C. Chin, pp 70-78, 2001).
- [11] M. Holland, S. Kokkelmans, M. Chiofalo, R. Walser, *Resonance superfluidity in a quantum degenerate Fermi gas*, Proceedings of the International Conference Quantum Optics V, (Acta Physica Polonica A, pp 387-397, 2001).

Toward Cooper Pairing of Fermionic Atoms

Deborah Jin
JILA, UCB440
University of Colorado
Boulder, CO 80309
jin@jilau1.colorado.edu

Our previous work [1] introduced a new quantum system by cooling a trapped gas of Fermionic atoms to ultralow temperatures. An exciting possibility in this system is a phase transition to a Cooper-paired state, analogous to superconductivity in metals. If found experimentally, this predicted new phase in the atomic gas system would have enormous potential in elucidating the underlying physics of superconductivity. In particular, recent theoretical efforts have pointed out that Cooper pairing in the atom gas could very well occur in a regime of temperature compared to the Fermi temperature that is more similar to exotic high temperature superconductivity than to standard BCS superconductivity [3]. One of the primary challenges in realizing this predicted new phase is in cooling the gas to sufficiently low temperatures relative to the Fermi temperature. In this project we are cooling a Fermi gas indirectly through thermal contact with a directly cooled Bose gas. With the appropriate choice of bosonic and fermionic atoms, this system has the potential to reach further into the quantum regime than previous results. Additionally, the Bose/Fermi mixture opens up new possibilities for investigating a mixed quantum system.

We have built a new apparatus to produce Bose/Fermi mixtures using ^{87}Rb and ^{40}K atoms (Fig. 1). This work has involved developing a unique laser system, demonstrating a two-species MOT [3], implementing a magnetic trapping system, and performing evaporative and sympathetic cooling to ultralow temperature [4]. Pre-cooled atoms are loaded from the MOT into a purely magnetic trap. Once in this quadrupole magnetic trap (created using two coils in anti-Helmholtz configuration) the gas is transferred to a higher vacuum portion of the chamber simply by mechanically moving the magnetic trap coils using a commercial computer-controlled track. Here, the atoms are transferred into a Ioffe-Pritchard type magnetic trap and then cooled. Forced

evaporation is then used to cool the ^{87}Rb gas, while the ^{40}K gas is cooled sympathetically simply through its thermal contact with the ^{87}Rb gas.

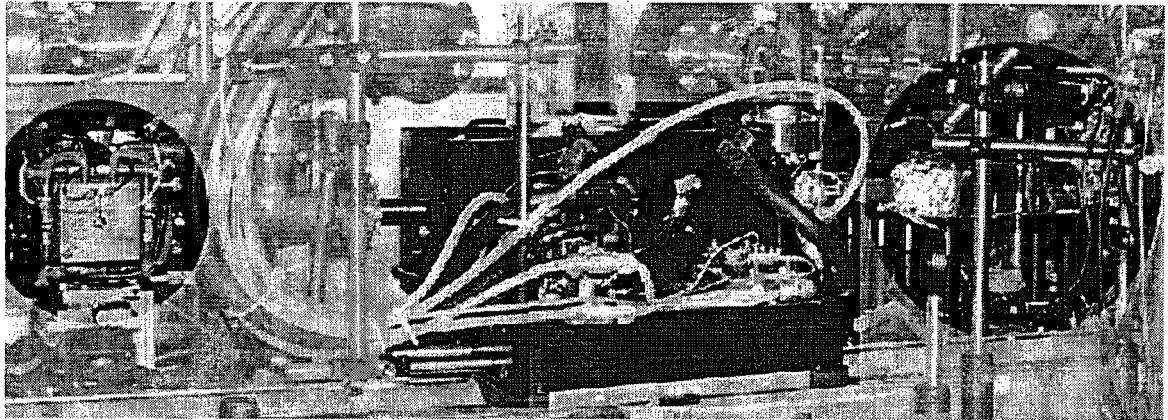


Fig.1. Bose-Fermi mixture apparatus. Three elements of the apparatus are highlighted in this photo – the glass MOT chamber (right), the quadrupole magnetic trap on a moving cart (middle), and the final magnetic trap around a second glass cell (left).

We first tested the apparatus by cooling ^{87}Rb alone down to the quantum regime. Starting with 10^8 ^{87}Rb atoms in the final magnetic trap, the gas is cooled by forced RF evaporation. After less than 1 minute of evaporation we clearly observe Bose-Einstein condensation in time-of-flight (TOF) expansion images of the gas (see Fig. 2). The gas is illuminated with a pulse of resonant light and the shadow is imaged onto a low-noise CCD camera. Fits to these images are then used to extract temperature and number.

Following the successful cooling of ^{87}Rb into the quantum regime, we added ^{40}K atoms to the magnetically trapped gas. Both isotopes are optically pumped into the stretched states before being loaded from the two-species MOT into the quadrupole magnetic trap. This improves the loading efficiency and avoids the problem of rapid trap loss due to spin-exchange collisions in the two-species gas. At the start of evaporation we have roughly 10^4 ^{40}K atoms along with 10^8 ^{87}Rb atoms in the final magnetic trap. As evidence of sympathetic cooling, we have observed that the ^{40}K gas cools as the ^{87}Rb is evaporatively cooled. Furthermore, the number of ^{40}K atoms shows a relatively small decrease during the evaporation. Preliminary results comparing the Bose and Fermi gas sizes in the magnetic trap suggest that the Fermi gas reaches a temperature of about 1/5 the Fermi temperature. After more detailed investigation of the cooling and the thermodynamics of the resulting Bose-Fermi mixture, we plan to use this new system to

investigate interactions in the mixed Bose/Fermi gas. An exciting possibility is that a boson-mediated attraction that could drive Cooper pairing of the Fermionic atoms at ultralow temperature.

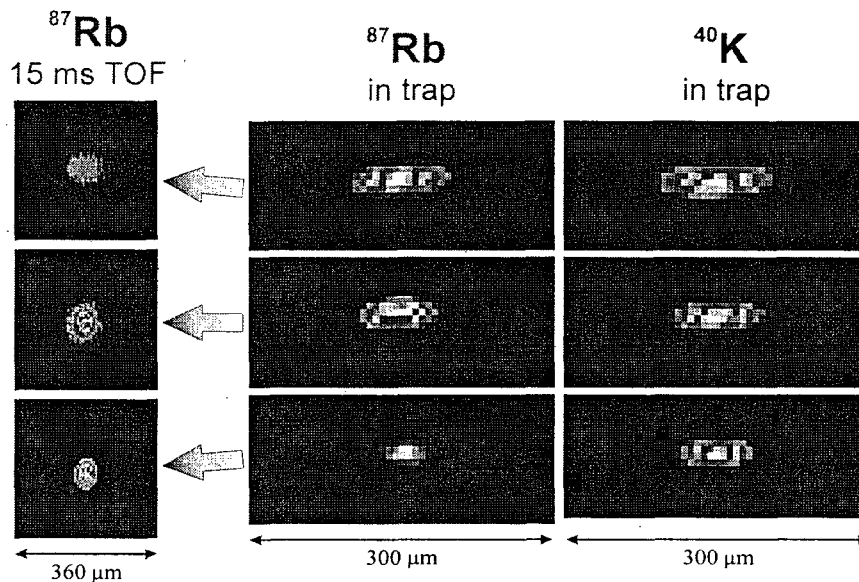


Fig.2. Absorption images of the ultracold bosonic and fermionic gases. On the right, the sizes of the simultaneously trapped gases are compared. In the quantum regime one expects the trapped fermionic ^{40}K gas to be larger than the bosonic ^{87}Rb gas. On the left, corresponding time-of-flight expansion images of the ^{87}Rb gas show Bose-Einstein condensation.

1. B. DeMarco and D. S. Jin, *Science* **285**, 1703 (1999).
2. M. Holland, S.J.J.M.F. Kokkelmans, M.L. Chiofalo, and R. Walser, *Phys. Rev. Lett.* **87**, 120406 (2001).
3. J. Goldwin, S. B. Papp, B. DeMarco, and D. S. Jin, *Phys. Rev. A* **65**, 021402 (2002).
4. S. Inouye, J. Goldwin, B. Newman, M. L. Olsen, B. DePaula, and D. S. Jin, in preparation.

Non-Perturbative Laser Atom Interactions for Nonlinear Optics

P.I.s: Henry C. Kapteyn and Margaret M. Murnane
Department of Physics and JILA
University of Colorado at Boulder, Boulder, CO 80309-0440
Phone: (303) 492-8198; FAX: (303) 492-5235; E-mail: kapteyn@jila.colorado.edu

Program Scope

The goal of this work is to study of the interaction of atoms and molecules with intense and very short (<20 femtosecond) laser pulses, with the purpose of developing new short-wavelength light sources, particularly at short wavelengths. We are also developing novel laser systems to enable this work.

Recent Progress

1. In work published in Physical Review Letters in 2002, we demonstrated an exciting new technique for making ultrashort light pulses. By inducing molecules in a gas to coherently spin, the very-fast time-dependent phase modulation induced by these molecular rotational quantum "wave packets" can spectrally-modulate and compress ultrashort light pulses. Using impulsively excited rotational wave packets in CO₂, we dramatically increased the bandwidth of a short-wavelength light pulse. This pulse was then compressed duration by an order of magnitude, simply by propagation through a fused silica window, *without the use of a pulse compressor*. This is a very general and novel technique for optical phase modulation, which can be applied to pulses in virtually any region of the spectrum from the IR to the VUV. It appears to be particularly useful for compressing light pulses in the VUV region of the spectrum, where conventional pulse compression techniques fail. (Refs. 7 and 12)
2. Very recently in related work, we proposed a new method for phase-matched frequency conversion in a gas that we call *transient birefringent phase-matching*. In this method, an intense linearly-polarized light pulse induces the molecules in an anisotropic molecular gas to align. A gas of molecules with an anisotropic polarizability normally exhibits no anisotropy since the molecules are randomly oriented. However, a random distribution of molecules can be aligned using an intense light field to induce a torque on any molecule not oriented either parallel or perpendicular to the laser field. In the case of an alignment pulse shorter than the rotational period of the molecule (typically less than a few picoseconds), the pulse exerts an impulsive torque on the molecules. This results in a change in the rotational angular momentum, and an excited distribution of rotational energy levels. Even after the alignment pulse has passed, this ensemble of molecules experiences a periodic realignment determined by the excited angular momentum states and the molecular rotational energy level structure. These alignments modify the macroscopic polarizability of the ensemble of molecules, creating a gas phase "quasi-crystal" and inducing time-dependent changes in the index of refraction. This birefringence created by an ensemble of aligned molecules can be used to phase match nonlinear frequency conversion. In particular, we calculated the conditions required to phase match third harmonic generation in a hollow-core fiber, and found them to be very reasonable. We also measured the induced birefringence. These results can be easily generalized to other nonlinear processes and interaction geometries. (Ref. 14)
3. In recent promising work, we observed what may be the first demonstration of a nonlinear-optical frequency conversion process driven by EUV light. By combining the fundamental

and second harmonic of an 800nm laser in a hollow-core fiber, we drive the process of high-harmonic generation, which in turn appears to drive a four-wave frequency mixing process in the EUV. The strong fundamental beam at frequency ω_1 (800nm) (where ω_n corresponds to a photon frequency of $n\omega$) generates odd-order harmonics very efficiently, in the range of ω_{15} - ω_{27} using argon gas. With the addition of only a small amount (few mW) of ω_2 light, these odd harmonics appear to be able to drive a low-order four-wave frequency mixing process such as $\omega_{20}=\omega_{21}+\omega_1-\omega_2$, to generate *even-order* harmonics. This may be, in effect, a *cascaded* process whereby the odd-order harmonics are generated by a high-order HHG process, which in turn drive a low-order frequency mixing process to generate the even-order harmonics. For higher ω_2 powers, we observe high-order processes that might be attributed to either multiple-order cascaded processes, or the high-order frequency mixing processes (similar to HHG but with 2 colors) that have been identified previously. (Refs. 5, 8, 10, 15)

Future Plans

1. Our calculations show that our coherent “molecular modulation” techniques should be extremely well-suited for the generation of very short-duration, 1-10 fs light pulses in both the deep-ultraviolet and the vacuum-ultraviolet regions of the spectrum. We plan to pursue this technology, with the goal of developing a high-power deep-ultraviolet light source to be used to study ultrafast dynamics in chemical species, clusters, and materials. In this work, we plan to combine solid-state laser technology with excimer lasers. This work will make use of the frequency conversion techniques developed during the previous grant period to generate ultrafast “seed” pulses at 248nm, 193 nm, and possible 157 nm. These pulses can be amplified in excimer gain media to high (up to 1 mJ) pulse energy, with duration ~100-200 fs. These pulses can then be compressed using the molecular modulation technique to as short as 1-2 fs, with virtually no loss in pulse energy. This light source will have unprecedented characteristics that will make it possible to explore a new regime in ultrafast light-atom interactions, as well as studying molecular dynamics and coherent control in the UV on the very fastest time-scales.
2. We plan to demonstrate nonlinear frequency conversion in a gas by phase matching using the transient birefringence induced by an intense polarized laser pulse. We will begin by phase matching third harmonic generation. We have already derived the conditions for anisotropic phase matching, and measured the induced birefringence.
3. Our initial experiments in two-color high-harmonic generation give us an intriguing hint that we are on the verge of observing for the first time nonlinear optical processes in the extreme-ultraviolet region of the spectrum. We plan to pursue this work, and to attempt to understand in more detail how atoms interact with light at “ionizing” photon energies, in the extreme-ultraviolet region of the spectrum. A large part of this effort will involve using temporally-shaped light pulses, and computer-controlled “learning algorithm” techniques to extensively characterize the response of atoms to complex, ultrabroad bandwidth light pulses. This work will be coupled with theoretical models that attempt to duplicate experimental observations, as was done with our past high-harmonic generation work.
4. Finally, new techniques have been developed at JILA that make it possible to control not only the intensity “envelope” of an ultrafast light pulse, but also the absolute position of the individual oscillations of the electromagnetic field of the light; i.e. the “carrier-envelope offset” or *CEO*. Although the technology now exists, relatively few physical phenomena are actually sensitive to this parameter. High-field laser-atom interactions, and in particular high-harmonic generation, represent the most-prominent application that should be sensitive to this parameter. In particular, CEO stabilization may be useful for reducing the pulse-to-pulse

Spectroscopy of Nanoparticles Produced by Laser Ablation of Microparticles

John W. Keto

Physics Department, The University of Texas at Austin, Austin, TX 78712

keto@physics.utexas.edu

1.0 Introduction

Our current objectives are: (1) measure the surface and bulk electronic quantum states of nanocrystals produced by a unique method of synthesis--laser ablation of microspheres (LAM), and (2) study the photoluminescence of nanoparticles in nanocomposites. Surface defect states produced by LAM are expected to be different from those grown chemically; and the knowledge of these defect states are essential to their use as optical devices. In contrast to chemical synthesis of nanocrystals, LAM is compatible with standard microelectronics fabrication techniques.

Using near-field scanning microscopy (NSOM) and microluminescence techniques, we are working to obtain the spectra of single nanocrystals (NC) correlating their spectra with size. When using microluminescence, particles are correlated to a pattern of scratches on a substrate which is later scanned with AFM. Single particle spectra will be compared with spectra obtained in a supersonic jet apparatus using resonance excitation followed by photoionization (REMPI) with time-of-flight mass analysis. In the latter experiments, semiconductor NC produced by LAM will be precooled to ~150 K and then expanded through a pulsed nozzle to achieve phonon temperatures less than 20K. Such experiments have the advantage of obtaining spectra in vacuum--free of substrate and environmental effects; and REMPI can obtain spectra of nonradiative, surface defect states. We hope that a comparison of the single-particle fluorescence spectra of nanoparticles with REMPI will develop a clearer understanding of the quantum states for semiconductor NC formed by LAM.

2.0 Single-particle spectra of semiconductor clusters

Our first experiments to measure microluminescence from isolated Si-NC produced by LAM were unsuccessful. Fluorescence was quenched either by nonradiative trap states on the surface of the particle or the bulk bandgap was filled by strain produced by surface reconstruction.¹ Following this initial failure, we prepared samples of silicon nanoparticles produced by LAM in He/H₂ and pure He carrier gases. In the case of the He/H₂ carrier gas, hot nanoparticles (T~2000K) ejected into the cooling He/H₂ laser plasma after nucleation may grow a hydride capping layer before surface reconstruction. A second set of samples produced in pure He carrier gases were exposed to air after collection so they formed native oxide coatings; a third set of samples were first exposed to H₂ at the collection wafers. All three types of particles produced no fluorescence when excited at 488 nm.

Since surface defects have proven to be less of a problem for CdSe NC, we measured spectra of isolated, individual particles collected on sapphire substrates. Charging and bleaching was not a problem, and we found that 50% of the nanoparticles observed were fluorescent. We did not observe the blinking of the particles as observed by Bawendi, and coworkers,² perhaps because of dry collection. An example spectrum is shown in Fig. 1 where we observed a broadened spectrum as expected for excitons at room temperature; the doublet structure suggests a small cluster of nanoparticles consistent with its large Rayleigh scattering intensity. Subsequent experiments attempting to observe similar particles at low temperatures were not successful. Analysis by XRD using high-resolution TEM of particles produced during the same run and captured on carbon grids

¹Bare silicon nanoparticles with surface reconstruction are expected to be metallic, see Lei Liu, C. S. Jayanthi, and Shi-Yu Wu, "Factor Responsible for the Stability and the Existence of a Clean Energy Gap of a Silicon Nanocluster," to be published J. Appl. Phys.

²Shimizu, K.; Emedocles, S. A.; Neuhauser, R.; Bawendi, M. G. Stark spectroscopy investigation of spectral diffusion in single CdSe quantum dots Proc. - Electrochem. Soc., 98-19 (Quantum Confinement: Nanostructures), 1999, pp. 280-285

intensity fluctuations of the high-harmonic generation source. We plan to use phase stabilized ultrafast laser-amplifier sources to study absolute-phase sensitive nonlinear optics.

Publications (refereed) as a result of DOE support

1. P. E. Zeek, R. Bartels, M. M. Murnane, H. C. Kapteyn, and S. Backus, "Adaptive pulse compression for transform-limited 15fs high-energy pulse generation," *Opt. Lett.* **25**, 587 (2000).
2. R. Bartels, S. Backus, E. Zeek, L. Misoguti, G. Vdovin, I. P. Christov, M. M. Murnane, H. C. Kapteyn, "Shaped-pulse optimisation of coherent soft-x-rays," *Nature* **406**, 164-166, 2000.
3. R. Bartels, S. Backus, I. P. Christov, M. M. Murnane, H. C. Kapteyn, "Attosecond timescale feedback control of coherent x-ray generation", invited paper, *Chemical Physics* **267**, 277 (2001).
4. S. Backus, R. Bartels, S. Thompson, R. Dollinger, H. C. Kapteyn, M. M. Murnane, "High efficiency, single-stage, 7 kHz high average power ultrafast laser system", *Optics Letters* **26**, 465 (2001).
5. L. Misoguti, S. Backus, C. Durfee, R. Bartels, M. Murnane and H. Kapteyn, "Generation of broadband VUV light using third-order cascaded processes", *Physical Review Letters* **87**, 13601 (July 2, 2001).
6. I.P. Christov, M. M. Murnane and H.C. Kapteyn, "Attosecond time-scale intra-atomic phase matching of high harmonic generation", *Physical Review Letters* **86**, No. 24, 5458 (2001).
7. R. Bartels, T. Weinacht, N. Wagner, M. Baertschy, C. Greene, M. Murnane, H. Kapteyn, "Phase Modulation of Ultrashort Light Pulses using Molecular Rotational Wavepackets", *Physical Review Letters* **88**, 019303 (2002).
8. C. Durfee, L. Misoguti, S. Backus, R. Bartels, M. Murnane and H. Kapteyn, "Phase Matching in Cascaded Third-Order Processes, *JOSA B* **19** (4): 822-831 (2002).
9. S. Christensen, H.C. Kapteyn, M.M. Murnane, and S. Backus, "Simple, high power, compact, intracavity frequency-doubled Q-switched Nd:YAG laser," *Review of Scientific Instruments* **73** (5): 1994-1997 (2002).

Publications (not refereed) as a result of DOE support

10. L. Misoguti, C. Durfee, S. Backus, M. Murnane, H. Kapteyn, "Generation and measurement of ultrafast tunable VUV light", *OSA Proc. Ultrafast Phenomena XII* (Springer Series in Chemical Physics 66), p. 112.
11. R. Bartels, S. Backus, I. Christov, L. Misoguti, E. Zeek, M. Murnane, H. Kapteyn, "Coherent Control of XUV Radiation", *OSA Proc. Ultrafast Phenomena XII* (Springer Series in Chemical Physics 66), p. 42.
12. R. Bartels, T. Weinacht, M. Baertschy, N. Wagner, C. Greene, M. Murnane, H. Kapteyn, "Self-Compression of Ultrafast Optical Pulses using Molecular Phase Modulation", *OSA Proc. Ultrafast Phenomena XIII* (Springer Series) to be published.
13. S. Backus, R. Bartels, S. Thompson, S. Christensen, H. Kapteyn, M. Murnane, "High average power, 10kHz, ultrafast laser system", *OSA Proc. Ultrafast Phenomena XIII* (Springer Series) to be published

Publications submitted as a result of DOE support

14. R. Bartels, N. Wagner, M. Barschety, J. Wyss, M. Murnane, H. Kapteyn, "Phase matching conditions for nonlinear frequency conversion using aligned molecular gasses", submitted to *Optics Letters*.
15. L. Misoguti, R. Bartels, I.P. Christov, S. Backus, M. Murnane, H. Kapteyn, "Nonlinear Optics in the Extreme Ultraviolet", submitted to *Physical Review Rapid Communications*.

News articles as a result of DOE support

1. "Physicists progress towards x-ray laser", *INSIDE R&D ALERT*, John Wiley & Sons, Inc., July 2000.
2. "Pulse-Shaping Yields Efficient X-Ray Generation", *Photonics Spectra*, Tech. World Briefs, Nov. (2000).
3. "Pulse Shaping Improves Efficiency of Soft-X-Ray Generation", *Physics Today*, Search & Discovery, Sept. 2000.
4. "Coherent Control of Soft-X-Rays", *Optics News in 2000*, *Optics & Photonics News*, Dec. 2000.
5. "Single-stage system boasts high power", *Eye on Technology in OE Magazine*, June 2001.
6. "Powerful Ultrafast Sources get Small", *Laser Focus World*, World News Section, August 2001.
http://fw.pennnet.com/Articles/Article_Display.cfm?Section=Articles&Subsection=Display&ARTICLE_ID=113661
7. *Photonics Spectra*, "Generation of Broadband VUV Light", Fall 2001.

demonstrated that the particles had become Cd rich over several weeks of storage (in argon) while waiting access to the microluminescence apparatus. Oxidation resulted in loss of Se in the form of SeO_2 .

In order to prevent the formation of surface states upon exposure to atmosphere, single particle spectra of isolated nanoparticles will require that particles captured on sample wafers be transported within UHV to a microluminescence or near-field spectroscopy apparatus. We plan to add such a diagnostic chamber to a recently constructed, apparatus capable of LAM followed by collection in UHV.

3.0 Nanocrystals in solution

Though our ultimate goal is to prepare dry samples for single particle spectroscopy, we now collect NC at large density in solution. The capping molecules can slow oxidation sufficiently² to test if the as produced particles are fluorescent. Particles are tested using a fluorimeter to determine the quantum efficiency for fluorescence and to measure the room temperature absorption and fluorescence spectra. We first tried supersonic impaction into either Nonanoic acid or a solution of 10% by mass Tri-octylphosphine oxide (TOPO) in octanol. We can recirculate the solution through the collection region many times and hence produce very high densities of nanocrystals in the liquid.

Stabilization of NC in surfactants

Nonanoic acid as a collection liquid has several interesting properties. It has a strong affinity for the surface of the CdSe NC, however, the surface passivation is not complete, resulting in loose flocculation of the particles. This property is valuable because it allows nanoparticle solutions to be further concentrated from the collected solution and even "slurries" of nanoparticles can be produced approaching 25% mass density. Unfortunately, the incomplete surface capping leads to an inability to carry out size selective precipitation so as to narrow size distribution to a ~5% dispersion.

We have experienced similar behavior with silver nanoparticles captured in Nonanoic acid. As produced, the sample solutions are opaque and a dark gray to black in color. If allowed to settle, a dense precipitate forms at the bottom of the test tube. We find, however, that we can stabilize the nanoparticles in solution by annealing the sample at temperatures from 75 to 140 C for several hours. A sequence of beautiful color changes occurs with time, progressing from a muddy brown color, to dark orange, and translucent yellow. Finally the samples become as transparent as water, even at nanoparticle densities of ~10 mg g/ml. Once transparent, it is difficult to remove the particles, even by centrifugation. Measuring the degree of light extinction using a spectrophotometer, we found a thermally activated, first order stabilization rate with an energy barrier of 0.44 eV/molecule. We believe this successful suspension of the particles results from a change in the surface coverage, due to a change in surface orientation for binding of the surfactant molecule.

We confirmed this model by measuring the Raman spectra of Nonanoic molecules on the surface of the nanoparticles. This was achieved using a micro-Raman apparatus. Because of enhanced Raman scattering for molecules bound to the surface, spectra could be obtained for molecules bound to the surface of only a few nanoparticles. Samples were prepared placing a drop of a dilute solution of nanoparticles onto silicon collection wafers, excess Nonanoic acid was then removed by evaporation at room temperature for a period of 24 hrs. Non-annealed samples showed symmetric and antisymmetric stretch modes for the COOH group of Nonanoic acid and for the carbon backbone we observed both wagging and stretch modes. For nanoparticles prepared from annealed samples the backbone modes were absent and the antisymmetric COOH mode decreased in intensity relative to the symmetric one. Both changes are consistent with a greater

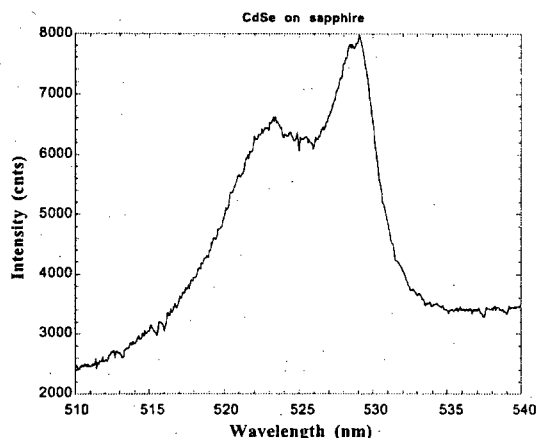


Fig. 1. Microluminescence of CdSe NC collected dry on sapphire substrates. The particles were produced in 1 atm of N_2 and collected dry on sapphire substrates.

fraction of of the surface bound molecules having an "upright" orientation relative to the surface plane of the nanoparticle.

Direct-gap fluorescence of Si-NC

Si-NC were produced and collected dry on carbon films and as suspensions in ethylene glycol. The NC were produced both in a pure helium aerosol and a He/10% H_2 aerosol. In recent studies of Si-NC formed by ion implantation in SiO_2 , Min, *et al.* found annealing samples in hydrogen removed the fluorescence from defects in implanted SiO_2 , it also significantly increased the quantum efficiency for size selective fluorescence centered at 780 nm.³ They surmised that the diffusion of hydrogen to the surface of the Si-NC passivated dangling bonds. We hoped that capping the bonds at the creation of the particle would similarly prevent non-radiative trap states. HRTEM of the samples collected on carbon films demonstrated that the mean size was ~ 3 nm and particles larger than 10 nm were crystalline. Solvents used in preparing the suspensions were degassed in vacuum to remove dissolved gases. An "as made" UV-visible absorption spectra is shown in Fig. 2. The absorption spectra of the silicon microparticles (MP) are also shown in Fig. 2 with the known $\Gamma_{25}-\Gamma_{15}$ direct gap band edge. The spectrum of the MP is similar to bulk silicon. The absorption edges for nanoparticles formed in both aerosols are similar to that observe by Wilcoxon, *et al.*⁴ for 2 nm diameter NC grown in inverse micelles. The absorption seen in Fig. 2 is small; we estimate an absorption cross section of 10^{-17} cm^2 at 250 nm, nearly 10^{-2} that of the Mie absorption calculated for similarly sized metal nanoparticles.

Photoluminescence spectra were taken with 300 nm wavelength excitation. Surprisingly, only the Si-NC sample prepared in pure helium exhibited weak PL. The observed spectrum, shown in Fig. 3, is very similar to that of Wilcoxon, *et al.* They attributed the uv emission to direct band gap recombination which is blue-shifted due to quantum confinement of the small particles. They also observed a small absorption feature around 500-550 nm that yielded a smaller emission near 600 nm which was attributed to surface or defect recombination because its position was independent of mean size. Our fluorescence efficiency is about an order of magnitude less than Wilcoxon's, perhaps due to the longer excitation wavelength of 300 nm vs their 245 nm. The weakness in fluorescence is due to the QE and the small absorption cross section at 300 nm.

The very weak fluorescence at 665 nm is shorter in wavelength and narrower than the indirect gap emission observed by Min, *et al.*³, likely due to a smaller size. We do not see the 600 nm emission assigned to oxide defects by Wilcoxon, *et al.*

We are currently measuring PL at excitation wavelengths varying from 250 to 500 nm. We are also using anhydrous and oxygen free solvents and handle the solvents in a glove box to eliminate the questions of impurities from those sources.

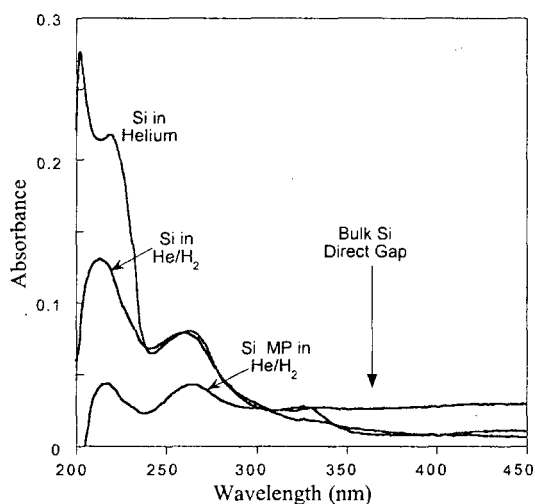


Fig. 2 Absorption spectra for Si-NC in ethylene glycol. A spectra for a sample of Si microparticles (Si MP) prepared without the laser is included.

³ K. S. Min, K. V. shcheglov, C. M. Yang, Harry A. Atwater, M. L. Brongersma, and A. Polman, "Defect-related versus excitonic visible light emission from ion beam synthesized Si nanocrystals in SiO_2 ," *Appl. Phys. Lett.* **69**, 2033(1996).

⁴ J. P. Wilcoxon, G. A. Samara, and P.N. Provencio, "Optical and electronics properties of Si nanoclusters synthesized in inverse micelles, *Phys. Rev. B* **60**, 2704 (1999)

4.0 Future Research

We have also built and tested a new design for a powder feeder so that semiconductor NC produced by LAM can be expanded in a supersonic jet. The new aerosol generator employs a small drum head driven by an oscillating solenoid. Powder resting on the drum head is driven vertically into the atmospheric gas and then descends slowly. As the gas column traverses the cloud particles are carried down stream toward the nozzle. We have measured particle densities of 10^7 cm^{-3} in the output tube of this device. The design is compact, operates better at the high pressures preferred by the nozzle, and operates independently of the pressure and flow rate of the aerosol.

We have finished the construction of an apparatus to deposit nanoparticles on single, crystal, clean substrates held in ultra-high vacuum. The samples can then be moved into a second chamber where thin films of high band-gap semiconductors or glasses can be grown by laser or ion beam sputtering. The apparatus has achieved pressures of 10^{-12} Torr, and neutralized ion-beam sputtering has been demonstrated. Films of hydrogenated Si nanoparticles have been passivated by SiO_2 coating with ~ 10 nm thickness. We have also produced films of GaN nanoparticles passivated by AlN films. In addition to the spectroscopy experiments above, single particle spectroscopy and measurements of the second and third order nonlinear susceptibilities will be made on these new samples.

5.0 DOE Supported Publications

1. H. Htoon, J. W. Keto, O. Baklenov, and A. L. Holmes, Jr., C. K. Shih, "Cross-sectional Nanophotoluminescence Studies of Stark Effects in Self-Assembled Quantum Dots," *Appl. Phys. Lett.* **76**, 700-702(2000).
2. W.T. Nichols, G. Malyavanatham, M.P. Beam, D.E. Henneke, J.R. Brock, M.F. Becker, and J.W. Keto, "Synthesis of nanostructured wc films by supersonic impaction of nanoparticle aerosols," *Nanophase and Nanocomposite Materials III, Vol. 581*, (Material Research Soc., Pittsburg), p. 193-198, 2000.
3. H. Htoon, Hongbin Yu, D. Kulik, J. Keto, C.K. Shih, O.I Baklenov, and A. L. Holmes, "Nanophotoluminescence studies of self-assembled quantum dots," *Self-organized Processes in Semiconductor Alloys-Vol. 583* (Material Research Soc., Pittsburg), p. 105-111, 2000.
4. S. K. Jo, J. H. Kang, X. Yan, J. M. White, B. Gong, J. G. Ekerdt, J. Keto, and J. Lee, "Direct absorption of gas-phase atomic hydrogen by Si(100): a narrow temperature window," *Phys. Rev. Lett.* **85**, 2144(2000).
5. William T. Nichols, Gokul Malyavanatham, Dale E. Henneke, James R. Brock, Michael F. Becker, John W. Keto, and Howard D. Glicksman, "Gas and Pressure Dependence for the Mean Size of Nanoparticles Produced by Laser Ablation of Microparticles in Aerosols", *J. of Nanoparticle Res.* **2**, 141-145(2000).
6. James M. Kohel and J. W. Keto, "Two-photon laser-assisted reactions in Xe and Cl_2 gas mixtures," *J. Chem. Phys.* **113**, 10551(2001).
7. W.T. Nichols, D.E. Henneke, G. Malyavanatham, M.F. Becker†, J.R. Brock, and J.W. Keto, and H. D. Glicksman, "Large scale production of nanocrystals by laser ablation of aerosols of microparticles," *Appl. Phys. Lett.* **78**, 1128-1130(2001).
8. W. T. Nichols, G. Malyavanatham, D. T. O'Brien, D. Kovar, M. F. Becker, and J. W. Keto, "Supersonic nanocrystal deposition for nanostructured materials," *Mat. Res. Soc. Symp. Proc.* **703**, (Material Research Soc., Pittsburg, 2002), p 5.51-5.56.
9. Dale E. Henneke, William T. Nichols, Gokul Malyavanatham, Michael F. Becker and John W. Keto, "Reduced flocculation of silver nanocrystals in nanoic acid: a thermal induced change in surface structure observed with Raman spectroscopy," submitted.

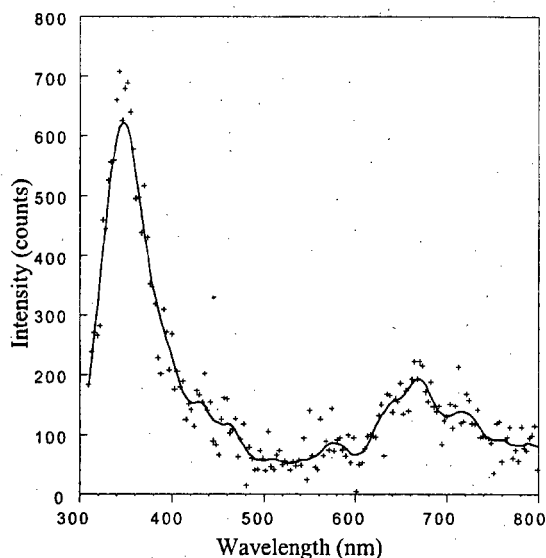


Fig 4. Plot of Si-NC luminescence. The PL spectra was obtained by subtraction of the ethylene glycol spectra (Raman peak) from the Si-NC data. A "smoothing" fit was applied as an aid to the eye.

- “Physics of Low-Dimensional Bose-Einstein Condensates”, Grant No. DE-FG02-01ER15203

Eugene B. Kolomeisky (PI)
Department of Physics
University of Virginia
382 McCormick Road
PO Box 400714
Charlottesville, VA 22904-4714
ek6n@virginia.edu

- The project consists in investigating fundamental properties of low-dimensional superfluids (Bose-condensed alkali gases in strongly anisotropic traps, for example) and related systems within a wider scope of the DOE Nanoscale Science, Engineering, and Technology Initiative.

- **Recent Progress.** During the period of September 2001 – August 2002 we have been working on several (mostly completed) projects described below in more detail:

1. ***Superfluid flow past an obstacle*** [with T. J. Newman (Co-PI) and X. Qi (graduate student)]. A direct measure of superfluidity is the possibility of dissipation-free flow of the fluid under question past an obstacle. We studied this problem analytically and numerically in one spatial dimension using a one-dimensional hydrodynamic theory that we developed earlier in Phys. Rev. Lett. **85**, 1146 (2000). The outcome of the investigation is a phase diagram of the system representing the regions of normal and superfluid behavior depending on the flow velocity and the properties of the obstacle as well as insight into the mechanism by which superfluidity breaks down. We found that although the sound velocity plays a crucial role in the stability of the superflow, both subsonic and *supersonic* superfluidity is possible. The existence of supersonic regime is an entirely new finding, and is facilitated if the effective potential created by the obstacle is smooth. We have also found that the onset of normal behavior can be linked to the generation of solitons previously identified in Phys. Rev. Lett. **85**, 1146 (2000). A paper detailing these findings will be written up within the next few months as we are currently studying similar problems in two spatial dimensions.

2. ***Manifold self-localization in a deformable medium*** (with J. P. Straley), submitted to Physical Review B. The concepts of domain walls, flux lines, and interfaces (manifolds, for brevity) are central in condensed matter physics. In all known experimental situations these objects are placed in a medium which could be a magnet, superconductor, or just a plain crystal. The medium deforms in response to the presence of the manifold. This deformation may provide an effective “self-localizing” potential for the manifold. We studied how this self-localizing effect influences manifold properties. We found that the manifold can either become self-localized, i.e. the deformation field will follow the manifold displacement, or it will

remain free. The precise conditions dependent upon space dimensionality and strength of the manifold-medium coupling are established.

3. ***Quantum fluctuations of charge and phase transitions of a large Coulomb-blockaded quantum dot*** [with Robert M. Konik (postdoctoral associate) and X. Qi], published in Physical Review B. Quantum dots are nanometer-scale structures hosting a few to a few thousand electrons and coming in a variety of forms. A useful mental picture of a dot is that of a container for electrons connected to a reservoir through a tunneling junction and placed nearby a gate electrode. The role of the gate electrode is to create favorable electrostatic conditions for the dot to host a desirable number of electrons. This number is controlled experimentally and is not necessarily integer. On the other hand, the electrons are discrete, and can only enter the dot one by one. As a result, the electrons enter the dot only at special values of the gate voltage, and most of the time the dot population does not respond to changes in the gate voltage. This phenomenon predicted in the mid 80s and first observed in the early 90s is called Coulomb blockade. One of its hallmarks is the dependence of the population of the dot on the gate voltage consisting of plateaus corresponding to an integer number of electrons on the dot – the celebrated Coulomb staircase. This classical picture is modified qualitatively even at zero temperature because in reality the dot is never completely isolated from the reservoir. Earlier studies concluded that even infinitesimally weak coupling between the dot and reservoir will smear the Coulomb staircase. In our work the whole problem is re-examined for the case when the system is placed in a strong magnetic field (which means electrons are effectively spinless), and the electrons are interacting. We found that the old conclusion that the Coulomb staircase will be always smeared is just one of the possible answers. Depending on the way the dot and reservoir are coupled, and depending on the strength of interaction between the electrons, a modified staircase can survive in certain cases. One of our most intriguing predictions is the existence of the range of parameters where the population of the dot jumps from a near integer value to a region of stable population centered about a *half-integer* value. The origin of this effect is purely quantum-mechanical and remotely similar to the classical effect of inverted pendulum. The results of this work were delivered at the 2001 Meeting of the Southeastern Section of the APS (by E. B. Kolomeisky), and at the 2002 March Meeting of the APS (by R. M. Konik). We have also solved similar problem and arrived at similar conclusions for electrons with spin. A paper detailing this study will be written up soon.
4. ***The Bose molecule in one dimension*** (with J. P. Straley) submitted to Physical Review B. We consider a collection of *attractive* bosons with short-range interactions in one dimension. This setup has been recently realized experimentally in a Li-7 vapor [L. Khaikovich et al., Science **296**, 1290 (2002); K. E. Strecker et al., Nature **417**, 150 (2002)] confined to an atomic trap which is so tight in two directions, that the system can be regarded as one-dimensional with respect to the third direction. This system is interesting because it is an example of a many-body bound state having the form of a well-localized “molecule”. Some of the properties of this molecule can be computed either exactly or using the Gross-Pitaevskii theory

thus shedding some light on the range of applicability of the mean-field approach. We have computed the Green function, momentum distribution, two-particle correlation function, and structure factor which all can be independently measured in experiment.

- **Future plans**

1. ***The Bose atom in one dimension.*** In a series of applications it is important to understand the ground-state properties of a system of repulsive bosons with short-range interactions confined to one dimension in the presence of an attractive center, the “nucleus”. The examples include real atoms in superstrong magnetic fields, flux lines in superconductive films in the presence of a linear pin, and one-dimensionally confined Bose-condensates in the presence of an artificial small-size potential well. The last application is of particular interest because the strength of the “nuclear” attraction can be tuned (an experiment in that direction is under way in the group of Professor Sackett of our Department). Even in its simplest form this problem cannot be exactly solved. On the other hand, for fixed number of “electrons” the problem can be solved accurately in the limits of either strong or weak nuclear attraction. The former will involve the Gross-Pitaevskii theory while the latter will use our theory of Phys. Rev. Lett. **85**, 1146 (2000).
2. ***Quantum dissociation of a one-dimensional chain*** (with X. Qi). One of the most intriguing uses of carbon nanotubes and their bundles is as hosts for foreign atoms. The axial confinement imposed by the tubes provides favorable conditions to experimentally study various phases of matter in one dimension. Inspired by these developments we are looking at the ground-state properties of a one-dimensional chain of particles at zero temperature. We believe that the combined effect of zero-point motion and anharmonicity can lead to a dissociation of the chain which will be a nontrivial example of a liquid-gas transition in one dimension.

- **DOE sponsored publications**

E. B. Kolomeisky, R. M. Konik and X. Qi, *Quantum fluctuations of charge and phase transitions of a large Coulomb-blockaded quantum dot*, Phys. Rev. B **66**, 075318 (2002).

Program Title:

"Ion/Excited-Atom Collision Studies with a Rydberg Target and a CO₂ Laser"

Principal Investigator:

Stephen R. Lundeen,
Dept. of Physics
Colorado State University
Ft. Collins, CO 80523
Lundeen@Lamar.colostate.edu

Program Scope:

The program involves four projects, three involving the interaction of multiply-charged ion beams with a Rydberg target, and one involving multiply-excited Rb atoms in a MOTRIMS target.

- 1) Continued studies of charge transfer, aiming to reveal details about the L-distributions formed in the collisions.
- 2) Studies of X-rays emitted from the highly-excited Rydberg ions formed in these collisions.
- 3) Studies of the fine structure of high-L Rydberg ions, in order to extract measurements of dipole polarizabilities and quadrupole moments of the positive ion cores.
- 4) Stepwise excitation of a Rb MOT to 4D and higher Rydberg states within a MOTRIMS apparatus.

Recent Progress and Immediate Plans:

Project 1) This project was completed last year. A paper describing the results appeared this year and is listed among our publications.

Project 2) We completed the first phase of this experiment this year. By studying the variation with electric field of the X-ray spectrum emitted by H-like and He-like Silicon after capture of an electron from our Rydberg target, we were able to deduce the fraction of captures which resulted in a state of low m (-1, 0, 1). Fig. 1 shows a typical spectrum emitted by He-like Si. The two lines visible are: 1) K α decay from 2 to 1. 2) direct decay to the 1S ground state from the n ~ 72 states formed in capture. Fig. 2 shows the ratio of these two features as a function of the external electric field at

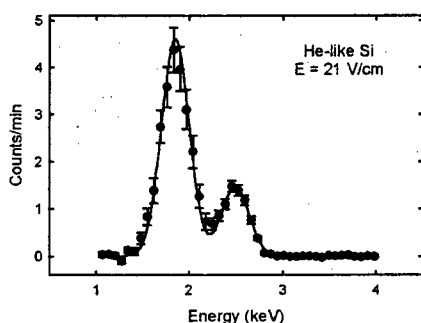


Fig. 1. X-ray spectrum from He-like Silicon after capture from the Rydberg target in the presence of a external electric field.

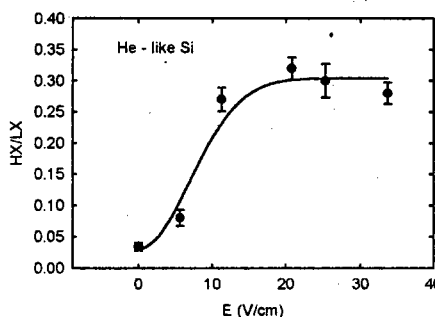


Fig. 2. Ratio of two spectral features in Fig. 1 as a function of applied E-field.

the point of emission. The enhanced decay to 1S results from the Stark mixing of high-L Rydberg states of low m. From the limiting ratio of these features, and independently from the ratio of feature 2) to the total charge transfer rate, we deduce a low m fraction of about 40%, much higher than a statistical distribution (4%). A paper reporting this result will appear shortly in Phys. Rev. A, and is listed in our publications.

A further study is planned extending the range of Rydberg targets and the range of bare ions studied. We would like to check the scaling with target n and ion charge Q of the critical electric field.

Beyond this, we are designing an improved apparatus including a "Stark Barrel" which will allow application of electric fields at arbitrary angles to the beam direction. The rate of HX emission as a function of electric field direction should give new information about the emitting populations.

Project 3) We decided last year to focus our effort here on measuring the fine structure of Rydberg Silicon ions, as a proof of principal for our proposed studies of Rydberg actinide ions. The Silicon studies are now progressing well. We have measured five fine structure intervals in the n=29 level of Si^{2+} , using microwave methods. Fig. 3 shows some typical data, and Fig. 4. shows the inferred fine structure. One problem we encountered was the presence of small stray electric fields (~ 100 mV/cm) within our microwave interaction regions. These cause Stark shifts of the observed transitions. In order to measure and correct for these shifts, we observed Helium fine structure resonances in the same apparatus. These have been previously studied, and their frequencies, as well as their Stark shift rates are well known. A short paper reporting these results is in preparation.

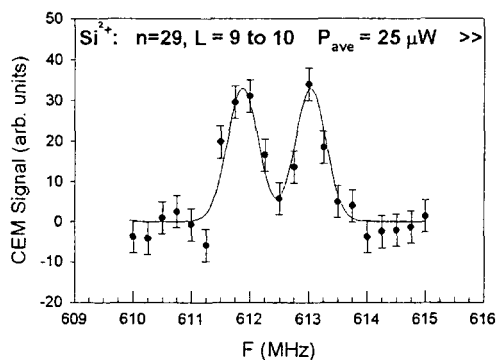


Fig. 3. Microwave resonance showing the transition from L=9 to L=10 in Si^{2+} , n=29.

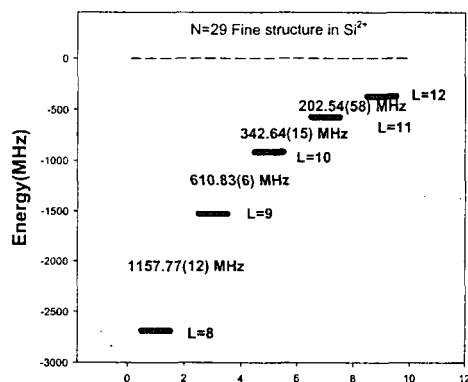


Fig. 4. Fine structure of the n=29 state of Si^{2+} , as determined from our recent study.

The next phase of the Silicon-Ion study will be to look at the fine structure of several other ionization states of silicon. It is hoped that these further studies will help to identify potential difficulties with the technique.

Project 4) As a first step in this project, we used our Solid state laser at 1529 nm to excited the Rb MOT to the $4^2\text{D}_{5/2}$ level. When this laser was on, the MOTRIMS spectrometer was able to distinguish collision events coming from all three initial states,

5S, 5P, and 4D. When the 1529 laser was off, the 4D events rapidly disappear, along with the 4D population. This observation was extremely suggestive, and it led us to realize the potential of the MOTRIMS technique for simultaneous measurement of relative cross sections and relative populations. A short paper describing this idea has been submitted for publication and is under review. It is included in our publication list.

In preparation for further studies of this type, we have improved our frequency locking method for the 1529 nm laser, and are preparing to pump it into the MOT area on a regular basis. Eventually, we also plan to send a sample of our TiSapphire laser, which can be used to further excite the MOT from the 4D state into nF states,

Recent Publications:

1) "Energy transfer in Ion-Rydberg-atom charge exchange," D.S. Fisher, S.R. Lundeen, C.W. Fehrenbach, and B.D. DePaola, Phys. Rev. A 63, 052712 (2001)

2) "Experimental studies of resonant charge transfer from Rydberg states of Highly-Charged Ions," S.R. Lundeen, D.S. Fisher, C.W. Fehrenbach, and B.D. DePaola, Physica Scripta T92, 71 (2001)

3) "Experimental studies of L-distributions from charge capture by Si^{3+} on Rydberg atoms", S.R. Lundeen, R.A. Komara, C.W. Fehrenbach, and B.D. DePaola, Phys. Rev. A 64, 052714 (2001)

4) "State selective charge transfer cross sections for Na^+ with excited rubidium: A unique diagnostic of MOT population dynamics," X. Flechard, H. Nguyen, S.R. Lundeen, M. Stauffer, H.A. Camp, C.W. Fehrenbach, and B.D. DePaola, submitted to Phys. Rev. A.

5) "Stark-induced X-ray emission from high Rydberg states of H-like and He-like Silicon ions," M.A. Gearba, R.A. Komare, S.R. Lundeen, W.G. Sturuss, C.W. Fehrenbach, B.D. DePaola, and X. Flechard, to be published, Phys. Rev. A.

Correlation in dynamic multi-electron systems

Jim McGuire

Department of Physics, Tulane University, New Orleans, LA 70118-5698

mcguire@tulane.edu

Both spatial electron correlation, arising from internal electron-electron interactions, and time correlation between electrons, arising from time ordering of the external interactions, can give rise to observable effects. Our general method [1-3] may be used for photon, as well as charged particle impact, and has been applied to two coupled-channel equations for 2s-2p transitions. Cross sections for double excitation, ionization with excitation in helium were evaluated in a full second Born calculations that include principal value terms. Our second Born calculations are compared to calculations in the independent electron approximation (iea), where spatial correlation between the electrons is removed. Comparison is also made to calculations in the independent time approximation (ita), where time correlation between the electrons is removed. We discuss the use of multiple times in the quantum N-body problem.

Most complex atomic and molecular systems cannot be adequately described in terms of independent transitions of electrons. In applications from molecular dynamics to quantum computing, correlation between electrons increases and modifies reaction pathways. These dynamic electronic connections can redistribute energy and facilitate transitions that would otherwise be forbidden. These correlations in time are caused by external interactions, such as strong electro-magnetic fields together with internal interactions, such as the Coulomb interactions between electrons or spin-spin interactions. These interactions can be used to shape and dynamically control nanostructures. The problem of time correlation in multi-electron systems has recently been addressed theoretically with inclusion of corresponding energy non-conserving terms. However, the effect of time correlation between electrons has not been previously confirmed by experiment, as reported here.

The focus of our work this year is time correlation in dynamic multi-electron systems. Interconnection of different electrons in time requires both internal electron correlation, which interconnects the electrons, as well as time ordering, which imposes a causal-like sequencing of interactions in quantum time propagation. Electron correlation is relatively well understood. Time ordering comes from the time-dependent Schrödinger wave equation, which determines the equation for the time evolution operator, $U(t_2, t_1)$, which describes how the system changes between time t_1 and time t_2 . The formal solution for the evolution operator may be expressed,

$$U(t_2, t_1) = \sum_{n=0}^{\infty} \frac{(-i\hbar)^n}{n!} \int_{t_1}^{t_2} dt^{n'} \dots \int_{t_1}^{t_2} dt^{n''} \int_{t_1}^{t_2} dt' T V(t^{n'}) \dots V(t^{n''}) V(t'). \quad (1)$$

Here $V(t)$ is the interaction (or sum of interactions) of a system of atoms with light or matter and T is the Dyson time ordering operator, which imposes the causality-like constraint that

$V(t^l)V(t^k) = 0$ if any $t^l < t^k$. The time ordering operator T provides a time connection between pairs of interactions due to the constraint that the interactions occur in the order of increasing time.

The independent time approximation (ITA) corresponds to independent time evolution of different electrons, namely,

$$U(t, t_0) = \Pi_j^N U_j(t, t_0) \quad (\text{ITA}) \quad (2)$$

Time correlation, corresponding to deviation from Eq.(2), arises from the enforcement of time ordering on the sequence of interactions, $V(t^n) \dots V(t'') V(t')$, which cause the system to change. The time ordering operator T may be decomposed into two terms, namely, $T = T_{\text{cor}} + T_{\text{unc}}$. The correlated term, T_{cor} , gives the time correlation between electrons and regulates sequencing of the Interactions $V(t)$. The uncorrelated term, T_{unc} , is the time independent part of T , which does not connect the various interactions $V(t)$ in time and thus eliminates both sequencing and time correlation in the time evolution of the system. For a two-electron transition occurring via $V_1(t)$ and $V_2(t)$ respectively, we have shown that in second order,

$$T_{\text{unc}} V_2(t'')V_1(t') = 1/2 (V_2(t'')V_1(t') + V_2(t')V_1(t'')), \quad (3a)$$

so that

$$T_{\text{cor}} V_2(t'')V_1(t') = 1/2 \text{sign}(t''-t') [V_2(t''), V_1(t')], \quad (3b)$$

Here $\text{sign}(t'' - t') = (t'' - t')/|t'' - t'|$ is a unit vector in the direction of increasing time, and $[V_2(t''), V_1(t')] = V_2(t'')V_1(t') - V_1(t')V_2(t'')$ explicitly requires a time connection between interactions at different times, t' and t'' . This represents non-local quantum time entanglement between electrons. The Fourier transform of T_{cor} gives the principal value part of the energy propagator. This quantum term violates conservation of energy for short times. This effect is not present in the propagation of classical waves.

In the independent electron approximation, where spatial correlation between electrons is removed, the quantum commutator $[V_2(t''), V_1(t')]$ is zero. Then each electron evolves independently in time, i.e. the evolution operator, $U(t_2, t_1)$, reduces to a product of single electron evolution operators. When spatial correlation between electrons is included, e.g. via two-body Coulomb electron-electron interactions, $[V_2(t''), V_1(t')]$ is non-zero, and the time evolution of different electrons may become entangled. Time correlation between electrons corresponds to cross correlation between the time propagation of amplitudes for different electrons, and describes how electrons communicate about time.

Time ordering is generally thought to be needed to understand the difference observed in double ionization of atoms by protons and anti-protons at high velocities. Nonetheless, there has been

no previous direct experimental evidence for time correlation between different electrons. Our data for ionization of atomic helium with concurrent excitation of a second electron into various magnetic sublevels of the 2p excited state now provides evidence for correlation in the time evolution of different electrons. This means, for example, that one sequence of interactions may differ from another, as illustrated by the equation for T_{cor} given above.

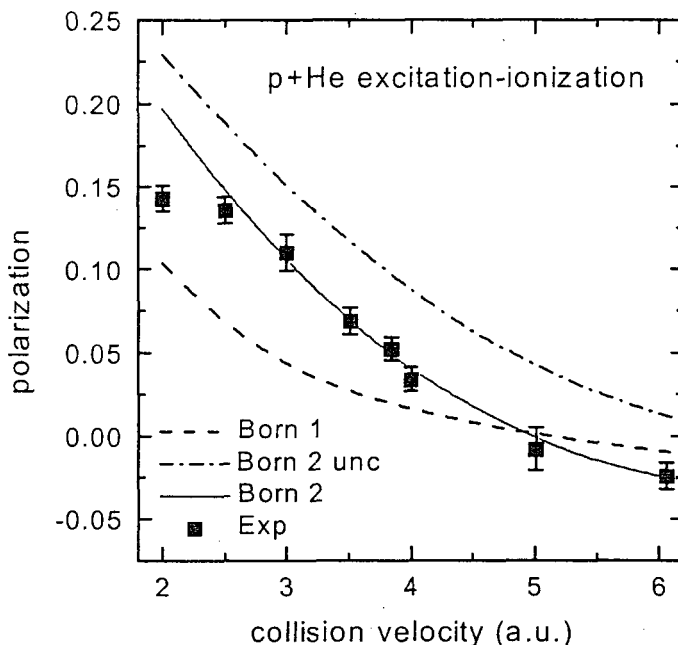


Fig. 2. Calculations with and without time correlation of electrons compared to experimental data. Here polarized light is emitted from helium following $1s - 2p$ excitation of one electron accompanied by ionization of the second electron. The polarization fraction is plotted as a function of the velocity of the incident proton. The first-order calculation (Born 1) has no time correlation, nor does the second-order calculation without time correlation (Born 2 unc). The full second-order calculation (Born 2) includes time correlation by including T_{cor} from Eq. (3a). The data is from Merabet et al..

In figure 1 we present both data and theory for the polarization of light emitted from the 2p level of excited helium following excitation of one electron and ionization of another by an incident proton. It is evident that a first-order theory does not describe either the magnitude or the energy dependence of the polarized light observed. A second-order calculation in the on-energy-shell (or energy-conserving) approximation with $T_{\text{cor}} = 0$ provides some improvement, but still does not agree with the data. Only the second-order calculation including time correlation between electrons is in good agreement with observation, except at the lowest energy shown, where it is expected that higher order terms in $V(t)$ are significant. The method applies to incident photons as well as electrons, protons and ions.

In many cases the effects of time correlation between electrons are small. This is fortunate in that the off-shell, time-entangled terms require more than one hundred times more computer time to evaluate than the simpler on-shell, energy-conserving terms. In calculations of dynamically

correlated systems of particles, an independent time (or on-shell or wide band) approximation without time correlation is widely used to save computational time and effort. When this relatively easy independent time approximation is valid, calculations of relatively complex systems become feasible.

We have applied the independent time approximation in a two-coupled channel calculation. In the first step we have calculated the probability for a 2s-2p transition in hydrogen by photon impact with and without time ordering. The expression without time ordering is analytic, while the inclusion of time ordering requires numerical integration.

Also we have investigated the use of multiple times in the quantum N-body problem. It is possible to describe time evolution using different times for different particles under certain conditions. In the independent particle approximation, where inter-particle interactions are removed, the N-particle evolution operator factors into N single-particle evolution operators. In this limit one may use either a single time, with a single energy-time Fourier transform, or N different times with a different energy-time transform for each particle. Coherence between single particle amplitudes is lost if relatively strong randomly fluctuating residual fields influence each particle independently. Then the use of different times for different particles is required. When spatial correlation is present the use of multiple times is not feasible, even when the evolution of the particles is uncorrelated in time.

In summary correlations in the time evolution between electrons can be significant. This time correlation between electrons arises from energy-non-conserving quantum fluctuations occurring for short times in intermediate states of the system.

References:

1. McGuire J H, Godunov A L, Tolmanov S G, Shakov Kh Kh, Schmidt-Boecking H, Doerner R and Dreizler R M, Phys. Rev A **65**, 052706 (2001).
2. Godunov A L and McGuire J H, J. Phys. B **34**, L223-9 (2001).
3. Godunov A L, McGuire J H, Shakov, Kh Kh, Merabet H, Hanni J, Bruch R, and Schipakov V S, J. Phys. B. **34**, 5055 (2001).
4. Godunov A L, Bruch R, Merabet H, Schipakov V S, and McGuire J H, J. Phys. B. **34**, 1 (2001).
5. Godunov A L, McGuire J H, Shipakov V S and Crowe A, J. Phys. B **35**, L1 - L7, (2002).

PROGRESS REPORT ELECTRON-DRIVEN PROCESSES IN POLYATOMIC MOLECULES

Investigator: Vincent McKoy

A. A. Noyes Laboratory of Chemical Physics
California Institute of Technology
Pasadena, California 91125
email: mckoy@its.caltech.edu

PROJECT DESCRIPTION

This project aims to develop and apply accurate, scalable methods for first-principles computational study of low-energy electron-molecule collisions. Because our focus in applications is on polyatomic molecules, for which calculations are highly numerically intensive, the code developed is designed to run efficiently on large-scale parallel computers, including workstation clusters as well as tightly-integrated supercomputers.

HIGHLIGHTS

Over the past year we have applied the unique capabilities of our scalable, parallel computational methodology to a variety of electron-molecule collision problems of high interest. We have also continued developing and testing extensions to that methodology which allow high-accuracy calculations on large polyatomic molecules.

Principal developments this year:

- Electron cross section sets for plasma-processing gases
- Studies of electron interactions with DNA bases
- Several research papers published and presentations given at leading conferences
- Continued development and application of computational methods for high-accuracy studies of large molecules

MATERIALS-PROCESSING GASES

During the past year we completed and published several studies of fluorocarbon etchants and other gases used in plasma-based materials processing. In order to develop cross section sets of use in understanding and modeling plasma chemistry, we have collaborated in much of this work with other experimental and theoretical scientists having complementary expertise. Thus, for example, our extensive study of elastic and inelastic electron-collision processes in tetrafluoroethene, C_2F_4 [1], when combined with electron-swarm experiments, ionization cross section measurements, and plasma simulations, formed the basis for development of a validated electron cross section set for C_2F_4 [2]. Other molecules that we have studied recently include tetraethoxysilane (TEOS) [3] and SF_6 , for which we are currently completing calculations.

DNA BASES

The same computational methodology that has enabled electron collision calculations on fluorocarbons and other large molecules used in the semiconductor industry can be

applied to the study of low-energy electron collisions with biological molecules. Recent experimental work has stimulated interest in electron interactions with the nucleotide bases that pair up to join the two strands of DNA and that encode genetic information. Aflatooni *et al.* [4] directly measured the energies of temporary anion states (shape resonances) for the gas-phase nucleotides, while Boudaïffa *et al.* [5] demonstrated that dissociative attachment, which is mediated by such shape resonances, can produce single- and double-strand breaks in DNA and thus acts as a mechanism of radiation damage.

As first steps toward a detailed analysis of low-energy electron interactions with the DNA bases, we carried out calculations of low-energy elastic scattering cross sections for adenine, thymine, and cytosine in the static-exchange approximation. For cytosine, we extended the calculation to include polarization effects in order to obtain better resonance positions. Our results including polarization place shape resonances at 1.5 and 4.0 eV, in reasonably good agreement with the measurements of Aflatooni *et al.* [4], which indicate resonances at 1.5 and 4.5 eV (Fig. 1). Interestingly, Aflatooni *et al.* also observe a resonance feature at 0.3 eV that does not appear to be present in our elastic cross section, and we are currently trying to understand this discrepancy.

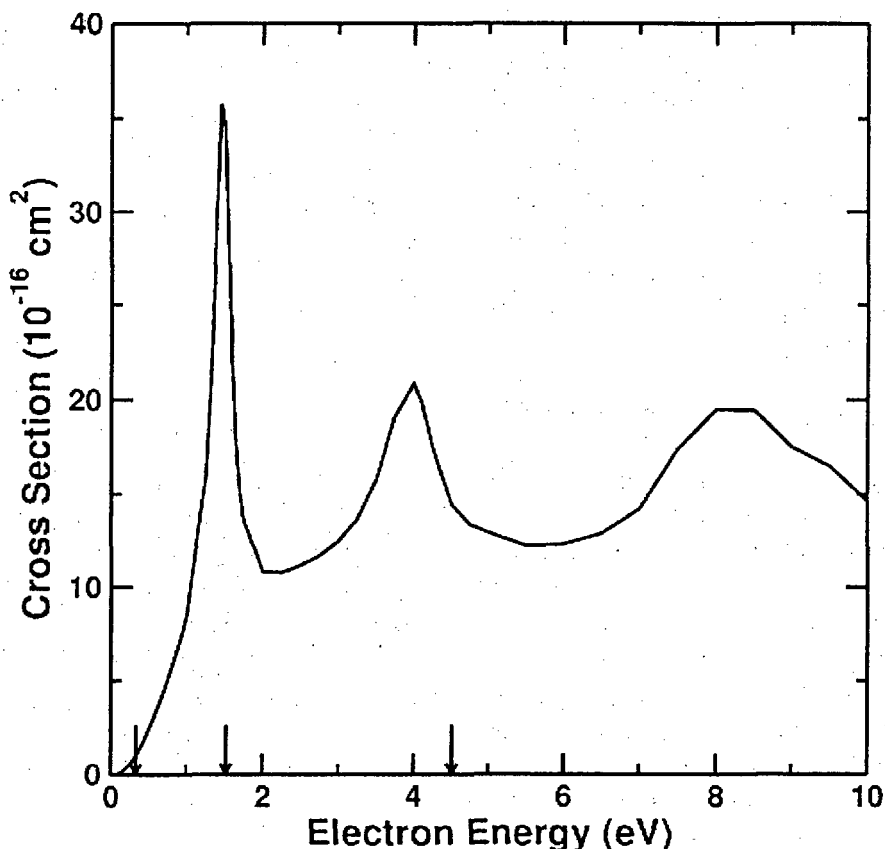


Figure 1. Computed integral elastic cross section (resonant component only) for cytosine. Arrows indicate locations of observed shape resonances [4].

PROGRAM DEVELOPMENT

We are continuing program development and debugging for multiconfiguration descriptions of target states based on compact MCSCF wavefunctions. This methodology provides a balanced description of the ground and excited states suitable for electron-impact excitation studies. Such calculations, moreover, remain feasible for the larger polyatomic molecules that form our principal focus. We are also further developing multiconfigurational treatments of polarization effects in elastic scattering and will be testing those developments on large molecules, including the DNA bases, over the coming year.

HARDWARE

The 32-processor cluster that we received from Intel Corp. has been placed into regular production use as a virtual parallel computer for our electron collision calculations. The cluster is also used for our code development work. We continue to make periodic software upgrades as new drivers and libraries become available.

Large-scale parallel computers continue to be important to our work. We currently have access locally to a 128-processor Origin 2000 and a 32-processor Superdome system; in the near future, we expect to have access to new terascale clusters at Caltech and LSU. We will also be working with researchers at NCSA (Daniel Reed and coworkers) to port our code to an innovative cluster of Sony Playstation 2 processors.

PLANS FOR COMING YEAR

We will continue our calculations on the DNA bases, obtaining initial cross sections for guanine and incorporating polarization effects in cases other than cytosine. Because the DNA bases exist in several different isomers of nearly equal energy (tautomers), we would also like, in at least some cases, to explore for differences in scattering between different tautomers of the same base. The procedures for efficient treatment of polarization in large molecules that we have developed as part of this DOE-sponsored project will continue to play a critical role in this work. As time permits, we are also interested in looking at electron scattering by related molecules, especially the RNA base uracil.

We also plan to continue work on electron collision processes related to materials processing. In particular, we are wrapping up work on elastic and inelastic collisions with SF₆ for publication in the near future. We will continue with program development, including implementation, testing, and application of multiconfigurational target descriptions adapted to larger polyatomic molecules. Those code-development activities will include targeted test calculations on smaller molecules as well as production calculations on larger polyatomics.

REFERENCES

- [1] C. Winstead and V. McKoy, *J. Chem. Phys.* **116**, 1380 (2002).
- [2] K. Yoshida, S. Goto, H. Tagashira, C. Winstead, V. McKoy, and W. L. Morgan, *J. Appl. Phys.* **91**, 2637 (2002).
- [3] W. L. Morgan, C. Winstead, and V. McKoy, *J. Appl. Phys.* **92**, 1663 (2002).

- [4] K. Aflatooni, G. A. Gallup, and P. D. Burrow, *J. Phys. Chem. A* **102**, 6205 (1998).
[5] B. Boudaïffa, P. Cloutier, D. Hunting, M. A. Huels, and L. Sanche, *Science* **287**, 5458 (2000).

PROJECT PUBLICATIONS

Publications and presentations related to this project during the past year:

1. "Electron-Molecule Collisions in Processing Plasmas," V. McKoy and C. Winstead, First International Symposium on Advanced Fluid Informatics, Sendai, Japan, 4-5 October, 2001 (*invited talk*).
2. "Electron Collisions with Hexafluorocyclobutene, $c\text{-C}_4\text{F}_6$," C. Winstead and V. McKoy, Fifty-Fourth Gaseous Electronics Conference, State College, Pennsylvania, 9-12 October, 2001.
3. "Electron-Molecule Collisions in Processing Plasmas," V. McKoy and C. Winstead, Forty-Eighth International Symposium of the American Vacuum Society, San Francisco, California, 28 October-2 November, 2001 (*invited talk*).
4. "Low-Energy Electron Scattering by CH_3F , CH_2F_2 , CHF_3 , and CF_4 ," M. T. do N. Varella, C. Winstead, V. McKoy, M. Kitajima, and H. Tanaka, *Phys. Rev. A* **65**, 022702 (2002).
5. "Electron Collisions with Tetrafluoroethene, C_2F_4 ," C. Winstead and V. McKoy, *J. Chem. Phys.* **116**, 1380 (2002).
6. "Electron Transport Properties and Collision Cross Sections in C_2F_4 ," K. Yoshida, S. Goto, H. Tagashira, C. Winstead, V. McKoy, and W. L. Morgan, *J. Appl. Phys.* **91**, 2637 (2002).
7. "Electron Collision Cross Sections for Tetraethoxysilane (TEOS)," W. L. Morgan, C. Winstead, and V. McKoy, *J. Appl. Phys.* **92**, 1663 (2002).
8. "Developing Cross Section Sets for Fluorocarbon Etchants," C. Winstead and V. McKoy, to appear in *Proceedings of the Third International Conference on Atomic and Molecular Data and Their Applications, Gatlinburg, Tennessee, 24-27 April, 2002* (*invited talk*).
9. "Quickly Generating Databases," C. Winstead, Third International Conference on Atomic and Molecular Data and Their Applications, Gatlinburg, Tennessee, 24-27 April, 2002 (*panelist*).

ATOMIC COLLISIONAL PROCESSES INVESTIGATED THROUGH THE GENERALIZED OSCILLATOR STRENGTH

Alfred Z. Msezane

amsezane@ctsps.cau.edu

Department of Physics and Center for Theoretical Studies of Physical Systems
Clark Atlanta University, Atlanta, Georgia 30314

The generalized oscillator strength (GOS), introduced by Bethe, is an important property of the atom which manifests the atomic wave function directly and the dynamics of atomic electrons. Here two major thrusts are pursued:

- 1) The formulation of small-angle electron scattering using Dispersion Relations representation of the GOS requires the accurate calculation of Regge pole trajectories and residues; and
- 2) Correlation effects are investigated within the GOS description of scattering problems, particularly for larger values of the momentum transfer, q , where nondipole effects become manifest.

A. Regge Poles Calculation for Singular Potentials

The full understanding of atom-diatom collisions and the dynamics of molecules and chemical reactions is a subject of considerable continuing interest and fundamental importance [1-6]. Crucial to gaining insights into all chemical reactivity is understanding the role played by dynamic scattering resonances in chemical reactions, a key to laser control of reactions. The standard procedure of summing a large partial wave expansion offers no physical insight into the underlying physical process. New information and physical insights are provided by the analysis that identifies complex angular momentum (Regge pole) resonances of the S-matrix in the complex angular momentum (CAM) plane. In the CAM techniques, the key quantities that appear in the theory are the energy dependent Regge pole positions, l_n , and the corresponding residues, r_n , where $n = 0, 1, 2, \dots$. The position of the Regge pole determines the angular velocity and angular lifetime of the decaying complex system, while the residue defines the magnitude of the resonance contribution to the differential cross section (DCS) [1]. The CAM methods have the advantage that the calculations are based on a rigorous definition of resonances, viz. as singularities of the S-matrix.

The successful application of the CAM approach in describing heavy particle collisions [1], including chemical reactions [7], and the formulation of small-angle electron scattering from atoms using Dispersion Relations [8,9] have inspired the development of various theoretical, particularly analytical, methods to calculate Regge poles [10-14]. The recent development of bounding methods for generating converging bounds to Regge poles of rational fraction scattering potentials, represents a significant breakthrough [15]. The generation of Regge pole positions and residues for singular potentials (diverging faster than r^{-2} at the origin), inherent to heavy particle collisions, such as atoms and molecules, is one of the most challenging problems

in atomic scattering analysis because a singular eigenvalue problem, defined in the context of a non-Hermitian Schrödinger operator, is involved, with currently no general, high precision, working method.

The Regge pole representation for analyzing electronic, atomic, and molecular scattering, defines an efficient resummation procedure for large partial wave expansions [1]. Our group has developed various methodologies for calculating mainly Regge pole positions [11, 12, 14, 15] and, most recently residues [16]. In [11] the Langer transformation is exploited to map the two singular points of the potential into one singularity at ∞ . The problem then becomes analytically tractable because all the solutions are entire functions with no singularities in the open complex z plane. Novel methods [12, 14] have also been developed for the accurate calculation of Regge poles trajectories for singular potentials. The approaches assume the existence of a close pair of turning points of the effective potential responsible for the Regge poles in the CAM plane and exploit the Bohr-Sommerfeld quantization condition. Bounding methods for generating converging bounds to Regge poles of rational fraction scattering potentials have been developed [15]. Recently, a very efficient formalism, based on the Multi-scale Reference Function representation of Tymczak *et al* [Phys. Rev. Lett. **80**, 3673 (1998)], has been presented [16] for calculating Regge pole positions and residues.

B. Correlation Effects in the GOS.

B.1. Correlation Effects in the GOS of the Mg $3^1S - 3^1P$ Transition

We have investigated correlation effects in the GOS of the Mg $3^1S - 3^1P$ transition using the Random Phase Approximation with Exchange (RPAE) and found that at small q the most important correlation effects come from the $3s - 3p$ coupling [17]. However, at large q the important correlation effects are contributed mainly by the continuous states of the $2p - nd$ channel.

B.2. Determination of Discrete Transitions Multipolarity through the GOS

[Collaboration with M. Ya. Amusia, Hebrew University, Israel and Ioffe Institute, Russia and L.V. Chernysheva, Ioffe Institute, Russia, Z. Felfli, Clark Atlanta University. CTSPS]

A recent experiment attributed the measured GOS for the dipole forbidden Ar $3p-4p$ transition to a quadrupole contribution [18]. Using the RPAE, it has been found [19] that the experiment [18] actually measured the combined monopole, the dominant component, and quadrupole transitions. The inelastic cross section of a fast charged particle from an atom is simply proportional to the GOS. Through studying the GOS of discrete atomic transitions, the multipolarity of the corresponding transitions can be determined [20]. By investigating the small $q \rightarrow 0$ behavior of the GOS, it is easy to separate the dipole and nondipole transitions.

In [20] we have addressed two important questions:

What does “fast” charged particle mean in the context of describing the inelastic scattering cross section using the GOS concept? and, To what extent are the GOS’s affected by interelectron correlations?

An interesting consequence of the simultaneous excitation of the quadrupole and monopole levels is the connection with their decay rates. Although they are excited with almost the same probability, they nevertheless decay differently. Indeed, a monopole level decays via the emission of two photons, which is almost impossible. However, a quadrupole level decays through emitting a quadrupole photon, which is by a factor of α^{-2} smaller than that of an ordinary dipole photon. Consequently, with increase of time, an excited gas of Ar atoms, for example, will be populated only through the $3p-4p$ monopole transition. We have demonstrated this by performing calculations using the RPAE for Ne, Ar, Kr and Xe outer $np \rightarrow (n+1)p, (n+2)p$ transitions for both monopole and quadrupole excitations, when q varies from 0 to 8 a.u. [20].

Future Plan

We continue to:

Develop methodologies for calculating Regge poles trajectories and residues for singular potentials, with emphasis on obtaining bounds.

Investigate correlation effects in the GOS’s for discrete atomic transitions (dipole, monopole, quadrupole and octupole), both dipole and nondipole.

References and Publications

- [1] J. N. L. Connor, *J. Chem. Soc. Faraday Trans.* **86**, 1627 (1990)
- [2] R. E. Wyatt and J. Z. H. Zhang, Eds. *Dynamics of Molecules and Chemical Reactions* (Dekker, New York, 1996)
- [3] D. Skouteris et al., *Science* **286**, 1713 (1999); J. F. Castillo and D. E. Manolopoulos, *Faraday Discuss.* **110**, 119 (1998)
- [4] R. Cote and A. Dalgarno, *Phys. Rev. A* **62**, 012709 (2000)
- [5] B. K. Kendrick *et al*, *Phys. Rev. Lett.* **84**, 4325 (2000); *J. Chem. Phys.* **114**, 8796 (2001)
- [6] D. Vranceanu, **A. Z. Msezane**, D. Bessis, J. N. L. Connor and D. Sokolovski, *Chem Phys. Lett.* **324**, 311 (2000)
- [7] D. Sokolovski, J. N. L. Connor and G. C. Schatz, *J. Chem. Phys.* **103**, 5979 (1995); *-Chem. Phys. Lett.* **238**, 127 (1995); D. Sokolovski, *Phys. Rev. A* **62**, 024702 (2000)
- [8] Z. Felfli, **A. Z. Msezane** and D. Bessis, *Phys. Rev. Lett.* **81**, 963 (1998)
- [9] **A. Z. Msezane**, Z. Felfli and D. Bessis, *Phys. Rev. A*, **65**, 050701(R) (2002)
- [10] D. Sokolovski, C. Tully and D. S. F. Crothers, *J. Phys. A* **31**, 1 (1998)
- [11] D. Vranceanu, **A. Z. Msezane** and D. Bessis, *Phys. Rev. A* **62**, 022719 (2000); *Chem. Phys. Lett.* **311**, 395 (1999)
- [12] S. Naboko, Z. Felfli, N. B. Avdonina and **A. Z. Msezane**, in *Proc. Second Int. Workshop on Contemp. Approaches in Math. Phys.*, Eds. J. Govaerts et al. (World Scientific, Singapore, 2002), In Press.
- [13] S. A. Sofianos, S. A. Rakityansky and S. E. Massen, *Phys. Rev. A* **60**, 337 (1999)

- [14] N. B. Avdonina, S. Belov, Z. Felfli, **A. Z. Msezane** and S. Naboko, Phys. Rev. A **65**, In Press (2002)
- [15] C. R. Handy and **A. Z. Msezane**, J. Phys. A **34**, L531 (2001)
- [16] C.R. Handy and **A.Z. Msezane**, Phys. Rev. A**66**, Rapid Commun. In Press (2002)
- [17] Zhifan Chen and **A.Z. Msezane**, J. Phys. B **35**, 815 (2002)
- [18] X.Q. Fan and K.T. Leung, Phys. Rev. A **62**, 062703 (2000)
- [19] **A.Z. Msezane**, Z. Felfli, M. Ya Amusia, Z. Chen and L.V. Chernysheva, Phys. Rev. A **65**, 054701 (2002)
- [20] M. Ya Amusia, L.V. Chernysheva, Z. Felfli and **A.Z. Msezane**, Phys. Rev. A, to be submitted (2002)
- [21] M. Ya. Amusia, L.V. Chernysheva, Z. Felfli and **A.Z. Msezane**, Phys. Rev. A**65**, 0620705 (2002) "Cross Sections of Discrete-Level Excitation of Noble-Gas Atoms in Compton Scattering".

Study of near-field optical interactions between a molecule and a laser illuminated metal tip

Lukas Novotny (novotny@optics.rochester.edu)

University of Rochester, The Institute of Optics, Rochester, NY, 14627.

1 Program Scope

Near-field optics has extended the range of optical measurements beyond the diffraction limit and stimulated interests in many disciplines, especially material sciences and biological sciences. In the most widely adapted aperture approach light is sent down an aluminum-coated fiber tip of which the foremost end is left uncoated to form a small aperture. Light emitted by the aperture interacts with the sample surface at close proximity and by raster scanning the tip over the sample surface an optical scan image can be recorded. Unfortunately, only a tiny fraction of the light coupled into the fiber is emitted through the aperture because of the cut-off of propagation of the waveguide modes. The low light throughput and the finite skin depth of the metal are the limiting factors for improving spatial resolution beyond 50nm .

To overcome the limitation of the aperture technique, we have recently introduced a new near-field optical method which allows to perform spectroscopic measurements with spatial resolutions on the order of $10 - 20\text{nm}$ [1]. The method makes use of the strongly enhanced electric field close to a sharply pointed metal tip under laser illumination. The tip is held in close proximity over the sample surface by means of a sensitive mechanical feedback system. A laser beam is focused by a high numerical aperture objective on the sample surface and the tip is laterally positioned into the focal spot. The laser wavelength and polarization are optimized to maximize the field enhancement at the metal tip. The enhanced fields near the tip form a local excitation source which allows for a highly confined optical interaction with the sample surface [2, 3]. An optical image of the sample is recorded by raster scanning the sample and detecting for each position the emitted photons. To optimize the near-field contrast we make use of nonlinear optical interactions between tip and sample such as second-harmonic (SH) generation or two-photon absorption. The experimental setup is shown schematically in Fig. 1. The laser excitation source is a Ti:Sapphire laser and an OPO working both in fs and ps mode.

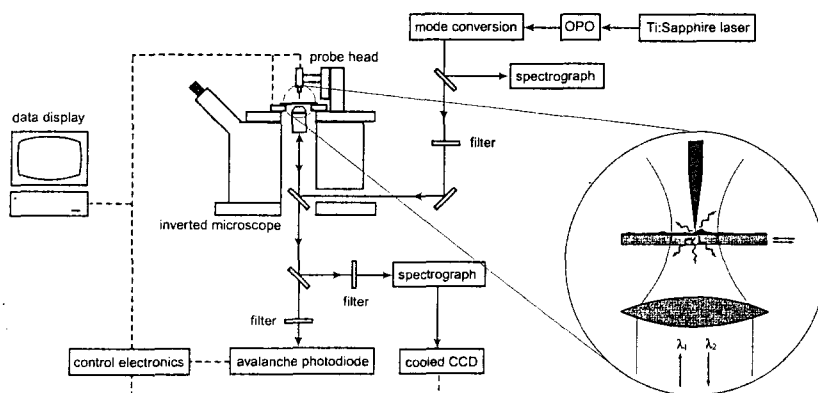


Figure 1: *Experimental setup.* The enhanced optical field near a laser irradiated metal tip is used to locally excite a nonlinear spectroscopic response in the sample beneath the tip.

2 Recent Progress

Most recently we have investigated the relationship between field-enhancement and fluorescence quenching by the metal tip. The metal tip locally enhances the electric field, but also quenches fluorescence emission of the sample by introducing a non-radiative decay channel for the electronic excited states. The goal of this project is to study the optical interaction between a laser irradiated tip and a single molecule. However, for our initial studies we chose a sample with J-aggregates which consist of strongly coupled molecules embedded in a thin polymer strand. This system has the advantage that the local excitation of a fluorophore by the tip becomes rapidly delocalized over a large distance thereby reducing the perturbing influence of the tip. As shown in Fig. 2 we have been able to image samples of J-aggregates by two-photon excited fluorescence [4]. Because the tip is used as local excitation source instead of a local scattering center we are able to record the emission spectrum for each image pixel. This allows us to spectrally identify the molecules involved in the near-field optical interaction and also to estimate the coupling strength between the molecules. The spatial resolution of the optical near-field image in Fig. 2 is smaller than 20nm. To date, this is the highest reported spatial resolution of an optical spectroscopic measurement.

Besides the high-resolution, an important feature of the image shown in Fig. 2 is the fluctuations which occurred in the fluorescence from line to line. This is due to fluctuations in the strength of the field enhancement. We have observed that the level of field enhancement varies strongly from tip to tip, and we have found that most tips have a field enhancement which is too small for useful imaging. This is despite the relative homogeneity of the tip shapes, which we verify using a scanning electron microscope. The tips are etched from gold wire in hydrochloric acid, and have a typical tip radius of 15 nm and a cone angle of 30 degrees. However, even for a tip such as the one used in Fig. 2 the enhancement can fluctuate from line to line. We suspect that shape resonances critically influence the enhancement, and that small changes to the tip dimensions result in large effects, both in the tip enhancement, and in the coupling between the external laser and the tip. Therefore, mechanical forces acting on the tip during the course of the scan may modify the tip shape and can change the image contrast. Also, long-term drift of the instrument can change the tip position within the laser focus.

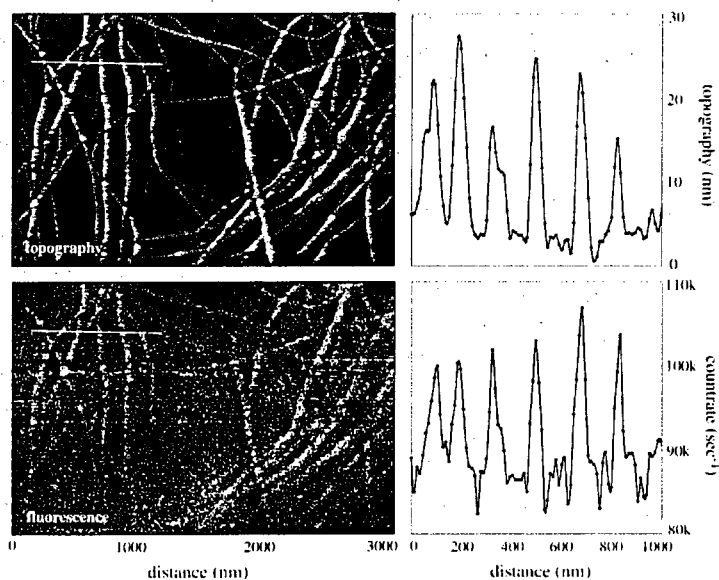


Figure 2: High-resolution near-field image of PIC J-aggregate strands. The optical image is acquired by recording the fluorescence from the J-aggregates following two-photon excitation by the enhanced field near a laser irradiated gold tip. The optical resolution exceeds the topographical resolution and is limited by the actual size of the strands. The figures to the right are cross-sections along the white lines. From Ref. [4].

To investigate the role of fluorescence quenching we measured the fluorescence rate as a function of the proximity of the tip to the sample. Shown in Figure 3 is a fluorescence image of a J-aggregate sample and an approach curve which shows a sharp increase of fluorescence in the last 5 nm of the tip-sample separation. This is the range in which the effect of non-radiative energy transfer to the tip is the strongest. However, the measurement in Fig. 3 shows that for the J-aggregates the increase in fluorescence outpaces any quenching phenomenon, which is what we expect from the delocalized excited state of the J-aggregate.

We then used the same tip to image individual CdSe quantum dots (QD). Quantum dots behave like individual fluorophores but they have the beneficial property that they can be localized topographically. The initial image shown in Figure 4 is indicative of the quenching effects of the tip for single, localized quantum systems. While the signal to background ratio is lower than for J-aggregates, the important point is that it is possible to see near-field induced fluorescence from single quantum dots. It is then a matter of finding a tip with suitably high enhancement in order to record a near-field image with sufficient contrast.

Since the relationship between tip shape and strength of the field enhancement is not completely understood, another set of experiments has dealt with the non-linear properties of the metal tips themselves. We have found that we can relate the strength of several non-linear signals to the field enhancement produced by the tip. The field enhancement at the tip leads to very high field strengths, which is what makes the anharmonic response of the tip important. Second-harmonic (SH) generation is easily detectable and we have shown that the SH count rate is an indirect measure for the strength of field enhancement [5]. Since SH generation is confined to the very end of the tip it can be modelled accurately by a dipole aligned along the tip axis. SH generation is driven by the external laser field component that is parallel to the tip axis, and so by scanning the tip through focused beams, the longitudinally polarized components of these fields can be spatially mapped. This has the additional benefit of providing a signal which can be used to align the tip into the laser focus during a near-field experiment.

Because of the strong field gradients associated with the strongly confined optical field near the metal tip the standard dipole approximation and related selection rules might not be sufficient. For spatially large quantum systems such as quantum dots it is necessary to consider higher-order multipole transitions. Our recent theoretical studies have shown that the electric dipole approximation breaks down for quantum dots in the vicinity of a sharp tip [6]. The possibility of selectively exciting electric quadrupole transitions would extend the spectroscopic information content and open up new exciting experiments. Quadrupole transitions lead to a modification of the absorption spectrum and to an increase of the overall absorption strength.

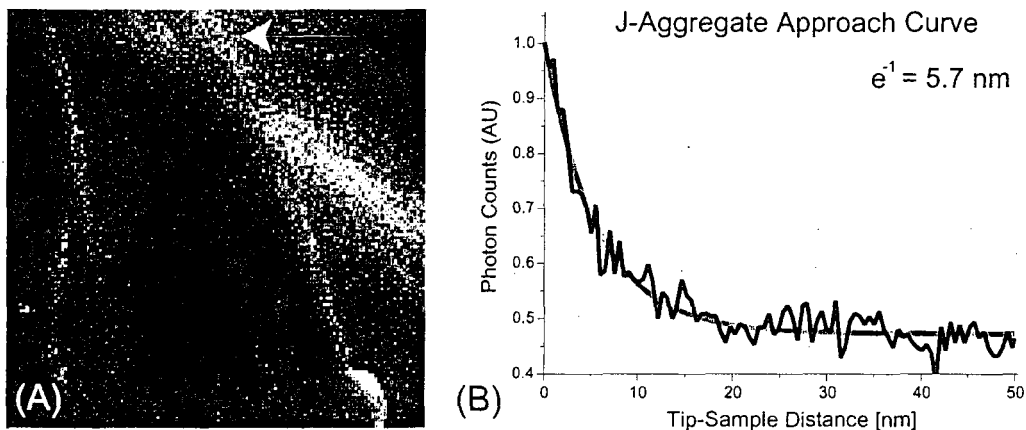


Figure 3: Approach curve for a tip placed above a single PIC J-aggregate strand. (A) Two-photon excited fluorescence image (image size $1 \times 1 \mu\text{m}^2$) (B) Approach curve recorded above the location indicated by the arrow. The fluorescence decay is fitted to an exponential decay with a decay constant of 5.7 nm.

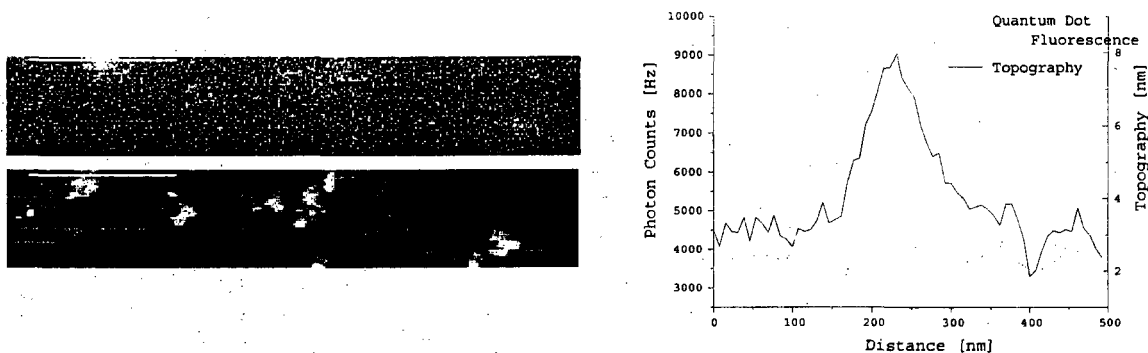


Figure 4: Two-photon excited fluorescence image of individual CdSe quantum dots. (A) Near-field and corresponding topographic images (B) Line scans of the fluorescence and topography from the regions indicated by the white strips.

Thus, by using a laser illuminated metal tip as an excitation source we can make use of two enhancement mechanisms: the first is due to the *strength* of the enhanced field at the laser illuminated metal tip and the other is related to the *gradient* of the enhanced field. The first enhances the dipole interaction, whereas the latter increases the strength of quadrupole transitions. We believe that an understanding of quadrupole selection rules is important for situations where single quantum systems (molecules, quantum dots, ...) are embedded in a complex environment. Our theoretical studies predict that every third photon absorbed by a quantum dot near a gold tip is mediated by a quadrupole transition [6].

3 Future Plans

Our goal is to fundamentally understand the field enhancement process and to quantify the quenching mechanism for single quantum systems in the vicinity of the tip. We will investigate different tip shapes and multiphoton excitation schemes. Recently, we have calculated magnetic dipole transitions in spherical quantum dots and determined that the selection rules are identical with the electric quadrupole transitions [7]. To experimentally test magnetic dipole transitions we have set up an experiment in which a strongly focused, azimuthally polarized laser beam is used as an excitation source for individual quantum dots. This laser mode has the unique property that it exhibits a zero electric field in the focus whereas the magnetic field is strongly enhanced [8].

References

- [1] E. J. Sanchez, L. Novotny, and X. S. Xie, *Phys. Rev. Lett.* **82**, 4014, 1999.
- [2] J. Wessel, *J. Opt. Soc. Am. B*, **2**, 1538, 1985.
- [3] L. Novotny, R. X. Bian, and X. S. Xie, *Phys. Rev. Lett.* **79**, 645, 1997.
- [4] M. R. Beversluis, A. Bouhelier, A. Hartschuh, and L. Novotny, *Opt. Lett.*, in preparation, 2002.
- [5] A. Bouhelier, M. Beversluis, A. Hartschuh, and L. Novotny, *Phys. Rev. Lett.*, submitted, 2002.
- [6] J. R. Zurita-Sanchez and L. Novotny, *J. Opt. Soc. Am. B* **19**, 1355, 2002.
- [7] J. R. Zurita-Sanchez and L. Novotny, *J. Opt. Soc. Am. B*, in press, 2002.
- [8] A. Heaney, M. Hahn, T. D. Krauss, and L. Novotny *Appl. Phys. Lett.*, in preparation, 2002.

DOE sponsored publications (2000-2002): Refs. [5], [6], [7].

Energetic Photon and Electron Interactions with Positive Ions

Ronald A. Phaneuf,
Department of Physics /220
University of Nevada
Reno NV 89557-0058
phaneuf@physics.unr.edu

Program Scope

This program is focused on experimental studies of ionization of positive ions by photons and electrons. The objective is a deeper understanding of multielectron interactions in atomic ions. Monenergetic beams of photons and electrons selectively probe the electronic structure and dynamics of positively charged ionic systems using merged-beams and crossed-beams techniques. In addition to precision spectroscopic data for ionic structure, quantitative measurements of cross sections for photoionization and electron-impact ionization provide critical benchmarks for the theoretical calculations that generate opacity databases. The latter are critical to models of astrophysical, fusion-energy and laboratory plasmas. Examples of particular relevance to DOE interests include the Z pulsed-power facility at Sandia National Laboratories, which is the world's brightest and most efficient x-ray source, and the National Ignition Facility under development at Lawrence Livermore National Laboratory for high-energy-density science, fusion energy and defense-related research.

Recent Progress

Photoionization of Ions at the Advanced Light Source

The photoionization of C^{2+} was selected for study in collaboration with the University of Giessen, Germany (A. Müller and S. Schippers). Photoionization of C^{2+} is the time reversal of the recombination of electrons with C^{3+} , which that group had measured previously at a heavy-ion storage ring facility in Europe. The same intermediate autoionizing states may be populated by both processes, and the principle of detailed balance relates the photo-recombination and photoionization cross sections on a state-to-state basis. The situation is complicated by the presence of a significant metastable fraction (estimated at 40%) in the C^{2+} primary ion beam. Figure 1 presents a comparison of the photoionization results with a state-of-the-art R-matrix calculation by B. McLaughlin for photoionization of both ground-state and metastable C^{2+} . This comparative study was published as a letter in the Journal of Physics B [1].

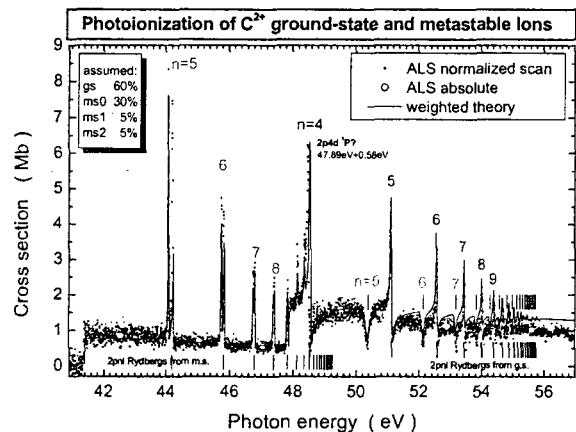


Figure 1. Comparison of absolute experiment and theory (curve) for photoionization of a mixture of ground-state and metastable C^{2+} .

The first photoionization experiments with multiply charged metallic ions were completed at the ALS using a resistively-heated refractory metal oven developed at the University of Nevada for the permanent-magnet ECR ion source at ALS. Photoionization cross-section measurements were completed for potassium-like Sc^{2+} sequence in collaboration with the Giessen group as part of a series of measurements on ions of the potassium isoelectronic sequence. The Sc^{2+} photoionization measurements were compared with storage-ring measurements of electron recombination with Sc^{3+} . Application of the principle of detailed balance made it possible to determine the metastable fractions in the Sc^{2+} ion beam. A report on this comparative study was submitted to Physical Review Letters. High-resolution measurements were also completed for Mg^+ , Al^+ and Al^{2+} in collaboration with Daresbury Laboratory, U.K. (J. B. West) and Århus University, Denmark. (H. Kjeldsen and F. Folkmann). These measurements augment previous lower-resolution measurements made at the Århus light source, revealing additional structures. A detailed spectroscopic analysis performed for the sodium-like ions, Mg^+ and Al^{2+} is being prepared for publication.

To complement earlier measurements on O^+ , photoionization measurements were completed for F^{2+} and Ne^{3+} as part of a systematic study of the nitrogen isoelectronic sequence that will constitute the Ph.D. dissertation of A. Aguilar (expected completion in December, 2002). The results for photoionization of metastable O^+ were published in Physical Review Letters [2], and a more detailed spectroscopic analysis including photoionization of ground state O^+ has been prepared for publication.

Measurements of photoionization of Fe^{3+} were initiated as part of a systematic study of the iron isoelectronic sequence. The iron sequence is both important astrophysically and prominent in fusion plasmas. Preliminary data are shown in Figure 2. The origin of the strong and extremely broad resonance feature observed in the energy range 56-62 eV is under investigation. Such broad features significantly affect photon opacities. Photoionization measurements of Fe^{9+} ions will constitute the Ph.D. dissertation research of M. F. Gharaibeh.

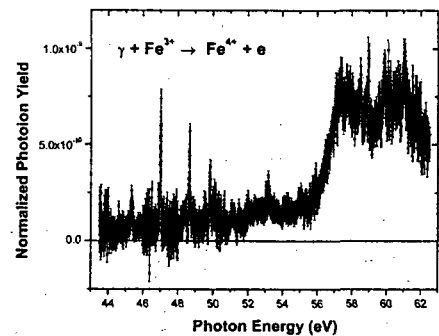


Figure 2. Preliminary results for photoionization of Fe^{3+} .

A manuscript on photoionization of CO^+ has been accepted for publication in Physical Review A [3]. A detailed report on the photon-ion merged-beams experimental technique was prepared, which includes as an example, a detailed comparison of absolute experiment and state-of-the-art R-matrix theory for photoionization of Ne^+ . The comparison reveals evidence for the role of three-electron promotions in photoionization, and has been submitted to Physical Review A. This project also provided support for research on photoionization of negative ions using the ion-photon-beam endstation at ALS [4].

During 2001-2002 reporting period, this part of the project (80% of effort) supported two graduate students (A. Aguilar and M. F. Gharaibeh) and two undergraduate students (A. Fuhrmann and T. Burris). S. Scully will join the project as a postdoctoral fellow in August, 2002.

Electron-Impact Ionization of Multiply Charged ions at the University of Nevada

During the past year, this part of the project focused on analysis of coincidence data for electron spectroscopy of metastable autoionizing states of Sodium-like Ar^{7+} , Cl^{6+} and S^{5+} . This marked the successful completion of the M.S. thesis research of M. Lu, and a manuscript based on this was published in Physical Review A [5]. Subsequent attempts to measure coincident ejected electron spectra due to electron-impact ionization of Ar^{6+} and Xe^{3+} yielded inconclusive results, indicating that a further reduction of 5-10 in the electron background count rate will be required. Several pathways to that end are being pursued. E. Emmons joined this project as a graduate student in April 2002.

During the 2001-2002 reporting period, this part of the project (20% of effort) supported two graduate students (M. Lu and E. Emmons).

Future Plans

Photoionization of Ions

Future research will be concentrated on systematic studies of photoionization of multiply charged ions along selected isoelectronic and isonuclear sequences. Measurements on the nitrogen isoelectronic sequence, which constitute the Ph.D. dissertation research of A. Aguilar (expected completion December 2002), will be analyzed in detail and prepared for publication. Collaborative research on photoionization of ions of the potassium isoelectronic sequence will continue with measurements on Ti^{3+} , complementing earlier work on Ca^+ and Sc^{2+} . The complementarity of photoionization and photo-recombination experiments will be further exploited in this continuing collaboration with the University of Giessen. Preliminary measurements on K-shell excitation of B^{9+} ions will also be extended. In addition, the measurements initiated recently on the iron isonuclear sequence with Fe^{3+} will be continued, and extended to other charge states. This will constitute the Ph.D. dissertation research of M. F. Gharaibeh.

Electron-Impact Ionization of Ions

A test case will be identified for a detailed comparison of the energy dependences of cross sections for electron-impact ionization at UNR and photoionization at ALS. This will constitute the M.S. thesis research of E. Emmons. Continued attempts to make the first definitive coincident electron-spectroscopy measurements from electron-ion collisions will focus on 2p-nl excitation-autoionization in the Ar isonuclear sequence, and 4d-nl excitation-autoionization in the Xe isonuclear sequence. In both cases multiple excitation channels with large cross sections are exhibited by total cross-section measurements

References to Publications of DOE-Sponsored Research (2000-2002)

1. *Photoionization of C^{2+} ions: time-reversed recombination of C^{3+} with electrons*, A. Müller, R.A. Phaneuf, A. Aguilar, M.F. Gharaibeh, A.S. Schlachter, I. Álvarez, C. Cisneros, G. Hinojosa and B.M. McLaughlin, J. Phys. B. (At. Mol. Opt. Phys.) **35**, L137 (2002).

2. *Photoionization of metastable O^+ ions: experiment and theory*, A.M. Covington, A. Aguilar, I.R. Covington, M. Gharaibeh, C.A. Shirley, R.A. Phaneuf, I. Álvarez, C. Cisneros, G. Hinojosa, J.D. Bozek, I. Dominguez, M.M. Sant'Anna, A.S. Schlachter, N. Berrah, S.N. Nahar and B.M. McLaughlin, *Phys. Rev. Lett.* **87**, 243002-1 (2001).
3. *The formation of long-lived CO^{2+} via photoionization of CO^+* , G. Hinojosa, A. M. Covington, R.A. Phaneuf, M.M. Sant'Anna, R. Hernandez, I.R. Covington, I. Dominguez, J. D. Bozek, A.S. Schlachter, I. Álvarez and C. Cisneros, *Phys. Rev A* (accepted for publication).
4. *Correlated processes in inner-shell photodetachment of the Na^- ion*, A.M. Covington, A. Aguilar, V.T. Davis, I. Álvarez, H.C. Bryant, C. Cisneros, M. Halka, D. Hansdorp, G. Hinojosa, A.S. Schlachter, J.S. Thompson and D.J. Pegg, *J. Phys. B. (At. Mol. Opt. Phys.)* **34**, L735 (2001).
5. *Electron Spectroscopy of Na-like autoionizing metastable ions*, M. Lu and R.A. Phaneuf, *Phys. Rev. A* **66**, 012706 (2002).
6. *Electron-impact ionization of multiply charged manganese ions*, R. Rejoub and R.A. Phaneuf, *Phys. Rev. A* **61**, 032706 (2000).
7. *Dielectronic recombination of lithiumlike Ni^{25+} ions: High-resolution rate coefficients and influence of external electric and magnetic fields*, S. Schippers, T. Bartsch, C. Brandau, A. Müller, G. Gwinner, G. Wissler, M. Beutelspacher, M. Grieser, A. Wolf and R.A. Phaneuf, *Phys. Rev. A* **62**, 022708 (2000).

Mode-specific polyatomic photoionization far from threshold: molecular physics at 3rd generation light sources

Erwin Poliakoff; Department of Chemistry, Louisiana State University, Baton Rouge, LA 70803, epoliak@lsu.edu

Scope of program

The goal of this research is to understand microscopic aspects of molecular photoionization using two related approaches: vibrationally-resolved high resolution VUV-photoelectron spectroscopy, and X-ray core-shell spectroscopy of chemically-constrained systems. Both projects are aimed at understanding fundamental, microscopic aspects of the photoelectron scattering dynamics, and thereby helping to develop the capabilities of high energy spectroscopies. Progress has been achieved on both fronts.

Recent progress

The photoelectron studies performed to date concentrate on valence-shell processes, where we study mode-specific behavior in gas-phase molecular photoionization. These valence-shell studies are performed at the ALS. In experiments performed previously, we uncovered a new phenomenon, *resonantly amplified vibronic symmetry breaking* [J. Chem. Phys. **113**, 899 (2000); J. Chem. Phys. **114**, 4496 (2001)]. In previous studies, we focused on bending excitation accompanying CO₂ photoionization. In the past year, we have gone far beyond the initial preliminary study.

A. CO₂ photoelectron studies

In our new work on CO₂ $4\sigma_g^{-1}$ photoionization, we studied the energy dependence of the $v^+=010/v^+=000$ (bend), the $v^+=100/v^+=000$ (symmetric stretch) and the $v^+=001/v^+=000$ (asymmetric stretch) vibrational branching ratios. The energy dependent branching ratios demonstrate 2 new effects: (a) photoelectron-mediated vibronic coupling influencing the symmetry-forbidden *asymmetric stretch and bend*, and (b) resonant *suppression* of the excited symmetric stretch (cf. Fig. 1).

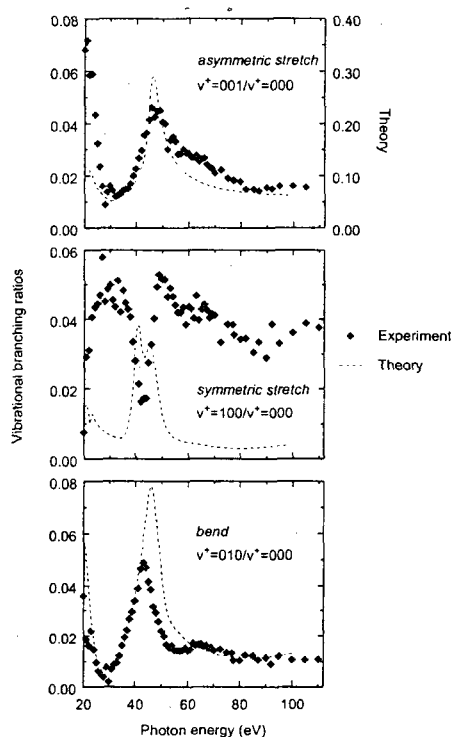


Figure 1. This shows the branching ratios for all of the fundamental vibrations following $4\sigma_g^{-1}$ photoionization of CO₂. Note the behavior of the symmetric stretch branching ratio, i.e., the resonant suppression of the excited vibrational level. The top and bottom frames show branching ratios for forbidden transitions (i.e., non-totally symmetric vibrations), and the energy dependences of these ratio curves suggest that the mechanism responsible for populating these levels is photoelectron-mediated symmetry breaking, and does not involve interchannel phenomena.

B. CS₂ photoelectron studies

New results on have also been obtained for $5\sigma_u^{-1}$ photoionization of CS₂. As was seen for CO₂, the results show pronounced mode-specificity, but the behavior is not the same as what is observed for CO₂. In particular, Fig. 2 shows that all of the branching ratios studied were relatively flat, *except for the asymmetric stretching and the bending vibrations*. This is suggestive that the localization of the quasibound continuum electron is qualitatively different for the CS₂ case; moreover, it is different from any other system previously studied with vibrational resolution.

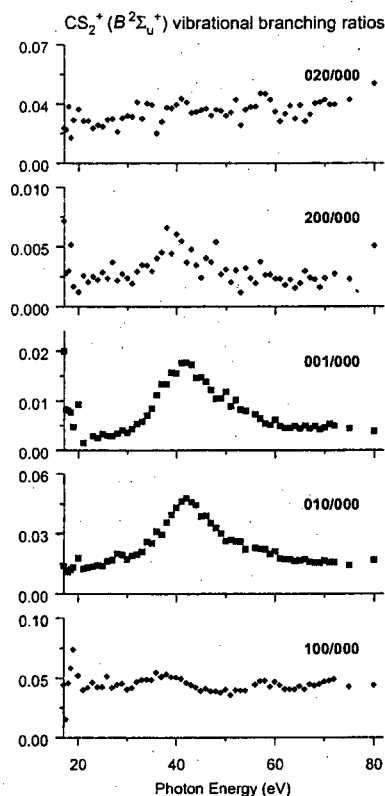


Figure 2. This figure shows an example of mode specificity, i.e., the single quantum excitation branching ratio shows a very strong enhancement for the bending branching ratio (010) and the asymmetric stretch (001), while all of the other branching ratios are comparatively flat. These results show that the response of the resonance to alternative vibrational motions is different than has been observed for any other molecule. The implication is that the localization of the quasi-bound electron is different from previously studied cases.

C. Other photoelectron studies

Several other systems were investigated, and space limitations preclude a full description. It is useful to study systems without inversion symmetry, so N₂O $7\sigma^{-1}$ photoionization was studied. This enhances asymmetric stretching vibrations while preserving the selection rule against bending excitation. It was determined that the vibrational branching ratio curves naturally arranged themselves into “families” of curves, and these data are currently being written up for publication. In an effort to extend these studies beyond simple linear systems, measurements have been performed on BF₃ and aromatic ring systems. Pronounced energy dependent effects are observed in these vibrationally-resolved studies, and the data are currently being analyzed.

D. Instrumentation Development

The research described above uses existing instrumentation. We are also designing and building new instrumental capabilities. There are two principal efforts in this regard. First, we have designed and tested a skimmed molecular beam source that is compatible with synchrotron radiation source vacuum constraints, and it is working well. Secondly, we have begun work on a coincidence apparatus that will be used with the supersonic beam source, and this will be commissioned soon.

E. Core-shell studies of chemically tailored systems

In addition to the valence-shell work, core shell studies were performed. A theme of both the valence and core shell research is to illuminate connections between molecular geometry and ionization dynamics. For the core shell work, we chemically constrain some aspect of the structure, and investigate the effect on the ionization spectrum. Structural changes are known to influence molecular XANES (X-ray absorption near edge structure) spectra, but the effect of bond angle has not been investigated in detail. In order to understand the systematics of such changes, XANES spectra were acquired for bis diphenylphosphino alkane tetracarbonyl chromium, $\text{Cr}(\text{CO})_4\text{PPh}_2(\text{CH}_2)_n\text{PPh}_2$, $n = 1-3$. They were studied because they allow adjustment of the bond angle about absorbing atoms (P being the principal focus in this study). Spectra were taken at CAMD at a double crystal monochromator beamline at port 5A. We see in Fig. 3 that the continuum features at the P K-edge are very different for the different bidentate ligands, indicating that the electron backscattering is strongly affected by bond angle.

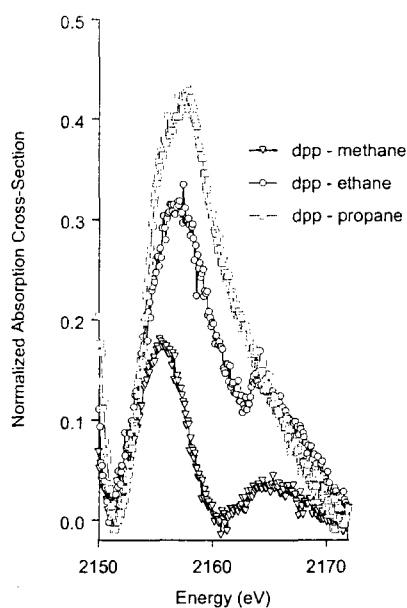


Figure 3. $\text{Cr}(\text{CO})_4\text{dpp-n}$ [$n = \text{CH}_2$, $(\text{CH}_2)_2$, and $(\text{CH}_2)_3$] XANES spectra taken at the phosphorus K-edge (ca. 2142 eV) after subtraction of nonresonant background. Features are broadening and changing position.

In addition to the study on sterically constrained Cr compounds, we completed a study on cyclic sulfides where the C-S-C bond angle was controlled via the ring size of the heterocycle. Preliminary results on this project were included in the research proposal, and that work has been verified and the analysis is now complete. A paper has been submitted to the *Journal of Chemical Physics* that includes results on both types of cyclic systems described above. Additionally, we performed related core-shell spectroscopies for sulfides adsorbed on Ag crystals, and found that subtle differences in the adsorption geometry exerted dramatic leverage on the sulfur K-edge XANES spectra. These results have also been submitted for publication.

F. Core-shell results relevant to combustion

Finally, my group has been collaborating extensively with Prof. Barry Dellinger of the LSU Chemistry Department. We have been using hard x-ray absorption spectroscopy (principally XANES) to elucidate the mechanisms of surface-mediated production of dioxins from chlorinated precursors. While this work is funded separately by an exploratory grant from the NSF Division of Materials Research (Biocomplexity Program), the methods used and the training afforded my students from this environmental work directly benefits this DOE-funded project. It is likely that interesting target compounds of *both* environmental chemistry and AMO physics interest can be identified in the course of these studies. One paper has been submitted, and another is in preparation.

Future plans

The accomplishments described for the VUV photoelectron spectroscopy experiments demonstrate the utility of obtaining high resolution photoelectron spectra over a wide range of energies. However, Doppler broadening becomes more severe as the photoelectron kinetic energy increases, so a skimmed supersonic beam is under development for obtaining high resolution data on closely spaced levels at higher photon energies. This will be particularly useful for higher quanta excitations in the triatomic samples, as well as for more complex molecular targets. The same supersonic beam will also be useful for high resolution, energy-dependent studies of molecular clusters (principally dimers). Finally, we are building an apparatus for velocity-map imaging studies using synchrotron radiation excitation.

Publications:

One paper (a **Communication** in J. Chem. Phys.) has appeared based on the work described here; 3 others have been submitted. Those papers are listed below. In addition, manuscripts are currently being written for 4 others (the CO₂ full paper, the CS₂ study, the N₂O work, and the BF₃ investigation).

G.J. Rathbone, E.D. Poliakoff, J.D. Bozek, and R.R. Lucchese, *Resonantly amplified vibronic symmetry breaking*, J. Chem. Phys. **114**, 8240 (2001)

E.E. Doomes, P.N. Floriano, R.W. Tittsworth, R.L. McCarley, and E.D. Poliakoff, *Anomalous XANES spectra of octadecanethiol adsorbed on Ag(111)*, J. Phys. Chem. B (submitted)

E.E. Doomes, R.W. Zuraes, R.L. McCarley, E.D. Poliakoff, *Correlations between heterocycle ring size and X-ray spectra*, J. Chem. Phys. (submitted)

G. Farquar, S.A. Alderman, E.D. Poliakoff, and B. Dellinger, *X-ray Spectroscopic Studies of the High Temperature Reduction of Cu(II)O by 2-Chlorophenol on a Simulated Fly-Ash Surface*, Environ. Sci. Technol. (submitted)

Research Summary
August, 2002

“Isotopically Enriched Thin Films and Nanostructures by Ultrafast Pulsed Laser
Deposition”

Peter P. Pronko, PhD
University of Michigan
Center for Ultrafast Optical Science
Department of Electrical Engineering and Computer Science
6109 IST Bldg., 2200 Bonisteel Boulevard
Ann Arbor, MI 48109
pronko@eecs.umich.edu

Program Scope and Definition

This program of study is directed at developing, understanding and applying the unusual phenomena of spontaneous isotopic enrichment of the lighter isotopes of an element along the central axis of ultrafast laser ablation plasmas. A model is proposed whereby the spontaneous magnetic fields, both toroidal and longitudinal, which are known to exist in such laser plasmas, act to confine the emitted ionic component of the plume and to induce centrifuge like rotation that produces the observed enrichments. Our early work at 780 nm, 120 fs, 2×10^{14} W/cm² demonstrated the generality of the phenomena for isotopic elements in the periodic table up to mass 73. Our research under this program has demonstrated similar separation effects for chemical species of ablated binary compounds such as the Ni/Cu alloy at 5×10^{15} W/cm². Comparison of these results with those obtained by conventional plasma centrifuges provides alluring similarities and reinforces the proposed model.

Recent Results

Enhancement of Ionic and Isotopic Yield

Recent experiments, in the 10^{16} W/cm² range, have been directed at developing methods to enhance the ionic component of the plume, which normally also contains a large neutral fraction. The neutral fraction may or may not contain the enrichment, depending on the point in the expansion process where it achieved the neutral state. Experiments have been performed whereby the initial ablation plasma, while still in the one-dimensional expansion state, is subjected to a second time-delayed laser pulse. These time delays have been studied over the temporal range of 0.25 to 40 picoseconds. The mean plasma expansion distance for this time scale ranges from a small fraction of a micron to about 8 microns, well within the one-dimensional expansion region (typically taken to be on the order of the beam spot radius). It is found that the second pulse (with equal intensity to the first) produces a maximum 60% increase in the observed total ionic

fraction of a silicon plume for a time delay on the order of 10 picoseconds. By comparing this effect using S and P polarized light it is determined that the second pulse affects the plasma through a predominantly resonance absorption process, the maximum of which is theoretically predicted to occur at 10 ps. This is confirmed by extracting the purely resonance portion of ionic yield and comparing it to theory. In addition to the increase in ionic yield at the optimum time delay, a study has been made of the isotopic enrichment of boron, from boron nitride, with and without the second pulse. It is observed that the second pulse affects the isotopic enrichment in a similar fashion as the ionic yield, producing a weighted average of 26% increase in central axis light isotope enrichment for the observed charge states of +1 to +3. For the specific charge state +2 the isotopic enrichment is seen to approach 60%.

Nanostructure Formation in a Femto-Jet Nozzle

The laser plumes produced from the ablation of a solid target contain, in their combined ionic and neutral components, sufficient flux to produce either thin films or nano-particle clusters, depending on the ablated material and laser irradiation conditions. The program of study being reported on here has, as one of its goals, to produce thin films and nanostructures that have isotopically enriched components. In our earlier work we examined the production of very high quality epitaxial thin films of tin dioxide (SnO_2) on sapphire by ultrafast pulsed-laser deposition. More recently we have been studying the controlled formation of nano-clusters through the use of expansion dynamics associated with the transition from a one-dimensionally confined plasma condition to that of a three dimensional free expansion. It is proposed that the one-dimensional confinement is strengthened and sustained by the classical pinch effect from the toroidal magnetic field present in the early stages of plasma expansion in these ultrafast plumes. Sub-micron and micron clusters of germanium, Ni/Cu alloy, and BaTiO_3 have been made this way. Single and double pulse experiments have been conducted for some of this work as well. Figure 1 shows clusters fabricated in this fashion for a 57/43 atom-ratio alloy of Cu/Ni. Mean cluster size is determined to be 250 nm. These clusters are essentially spherical and appear to be deposited in the solid state. In contrast to this, we have fabricated germanium clusters that appear to be deposited as spherical liquid droplets. These are shown in Fig. 2. The curious annular appearance of the germanium clusters, with depressed centers, suggests that these shapes occur during flow and quenching of the liquid after deposition. Cluster size distribution analysis reveals that a double pulse deposition (both pulses equal intensity) will result in larger mean cluster sizes being formed compared that of a single pulse (400 nm compared to 262 nm). The liquid state deposition for Ge compared to the solid-state deposition for Cu/Ni is consistent with their respective freezing temperatures. For germanium it is 930 C whereas for the Cu/Ni alloy it is 1300 C. It would appear from this that the temperature at which these clusters are deposited is in a range between these two values. The measured plasma-temperature (T_e) in the free expansion zone near the deposition substrate is measured to be on the order of 4000 C. The clusters form well before this point and are able to cool considerably during transport to the substrate where they are deposited.

Future Plans

Work will continue on the multi-pulse technique with the goal of better understanding how the enhancements from the second pulse affect the ionic yield, the isotope enrichment, and the mean cluster size. Plans are being made to investigate multi-pulse enhancements, where third, fourth, and higher numbers of pulses are used. Fundamental studies will be carried out on better understanding the femto-jet nozzle phenomena. Experiments are being conducted using a time resolved Langmuir probe to study the plasma temperature in the free expansion zone as a function of laser pulse intensity for single and multi-pulses. These results will be correlated with cluster size and density distributions. Attempts will be made to demonstrate isotopically and chemically enriched cluster formation as a follow on to these materials fabrication experiments.

Publications:

“Angular Distributions for Mass Enrichment of Heavy Ions in Ultrafast-Laser Ablation Plasmas”, P.A. VanRompay, Z. Zhang, and P.P. Pronko (submitted to Physical Review-A).

“Ionic Characterization of Laser Produced Plasmas using a Pair of Time-Correlated Collinear Femtosecond Pulses”, Z. Zhang, P.A. VanRompay, and P.P. Pronko (submitted to Applied Physics Letters).

“Microstructure of Epitaxial SnO₂ Thin Films Deposited on Sapphire Substrates Using Ultrafast Pulsed Laser Ablation”; L. Fu, J. E. Dominguez, X. Q. Pan, P. A. VanRompay, Z. Zhang, J. A. Nees, and P. P. Pronko (submitted to Journal of Applied Physics)

Conference Proceedings:

Invited presentation- European Materials Research Society, Strasbourg, France, June 17-21, 2002; “Critical Density Effects in Femtosecond Ablation Plasmas and Consequences for PLD Deposition”, P.P. Pronko, Z. Zhang, and P.A. VanRompay(submitted for publication in Applied Surface Science).

Conference on Lasers and Electro-Optics (CLEO/QELS), Long Beach, CA, May 19-24, 2002; “Enhanced Isotope Enrichment by Time-Delayed Laser-Pulse Pumping of Ultrafast Ablation Plumes”, P.A. VanRompay, Z. Zhang, and P.P. Pronko

Conference on Lasers and Electro-Optics (CLEO/QELS), Long Beach, CA, May 19-24, 2002; “Critical Density Effects in Sub-Picosecond Laser-Ablation of Silicon by Plasma-Absorption Ion-Energy Spectroscopy”, Z.Zhang, P.A. VanRompay, and P.P. Pronko.

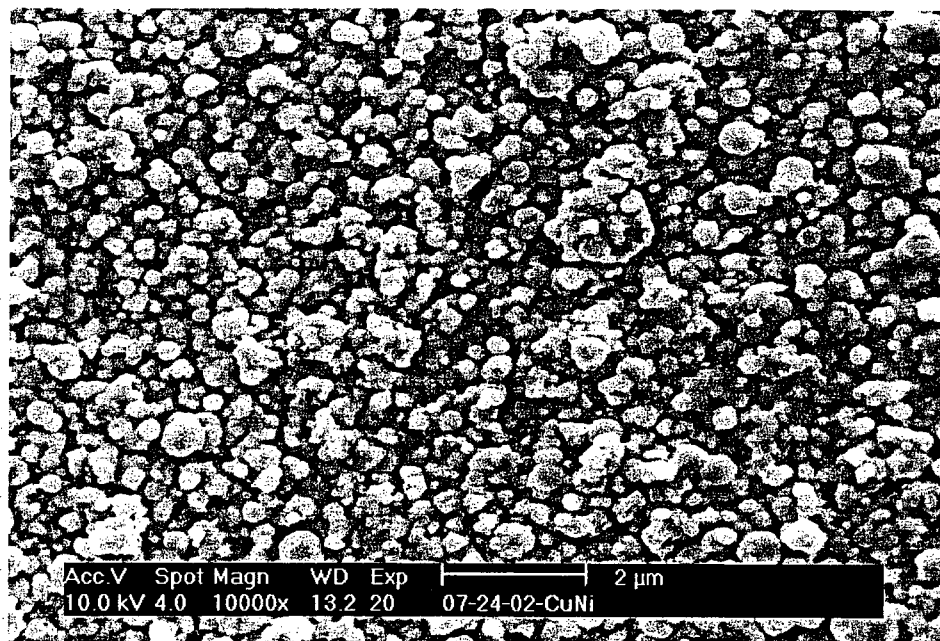


Figure 1 SEM image (magnification of 10,000X) of CuNi clusters deposited on silicon with single pulse.

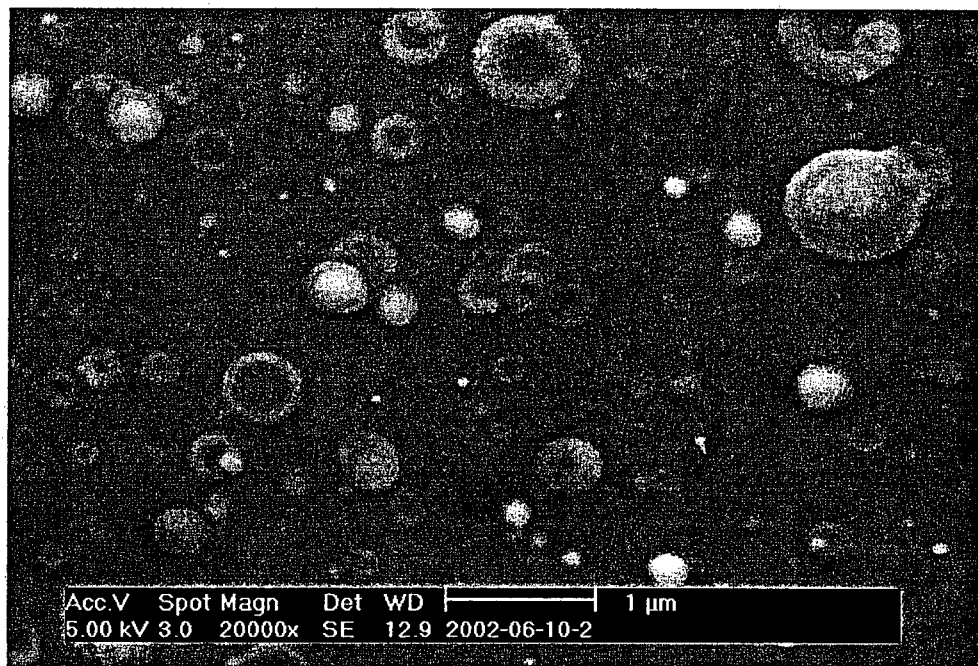


Figure 2. SEM Image (20,000X) of germanium clusters deposited using double pulse

Cold Rydberg Atom Gases and Plasmas in Strong Magnetic Fields

G. Raithel, University of Michigan

FOCUS Center, Physics Department, University of Michigan, 500 East University, Ann Arbor, MI 48109-1120

Scope and Plans

Recently, laser-cooling technology and well established methods of laser spectroscopy have converged into a new area in atomic and plasma physics, namely the study of cold plasmas and dense gases of cold Rydberg atoms. These novel systems, which can be generated by the photo-excitation of atom clouds collected in atom traps, allow one to prepare previously unattainable states of matter. Ionization, l -mixing, and recombination processes have been observed in these systems, as well as plasma oscillations. The extension of this research into the regime of strong magnetic (B) fields is of high interest, as B -fields are commonly used to confine plasmas, and plasmas and B -fields are ubiquitous in astrophysical environments.

The objective of this project is to study cold plasmas and dense gases of cold Rydberg atoms in a high- B -field environment. In particular, we want to elucidate the role highly diamagnetic Rydberg atoms play in such systems. Rydberg atoms in strong B -fields can have chaotic classical analogues, and have emerged as one of few systems that allow for laboratory tests of theories about quantum-classical correspondence in situations of classical chaos. In a different region of classical phase space, the magnetic field produces the dominant terms in the Hamiltonian, and the Coulomb interaction presents only a weak perturbation. The classical motion in this regime is regular and dominated by an $\mathbf{E} \times \mathbf{B}$ -drift of the atomic constituents. The effect of the Coulomb interaction is to weakly bind the gyration centers of the drifting particles in a shallow potential. The motion exhibits three characteristic components: a cyclotron oscillation, a bounce oscillation parallel to \mathbf{B} , and an $\mathbf{E} \times \mathbf{B}$ drift that leads to a slow magnetron oscillation. The motion can be quantized, leading to exotic atomic states that have large values of the conserved canonical angular-momentum component l_z parallel to \mathbf{B} . Based on wave-function overlap arguments and selection rules for electromagnetic transitions, we expect strongly magnetized high- l_z states to be long-lived. Further, semi-classical estimates of the density of states show that for B -fields of order of a few Tesla and Rydberg atom binding energies less than about 20 meV there are large numbers of high- l_z states a Rydberg atom can occupy. Therefore, we expect that Rydberg atoms in a collision-rich environment such as a strongly magnetized plasma predominantly evolve into high- l_z states.

The detailed goals of our research on strongly magnetized Rydberg atoms and cold plasmas are as follows:

- Characterization of the plasma and Rydberg atom components in a suddenly created, decaying cold plasma as a function of time, electron density and electron energy. Analysis of the Rydberg atom population with respect to ionization electric field and Rydberg-state lifetime.
- Determination of recombination cross sections of Rb^+ -ions vs. electron energy.
- Analysis of the plasma and the Rydberg atom components in steady-state plasmas continuously regenerated by cw lasers.
- Maximization of the plasma lifetime and the coupling parameter Γ in long-lived or continuously replenished quasi-steady-state strongly magnetized plasmas. Conditions may become favorable to form Wigner crystals.
- Radio-frequency and microwave spectroscopy of cold Rydberg atom gases and plasmas in strong magnetic fields.

We perform some theoretical studies on issues related to our experiments:

- We have calculated cross sections of microwave transitions, photo-ionization and radiative recombination of high- l_z magnetized Rydberg states.
- We plan a theoretical study of the validity of the Born-Oppenheimer approximation, which is the basis of our present quantum mechanical description of high- l_z Rydberg states in strong B -fields.
- Calculations on positronium Rydberg states in strong magnetic fields. In view of recent efforts on the formation and trapping of anti-hydrogen we believe that this subject is interesting.

Progress

State of the Experiment

A high- B trap with a B -field minimum tested up to 3.6 T forms the central part of our experiment. The construction of the superconducting high- B trap magnet and its cryostat has been completed. Using laser-cooling methods, a slow beam of Rb atoms has been prepared and sent from outside the cryostat into the high- B trap center. The brightness of the cold atomic beam has been optimized using superconducting magneto-optic traps (MOTs) created at the center of the cryostat as a sensitive probe for the flux of slow atoms.

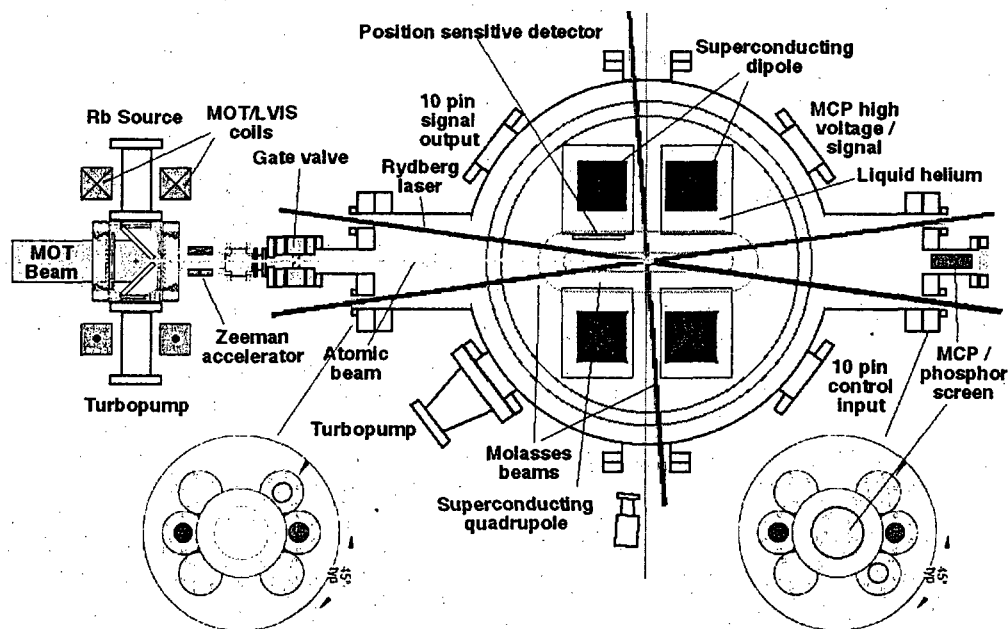


Figure 1: Outline of the beam preparation line and the high- B trap.

Trap magnet and cryostat

The four-coil superconducting trap magnet, which emerged from combined designing efforts at AMI and in my group, contains a main split-coil dipole magnet that provides a strong bias field at the trap center. A pair of racetrack-shaped coils with opposite current directions inserted into the dipole magnet adds a strong quadrupole field to the dipole field, thereby creating a Ioffe-Pritchard-type local minimum of the B -field, which acts as a magnetic trap for neutral atoms and as a magnetic bottle for ions and electrons. An auxiliary center tap on the split-coil dipole magnet can be used to move the trap minimum in axial direction and to thereby overlap it with the geometrical symmetry point of the coil arrangement. The magnet unit has six cold bores providing optical and instrumentation access from outside the cryostat; the cryostat has been built by Janis. The magnet has been successfully tested at a center field of 3.6 T and a current density in the racetrack coils of $12,000 \text{ A/cm}^2$. Under these conditions, the trap depth is 420 Gauss, which for Rb corresponds to a maximal velocity of trapped atoms of 2.3 m/s. Along the z -axis, i.e. the axis of the split-coil dipole magnet, the field follows $B = 3.6 \text{ T} + z^2 70 \text{ Gauss/cm}^2$. The curvatures of the field magnitude in the x and y -directions are about the same as in the z -direction.

Atomic-beam source

We have constructed a large vapor-cell pyramidal MOT to collect and pre-cool Rb atoms (left section in Fig. 1). A large collection rate of atoms is achieved by using large pyramid mirrors and a large MOT laser beam (about 4 cm diameter). To produce the MOT laser light, a master diode laser system is locked about 15 MHz below the $F = 3 \rightarrow F = 4$ transition of the ^{85}Rb D2-line using standard saturation spectroscopy. The master diode is microwave-modulated at a frequency of 3.02 GHz to provide a frequency sideband coincident with the ^{85}Rb repumping transition ($F = 2 \rightarrow F = 3$ transition of the D2-line). Half the useable

output of the master laser is used to injection-lock a slave diode laser system; the output of the latter is sent through a single-mode fiber to produce a Gaussian MOT laser beam with 25 mW power. The other half of the master laser output is used to injection-lock another slave laser system.

A 1 mm-sized hole in the tip of the pyramidal mirror allows atoms collected in the MOT to be emitted in form of a slow atomic beam. The atomic beam can be turned on and off in rapid sequence (of order 1 ms switching time). When the atomic beam is turned off, the MOT lacks a fast trap loss mechanism, and it becomes as bright as a normal vapor-cell MOT (upper left in Fig. 2). The atomic beam is turned on by overlapping the MOT trap center with the 1 mm diameter extraction column, which is defined by the hole in the pyramidal mirror and the direction of the incident MOT laser beam (Fig. 1). In that case, all cold atoms entering the extraction column get ejected due to radiation-pressure imbalance, thereby forming the cold atomic beam. Since the atomic beam presents a fast trap loss mechanism, the MOT becomes quite dim. Further, because the transfer of atoms from the MOT into the cold atomic beam is localized to a line passing through the MOT center, the MOT appears doughnut-shaped when viewed from a direction close to that line (see upper right in Fig. 2).

Superconducting magneto-optic traps

To optimize the atomic beam, we have used the superconducting coils to create magnetic-field configurations suitable to operate MOTs at the center of the high-*B* magnet. The laser light for the secondary MOTs is provided by an independent microwave-modulated diode laser system. Sending small opposite currents through the dipole coils (see Fig. 1) yields a usual 3D MOT configuration (lower left of Fig. 2). Simultaneous operation of the dipole coils and the racetrack coils with suitable small currents yields a 3D MOT configuration with different axes (lower row in Fig. 2, second from the left). When the racetrack coils are operated alone and at small current, we obtain 2D MOTs.

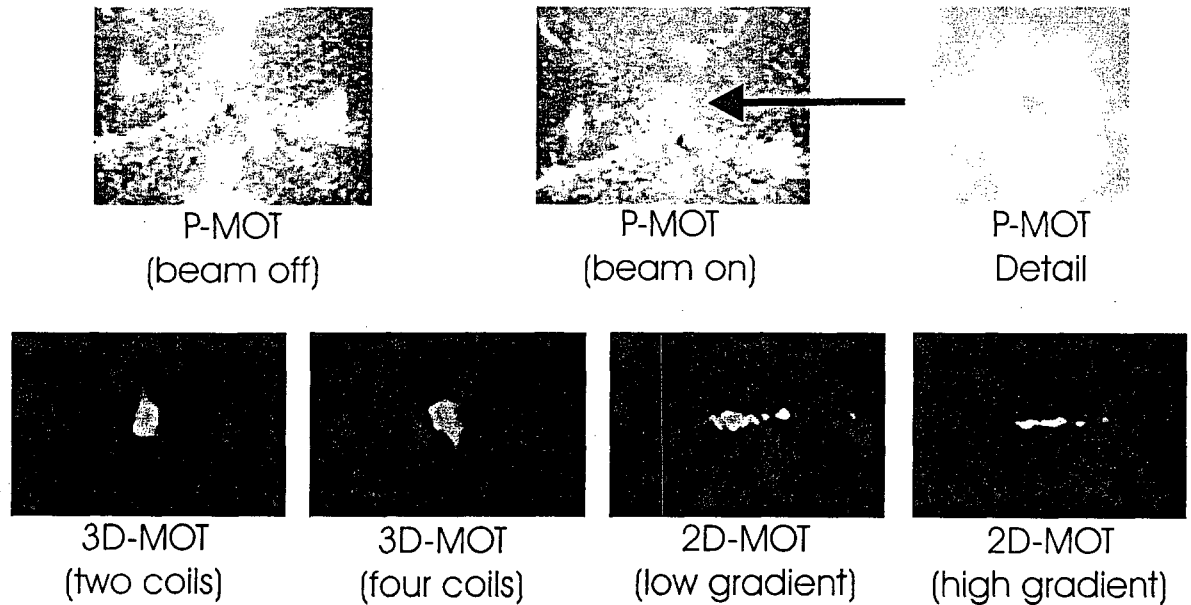


Figure 2: Top row: Primary pyramidal MOT used for atomic-beam generation. The atom cloud and multiple mirror images of it are visible. The linear structures in the background of scattered light indicate the corners of the pyramidal MOT mirror. Bottom row: Secondary MOTs produced at the cryostat center using two or four superconducting coils.

The successful operation of the secondary MOTs has shown that the primary (pyramidal) MOT produces an atomic beam that reaches the center of the high-*B* trap magnet. It has been demonstrated that the atomic-beam apparatus and the laser beams used for the secondary MOT and - later - for the high-*B* molasses are functional with the cryostat cooled to L-He temperature: there is no excessive differential thermal contraction of cryostat parts, and no excessive fogging of cryostat windows. We have developed robust and fast strategies to align the atomic beam. An analysis of the positions of the MOTs displayed in the lower row of Fig. 2 has

also shown that the system of four superconducting coils has been manufactured well enough that there is no noticeable displacement of the various field symmetry points from the intersection point of the six optical access channels. The high quality of the cryo-pumped vacuum has been confirmed by the observation of magnetic trapping times larger than one minute.

Without further action, atomic-beam sources such as ours produce beams with an average velocity of about 10 m/s. Thus, under low- B conditions our atomic beam droops by a few cm on its way to the cryostat center. This is considerably more than the radius of various apertures along the atomic-beam path. The loading efficiency of the secondary MOTs is therefore limited by the fact that - without further action - only the atoms at the high-velocity end of the atomic-beam velocity distribution are transferred. Later, when the system will be operated in a high- B molasses configuration, only atoms exceeding a velocity of about 20 m/s will be able to overcome the repulsive magnetic-dipole potential of the high- B trap and to become trapped. Because of these issues, an additional pusher laser beam produced by another diode laser system has been introduced. The pusher beam, which has 1 mm diameter and propagates collinear with the atomic beam, accelerates the atoms to > 20 m/s. The pusher beam intensity and polarization have been optimized using the brightness of a secondary superconducting MOT as a meter for the transfer efficiency. As expected, the pusher laser has resulted in a large increase in the loading rate of the secondary MOTs.

High- B molasses

We presently work on the realization of a 3.2 Tesla high- B molasses. ^{85}Rb atoms reaching the trap center in the state $|m_J = 2.5, m_S = 0.5\rangle$ will be captured by a six-beam optical molasses. The molasses lasers are blue-shifted from the field-free resonance by 48 GHz. To be able to lock and scan the molasses laser, we have constructed a temperature-stabilized scanning Fabry-Perot-interferometer. Labview software is used to simultaneously control the magnets (two supplies for superconducting coils, two supplies for the pyramidal MOT, a couple of supplies for shimming coils) and to conduct the molasses search scans. Recently, we have run the whole system at a trap field of 3.2 T and have conducted a first one-hour search for the high- B molasses. While we have not seen the high- B molasses yet, we are encouraged by the fact that we are now able to simultaneously run all laser systems, the primary MOT, the cryostat, and the high- B trap magnet at large trap fields.

Rydberg atoms

A pulsed YAG and dye laser system suitable to excite Rb Rydberg atoms has been moved into the lab and has been prepared for its use. Two new cooled dye circulators have been built. A set of construction drawings for the Rydberg atom and plasma manipulation electrodes has been completed, and most materials required to build them have been bought. A position-sensitive two-stage MCP detector with a phosphor screen is currently being checked in a small test setup. High-voltage power supplies and amplifiers, needed to drive the MCP detector and the electrodes, have been constructed.

Publications which acknowledge DoE support:

"Ponderomotive optical lattice for Rydberg atoms," S. K. Dutta, J. R. Guest, D. Feldbaum, A. Walz-Flannigan, G. Raithel, *Phys. Rev. Lett.* **85**, 5551 (2000).

"High-angular-momentum Rydberg states in cold Rydberg gases," S. K. Dutta, D. Feldbaum, A. Walz-Flannigan, J. R. Guest, and G. Raithel, *Phys. Rev. Lett.* **86**, 3993 (2001).

"Spectroscopy of Rydberg Atoms in Non-neutral Cold Plasmas," D. Feldbaum, N. V. Morrow, S. K. Dutta, G. Raithel, in *Non-Neutral Plasma Physics IV*, eds. F. Anderegg, L. Schweikhard, C. F. Driscoll (AIP Conference Proceedings, Volume 606, New York 2002).

"1-Changing Collisions in Cold Rydberg Gases", A. Walz-Flannigan, D. Feldbaum, S. K. Dutta, J. R. Guest, G. Raithel, in *Photonic, Electronic and Atomic Collisions (XXII ICPEAC Proceedings)*, eds. J. Burgdörfer, J. S. Cohen, S. Datz, C. R. Vane (Rinton Press, Princeton, NJ, 2002).

"Tunneling resonances and Coherence in an Optical Lattice," B. K. Teo, J. R. Guest, G. Raithel, *Phys. Rev. Lett.* **88**, 173001 (2002).

"Magnetic Behavior of Atoms in Gray Optical Lattices," J. R. Guest, B. K. Teo, N. V. Morrow, G. Raithel, submitted.

"Coulomb Expansion of Laser-Excited Ion Plasmas," D. Feldbaum, N. V. Morrow, S. K. Dutta, G. Raithel, submitted.

Measurement of Electron Impact Excitation Cross Sections of highly ionized atoms

A. J. Smith

Department of Physics, Morehouse College, Atlanta GA 30314.

Unfunded Liaison/Collaborator: Peter Beiersdorfer

Lawrence Livermore National Laboratory, Livermore, CA 94550

August 21, 2002

1. Introduction

We use the Lawrence Livermore National Laboratory electron beam ion trap EBIT-I to study x-ray emissions from highly ionized atomic species with low to intermediate values of Z . The atoms are ionized trapped and excited by a magnetically compressed, nearly monoenergetic (50 eV FWHM) electron beam. We also use high resolution Bragg crystal spectrometers as well low resolution solid-state spectrometers to observe photons emitted at 90° to the electron beam. We look at various processes including dielectronic recombination (DR), direct (electron impact) excitation (DE), and radiative recombination (RR). Our measurements provide basic atomic data relevant to a better understanding of the physics of highly ionized atoms. Our data is also used for development of spectral codes used in the diagnostics of high density and high temperature plasmas.

2. Dielectronic recombination in heliumlike Ti^{20+} and Cr^{22+}

We have measured the resonance strengths for dielectronic recombination in heliumlike titanium and chromium using techniques similar to those that we used for our argon measurements. DR is a resonant process in which a free electron is captured, and a bound electron is simultaneously excited to a higher level. The doubly excited state so formed may be stabilized by the emission of a photon. These so called satellite transitions have energies close to that of a resonant transition of the recombining ion, since the presence of the observer electron does not significantly modify the upper levels of the satellite lines. Using a low resolution solid state spectrometer we observe x-ray photons from the decay of either one of the excited electrons. In these measurements we also observe radiative recombination (RR) into the $n=2$ shell; this process is the inverse of photoionization. We have observed the KLM, KLN, KLO, and KLP resonances in $TiXXI$ and $CrXXIII$. In the KLM series, a K-shell electron is excited to an L-shell, while a free electron is captured into an M-shell. For each resonance we obtain resonance strengths for the $n = 2 - 1$ branch as well as for the $n = j - 1$, for $j = 3$ (KLM), 4(KLN), 5(KLO), and 6(KLP). We normalize the observed resonance strengths to radiative recombination cross sections, which can be calculated to a high degree of accuracy. Our measurements are compared with MCDF calculations, and with similar measurements found in literature.

3. Level-specific DR resonances in heliumlike Ti^{20+} and Cr^{22+}

In these measurements we use the LLNL EBIT and a high resolution Bragg crystal spectrometer to make accurate measurements of line positions and line intensities following dielectronic recombination in highly charged ions. We sweep the electron beam energy across individual DR resonances, and thus we are able to measure level specific resonance strengths for the strongest DR resonances in doubly excited lithiumlike and berylliumlike titanium and chromium. We also use MCDF code to calculate the excitation energies as well as the pho-

ton energies for these transitions. We compare observed to predicted wavelengths as well as observed to predicted resonance strengths. Our measurements include not only the KLL resonances, which have been observed in many tokamak spectra, but also KLM and KLN resonances which are not easily observed in tokamak spectra.

4. Polarization of He-like Ti^{22+} and V^{23+}

EBIT x-rays are polarized, and the EBIT high resolution spectrometers use crystals that have polarization dependent reflectivities. Measured intensities of EBIT x-rays must be corrected for the polarization. In most cases we rely on predicted polarizations to determine the corrections we need for lines we observe. These can be calculated from the partial cross sections for excitation to various magnetic sub-levels. It is also possible to measure the polarization of a line using two polarization sensitive spectrometers. In separate measurements, we have measured the polarizations of K-shell x-ray transitions in TiXX and TiXXI and of the $K\beta_2$ line heliumlike VXXIV .

5. Planned Research

Our new proposal which started in May, 2002 will concentrate on investigating various discrepancies between theory and experiment with regards to various electron-ion interactions. The discrepancies were discovered during our project that just ended. We propose to measure accurate cross sections for DE in heliumlike argon as the first step in our effort to understand how highly charged heliumlike ions interact with electrons. This will be followed by similar studies in heliumlike Ne and Al.

6. Acknowledgments

We gratefully acknowledge support by the Office of Basic Energy Science, Chemical Sciences Division. This work was performed under the auspices of the Department of Energy

by Lawrence Livermore National Laboratory under contract No. W-7405-ENG-48 and by Morehouse College under contract No. DE-FG02-98ER14877.

7. Publications List

- [1] "Ratios of $n = 3 - 1$ Intercombination to Resonance Line Intensities for Heliumlike ions with Intermediate Z -values," A. J. Smith, P. Beiersdorfer, K. J. Reed, A. L. Osterheld, V. Decaux, K. Widmann, and M. Chen, *Phys. Rev. A* **62** 012704 (2000).
- [2] "Recent Livermore Excitation and Dielectronic Recombination Measurements for Laboratory and Astrophysical Spectral Modeling," P. Beiersdorfer, G. V. Brown, M. -F. Gu, C. L. Harris, S. M. Kahn, S. -H. Kim, P. A. Neill, D. W. Savin, A. J. Smith, S. B. Utter, and K. L. Wong, Conference contribution for the "Int. Seminar on Atomic Processes", Toki, Japan; published as a NIFS proceeding.
- [3] "Experimental M1 transition rates of coronal lines from Ar X, Ar XIV, and Ar XV" E. Träbert, P. Beiersdorfer, S. B. Utter, G. V. Brown, H. Chen, C. L. Harris, P. A. Neill, D. W. Savin, A. J. Smith, *Astrophys. J* **541**, 506 (2000).
- [4] "Measurement of the Polarization of the $K\beta_2$ line of V^{21+} ", A. J. Smith, P. Beiersdorfer, E. Träbert, K. J. Reed, presented at the 3rd US-Japan Plasma Polarization Spectroscopy workshop, June 18-21, 2000, at the Lawrence Livermore National Laboratory, Livermore, CA, published in proceedings.
- [5] "Polarization spectroscopy of K-shell x-ray transitions of highly-charged Ti and Fe ions excited by an electron beam", C. Harris, P. Neil, P. Hakel, R. C. Mancini, A. S. Shlyaptseva, P. Beiersdorfer, S. Uter, G. Brown, A. J. Smith, E. Träbert, H. Zhang, and R. E. H. Clark, proceedings of APIP conference, Gatlinburg, TN April 2002.

DYNAMICS OF FEW-BODY ATOMIC PROCESSES

Anthony F. Starace

*The University of Nebraska
Department of Physics and Astronomy
116 Brace Laboratory
Lincoln, NE 68588-0111
Email: astarace1@unl.edu*

PROGRAM SCOPE

The major goal of this project is to understand the physics underlying the interaction of real atomic systems with strong external fields. Nearly all the atomic systems considered for study are many-electron systems. We treat their interactions, i.e., electron correlations, as accurately as possible. The strong external fields considered are mainly intense laser fields. In some cases our studies are supportive of and/or have been stimulated by experimental work carried out by other investigators funded by the DOE AMO physics program.

RECENT PROGRESS

A. Angular Distributions for Double Ionization of Li^- by an Ultrashort, Intense Laser Pulse
[G. Lagmago-Kamta and A. F. Starace, *Phys. Rev. A* **65**, 053418 (2002)]

We have presented a detailed account of a two-active-electron (TAE) approach for solving the time-dependent Schrödinger equation (TDSE) for the interaction of a multi-electron system with an ultrashort, intense, and linearly polarized laser pulse. A technique for obtaining angular distributions for double ionization by such pulses has also been described. The approach for solving the TDSE in the TAE approximation is full dimensional and accounts for correlations between the two electrons, as well as the polarization of the core. It is based on a configuration-interaction expansion of the time-dependent wave function in terms of one-electron atomic orbitals. Applying the method to the lithium negative ion (Li^-), we display the time-dependent dynamics of the photodetachment process. For low intensities, our results for the detachment yield follow expectations from lowest-order perturbation theory and agree satisfactorily with \mathcal{R} -matrix calculations. Our results for angular distributions indicate that following multiphoton double ionization by an intense laser field, electrons are predominantly ejected along the laser polarization axis; however, a significant number are ejected perpendicularly to this axis. An angular momentum-based analysis of these angular distributions indicates that, in the dipole approximation and for an initial $^1S^e$ state interacting with a linearly polarized laser field, double ejection of both electrons along the direction perpendicular to the laser polarization axis can only occur following absorption of an even number of photons, whereas multiphoton absorption of an odd number of photons does not lead to double ejection at these angles. A preliminary account of these results has been given earlier [*Phys. Rev. Lett.* **86**, 5687 (2001)].

B. Role of Rescattering in Intense Field Double Ionization Processes

[G. Lagmago-Kamta and A. F. Starace, *J. Mod. Optics* (in press)]

As described above, we have studied in the dipole approximation the interaction of Li^- with an ultrashort intense laser field, linearly polarized along the z -axis, via a direct numerical solution of the TDSE. In all cases, angular distributions for double ionization obtained for the multiphoton regime exhibit the influence of electron-electron correlations. In the case of intense fields, both electrons may be ejected perpendicularly to the laser polarization axis; this does not occur for the single photon, weak field case. In this work, we have shown that very general symmetry and angular momentum selection rules for a two-electron wave function having initially $L = 0$ permits this perpendicular ejection only for the case in which an even number of photons is absorbed.

In addition, we have carried out numerical experiments on single and double ionization by a single cycle pulse (SCP) and by a double half-cycle pulse (DHP) that show that single and double ionization are larger for the SCP than for the DHP. Since rescattering only occurs for the SCP case, these results suggest that the rescattering mechanism enhances both single and double ionization. On the other hand, angular distributions for double ionization by a half-cycle pulse, for which rescattering does not apply, show the existence of a significant shakeoff contribution to double ionization, in which one electron is ejected in the direction opposite to that of the laser field force direction.

C. GeV Electrons from Ultra Intense Laser Interactions with Highly Charged Ions

[S. Hu and A. F. Starace, *Phys. Rev. Lett.* **88**, 245003 (2002)]

We have begun to investigate laser interactions with highly charged ions using a three-dimensional Monte Carlo simulation. Initially, we have studied hydrogenic highly charged ions. We have first demonstrated that free electrons cannot be accelerated to GeV energies by the highest intensity lasers because they are quickly expelled from the laser pulse before it reaches peak intensity. We have shown that highly charged ions exist that (1) have deep enough potential wells that tunneling ionization is insignificant over the duration of an intense, short laser pulse, and (2) have potentials that are not too deep, so that the laser pulse is still able to ionize the bound electron when the laser field reaches its peak intensity. We have shown that when the ionized electron experiences the peak intensity of the laser field, then it is accelerated to relativistic velocity along the laser propagation direction (by the Lorentz force) within a fraction of a laser cycle. Within its rest frame it then "rides" on the peak laser amplitude and is accelerated to GeV energies before being expelled from the laser pulse.

D. Control of Entanglement of Two Interacting Spin 1/2 (Heisenberg) Systems

[G. Lagmago-Kamta and A. F. Starace, *Phys. Rev. Lett.* **88**, 107901 (2002)]

Entanglement is a nonlocal correlation between quantum systems that does not exist classically. Quantum entanglement has become recognized as crucial in various fields of quantum information, including quantum cryptography, quantum teleportation, and quantum computation. Potential applications of entanglement in these fields have stimulated research on ways to quantify and control it. In particular, considerable attention has been paid to interacting

Heisenberg spin 1/2 systems, which may have applications in gate operations in solid state quantum computation processors. A major limitation on such applications, however, is that entanglement in such systems normally vanishes above some finite critical temperature T_c . We have shown that an external constant magnetic field, combined with anisotropic spin interactions, may be used to overcome the temperature barrier in particular interacting spin 1/2 systems, thereby allowing one to entangle the spins at any finite temperature. Specifically, we have shown that for the case of two interacting spin 1/2 qubits whose interaction is anisotropic (i.e., different in different directions) the critical temperature (above which entanglement no longer exists) is dependent on the magnitude of the magnetic field, which is chosen to be constant along the z axis. This is different from the case in which the interaction of the two spins is isotropic (i.e., independent of direction), in which case T_c is independent of the magnetic field strength. We have shown that in the case of anisotropic interactions T_c depends on the magnetic field value, and that for a sufficiently strong magnetic field there always exists entanglement. More generally, we have shown that through variation of the anisotropy of the interaction and the value of the magnetic field one can control the extent of entanglement of two interacting spin 1/2 systems. The absence of a temperature barrier may hasten the development of practical devices in the various fields of quantum information.

FUTURE PLANS

Our group is currently carrying out research on the following projects: (1) A more detailed analysis of the role of rescattering effects on double ionization of two-electron systems, including investigation of the variation of these effects with two-electron energies; (2) A systematic analysis of the energy spectrum of GeV electrons produced by intense laser pulses interacting with highly-charged ions and the dependence of this spectrum upon laser parameters, including focal effects; (3) Investigation of the triply differential cross section for single-photon, double ionization of He using a perturbative method employing a Green's function in parabolic coordinates and including examination of circular and elliptical dichroism effects as well as non-dipole effects; (4) Investigation of the dynamic polarizabilities and multiphoton ionization cross sections for two-electron systems using a variationally stable, coupled-hyperspherical channel approach capable of producing benchmark results and including an examination of the role of logarithmic terms in describing the two-electron systems near the triple coalescence point; (5) Investigation of the role of external static fields on the entanglement of interacting spin 1/2 (Heisenberg) systems, with analysis of (i) means to control the entanglement and (ii) applications in various fields of quantum information (computation, cryptography, and teleportation). Nearly all proposed projects involve large-scale numerical computations.

PUBLICATIONS

- [1] M. Masili and A.F. Starace, "One- and Two-Photon Detachment Cross Sections and Dynamic Polarizability of H^- Using a Variationally Stable, Coupled-Channel Hyperspherical Approach," *Phys. Rev. A* **62**, 033403 (2000).
- [2] C.-N. Liu and A.F. Starace, "Mirroring and Mimicking of Partial Cross Sections in the

Vicinity of a Resonance,” *Physics Essays* **13**, 215 (2000).

- [3] G. Lagmago Kamta and A.F. Starace, “Angular Distributions for Double Ionization of Li^- by an Ultrashort, Intense Laser Pulse,” *Phys. Rev. Lett.* **86**, 5687 (2001).
- [4] G. Lagmago Kamta and A.F. Starace, “Angular Distributions for Double Ionization by an Ultrashort, Intense Laser Pulse: The Case of Li^- ,” in *Super-Intense Laser-Atom Physics*, edited by B. Piraux (Kluwer, Dordrecht, The Netherlands, 2001), pp 143-152.
- [5] S.X. Hu and A.F. Starace, “GeV Electrons from Ultra-Intense Laser Interaction with Highly-Charged Ions,” *Phys. Rev. Lett.* **88**, 245003 (2002).
- [6] G. Lagmago Kamta and A.F. Starace, “Anisotropy and Magnetic Field Effects on the Entanglement of a Two Qubit Heisenberg XY Chain,” *Phys. Rev. Lett.* **88**, 107901 (2002).
- [7] G. Lagmago Kamta and A.F. Starace, “Multielectron System in an Ultrashort, Intense Laser Field: A Nonperturbative, Time-Dependent Two-Active Electron Approach,” *Phys. Rev. A* **65**, 053418 (2002).
- [8] G. Lagmago Kamta and A.F. Starace, “Two-Active Electron Approach to Multielectron Systems in Intense Ultrashort Laser Pulses: Application to Li^- ,” *J. Mod. Optics* (in press).

FEMTOSECOND AND ATTOSECOND LASER-PULSE ENERGY TRANSFORMATION AND CONCENTRATION IN NANOSTRUCTURED SYSTEMS

Progress Report on DOE Grant No. DE-FG02-01ER15213

Mark I. Stockman

Department of Physics and Astronomy, Georgia State University, Atlanta, GA 30303

E-mail: mstockman@gsu.edu

1. Program Scope

The scope of the program includes a theoretical study of ultrafast (femtosecond and attosecond) optical processes in nanosystems. Both linear and nonlinear optical processes are within the scope of this project. The project focuses on the ultrafast localization and transformation of optical excitation energy and the corresponding generation and localization of the local fields on the nanoscale. Transfer of energy between optical modes (parametric processes such as generation of harmonics), nanoscale transport of optical energy in space, and transformations of the optical energy into other kinds of energy, e.g., by processes of light-induced electron-electron scattering, are included. Ways to control the processes of ultrafast energy localization and transformation on the nanoscale, in particular, by coherent control, are within the scope of the project.

2. Recent Progress

This sponsored research during the current grant period has focused on problem of controlling localization of the energy of ultrafast (femtosecond) optical excitation on the nanoscale. This is a formidable problem since it is impossible to achieve such concentration by optical focusing due to the nanosize of the system. It turns out also impossible to achieve the nanoscale localization of energy by using a near-field excitation alone (e.g., by means of a NSOM), because there always are delocalized eigenmode of the system overlapped in spectrum with localized eigenmodes¹ (see also Refs. 2-4) which would lead to delocalization of energy in a femtosecond-scale interval of time. We have proposed a method based on the coherent control that uniquely allows one to define the spatial localization of ultrafast excitation energy on the nanoscale,⁵ see also Refs. [6-11]. Another branch of our research has dealt with interaction and relaxation processes in systems of interacting electrons studied by means of the Kadanoff-Baym-Keldysh nonequilibrium Green's function technique,¹² see also Ref. 13.

The properties of polar excitations (eigenmodes) on nanoscale (called conventionally surface plasmons in nanosystems) are of principal importance for the entire field of the interaction of light with nanosystems. We suggested in early 1990s that in disordered nanosystems (especially, fractal clusters) eigenmodes are strongly localized due to Anderson localization. Later, there have been obtained mounting evidence that the strongly localized eigenmodes do exist. However, we have observed in numerical experiments that also non-localized eigenmodes are always present. This problem has been resolved in our paper¹ where we have analytically proved a theorem there can exist no nanosystem all eigenmodes of which are Anderson localized. This theorem follows from a rigorously proven fact that any Anderson-localized eigenmode is dark, i.e., it does not interact with external far-zone fields (it cannot be excited or observed by plane waves).

We have found¹⁻⁴ that surface plasmons of nanosystems have properties of both localized and delocalized states simultaneously. Their topology is determined by separate small-scale "hot spots" that are distributed and coherent over a length that may be comparable to the total size of the system. Coherence lengths and oscillator strengths vary by orders of magnitude from mode to mode at nearby frequencies. The existence of dark vs. luminous eigenmodes is established (the dark eigenmodes do not

contribute to optical responses, and the luminous eigenmodes do) and attributed to the effect of charge- and parity-conservation laws.

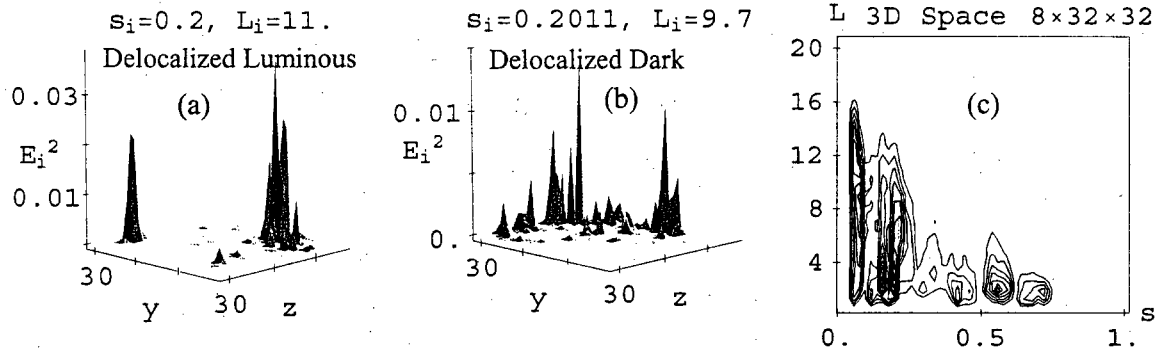


Figure 1. Examples of the delocalized luminous eigenmode (a) and delocalized dark eigenmode (b); the eigenvalues s_i and localization (coherence) radii L_i of the eigenmodes are shown. The distribution of the eigenmodes over their localization radius L and spectral parameter s is plotted as a contour map (c). Adapted from Ref. 1.

The results of our computations for random planar nanostructures are illustrated in Fig.1 (Ref. 1). Note that these results are obtained in spectral representation and, correspondingly, are material-independent.

The topology of the eigenmodes [Fig.1(a) and (b)] shows the above-mentioned topology of localized hot spots that are spread over the entire system. Fig.1(c) displays the distribution over the localization lengths L , which is very wide, from the minimum scale to the radius of the entire system (16 units in the scale of the figure). This result is of principal importance for nanoplasmonics: at any given value of the spectral parameter s (that uniquely relates to physical frequency for any given material), there always are delocalized as well as localized surface plasmons. This implies in particular that it is impossible to localize energy on the nanoscale in a resonant nanosystem by locally exciting it, because the delocalized eigenmodes will spread this energy across the entire extent of the system. *This is a fundamental result, but it is difficult to overestimate its importance for applications, because many of them, in particular, nano-photomodification and probing, require optical fields localized at nanoscale where such fields are formed by the surface plasmons.*

Based on our understanding of the dynamic properties of surface plasmons, we have proposed coherent control of ultrafast energy localization at nanoscale.⁵⁻¹¹ Our idea is to excite a spectrally-wide packet of surface plasmons and give the plasmons at a given frequency a certain distinctive phase. The set of such phases constitute the degrees of freedom by means of which we control the system to localize the excitation energy at a given nano-site at a given time.

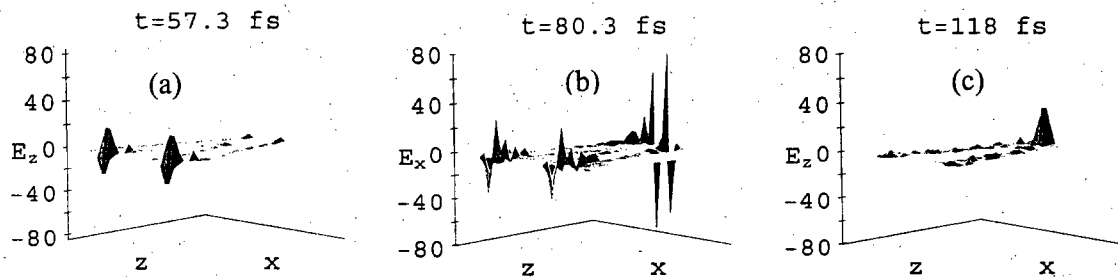


Fig. 2. Spatial distributions of local electric fields (in the units of the exciting pulse amplitude) at the nanosystem for moments of time indicated. The duration of the exciting pulse is 50 fs, and the phase modulation parameter $\alpha = -0.3$ [1].

The results of the simulations [1] for a V-shaped planar nanostructure made of silver (8 nm thick) subjected to a phase-modulated 25-fs exciting light pulse (the carrier frequency $\hbar\omega_0 = 0.8$ eV) with a negative linear chirp are illustrated in Fig. 2. This example shows that, as the pulse progresses, the maximum of the local fields and, correspondingly, the energy of the excitation on the nanoscale move from the opening of the nanostructure [see Fig. 2(a)] toward the apex where they strongly concentrate for a significant time interval on the femtosecond scale from 80 to 118 fs [see Fig. 2 (b) and (c)]. The maximum local field at the apex exceeds the exciting field by almost two orders of magnitude, which means that the local optical intensity is enhanced by four orders of magnitude. In the absence of the phase modulation, and for a different sign of the chirp, the concentration of energy is absent. *The predicted energy concentration may be used to energize or control the nanostructures for computations on the nanoscale, for directed nano-modification, to excite nonlinear photoprocesses localized at the nanoscale for ultrafast optical probing, and in other fields.*

Finally, we briefly mention our work^{12,13} on the electrons in a quantum well with the Coulomb interaction between them in the presence of an optical field in the framework of the Kadanoff-Baym-Keldysh method. We have found that the Coulomb interaction causes optical transitions to acquire non-zero spectral width even for very low population of the excited electrons. This is due to the fact that optical transitions move to electrons from states far below the Fermi surface to states high above the Fermi surface. For these states, Landau's Fermi-liquid theory of almost non-interacting quasiparticles is no longer valid. The quasiparticles acquire finite lifetimes, which causes broadening of their spectra. *This result is of principal importance for the optics of semiconductor quantum dots and metallic nanoparticles. In particular, in metals, such broadening is much stronger, which may explain why the metal nanoparticles do not exhibit discrete electron spectra in contrast to quantum dots.*

3. Future Plans

For the nearest future we plan to further develop the areas that we initiated the previous period, and to explore some new directions. The following research projects are in progress, or planned for the near future.

1. The ultrafast concentration of energy in nanosystems with structural defects. This is a necessary step before proposing arrangements for the experimental observation of the effect, because no fabricated nanosystem is ideal.
2. The perturbative nonlinear theory of the coherent control of ultrafast energy localization in nanosystems. This project will invoke effects of the second- and third-order nonlinearity on the energy concentration in nanosystems.
3. Energy transformations in semiconductor nanoparticles interacting with metallic nanosystems. We expect to reveal various processes of the relaxation and the exchange of energy and polarization between the electrons of the semiconductor nanoparticles and the surface plasmons of the nanostructure in its vicinity.
4. Theory of the imaging of nanostructures by NSOMs. This theory will invoke interaction of the surface plasmons of the nanostructure with modes of the NSOM.

References

- ¹ M. I. Stockman, S. V. Faleev, and D. J. Bergman, *Localization vs. Delocalization of Surface Plasmons in Nanosystems: Can One State Have Both Characteristics?*, Phys. Rev. Lett. **87**(16), 167401-1-4 (2001).
- ² D. J. Bergman, M. I. Stockman, and S. V. Faleev, *Anderson Localization vs. Delocalization of Surface Plasmons in Nanosystems*, APS March 2002 Meeting (Indianapolis, Indiana, March 18-22, 2002), Bulletin of American Physical Soc. **47**, 1265 (2002).

-
- ³ D. J. Bergman, M. I. Stockman, and S. V. Faleev, *Anderson Localization vs. Delocalization of Surface Plasmons in Nanosystems*, QELS 2002 (Long Beach, CA, May 19-24, 2002), Talk QF86, QELS 2002 Technical Digest, pp. 259-260, OSA, 2002.
- ⁴ D. J. Bergman, M. I. Stockman, and S. V. Faleev, *Anderson Localization vs. Delocalization of Surface Plasmons in Nanosystems*, Proceedings of the Progress in Electromagnetics Research Symposium 2002 (PIERS 2002) (July 1 - 5, 2002, Cambridge, Massachusetts, USA), p. 841 (Invited Talk).
- ⁵ M. I. Stockman, S. V. Faleev, and D. J. Bergman, *Coherent Control of Femtosecond Energy Localization on Nanoscale*, Phys. Rev. Lett. **88**(5) 067402-1-4 (2002).
- ⁶ M. I. Stockman, S. V. Faleev, and D. J. Bergman, *Coherently-Controlled Femtosecond Energy Localization on Nanoscale*, Appl. Phys. B **74**(9), 63-67 (2002) [Appl. Phys. On-Line: <http://dx.doi.org/10.1007/s00340-002-0868-x>].
- ⁷ M. I. Stockman, S. V. Faleev, and D. J. Bergman, *Femtosecond Energy Localization on Nanoscale Controlled by Pulse Phase*, APS March 2002 Meeting (Indianapolis, Indiana, March 18-22, 2002), Bulletin of American Physical Soc. **47**, 734 (2002).
- ⁸ M. I. Stockman, S. V. Faleev, and D. J. Bergman, *Femtosecond Energy Concentration in Nanosystems Coherently Controlled by Excitation Phase Modulation*, In: Technical Proceedings of the Second International Conference on Computational Nanoscience and Nanotechnology (NanoTech 2002 - ICCN 2002), pp. 380-382 (Computational Publications, Boston, Geneva, San Francisco, 2002).
- ⁹ M. I. Stockman, S. V. Faleev, and D. J. Bergman, *Femtosecond Energy Concentration in Nanosystems Coherently Controlled by Excitation Phase*, The Thirteenth International Conference on Ultrafast Phenomena (Vancouver, BC, Canada, May 12-17, 2002), Talk ME41-1, Technical Digest, pp. 135-136, OSA, 2002.
- ¹⁰ M. I. Stockman, S. V. Faleev, and D. J. Bergman, *Femtosecond Energy Concentration in Nanosystems Controlled by Excitation Phase*, Proceedings of the Progress in Electromagnetics Research Symposium 2002 (PIERS 2002) (July 1 - 5, 2002, Cambridge, Massachusetts, USA), p. 842 (Invited Talk).
- ¹¹ M. I. Stockman, S. V. Faleev, and D. J. Bergman, *Femtosecond Energy Concentration in Nanosystems: Coherent Control*, Sixth International Conference on Electronic Transport and Optical Properties of Inhomogeneous Media (ETOPIM-6) Abstracts, Salt Lake City, Utah, 14-19 July, 2002, p. 160 (University of Utah, 2002).
- ¹² S. V. Faleev, and M. I. Stockman, *Self-Consistent Random-Phase Approximation and Intersubband Absorption for Interacting Electrons in Quantum Well*, Phys. Rev. B (2002) [Accepted for publication].
- ¹³ S. V. Faleev, and M. I. Stockman, *Self-Consistent Random-Phase Approximation for Interacting Electrons in Quantum Wells and Intersubband Absorption*, APS March 2002 Meeting (Indianapolis, Indiana, March 18-22, 2002), Bulletin of American Physical Soc. **47**, 1189 (2002).

CORRELATED CHARGE-CHANGING ION-ATOM COLLISIONS

J. A. Tanis

Department of Physics, Western Michigan University, Kalamazoo, MI 49008-5151

Email: tanis@wmich.edu

I. PROGRAM SCOPE

This work involves the experimental investigation of excitation and charge changing in ion-atom collisions, with connections to electron-ion collisions and photon-induced processes. Major emphases are the study of the electron-electron interaction (i.e., correlation) and multielectron transitions as related to various collision phenomena. Processes studied are of interest from both fundamental and applied points of view. Measurements are carried out mainly by means of electron spectroscopy, but COLTRIMS techniques are utilized in some cases. While the bulk of the measurements have been conducted at WMU, additional experimental work has been carried out at the J.R. Macdonald Laboratory (Kansas State) and at GANIL (Caen, France). Summaries of work completed and work in progress are given immediately below.

II. RECENT PROGRESS

1. Superelastic electron scattering from metastable $1s2s\ ^3S$ states of low Z ions

Superelastic scattering occurs when an electron gains energy as a consequence of being scattered by an initially excited atomic system in such a way as to deexcite the parent system. We have investigated superelastic scattering for quasi-free H_2 electrons colliding with metastable $1s2s\ ^3S$ C^{4+} and O^{6+} ions in measurements conducted at WMU using the tandem Van de Graaff accelerator. Scattered electrons were observed using a parallel-plate electron spectrometer mounted at 0° to the incident beam axis. The resulting superelastic cross sections at 180° scattering angle for $1s2s\ ^3S \rightarrow 1s^2\ ^1S$ deexcitation show a strong dependence on the collision energy and on the atomic number of the metastable ion. Because of the change in spin (from 3S to 1S) the scattering process must involve electron exchange. Calculated R-matrix cross sections for superelastic scattering (in collaboration with T. Gorczyca from WMU) were obtained from time-reversed electron impact excitation cross sections using the principle of detailed balance. The calculated results show that the differential cross section at 180° is approximately inversely proportional to the collision energy and exhibits a dependence on the atomic number of the metastable ion that is significantly different from that for the total scattering cross section. This anisotropy of the angular differential cross section was shown to be important in the interpretation of the measured cross sections. This work was recently published in *Physical Review A* (see publication list).

2. Electron correlation in hollow-state formation in Li-like ions

Double-K-shell vacancy production, i.e., so-called hollow states, in Li-like Be^+ , B^{2+} , C^{3+} , and O^{5+} ions colliding with helium in the velocity range 3-9 a.u. has been investigated using high-

resolution projectile Auger spectroscopy. The measurements were conducted mainly at WMU, with a few of the higher energy data being obtained at Kansas State (in collaboration with M. Benis and P. Richard). State-selective measurements show that doubly vacant K-shell states in Be^+ ions are mainly produced by ionization followed by excitation leading to $2i2i'$ and $2i3i'$ configurations, while for B^{2+} and C^{3+} , both ionization-excitation and double-excitation contribute to the formation of hollow states leading to $2i2i'$, $2i3i'$ (only in B^{2+}), and $2i2i'2i''$ configurations. For O^{5+} , only $2i2i'$ configurations are seen. Both nucleus-electron ($n-e$) and electron-electron ($e-e$) interactions are found to be responsible for formation of the hollow states, with the $e-e$ contribution becoming clearly dominant at the higher velocities. Furthermore, from the observation of specific excited states, both "shake" and "dielectronic" manifestations of the $e-e$ interaction can be identified. Significant variations in the electron correlation strength as a function of collision velocity and atomic number occur for the ions studied. These results provide quantitative insight into the role and importance of the $e-e$ interaction in causing additional K-shell electronic excitation (or ionization), following an initial K-shell vacancy producing event by a different perturber (an ion or photon). These data provide a basis for comparison with future planned photon-induced studies for these same ions. This work formed the Ph.D. dissertation project of Mr. Ali Alnaser (graduation date 8/02).

3. Interference in electron emission from H_2 by fast ions

Interference effects, analogous to Young's two-slit experiment, are expected to occur when electrons are ejected coherently within a multi-center molecular field [1]. In this work, ionization of H_2 , a molecule composed of two indistinguishable atoms, by fast ions has been investigated. Calculations predict that the ratio of electron emission from H_2 compared to two independent H atoms should exhibit an oscillatory structure described by $[1+\sin(kd)/kd]$, where k is the outgoing electron momentum and d is the internuclear separation. At WMU, measurements for 3 and 5 MeV H^+ impact have been conducted, and just recently new data have been obtained at GANIL (Caen, France) for 68 MeV/u Kr^{33+} ions to complement our earlier measurements at that facility [1]. Electron emission cross sections were measured at WMU for electron energies ranging from ~ 3 -250 eV at observation angles of 30° , 45° , 90° , 135° , and 150° with respect to the incident beam. A sinusoidal variation was observed for electron energies less than ~ 250 eV in general agreement with the model calculations. Calculated Born cross sections for the momentum transferred as a function of the scattering angle support the observations. New measurements are presently underway for 1 and 10 MeV H^+ projectiles to compare with recent theoretical work [2]. This work, which is ongoing, forms the Ph.D. dissertation project of Mr. Sabbir Hossain (expected completion 12/03). Additionally, two high school students from the Kalamazoo Area Mathematics and Science Center have been instrumental in constructing a code to carry out the Born calculations.

4. Excited-state enhancement due to Pauli exclusion in electron transfer

Single-electron transfer to autoionizing $2i2i'$ configurations in metastable $\text{F}^{7+}(1s2s^3S)$ and double transfer to the same $2i2i'$ configurations in $\text{F}^{8+}(1s)$ are being investigated for \sim MeV/u collisions of these ions with He and Ne. The measurements are being done at WMU. An anomalously large intensity is observed for the formation of the triply spin-aligned metastable $1s(2s2p^3P)^4P$ state in single capture to $\text{F}^{7+}(1s2s^3S)$ and in double capture to $\text{F}^{8+}(1s)$. This 4P

state is larger in all cases than the similarly configured $1s(2s2p^3P)^2P$ and $1s(2s2p^1P)^2P_+$ states. Analysis suggests that the enhancement of the 4P state for both single and double transfer is a consequence of the Pauli exclusion principle [3]. Specifically, for $F^{7+}(1s2s^3S)$ a transferred electron that has the same spin as the existing electrons is blocked from going into $1s$ or $2s$ and is instead "forced" into $2p$ (or a higher level). In the case of double transfer to $F^{8+}(1s)$, the first electron having the same spin as the existing $1s$ is forced into $2s$, while the second like-spin electron is blocked from going into $1s$ or $2s$, thereby being forced into $2p$. Thus, the Pauli exclusion that prevents electrons from being transferred into $1s$ (or $2s$) has the effect of enhancing the 4P state. Such effects, so far studied only for electron transfer to the 4P state in F^{7+} and F^{8+} , may be useful for controlling or enhancing this or other specific excited ionic states. Results of this work are presently being prepared for publication. Some of this work formed the basis for the Honors College thesis project of Mr. Joseph Pole (graduated 4/02).

5. Dissociative ionization of spatially aligned D_2 by fast highly charged ions

Recent work has shown that the initial orientation of a molecule relative to an incident ion can be a significant factor in determining the outcome of molecular ionization and fragmentation processes [4]. While most work to date has focused on one-electron processes, similar effects might be expected for two-electron processes. In this latter regard, double-ionization and ionization-excitation of D_2 leading to dissociation of D_2 molecules by 19 MeV F^{8+} ions were studied using a COLTRIMS technique at the KSU LINAC in collaboration with Profs. P. Richard and C.L. Cocke. The vector momenta of at least one molecule fragment and one ejected electron resulting from these collisions were fully determined. Measurement of this fragment yields the molecular alignment at the time of the collision as well as the dissociative state of the molecular ion. Results to date indicate that double ionization of D_2 by incident 1 MeV/u F^{8+} is more likely to occur when the molecular axis is initially oriented perpendicular to the beam axis. The reason for this effect is not yet understood. However, interference effects similar to those observed in electron emission from H_2 (discussed above) are a suspected cause. Preliminary analysis based on a simple theoretical interference model appears to be consistent with the data. These data and their analysis are primarily the responsibility of Dr. Allen Landers.

III. FUTURE PLANS

The primary emphasis of our research is the study of electron dynamics as manifested in ion-atom collisions, and their corresponding connections to electron-ion collisions and photon-induced processes. New efforts based on our previous work will be conducted. Specific planned projects include: (1) experimental and theoretical investigation of interference effects in the coherent emission of electrons from H_2 by fast protons and other projectiles, (2) detailed study of the role of Pauli exclusion in leading to few-electron ionic excited states, and (3) determination of the role of electron correlation in producing doubly vacant K-shell excited states in atomic Li following ion bombardment. Most of this work is expected to be done at WMU, with some additional work being done in collaborative efforts with researchers at other universities and laboratories.

[1] N. Stolterfoht *et al.*, Phys. Rev. Lett. **87**, 023201 (2001).

[2] R. Rivarola, *et al.*, submitted to Phys. Rev. Lett., private communication.

[3] T. Kirchner and M. Horbatsch, *Phys. Rev. A* **63**, 062718 (2001).

[4] R. Dörner *et al.*, *Phys. Rev. Lett.* **81**, 5776 (1998).

IV. PAPERS PUBLISHED OR ACCEPTED DURING 2000-2002

"Two- and Three-body Effects in Fast Ion-Atom Collisions: Analogies between Photon and Charged Particle Impact," N. Stolterfoht, B. Sulik, J.A. Tanis, J.-Y. Chesnel, L. Gulyás, F. Frémont, D. Lecler, D. Hennecart, X. Husson, J.P. Grandin, M. Grether, Cs. Koncz, and B. Skogvall, X-ray and Inner-Shell Processes, 18th International Conference, AIP Conference Proceedings 506, (AIP, New York, 2000), pp. 427-443.

"One- and Two-K-Shell Vacancy Production in Atomic Li by 95 MeV/u Ar¹⁸⁺ Projectiles," J.A. Tanis, J.-Y. Chesnel, F. Frémont, D. Hennecart, X. Husson, D. Lecler, A. Cassimi, J.P. Grandin, J. Rangama, B. Skogvall, B. Sulik, J.-H. Bremer, and N. Stolterfoht, *Phys. Rev. A* **62**, 032715 (2000).

"Double-K-Shell Vacancy Production in Li-like C³⁺ Ions Colliding with Helium," A.S. Al-Naser, A.L. Landers, D.J. Pole, H. Knutson, and J.A. Tanis, *Physica Scripta T* **92**, 265 (2001).

"Coherence in Two-Electron Transfer in F⁸⁺ + Ne Collisions," A.L. Landers, D.J. Pole, A.L. Erickcek, S.M. Ferguson, J.-Y. Chesnel, B. Sulik, and J.A. Tanis, *Physica Scripta T* **92**, 354 (2001).

"Photoelectron Diffraction Mapping: Molecules Illuminated from Within," A.L. Landers, Th. Weber, I. Ali, A. Cassimi, M. Hattass, O. Jagutzki, A. Nauert, T. Osipov, A. Staudte, M.H. Prior, H. Schmidt-Böcking, C. L. Cocke and R. Dörner, *Phys. Rev. Lett.* **87**, 013002 (2001).

"Evidence for Interference Effects in Electron Emission from H₂ Colliding with 60.5 MeV/u Kr³⁴⁺ Ions," N. Stolterfoht, B. Sulik, V. Hoffmann, B. Skogvall, J.-Y. Chesnel, J. Rangama, F. Frémont, D. Hennecart, A. Cassimi, X. Husson, A. Landers, J.A. Tanis, M.E. Galassi, and R.D. Rivarola, *Phys. Rev. Lett.* **87**, 023201 (2001).

"Superelastic Scattering of Electrons from Highly Charged Ions with Inner Shell Vacancies," P.A. Závodszky, H. Aliabadi, C.P. Bhalla, P. Richard, G. Tóth, and J.A. Tanis, *Phys. Rev. Lett.* **87**, 033202 (2001).

"Superelastic Scattering of Electrons from Metastable He-like C⁴⁺ and O⁶⁺ Ions," A.S. Alnaser, A.L. Landers, D.J. Pole, S. Hossain, O.A. Haija, T.W. Gorczyca, J.A. Tanis, and H. Knutson, *Phys. Rev. A* **65**, 042709 (2002).

"Internal Dielectronic Excitation in Highly Charged Ions Colliding with Surfaces," G.A. Machicoane, T. Schenkel, T.R. Niedermayr, M.W. Newmann, A.V. Hamza, A.V. Barnes, J.W. McDonald, J.A. Tanis, and D.H. Schneider, *Phys. Rev. A* **65**, 042903 (2002).

"Mechanisms of Photo Double Ionization of Helium by 530 eV Photons", A. Knapp, A. Kheifets, I. Bray, Th. Weber, A.L. Landers, S. Schössler, T. Jahnke, J. Nickles, S. Kammer, O. Jagutzki, L. Ph. H. Schmidt, T. Osipov, J. Rösch, M. H. Prior, H. Schmidt-Böcking, C. L. Cocke, and R. Dörner, *Phys. Rev. Lett.* **89**, 033004 (2002).

"Analogies between photon and fast-ion impact in the production of hollow lithium," J.-Y. Chesnel, J.A. Tanis, B. Sulik, B. Skogvall, J. Rangama, F. Frémont, J.-H. Bremer, A. Cassimi, D. Hennecart, V. Hoffmann, X. Husson, A. L. Landers, and N. Stolterfoht, *Photonic, Electronic, and Atomic Collisions (XXII ICPEAC)*, edited by J. Burgdorfer, J. Cohen, S. Datz, and C. Vane, (Rinton Press, Princeton, 2002).

The Nuclear Moments of ^{133}Cs

Carol E. Tanner and Vladislav Gerginov
 University of Notre Dame
 College of Science
 Department of Physics
 225 Nieuwland Science Hall
 Notre Dame, IN 46556-5670

carol.e.tanner.1@nd.edu and vladislav.p.gerginov.1@nd.edu

We present our results for the ^{133}Cs $6p\ ^2P_{3/2}$ state hyperfine energy splittings in Table 1. Theory [1] predicts that the magnetic octupole contribution lies below the uncertainty of previous measurements [2]. Our new measurements reduce the uncertainty in the frequency intervals by an order of magnitude. With our new results, we can improve upon the known values of the magnetic dipole and electric quadrupole contributions to the frequency intervals and make the first determination of the magnetic octupole contribution. Precise measurements of hyperfine structure play an important role in the development of the atomic theory and provide tests for theories of nuclear structure. Our measurements are also motivated by their connection to the observation of parity non-conservation in atomic cesium [3] where the interpretation of the results in terms of the weak interaction depends on accurate knowledge of both atomic and nuclear wave functions.

Table 1: Hyperfine energy splittings and nuclear multi-pole coefficients.

$\Delta_{32} \equiv \nu(6p\ ^2P_{3/2}(F'=3)) - \nu(6p\ ^2P_{3/2}(F'=2))$	151.225(3) MHz
$\Delta_{43} \equiv \nu(6p\ ^2P_{3/2}(F'=4)) - \nu(6p\ ^2P_{3/2}(F'=3))$	201.286(3) MHz
$\Delta_{54} \equiv \nu(6p\ ^2P_{3/2}(F'=5)) - \nu(6p\ ^2P_{3/2}(F'=4))$	251.092(3) MHz
Magnetic Dipole Contribution A	50.2882(4) MHz
Electric Quadrupole Contribution b	-0.494(3) MHz
Magnetic Octupole Contribution c	0.00062(16) MHz

Our experimental approach uses a dense well-collimated thermal atomic beam and perpendicular laser excitation. Two highly stabilized laser diodes (850 nm) are used to record high-resolution spectra. One laser scans the hyperfine structure of the $6s\ ^2S_{1/2}$ $F=3,4 \rightarrow 6p\ ^2P_{3/2}$ $F'=2,3,4,5$ transitions. The second is a reference laser that is absolutely locked near a single hyperfine transition in a vapor cell. Portions of the output from each laser are combined on a fast photodiode where the frequency of the heterodyne beat note provides a high-resolution absolute frequency calibration.

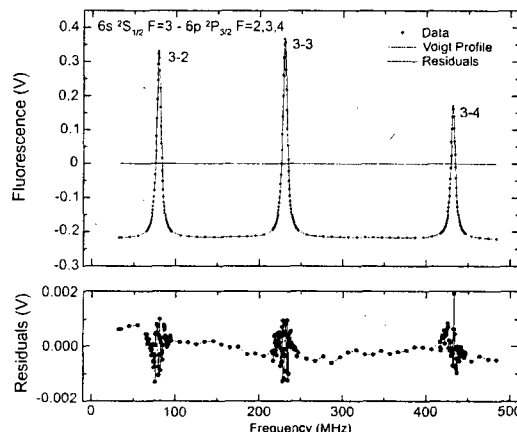


Figure 1: Laser heterodyne frequency calibrated spectrum using two diode lasers.

A typical spectrum starting from the $F=3$ ground state of Cs is shown in the Figure 1. For each data point, the difference frequency between the two lasers is locked to specific values and a computer reads and averages both fluorescence voltage and frequency values. Analysis of the spectrum is performed using a customized Fortran data-fitting program based on Levenberg-Marquardt method. The data is fitted with three Voigt profiles (a convolution between Gaussian and Lorentzian line shapes) and nonlinear backgrounds that take into account the velocity distribution of the residual Cs cloud in the chamber. Combining the results of many repeated measurements, the frequency differences between pairs of peaks is determined to a precision of approximately 3 kHz.

Our future plans for this project include an improved measurement of the $6p\ ^2P_{1/2}\ F'=3$ to 4 hyperfine splitting using the atomic beam developed for the present measurements. This measurement will require diode lasers capable of exciting the $6s\ ^2S_{1/2} \rightarrow 6p\ ^2P_{1/2}$ transition at 894 nm. In collaboration with atomic theorist W. Johnson and A. Derevianko, we expect to report the first results for the nuclear magnetic octupole moment of the ^{133}Cs nucleus. Finally, we are planning to use our atomic beam apparatus and diode lasers in conjunction with a pulsed laser frequency comb at NIST-Boulder to perform absolute wavelength measurements of both the $6s\ ^2S_{1/2} \rightarrow 6p\ ^2P_{1/2}$ and the $6s\ ^2S_{1/2} \rightarrow 6p\ ^2P_{3/2}$ transitions. These absolute optical frequencies are important to a new experimental determination of the fine structure constant [4] and for the interpretation of atom interferometer experiments [5] involving Cs atoms.

References:

- [1] W. Johnson and A. Derevianko, private communication.
- [2] C.E. Tanner, C. Wieman, *Physical Review A*, **38**, 1616 (1988).
- [3] C. S. Wood, S. C. Bennett, D. Cho, B. P. Masterson, J. L. Roberts, C. E. Tanner, and C. E. Wieman, *Science* **275**, 1759 (1997).
- [4] Th. Uhdem, J. Reichert, R. Hozwarth, and T.W. Hänsch, *PRL* **82**, 3568-3571 (1999).
- [5] Th. Uhdem, J. Reichert, T.W. Hänsch, M. Kourogi, *PRL* **62**, 031801-1 (2000).

Recent Publications:

- "Lifetime measurements of the cesium $5d\ ^2D_{5/2,3/2}$ and $11s\ ^2S_{1/2}$ states using pulsed-laser excitation", D. DiBerardino and C. E. Tanner, *Phys. Rev. A* **57**, pp. 4202-4211, June 1998.
- "Fast-beam laser lifetime measurements of the cesium $6p\ ^2P_{1/2,3/2}$ states," R. J. Rafac, C. E. Tanner, A. E. Livingston, and H. G. Berry, *Phys. Rev. A* **60**, pp. 3648-3662, November 1999.
- "Diode lasers for fast-beam laser experiments," V. Gerginov, B. Laughman, D. DiBerardino, R. J. Rafac, S. T. Ruggiero, and C. E. Tanner, *Opt. Comm.* **187**, pp. 219-230, January 2001.
- "Imperfect Detectors in Linear Optical Quantum Computers", S. Glancy, J.M. LoSecco, H.M. Vasconcelos, and C.E. Tanner, *Phys. Rev. A* **65**, 062317-1 to 7, June 2002.
- "Fiber-Optic Bundle Light-Collection Systems and Calculations of Collection Efficiency," S. Boone, V. Gerginov, D. DiBerardino, R.J. Rafac, and C.E. Tanner, *Opt. Com.* **210**, pp. 67-77, September 2002.

Quantum Dynamics of Ultracold Fermionic Vapors

John E. Thomas
Physics Department, Duke University
Durham, NC 27708-0305
e-mail: jet@phy.duke.edu

1. Scope

The purpose of this program is to study collective quantum dynamics of a mechanically driven ultracold gas of ${}^6\text{Li}$ fermions, contained in an ultrastable CO_2 laser trap. Mixtures of the two lowest hyperfine states of ${}^6\text{Li}$ exhibit magnetically tunable s-wave scattering interactions ranging from zero to strongly attractive or strongly repulsive. For this reason, this two-component mixture is particularly well suited for exploring fundamental interactions in Fermi gases. Pairing interactions in this system are predicted to lead to a Fermi superfluid phase at experimentally accessible temperatures, providing an atomic gas analog of a superconductor. Since the interaction strength and density can be experimentally controlled, it may be possible to study fundamental new features of spin pairing and superconductivity, such as the crossover from weak BCS pairing to Bose condensation of strongly bound pairs.

2. Recent Progress

During the past year we have made substantial progress, producing a degenerate Fermi gas by direct evaporative cooling in the CO_2 laser trap. Further, we have begun to characterize the magnetic field dependent interactions and loss in the trapped two-component ${}^6\text{Li}$ mixture as a prelude to the study of collective dynamics.

Our experiments employ an ultrastable CO_2 laser trap which is used to confine arbitrary mixtures of ground hyperfine states of ${}^6\text{Li}$ atoms by loading from a standard magneto-optical trap (MOT). Further cooling is accomplished by direct evaporation in the CO_2 laser trap. The CO_2 laser trap has depth of $700\ \mu\text{K}$ and a very low optical scattering rate of only two photons per atom per hour as a consequence of the long wavelength. The trapping laser achieves very low intensity noise, suppressing noise-induced heating. Extremely low residual heating rates of just $5\ \text{nK/sec}$ are measured and a lifetime of 400 seconds is achieved, comparable to the background gas limit at 10^{-11} Torr.

All-Optical Production of a Degenerate Fermi Gas

In the past year, we have for the first time produced a degenerate Fermi gas by all-optical methods [1]. The CO₂ laser trap consists of a single beam which is focused into the MOT region. A 50-50 mixture of the two lowest hyperfine states of ⁶Li is loaded from the MOT. Initially, approximately 3.5 million atoms are contained in the CO₂ laser trap at a temperature of 140 μK, identical to the measured MOT temperature during the loading stage. During this loading phase, the CO₂ laser beam is recollimated and retroreflected after passing through the MOT region to increase the trap depth.

A unique feature of the trapped mixture is that the scattering length vanishes at zero magnetic field, enabling the loading and evaporation stages to be separately controlled. To obtain a nonzero scattering length, we apply a 100 G magnetic field after the loading phase, yielding a scattering length of $\simeq -100 a_0$. Rapid evaporation follows, during which time the retroreflected CO₂ laser beam is adiabatically blocked over a few seconds. After this procedure, approximately 1.2 million atoms remain at a temperature of 50 μK, about 1/14 of the single beam trap depth. At this point, evaporation stagnates, since there are too few atoms with enough energy to leave the trap.

Further cooling employs forced evaporation, accomplished by slowly lowering the CO₂ laser power by a factor of about 100. After 40 seconds of lowering, degeneracy is achieved. The trap is adiabatically recompressed to full depth, preserving the phase space density. The atoms are released and the temperature is determined by time-of-flight imaging. Approximately 300 thousand atoms remain at a temperature just above 4 μK, about 0.55 of the Fermi temperature. The method provides a degenerate two-component mixture of the two lowest hyperfine states of ⁶Li, a promising system for observing Fermi superfluidity.

In the past few months, we have installed a new high field magnet system which provides fields up to 1100 G in the trap region. Using this magnet, we have performed evaporation at 900 G, where the scattering length is expected to be several thousand a_0 , yielding a unitarity limited elastic scattering cross section. In this case, degeneracy is achieved in just a few seconds and temperatures less than 0.3 of the Fermi temperature are attained.

Measurement of the Zero Crossing in a Feshbach Resonance of ⁶Li Fermions

A crucial feature of the ⁶Li system is the existence of a Feshbach resonance in mixtures of the two lowest hyperfine states. In a Feshbach resonance, the energy of the colliding two-particle state is magnetically tuned into resonance with a bound molecular state. This leads to a resonant enhancement in the scattering length, enabling magnetically tunable strongly attractive or repulsive interactions. The resonance is predicted to occur at a magnetic field near 850 G. Experimental verification of the

resonance is of paramount importance for studies of fundamental interactions in this system.

As a first step, we have measured the zero crossing associated with the expected Feshbach resonance in ${}^6\text{Li}$. When a Feshbach resonance occurs, the scattering length rapidly changes from a background value to a large positive or negative value as the magnetic field is varied. In mixtures of the two lowest states of ${}^6\text{Li}$, the background scattering length increases from zero at zero magnetic field to large and negative as the field is increased. In the vicinity of the Feshbach resonance, the scattering length initially becomes large and positive as the resonance is approached from the low field side. Hence, the scattering length must cross zero at some point before the Feshbach resonance. The predicted zero crossing is between 500 and 550 G.

To measure the zero crossing, we use evaporation in a trap of fixed depth. After 40 seconds of evaporation, we measure the temperature and the number of remaining atoms as a function of the magnetic field strength at which the evaporation is induced. At a field of 528 ± 2 G, we find that the temperature drop and atom loss are minimized. The temperature is consistent with that obtained for zero magnetic field, where we have previously shown that the scattering length is negligible by trapping the atoms for several hundred seconds at moderate temperature. Hence, the zero crossing occurs near 528 G. Using the best available interaction potentials, the NIST group has predicted that a Feshbach resonance should occur near 820 G. The zero crossing corresponding to this resonance is predicted to occur near 520 G, quite close to our measured result. Hence, our measurements suggest that a Feshbach resonance is likely to occur at the predicted location.

Magnetic Field-Dependent Collision-Induced Loss and Heating in ${}^6\text{Li}$ Mixtures

In bosonic systems, it is well known that substantial two and three body loss can occur near a Feshbach resonance. However, it is likely that such losses are in part suppressed for fermions as a consequence of Fermi statistics. If Fermi superfluidity is to be observable, it is necessary that the time scale over which loss occurs be long compared to the formation time of spin pairs. Hence, a study of collision-induced loss and heating is important for verifying that the ${}^6\text{Li}$ system is suitable for studies of superfluidity.

We have studied collision-induced loss by observing the number of atoms remaining after 1 second in a specified magnetic field. The atoms are first cooled by evaporation so that the temperature is $1/20$ of the trap depth. In this case, atom loss arising from evaporation is negligible. A magnetic field is applied for 1 second and the cloud is released to determine the number and temperature by time-of-flight absorption imaging.

We observe a broad loss and heating feature centered at 650 G. We find that at densities greater than $3 \times 10^{13}/\text{cm}^3$, the time scale for substantial loss is the order of a second, large compared to the formation time for spin pairs, which is expected to

be sub-millisecond. At fields of 900 G, we observe negligible loss and heating for time scales of a few seconds.

These initial results suggest that mixtures of the two lowest hyperfine states of ${}^6\text{Li}$ are suitable for studies of Fermi superfluidity in the vicinity of a Feshbach resonance.

3. Future Plans

After completion of our preliminary studies of magnetic field dependent interactions and loss, we plan to pursue a variety of experiments on the mechanical excitation of the trapped two-component gas. These experiments will begin by looking for shifts and hydrodynamic behavior in the parametric resonance spectrum of the trapped atoms.

An additional set of experiments will explore mechanical effects of magnetically tunable mean field interactions on the trapped cloud shape. These experiments will be accomplished by off-resonance imaging of the trapped cloud.

4. References to Publications of DOE Sponsored Research

- 1) S. R. Granade, M. E. Gehm, K. M. O'Hara, and J. E. Thomas, "All-Optical Production of a Degenerate Fermi Gas," *Phys. Rev. Lett.* **88**, 120405 (2002).

Laser-Produced Coherent X-Ray Sources

Donald Umstadter (dpu@umich.edu)

Frontiers of Optical, Coherent and Ultrafast Science (FOCUS), 1006 IST Bldg., University of Michigan, Ann Arbor 49109-2099

I. PROGRAM SCOPE:

We experimentally and theoretically explore the physics of ultra-high-intensity laser-plasma interactions and their applications to novel radiation sources. Our interests have shifted in the last few years from a more general study of high-field interactions [1] towards the more directed goal of developing keV-energy ultrashort-duration table-top x-ray sources [2]. One promising approach involves the scattering of ultra-powerful laser light from laser-accelerated electrons, resulting in Doppler-shifted high-order harmonic generation, which is predicted to reach keV energy using current technology. These studies have applications to the fields of relativistic nonlinear optics, ultrafast chemistry, biology, inner-shell electronic processes in atomic systems, and phase transitions in materials science.

II. RECENT PROGRESS:

A. Relativistic nonlinear Thomson scattering

It is now possible to create a sufficient photon density to study Thomson scattering in the relativistic regime. With increasing light intensity, electrons quiver during the scattering process with increasing velocities, approaching the speed of light when the laser intensity approaches 10^{18} W/cm². In this limit, the effect of light's magnetic field on electron motion should become comparable to that of its electric field, and the electron mass should increase because of the relativistic correction. Consequently, electrons in such high fields are predicted to quiver nonlinearly, moving in figure-eight patterns, rather than in straight lines, and thus to radiate photons at harmonics of the frequency of the incident laser light, with each harmonic having its own unique angular distribution. This is referred to as nonlinear Thomson scattering or relativistic Thomson scattering. Previously, we observed the generation of the second and third harmonics, with their unique angular patterning originating from this process [1]. More recently, we observed for the first time relativistic harmonics emitted along the laser axis. Third harmonic light was detected and discriminated spectrally and angularly from the harmonics generated from competing processes [3].

In this last year of the grant, we have extended this study to high-order harmonics [4], which we ascribe to scattering from relativistic electron beams, which were accelerated by the same laser pulse. It is shown that at high intensities, when the normalized electric field approaches unity, in addition to the conventional atomic harmonics from bound electrons, there is significant contribution to the harmonic spectrum from free electrons. The characteristic signatures of this are found to be the emission of even order harmonics, linear dependence on the electron density, significant amount of harmonics even with circular polarization and a much smaller spatial region over which these harmonics are produced as compared to the atomic case. Imaging of the harmonic beam shows that it is emitted in a narrow cone with a divergence of 2-3 degrees. Besides its promise as an efficient source of XUV radiation, the generation of high-order harmonics is of interest primarily from the fact that they can be produced by fewer nonlinear processes than low-order harmonics can and thus provide definitive signatures of their origin.

1. Experiments

The experiments were performed with a Ti:sapphire-Nd:glass laser system based on chirped-pulse amplification, which produces ≤ 2 -J, 400-fs pulses at 1.053- μm wavelength, focusable to a peak intensity of 10^{19} W cm⁻². As shown in Fig. 1, high harmonic emission from the plasma is measured using a Saye-Namioka spectrometer with a range of 200-30 nm. This covers the harmonic range of 6-30 for a fundamental wavelength of 1.053 μm . Harmonics are detected using an imaging MCP (dual plate + phosphor screen) coupled to a high sensitivity high dynamic range CCD camera. In the current experiment the laser beam is directed along the spectrometer axis and the gas jet and the MCP are located at the object and image planes respectively.

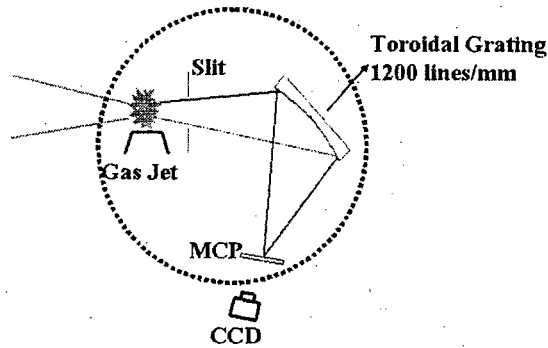


FIG. 1. Experimental setup used to spectrally and spatially resolve high-order harmonics.

Two different measurements were carried out to obtain data on the spatial region in which the harmonics were produced. As has been noted previously the odd harmonics were always stronger than the even order harmonics. One may conclude that the odd orders have contributions from both the bound and free electrons while the even orders only arise from the free electrons. Fig. 2 (a) shows the results obtained when linearly polarized light at low intensity and low density is used [4]. As expected only the odd orders (7th and 9th) are seen and the spatial extent is large as would be expected from the fact that bound harmonics would be produced in the focal volume when the intensity exceeds 10^{13} W/cm². The emission in the even order was much weaker than that in the odd orders. Data taken over the entire spectrometer range which extends to the 30th harmonic reveals a similar trend—namely that the even harmonics are weaker than the odd ones. Shots taken for other harmonic orders show similar results namely absence of all the even harmonics and large spatial extent of the region in which odd harmonics are produced (typically 100 μ m). In order to isolate the contribution from free electrons these experiments were done at high intensity and circularly polarized light was used. The results are shown in Fig. 2 (b). It is apparent that in addition to the 7th and 9th harmonic, which would be expected to arise from bound electrons, there is a clear signal coming from the 8th harmonic. It was checked that the even orders disappear at lower intensities or gas densities. The spatial extent of the harmonics from free electrons is seen to be significantly smaller ($< 20 \mu$ m) than the atomic harmonics.

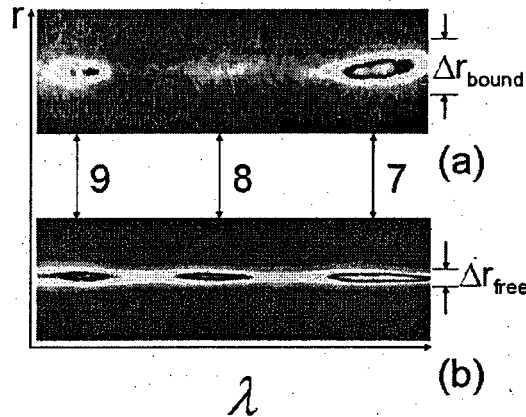


FIG. 2. Spatial profile of the high order harmonics (a, top) $I = 2 \times 10^{16}$ W/cm², $n = 10^{17}$ /cm³ and linear polarization (b, bottom) $I = 2 \times 10^{17}$ W/cm², $n = 10^{18}$ /cm³ and circular polarization.

The small angular divergence of the 11th harmonic seen in Fig. 3 can only be explained by nonlinear scattering (assuming a spread of laser k vectors at the focus) from the forward-going electron beam ("Compton" scattering) accelerated by means of a self-modulated wakefield [1] rather than free electrons in a stationary plasma [4].

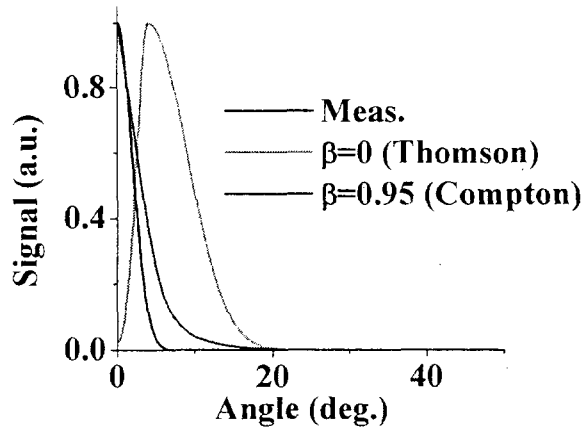


FIG. 3. Calculated spatial profile of the 11th harmonic for the case where the electron starts at rest (dashed curve) and for an initial velocity of $0.95c$ (dotted curve) and the measured profile (solid line).

Scattering from a laser-accelerated electron beam has several advantages over linear Compton scattering from a conventionally accelerated electron beam: (1) the acceleration length is 10,000 times shorter; (2) the conversion efficiency is much higher because the electron beam is laser-driven and self-aligned spatially and temporally with the laser focus; (3) the conversion efficiency is also higher and the scattered light is more energetic.

2. Theory

In collaboration with Prof. Y. Y. Lau, also from the Univ. of Michigan, we have begun to study theoretically the scattering of electrons from high-intensity lasers. The dependence of free electron orbits on the phase of an ultra-intense light field has never before been studied, although it is critical for a thorough understanding of basic phenomena such as Thomson scattering. Including this phase, we show that the familiar figure-8 motion of an electron that is superimposed onto the forward drift is more of an exception than the rule [5]. Specifically, an electron tends to drift across the laser path, and this transverse drift is not due to the ponderomotive force. The orbital periodicity, and therefore its nonlinear Thomson scattering spectrum, depend critically on the amplitude of the ultra-intense laser field and on the above-mentioned phase, but are otherwise insensitive to the laser frequency.

Fig. 4 shows the dependence of the fundamental frequency in the back-scattered direction ($\mathbf{n} = -\mathbf{z}$) as a function of a , for several values of θ_{in} . The radiation spectrum extends to frequencies much lower than the laser frequency ω_0 [5]. The reason for this behavior is that, as the electron drifts longitudinally at velocities close to the speed of light, the electron moves closer in phase with the laser and the figure eight frequency (of electron oscillations) decreases.

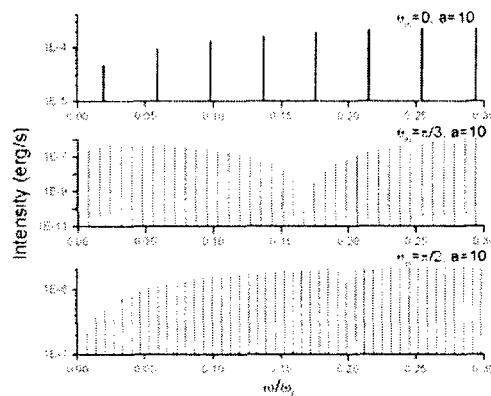


FIG. 4. Spectrum of Thomson back-scattered radiation, $(e^2\omega^2/4\pi^2c)|\mathbf{n} \times (\mathbf{n} \times \mathbf{F}_m)|^2$, in erg/s for $a = 10$. From top to bottom: $\theta_{in} = 0, \pi/3, \pi/2$. The spectrum for the $\theta_{in} = 0$ case peaks at $\omega = 6.26\omega_0$, with a value 0.00117 erg/s.

III. FUTURE PLANS

Our ongoing research is focused mainly on the study of short-wavelength generation with much shorter duration laser pulses and higher laser intensities. In this highly relativistic regime, the theoretical predictions [5] that were discussed in Sec. II A 2 can be tested. Access to this novel regime will be obtained with a laser system that has reached 10-TW peak power and 30-fs pulse duration. Additionally, experiments have begun on the scattering of short duration, high intensity laser pulses from counter-propagating MeV energy laser-accelerated electron beams. This geometry will permit the generation of much shorter wavelength radiation (keV energy), due to the relativistic Doppler shift [2,6]. Current efforts are being made in parallel to improve the energy, monochromaticity and emittance of laser produced electron beams via optical injection [2].

-
- [1] D. Umstadter, "Physics and Applications of Relativistic Plasmas Driven by Ultra-intense Lasers," *Phys. of Plasmas* **8**, 1774–1785 (2001) [invited].
 - [2] D. Umstadter, "Laser-Driven X-ray Sources for Ultrafast Metrology," *Yearbook in Science and Technology* [accepted for publication] (McGraw-Hill, New York, 2002).
 - [3] S.-Y. Chen, A. Maksimchuk, E. Esarey and D. Umstadter, "Observation of Phase-Matched Relativistic Harmonic Generation," *Phys. Rev. Lett.* **84**, 5528 (2000).
 - [4] S. Banerjee, A. R. Valenzuela, R.C. Shah, A. Maksimchuk and D. Umstadter, "High Harmonic Generation in Relativistic Laser Plasma Interaction," *Phys. Plasmas* **5**, 2393 (2002) [invited].
 - [5] F. He, Y. Y. Lau, D. Umstadter and T. Strickler, "Phase Dependence of Electron Orbits in an Ultra-intense Laser Field," *Phys. Plasmas* [accepted for publication] (2002).
 - [6] G. Mourou and D. Umstadter, "Extreme Light," *Scientific American*, May issue, p. 81 (2002).
 - [7] A. Maksimchuk, S. Gu, K. Flippo, D. Umstadter and V. Yu. Bychenkov, "Forward Ion Acceleration in Thin Films Driven by a High-Intensity Laser," *Phys. Rev. Lett.* **84**, 4108 (2000).
 - [8] D. Umstadter, S.-Y. Chen, G. Ma, A. Maksimchuk, G. Mourou, M. Nantel, S. Pikuz, G. Sarkisov and R. Wagner, "Dense and Relativistic Plasmas Produced by Compact High-Intensity Lasers," *Astrophysical Journal Supplement Series*, **127** 513-518, (2000).
 - [9] N. Saleh, K. Flippo, K. Nemoto, D. Umstadter, R. A. Crowell, C. D. Jonah, A. D. Trifunac, "Pulse Radiolysis of Liquid Water using Picosecond Electron Pulses Produced by a Table-top Terawatt Laser System," *Rev. Sci. Instr.*, **71**, 2305 (2000).
 - [10] A. Maksimchuk, M. Nantel, G. Ma, S. Gu, C. Y. Cote, D. Umstadter, S. A. Pikuz, I. Yu. Skobelev, A. Ya. Faenov, "X-Ray Radiation from Matter in Extreme Conditions," *J. Quant. Spectrosc. Radiat. Transfer.*, **65**, 367–385 (2000).
 - [11] F. B. Rosmej et al., "X-Ray Radiation from Ions with K-Shell Vacancies," *J. Quant. Spectrosc. Radiat. Transfer.*, **65**, 477-499,(2000).
 - [12] K. Nemoto, A. Maksimchuk, S. Banerjee, K. Flippo, G. Mourou, and D. Umstadter and V. Yu. Bychenkov, "Laser-triggered Ion Acceleration and Table Top Isotope Production," *Appl. Phys. Lett.* **78**, 595 (2001).

Author List

AUTHOR LIST

Bannister, M.E.	117
Beck, D.R.	125
Becker, Kurt H.	43
Belkacem, Ali	26, 101
Ben-Itzhak, Itzik	73
Berrah, Nora.	129
Bucksbaum, P.H.	133
Champion, R.L.	137
Chang, Z.	21, 77
Chapman, Michael	6
Chu, Shih-I.	13
Cocke, C.L.	69
Dalgarno, A.	141
Dantus, Marcos	144
DePaola, B.D.	81
DiMauro, L.F.	61
Ditmire, Todd.	17
Dunford, R.W.	54, 58
Esry, B.D.	93
Everitt, Henry O.	1
Feagin, James M.	7
Fischer, Charlotte Froese	150
Friedrich, Bretislav	148
Gallagher, T.F.	154
Gordon, Robert J.	22
Gould, Harvey	105
Gould, Phillip L.	157
Greene, Chris H.	160
Hagmann, S.	85
Hathiramani, D.	73
Holland, Murray J.	163
Hughes, Richard J.	5
Jin, Deborah	167
Jones, Robert R.	11
Kanter, E. P.	53
Kapteyn, Henry C.	170
Keto, John W.	172
Kolomeisky, Eugene B.	177
Krässig, B.	37
Krause, H.F.	38
Lin, C.D.	89
Lloyd, Seth.	3
Lundeen, Stephen R.	180
Macek, J.H.	40
McCurdy, C.W.	109
McGuire, Jim	183
McKoy, Vincent.	187
Monroe, Christopher	4
Msezane, Alfred Z.	191
Nelson, Keith A.	33
Novotny, Lukas.	195
Phaneuf, Ronald A.	199
Poliakoff, Erwin.	203
Pronko, Peter P.	207
Raithel, G.	211
Reinhold, C.O.	28
Rescigno, Thomas N.	47
Richard, Patrick.	48, 65
Robicheaux, F.	50
Rocca, Jorge J.	29
Schoenlein, Robert W.	113
Smith, A.J.	215
Starace, Anthony.	219
Stockman, Mark I.	223
Tanis, J.A.	227
Tanner, Carol E.	231
Thomas, John E.	233
Thumm, Uwe	49, 97
Umstadter, Donald	237
Zoller, Peter.	2